PREPARATION AND PROPERTIES OF BIODEGRADABLE MUNG BEAN STARCH AND BASIL SEED MUCILAGE FILMS BY CROSSLINKING WITH DIFFERENT ACIDS

NARUENART THESSRIMUANG

A THESIS SUBMITTED IN PARTIAL FULFILLMENT OF THE REQUIREMENT FOR THE DEGREE OF DOCTOR OF PHILOSOPHY IN APPLIED CHEMISTRY

DEPARTMENT OF CHEMISTRY FACULTY OF SCIENCE
KING MONGKUT'S INSTITUTE OF TECHNOLOGY LADKRABANG

2019
KMITL-2019-SC-D-010-043

PREPARATION AND PROPERTIES OF BIODEGRADABLE MUNG BEAN STARCH AND BASIL SEED MUCILAGE FILMS BY CROSSLINKING WITH DIFFERENT ACIDS

NARUENART THESSRIMUANG

A THESIS SUBMITTED IN PARTIAL FULFILLMENT OF THE REQUIREMENT FOR THE DEGREE OF DOCTOR OF PHILOSOPHY IN APPLIED CHEMISTRY

DEPARTMENT OF CHEMISTRY FACULTY OF SCIENCE
KING MONGKUT'S INSTITUTE OF TECHNOLOGY LADKRABANG

2019

KMITL-2019-SC-D-010-043

Thesis Title	Preparation and properties of biodegradable mung bean starch and basil seed mucilage films from crosslinking with different acids
Student Name	Naruenart Thessrimuang
Student ID	57605006
Degree	Doctor of Philosophy Program in Applied Chemistry
Department	Chemistry
Year	2019
Thesis Advisor	Assoc. Prof. Jutarat Prachayawarakorn

Abstract

Weak mechanical and highly hydrophilic properties of starches have limited their applications in packaging industry. In this study, mung bean starch (MBS) and basil seed mucilage (BSM) were investigated its film forming biopolymer potential. MBS and BSM films were prepared and modified by different types and contents of natural di-carboxylic acids—tartaric acid (TA), malic acid (MA) and succinic acid (SA)—with different levels of acidity and chemical structures. It was observed from FT-IR spectra, that there was the new peak at 1730 cm^{-1} assigned for the C=O stretching of the carboxylic and ester group. The result confirmed the formation of ester linkages between the starch and cross-linker. Moreover, the O-H stretching peak also shifted to lower wavenumber. X-ray diffraction patterns of the film cross-linked by TA, MA and SA exhibited lower crystallinity by higher contents of the acids. From SEM micrographs, the addition of three cross-linkers into MBS and BSM films led to smoother surface. Water absorption and degree of swelling of different MBS and BSM films clearly decreased with increasing cross-linker contents. When the content of the cross-linkers increased, the stress at maximum load and Young's modulus decreased. On the contrary, the strain at maximum load of MBS and BSM films significantly increased. For thermal property, thermal degradation temperature of all cross-linked films improved either by the addition of the cross-linkers or by the increasing contents of the acids. Finally, the cross-linked films degraded slower than the all-native films. From this study, the MBS film cross-linked by 30% SA presented the greatest overall properties, determined from degree of swelling, water absorption, water vapor permeability, gel fraction, tensile properties, thermal properties and soil burial test.

Keywords: Biodegradable film; Cross-linking; Starch; Modified starch

Acknowledgement

Firstly, I would like to express my sincere gratitude to my advisor Assoc. Prof. Dr. Jutarat Prachayawarakorn. Without her assistance and dedicated involvement in every step throughout the process, this thesis would have never been accomplished. I would like to thank you very much for your supporting and understanding. Moreover, I would also like to show gratitude to my committee, including Assist. Prof. Dr. Chidchanok meejaisue, Assoc. Prof. Dr. Somsak Woramongkolchai, Assist. Prof. Dr. Patchanee Charoenying and Assist. Prof. Dr. Panpailin seeharaj for their insightful comments. I greatly appreciate all teachers who have instilled invaluable knowledge to me while studying at the Faculty of Science, King Mongkut's Institute of Technology Ladkrabang. I would like to express my sincere appreciation to KMITL Research Fund (Grant No. KREF 046108) for financial support. I also would like to thank KMITL research and innovation services' proofreaders, Mr. Pratana Kangsadal and Prof. John Morris, for proofreading and editing the English in this thesis. I wish to acknowledge the supports from all staff members of the Industrial Chemistry and Polymer Technology Workshop. Last but not the least, I would like to thank my family and friends for their precious supporting me spiritually throughout writing this thesis and my life in general. This thesis stands as a testament to your unconditional love and encouragement.

Naruenart Thessrimuang

Contents

page

Contents (continue)

page

Contents (continue)

page

List of tables

page

List of figures

Page

List of figures (continue)

Page

List of figures (continue)

Page

Chapter 1

Introduction

1.1 Research Motivation

Presently, environmental concerns about increasing use of plastics and associated waste are rising; therefore, alternative renewable sources for replacing petroleum-based materials are widely searched and developed. This is because petroleum-based plastic is very hazardous to the environment. Bio-based materials could be used as appropriate substitutes for petroleum-based plastics, especially if their various properties can match those of plastic-based materials. A biodegradable film is in much need in various industries. Among bio-based polymers, starch is one of the most interesting materials for producing biodegradable films due to its abundance, transparency, renewability and low cost [1].

There are several sources of starch in Thailand. For example, mung bean (*Vigna radiate*) is generally grown in Southeast Asian countries. Mung bean starch (MBS) consists of two types molecular constituents: linear amylose (40-45%) and branched amylopectin (55-60%) [2]. MBS has higher amylose content than other legume starches [3]. Biodegradable films with higher amylose content normally exhibited higher tensile strength, Young's modulus and glass transition temperature than low amylose content ones [4-5].

The source of starch that motivated us to conduct this study is Basil seed (*Ocimum basilicum L.*). It is a mucilaginous polysaccharide source grown in various regions in Asia [6]. Basil seed mucilage (BSM) has been reported to be an acidic polysaccharide: the uronic acid content of *Ocimum bacilicum L.* is 7.32% high. Basil seed contains a high quantity of mucilage that has a lot of useful functional groups for chemical synthesis and has a full potential as a source for producing green-based biodegradable films.

In its native form, common starch is not very suitable for many applications and, therefore, must be chemically modified to obtain desirable properties. Cross-linking is a good method for enhancing the suitability of starch in various applications. However, conventional chemical reagents used for cross-linking starch are relatively expensive and toxic [7]. Therefore, natural cross-linkers are preferable such as tartaric acid (TA), malic acid (MA) and succinic acid (SA). These are natural organic acids existing in fruits vegetables. They can also be obtained from a fermentation process by microorganisms.

Di-carboxylic acid cross-linkers can produce chemical bridges, i.e., covalent bonds, between hydroxyl functional groups of polysaccharides molecules.

There have been many reports of cross-linking starch films via carboxyl groups, typically for starch that has a moderate amount of amylose. It has been reported that the solubility and degree of swelling in water of MA and SA-modified corn starch films were lower than those of the native film [8]. Li Shen et al. used citric acid (CA), SA, MA and 1,2,3,4-butanetetracarboxylic acid to improve corn starch films. They found that the addition of the acids improved the tensile strain and permeability property of corn starch films by providing cross-linking that can connect starch backbone chains. In addition, they also observed starch chain hydrolysis [9]. Regarding hydrophilicity, cross-linked potato starch was found to have a lower hydrophilicity when it was modified by malonic acid, and its hydrophilicity was lower as the amount of modifying malonic acid increased [10]. It was also revealed that cross-linking by MA and CA improved the gelatinization temperature film. Moreover, water absorption of film decreased when the amount of modifying MA or CA increased [11].

Consequently, the aims of this study were to develop and characterize a number of biodegradable films from MBS and BSM and to investigate the effects of different di-carboxylic acid cross-linkers i.e. TA, MA and SA on the mechanical and thermal properties of the cross-linked films. These acids represented acid molecules with different kinds of steric hindrance of the OH groups in their molecular structures. Native and cross-linked films with TA, MA and SA were characterized by Fourier transform infrared spectroscopy (FT-IR), scanning electron microscopy (SEM), X-ray diffractometry (XRD) and thermogravimetric analysis (TGA). Furthermore, water vapor permeability (WVP), degree of swelling, water absorption and gel fraction of different films were also examined.

1.2 Aims of this thesis study

1. To prepare biodegradable films from MBS and BSM by using glycerol as plasticizer.

2. To use TA, MA and SA as a cross-linker in order to improve the properties of the biodegradable films.

1.3 Scope of the Research

1. TA, MA and SA were used to crosslink and hydrolyze the polysaccharide structure of MBS and BSM. Glycerol was used as a plasticizer.

2. Various properties of biodegradable film were characterized by Fourier-transform infrared spectroscopy (FTIR), X-ray diffractometry (XRD), scanning electron microscopy (SEM), determinations of gel fraction, degree of swelling, water vapor permeability (WVP) and some tensile and thermal properties as well as soil burial test.

3. Study the effect of steric hindrance of OH groups in chemical structures of di-carboxylic acids; i.e. TA, MA and SA on properties of MBS and BSM films.

1.4 Anticipated Benefits

1. A biodegradable cross-linked polysaccharide film with desirable chemical and mechanical properties is produced.

2. The structure of MBS and BSM related to its film forming and barrier properties is insighted.

3. Proper acid types and content for detection of cross-linkages in starch films are investigated.

4. Reduction of plastic waste is a good target.

5. Added values for MBS and BSM are increased.

Chapter 2
Theory and literature reviews

2.1 Biodegradable Polymers

Nowadays, there are important environmental concerns caused by the use of petroleum-based materials. Improvement of biopolymers from plant-based resources that can mitigate the undesirable effects of petroleum-based polymers in the environment has reduced the demand for synthetic petroleum-based polymers. The objective was that these waste pollution from petroleum-based plastic was reduced in a landfill or treated in composting plants. These technologies presented a novel methodology for the controlling of plastics-based polymer waste. Additionally, management system of polymer waste is incorporated with the use of renewable resources to produce the polymers primarily; it is prospective that biodegradation of polymers might basically convert part of a green-based cycle [12-13]. Thus, the biopolymer materials have attracted attention by many researchers. One important aspect of using plant-based biopolymers is that they should provide an equal strength and elasticity to the petroleum-based polymer for a particular application [12]. Synthetic biopolymers from green-based resources i.e. cellulose and starch can offer biodegradable materials from inexhaustible green resources. Starch, one of the most abundant natural-based resources for polymer products, is biodegradable and inexpensive. With some modification and processing, starch can be used as an ideal "green" material that originates from nature and readily goes back into it [13].

2.2 Definition and general mechanism of biodegradation

The term "Biodegradable plastics" generally refers to plastic that decomposes naturally by an attack of microorganisms in an environment. Microorganisms are incapable to penetrate into plastic-based material due to lack of water-solubility and the large size of molecules of polymer, where biochemical progressions take place. Firstly, they have to excrete extra-cellular enzymes, which depolymerize the polymers outside the cells as showed in Figure 2.1. Consequently, if the mass of plastics could be adequately decreased to create water-soluble intermediates, these can be fed into the appropriate metabolic pathways and transferred into microorganisms and act on the surface of polymer; subsequently, the biodegradation could occur on surface erosion process. Furthermore, the end products of these metabolic progressions involve CO_2, H_2O and CH_4, composed with new biomass. However, non-biotic physical and chemical processes can also act on the polymer, either as a first stage merely or in parallel on the polymer. These non-biotic effects involve thermal polymer degradation, chemical hydrolysis and polymer chain scission by irradiation (photo-degradation) or oxidation process.

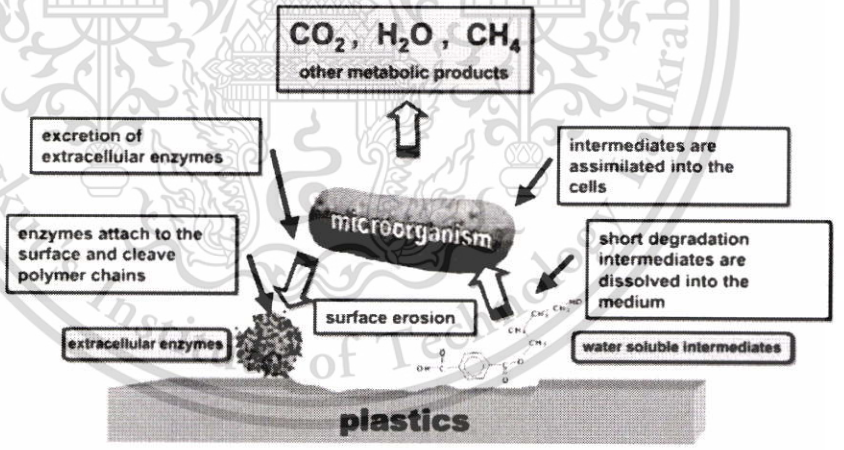

Figure 2.1

Mechanism of biodegradation of polymers [14]

Environmental factors not only influence the polymer to be degraded, but they also have a necessary effect on the microbial population and on the activity of the different microorganisms themselves. Parameters i.e. the presence or absence of oxygen, temperature, pH, salinity, humidity, and the supply of various nutrients are the key influences on the polymer degradation by microbial, and these surroundings might be considered when the biodegradation of polymers is examined [14].

2.3 Categorization of Biodegradable Polymers

Biodegradable plastics can be grouped into 4 main sessions [15-16]:

1. Polymers from chemical synthesis using renewable natural monomers or combined sources of petroleum and biomass, such as bio-polyester and poly-lactic acid (PLA).

2. Agro-polymers extracted from biomass (i.e., polynucleotides, polysaccharides, polypeptides, proteins). They are compostable and renewable polymers and could be processed directly, either fillers or plasticized or improved by chemical processes.

3. Polymers commonly obtained from the petroleum industry by chemical syntheses, such as poly-esteramide (PEA) and poly-caprolactone (PCL).

4. Polymers generated by genetically modified bacteria or by microorganisms during fermentation process used as the substrate. As examples, bacterial cellulose polyhydroxy alkanoates (PHA).

2.4 Introduction of Starch

2.4.1 Starch granules and molecular structure

Starch is the most plentiful reserve polysaccharide in plants. Nowadays, the main sources of starch extraction are roots, seeds and seeds primarily from potato, cassava, wheat, rice and maize. Starch can easily be extracted with high purity, resulting in a white, odorless powder and tasteless. Starch is also biodegradable and can demonstrate edible film behavior. In 2010, starch represented 22.2% of the global green-based packaging market (Pierce, 2011) [17]. Starch consists of two polymers amylose and amylopectin. Amylose is mainly a linear chain with α-1,4 linkages; whereas amylopectin is bonded by α-1,6 linkages. Amylopectin is the main component in starch, containing 40-50% [10]. The repeating units of amylose and amylopectin are similar (α-D-glucopyranose ring) but interconnected in different ways, as shown in Figure 2.2.

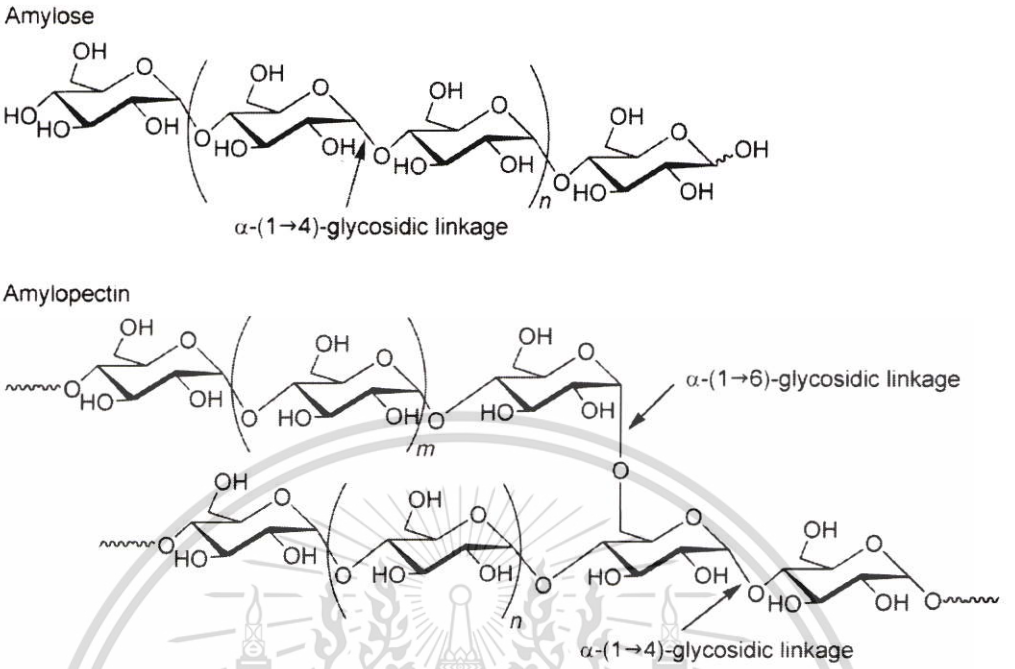

Figure 2.2 The structure of amylose and amylopectin [19]

In amylose, α-D-glucopyranose ring is connected by α(1,4) bond. Classically, the molecular weights of amylose are in the order of 10^5-10^6 g/mol. Amylose is generally well known as a linear molecule. The length of starch side chains ranges over 100 repeat units [19].

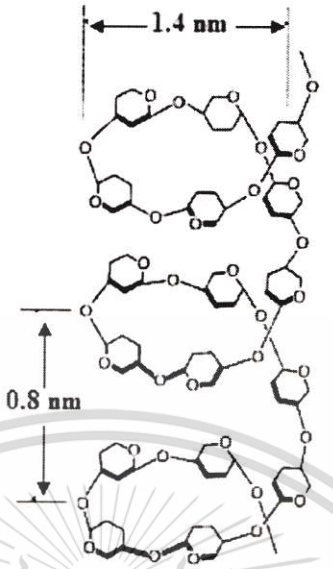

Figure 2.3 A single helix of amylose structure [20]

The structure of amylose leads to have a stiffer left-handed single helical structure or form a stiffer parallel double left-handed helix as shown in Figure 2.3. The single helix consists of six α-D-glucopyranose rings per cycle with a pitch of 0.8 nm [20].

Amylopectin is a branched molecule of starch. The α-D-glucopyranose ring is mostly linked by α (1,4) bonds and with α (1,6) bonds 5-6% at the point of the branch. It has molecular weight ranges 10^7—10^9 g/mol. The amylose content of several common starches is illustrated in Table 2.1 [21]. Starch is very hygroscopic and binds water reversibly but insoluble in cold water. Increasing the temperature, starch solution leads to decrease of hydrogen bonding in the starch granule hence the starch granules will start to gelatinize. Additionally, the starch granules would swell quickly to many times of its original volume. The linear amylose molecules of starch granules leach out of the granules into the solution resulting in suspension contained a mixture of swollen granules, linear amylose molecules, granule fragments which depend on the present of amount of water, then the granule of starch form a thick gel or paste. The gelatinization temperature of starch could be described as the temperature at which the granular swelling begins until the temperature when closely 100% of the granules are gelatinized [22]. The gelatinization temperature range of various starch sources is demonstrated in Table 2.1.

Table 2.1 Amylose content of common starches and starch gelatinization temperature range [21-22].

Starch	Amylose %	Gelatinization Temperature Range [°C]
Arrowroot	20.5	62-70
Corn	28	62-72
Oat	27	60.5-66
Manioc	15.7	61-67
Potato	20	59-68
Rice	18.5	65-72
Sago	25.8	62-68
Tapioca	16.7	58.8-70
Mung bean	35-40	63-74
Wheat	26	58-64

2.4.2 Structures of natural starch

As explained earlier, the linear amylose backbone chains lead to have helix structure either left-handed or right-handed. The left-handed form is energetically preferred to the right-handed form [23]. There are two ways the helical molecule (A-type and B-type) is packed in the crystalline phases of starch as illustrated in Figure 2.4. The helices of both A- and B-type crystals are packed parallel. Moreover, researchers also found Vh-type crystalline structure in starch complex formed between compounds and the single helix of amylose molecules, i.e.: dimethyl sulfoxide (DMSO), iodine, fatty acid and alcohol [24-25].

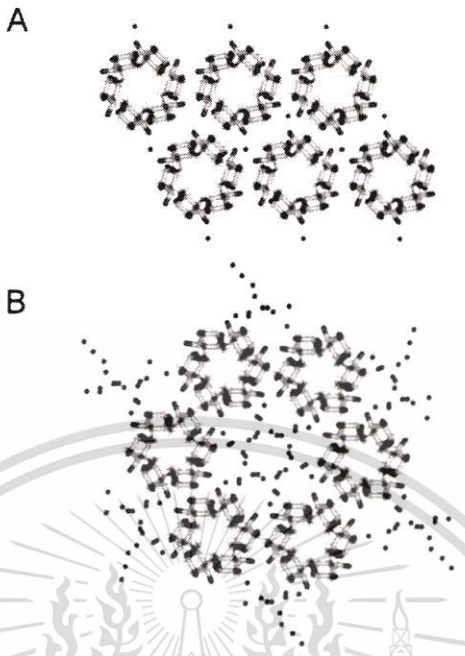

Figure 2.4 A-type and B-type of starch [20]

The stacks of amorphous and crystalline lamellae form larger rings or shells being in the order of 100~400 nm thick. The shells are semi-crystalline in nature as they contain both the crystalline lamellae and the amorphous, but they have also been considered as hard shells or crystalline. The rings are embedded in an amorphous matrix. The matrix was explained as soft shell, semi-crystalline shell or amorphous background. The granular rings, often-named "growth rings" as shown in Fig. 2.5, are normally thicker in their interior parts and thinner at the periphery of the granules. These shells contained both of semi-crystalline layers and amorphous [29].

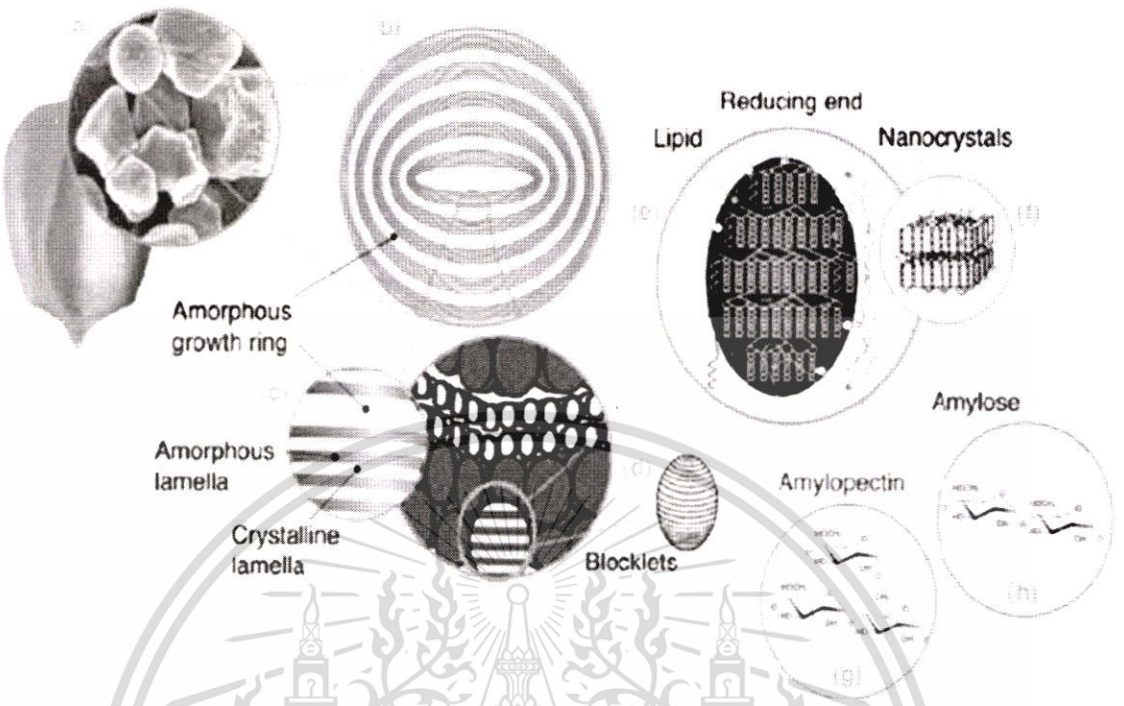

Figure 2.5 Granule structure of starch [28]

2.4.3 Gelatinization and glass transition temperature (T_g)

Gelatinization of starch was normally identified the destruction of the crystalline structure and eventually disruption of the granular of starch when water and heat were applied. Starch granules start to swell with the occurrence of excessive water (normally > 90 wt %) because the molecules of amylose were favorably solubilized in the water. Below a characteristic temperature identified as gelatinization temperature, the crystalline phase, generally combined of branched amylopectin structure and high molecular weight, still retains its integrity. Crystalline region starts to lose its crystalline order and swell irreversibly at above the gelatinization temperature [30]. When starch granules were considered as a polymer network, the swelling of the starch before the occurance of gelatinization can be considered as a reversible equilibrium. In this equilibrium, the affinity between the polymer network and the solvent generates osmotic pressure (favouring the swelling), which is equal to the restoring force (not favouring the swelling) resulting from the stiffness of polymer network. Obviously, enhancing the temperature or choosing the solvent that has a high affinity for starch will increasing swelling. Swelling above the gelatinization temperature is totally irreversible.

Since the degradation temperature was higher than T_g, therefore T_g of starch was experimentally unreachable. The water content has influenced on the T_g and

mechanical properties of starch. The addition of water can act as a strong plasticizing effect, resulting in notable depression in T_g [31]. The evaporation of water, the water content in starch is changed owing to the difficulty in keeping steady mechanical properties of the starch materials [32-33].

2.4.4 Retrogradation of starch

Retrogradation was another specific behavior of starch granules when reacting with molecules of water. If the mixture of gelatinized starch and water was cooled down to ambient temperature, there will be a strong driving force of starch chain rearrangement to crystallize. Then, water will generally be propelled out of the starch, resulting in phase separation. After cooling down, it was identified as retrogradation. In addition, there was different the thermodynamic force of crystallization between amylopectin and amylose due to their dissimilar conformations of molecular structure. A linear amylose structure has very long molecular chains as compared to branched amylopectin. Therefore, the amylose structure makes the formation of crystalline phase stronger than the amylopectin having abundant short linear molecular chains [34]. A very rapid phase separation observed when concentrated aqueous amylose solution was cooled down to room temperature. The transparent solution turns to opaque so fast, representing the presence of the polymer aggregates. The wavelength of the light was smaller than the size of the polymer aggregates. The size of the aggregates is larger than the wavelength of the light, making them visible [35-36].

2.4.5 Starch modifications

Native starch is not suitable as a packaging material because it cannot be shaped in films with sufficient mechanical properties (high tensile and flexural strength, percentage elongation) and is too sensitive to water. Subsequently, native starch must be modified, either by plasticization, blending with other materials, chemical modification, before native starch can be applied as biodegradable polymers [37].

The techniques for starch modification have been generally classified into 4 categories:

(1) Physical Modification i.e.; deep-freezing, osmotic-pressure treatment and heat-moisture treatment, etc.

(2) Chemical Modification involves cationization, esterification, etherification, cross-linking, oxidation and grafting, etc.

(3) Enzymatic modification includes the starch suspensions expose to enzymes primarily involving hydrolyzing enzymes that lead to high functional derivatives.

(4) Genetically modification includes the transgenic techniques targeting the various enzymes included in starch biogenesis [38].

Modified starch is combined into plastics to improve environmental degradation and fragmentation. Starch polymer composites and thermoplastic starch can substitute petroleum-based plastics in some applications. To overcome these limitations, the structure of starch can be improved through chemical and physical modifications, such as hydrolysis, oxidation and cross-linking process. Modified starch can be used for various applications. The alteration structure of starch is normally explained as 'chemical modification' due to the addition of chemicals. Chemical modifications include the improvement of a functional group of starch structure. The number and type of functional groups presented into the starch molecule depend on the required property in the end product. The terminal functionality depends on the starch source, the reaction conditions, the type and amount of its distribution and substituent along the molecule [39]. For example, the presentation of a hydroxypropyl group on starch molecules has been shown to improve its water solubility, swelling power, heat resistance and shear resistance. Disintegration of starch by introducing carbonyl groups and carboxyl via hydrolysis or oxidation is a common principle to make starch with lower viscosity. These functional groups can act as an internal plasticizer and can inhibit the affinity to retrograde [40].

2.4.6 Chemical Modification

Chemical modification includes the change of functional groups into the starch molecule, resulting in obviously improved physicochemical properties. The functional and chemical properties accomplished when improving starch by chemical substitution depend on starch source, reaction conditions, reactant concentration, extent of substitution (degree of substitution or molar substitution), reaction time, catalyst, pH, type of substituent and the distribution of the substituent in the starch molecule. These processes contain:

2.4.6.1 Etherification and Esterification

Etherification is the process of creating ether remarkably the elimination of alcohols forms petroleum products by rejoining with sulfuric acid. Esterification is described as any reaction (typically between an acid and an alcohol) that results in the production of ester formation. These methods mainly comprise substitution of hydrophilic -OH groups of starch structure by different hydrophobic functional groups resulting into succinylation, acetylation, carboxymethylation, hyproxypropylation and succinylation, etc [41].

2.4.6.2 Acid Treatment

The hydronium ion interacts the glycosidic oxygen molecules and subsequently, hydrolyzes the gloycosidic-linkage. Acid treatment improves the physicochemical properties of starch without destroying its granule structure. Firstly, acid interacts on the surface of the starch granule, and it increasingly penetrates the inner region. The breadths of the gelatinization endotherm and the gelatinization temperature have also been exhibited to increase on acid hydrolysis [41].

2.4.6.3 Oxidation

Oxidation of starch was created by changing starch structure with a required amount of oxidizing reagent under pH and controlled temperature. Oxidation initiates de-polymerization, which introduces carboxyl groups and carbonyl groups, results in a lower dispersion viscosity and, which hinders re-crystallization [41].

2.4.6.4 Cross-linking

Cross-linking of starch is proposed to form bonds between inter- and intra-molecular of polymer chains to strengthen the material structure. Cross-linking is produced by reaction with multifunctional reagents that are efficient of forming ether or ester bonds. The most generally used reagents such as ortho-phosphoric acid, phosphoryl chloride, epichlorohydrin and their salts, and di- or poly-carboxylic acids [42]. Cross-linking can be originated by chemical reaction via pH, heat, radiation or pressure. Covalent cross-linking is thermally and mechanically stable, *e.g.* starch films produced from cross-linked starch are more stable to soluble, swelling, shear, heat and acidic conditions. Additionally, cross-linking was shown to decrease the water-soluble of starch and to enhance barrier properties in starch-based coatings (Olsson *et al.*, 2013; Ghanbarzadeh *et al.*, 2011) [43-44].

2.4.7 Reactions of starch with di-carboxylic acid: esterification, cross-linking, plasticization and hydrolysis

Di-carboxylic acid is a natural organic acid with two carboxyl groups. Therefore, it can intra- and inter-connect with the –OH groups of starch to form ester linkages [45-46]. The reaction is a normal Fischer esterification reaction, which can be catalyzed by decreasing pH values or the adding Lewis acids. Cross-linking and di-esterification is a two-stage esterification process that has been demonstrated to be stimulated by high temperature approximately above 100 °C. It has been suggested that esterification of starch with di-carboxylic acid mainly substitute around the branching of amylopectin [47-48].

Mono-esterified starch can perform as an internal plasticizer of starch molecules by interrupting intra- and inter-molecular hydrogen bonds. However, unreacted cross-linker can act as an external plasticizer and enhance the flexibility of the starch structure in coatings and films (Reddy *et al.* 2010) [49]. Shuaiyang Wang *et al.* reported that di-esters could occur between two adjacent glucose residues, between two glucose chains in the same glucose residue on C3- and C6-position [50]. On the other hand, di-esters are considered to be cross-linkages due to increase in molecular weight. Cross-linking is required since it decreases solubility and swelling in water and rises viscosity.

Concurrent esterification of starch by di-carboxylic acid is hydrolysis. Although di-carboxylic acid is a weak acid, starch can simply be hydrolyzed owing to the low pH and high temperature. Increasing di-carboxylic acid content and high temperature promote degradation of starch backbone chain. The glycosidic oxygen is protonated during hydrolysis, and then, a water molecule is added. Therefore, molecular weight of starch backbone chain is reduced, which, in turn, increases permeability and diffusion in starch films. However, high temperature and low pH are both required, as revealed by Hirashima *et al.* (2005) [51]. Tests by those previous works with the addition of acids before and after gelatinization presented that no hydrolysis happened without sufficient temperature. To eliminate water, pre-drying at low temperature and then raising the temperature to introduce cross-linking can reduce excessive hydrolysis of starch molecules [52].

2.5 Mung bean starch (MBS)

Mung bean (*Vigna radiata (L.) R. Wilczek*) has been cultivated throughout Eastern and Southern Asia, Central Africa, China, South and North America and Australia, especially for its protein-rich grains. The advantages of crop's main are that, as a legume, that the growth has a short cycle (75-90 days), fits easily into crop rotations with cereals and needs little water. It grows well under most adverse semi-arid and arid conditions [53].

Mung bean is investigated as a good source of protein. Its different food products such as snacks and sweets foods have developed and became popular in the Indian subcontinent, whereas products like soups, cake and noodles evolved in oriental countries like Philippines, Iran as well as and Thailand. Technology and chemistry of mung bean has been presented previously by Engel *et al.* and Adsule *et al.*, who offered abundant information on the nutritional aspects, but only information on processing of mung bean is limited [54-55].

2.5.1 Chemical composition of MBS

The chemical compositions are randomly dispersed in the different parts of MBS. The major chemical constituents of mung bean dry matter are protein, fat, fiber, ash, carbohydrates, amino acids and fatty acids while micronutrients include vitamins and minerals. The average reported values of each chemical constituent are demonstrated in Table 2.2.

Table 2.2 Macronutrient compositions of MBS [56]

Compositions of MBS	Percentage by weight
Moisture	9.80
Crude protein	23.8
Crude lipid	1.22
Crude fiber	4.57
Ash	3.51
Carbohydrate	61
-Amylose	40
-Amylopectin	60

Nutritionally, mung bean appears to have good potential with lower fat content than soy bean, higher protein content than chickpea. The grain quality depends mainly on genetic factors, which is modified by agronomical performs.

2.6 Basil seed mucilage

Basil (*Ocimum basilicum L.*) is an associate of genus Ocimum. It is a popular, aromatic white-purple flowering herb grown in Iran and India [57]. The basil seed mucilage (BSM) extract contained two major fractions of glucomannan (43%), with the ratio of glucose to mannose 10:2, and (1,4)-linked xylan (24.29%) and a minor fraction of glucan (2.31%). Glucomannans are one of the important classes of plant-based polysaccharides, which containing COOH groups have a pKa value of 3.0. BSM polysaccharide is negatively charged due to the ionization of the carboxylic group [58-59]. BSM has a great potential to be applied as a thickening ingredient and stabilizing in food systems. Examination into rheological properties presented that BSM present a non-Newtonian pseudoplastic behavior [60]. Basil seed has shown to have reasonable amounts of mucilage with excellent functional properties, which is comparable with other commercial food hydrocolloids. Many researchers studies illustrated that BSM can produce films with reasonable mechanical properties and good appearance. Moreover, when compared with other polysaccharides, BSM has several important advantages, such as good rheological properties, low production cost, hydrophilic, biocompatible as well as biodegradable properties, which are features that enable it to have excellent producing biodegradable film-forming [61]. The average reported values of each chemical constituent are showed in Table 2.3.

Table 2.3 Chemical compositions of BSM [62]

Compositions of BSM	Percentage by weight
Moisture	3.91
Ash	4.18
Protein	2.90
Total sugar	88.39
Uronic acid	6.51
glucomannan	43
xylan	24.29
glucan	2.31
Carbohydrate	50
-Amylose	25
-Amylopectin	75
Molecular weight (KDa)	2320

2.7 Tartaric acid

Tartaric acid (TA) is an inherently appearing organic acid, TA with 2 hydroxyl and 2 carboxyl groups as shown in Figure 2.6. TA is the most water-soluble of the solid acidulants. It contributes a strong tart taste, which enhances fruit flavors, particularly grape and lime. This dibasic acid is produced from potassium acid tartrate, which has been recovered from various byproducts of the wine industry, including press cakes from fermented and partially fermented grape juice. The major European wine-producing countries, Spain, Germany, Italy, and France, use more of the acid than the USA.

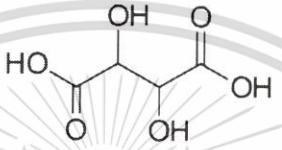

Figure 2.6 Structure of TA [8]

TA is often used as an acidulant in grape and lime-flavored beverages, gelatin desserts, jams, jellies, and hard sour confectionery. The acidic mono-potassium salt, more commonly known as 'cream of tartar,' is used in baking powders and leavening systems. Because it has limited solubility at lower temperatures, cream of tartar does not react with bicarbonate until the baking temperatures are reached; this ensures maximum development of volume in the finished product [48]. Material safety data, physical and chemical properties of TA are illustrated in Table 2.4 and Table 2.5, respectively.

Table 2.4 Material safety data of TA [63]

Information	Identification
Preferred IUPAC name	2,3-Dihydroxybutanedioic acid
Chemical name	Tartaric acid
Chemical Formula	$HOOC(CHOH)_2COOH$
RTECS	WW7875000
EC No.	201-766-0
Danger Hazard statements	 H318 causes serious eye damage
National Fire Protection Association (U.S.A.)	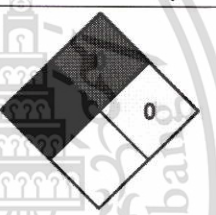 Health Hazard: 2 Flammability: 0 Reactivity: 0 Specific hazard: 0
CAS No.	87-69-4

Table 2.5 Physical and chemical properties [63]

Information	Identification
Physical state and appearance:	Solid (Crystalline solid)
Odor:	Odorless
Taste:	Acid
Molecular Weight:	150.09 g/mole
Color:	White
Melting Point:	168-172°C
Specific Gravity:	1.76
Acidity (pKa)	pKa_1 = 2.89, pKa_2 = 4.40
Dispersion Properties:	solubility in water, methanol, diethyl ether

2.8 Malic acid

Malic acid (MA) is an organic compound with the molecular formula $C_6H_6O_5$ as shown in Figure 2.7. MA is found as an obviously appearing organic compound in different fruits; it is a component of many foods. Presently, MA is most usually used as a preservative and food additive.

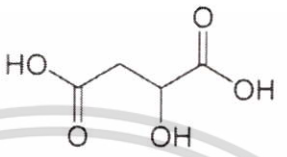

Figure 2.7 Structure of MA [8]

It is a relatively mild and innocuous when used in reasonable amounts. As a food supplement, it is normally observed beneficial for health and is exhibit in large amounts in apple juices. MA is most well-known for its high content in lychees, cherries, nectarines, bananas, peaches, tomatoes mangoes, strawberries and apple. MA is also used as a flavor enhancer for many candies and drinks because of its highly versatile nature; therefore, it has become an important part of nearly any food product [64]. Material safety data, physical and chemical properties of MA are shown in Table 2.6 and 2.7, respectively.

Table 2.6 Material safety data of MA [65]

Information	Identification
Preferred IUPAC name	2-Hydroxybutanedioic acid
Chemical name	Malic acid
Chemical Formula	$C_4H_6O_5$
RTECS	ON7175000
CAS No.	617-48-1
Danger Hazard statements	 H302 Harmful if swallowed
EC No.	230-022-8
National Fire Protection Association (U.S.A.)	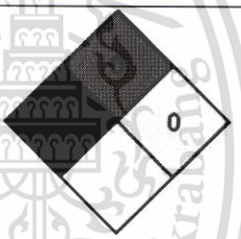 Health: 1 Flammability: 0 Reactivity: 0 Specific hazard: 0

Table 2.7 Physical and chemical properties [65]

Information	Identification
Physical state and appearance	Solid (Crystalline solid)
Odor	Odorless
Taste	Smoothly tart
Molecular Weight	134.09 $g \cdot mol^{-1}$
Color	White
Melting Point	127-132 °C
Density	1.609 $g\ cm^{-3}$
Acidity (pKa)	pKa_1 = 3.40, pKa_2 = 5.20
Solubility in water	558 g/L (at 20 °C)

2.9 Succinic Acid

Succinic acid (SA) is a natural di-carboxylic acid, which is colorless and odorless. Structure of SA is shown in Figure 2.8. SA is slightly soluble in acetone, ether, ethanol and glycerol and soluble in water. It that can be used in the food and beverage industries. SA may serve as a key building block for deriving various commodity chemicals including 1,4-butanediol, adipic acid, and tetrahydrofuran as well as biodegradable polymers such as polybutylene succinate and polybutylene succinate adipate. It is currently primarily produced from fossil fuels by a chemical synthetic process, which comes at a high environmental cost, particularly in the form of higher CO_2 emissions. As fossil fuel prices skyrocket and environmental awareness increases, biological processes for SA production may become both more economical and acceptable.

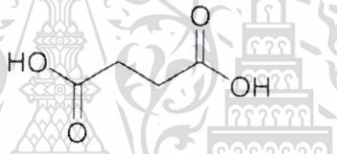

Figure 2.8 Structure of SA [66]

It is presently mostly produced from fossil fuels by a chemical process. However, biological processes for SA production may develop more reasonably competitive with increase in fossil fuel values. SA, an intermediate in tri-carboxylic acid cycle, is excreted as an end-product during anaerobic fermentation by some anaerobic and facultative anaerobic organisms [66]. Material safety data, physical and chemical properties of SA are shown in Table 2.8 and 2.9, respectively.

Table 2.8 Material safety data of SA [67]

Information	Identification
Preferred IUPAC name	Butanedioic acid
Chemical name	Succinic acid
Chemical Formula	$C_4H_6O_4$
EC No.	203-740-4
CAS No.	110-15-6
Danger Hazard statements	 H318: Causes serious eye damage.
RTECS	WM4900000
National Fire Protection Association (U.S.A.)	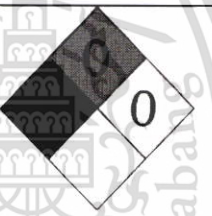 Health: 2 Flammability: 0 Reactivity: 0 Specific hazard: 0

Table 2.9 Physical and chemical properties [67]

Information	Identification
Physical state and appearance	Solid (Crystalline solid)
Odor	Odorless
Taste	Smoothly tart
Molecular Weight	118.09 $g \cdot mol^{-1}$
Color	White
Melting Point	184 °C
Density	1.56 g/cm^3
Acidity (pKa)	pKa_1 = 4.2, pKa_2 = 5.60
Solubility in water	58 g/L (20 °C) or 100 mg/mL

2.10 Plasticizer

A plasticizer is an important component affective the physicochemical properties of the films. Generally, to overcome brittleness caused by extensive intermolecular forces in the film; plasticizers are added, to allow the film to be easily moved from its forming support. Addition of plasticizer results in decrease in inter-molecular forces along the backbone chain of polymer, which subsequently enhances extensibility, flexibility, tear resistance and toughness of the film. Since plasticizer decreases inter-molecular forces, efficiently dilutes and softens structure of the film and increases the intermolecular spacing and chain mobility [68].

2.10.1 Glycerol

Glycerol (1,2,3-propanetriol) (Figure 2.9) is an odorless, colorless, viscous liquid and a sweet taste, derived from both petrochemical and natural feedstocks. The name of glycerol is derived from the Greek word for ''sweet,'' glykys, and the terms glycerine, glycerin and glycerol tend to be used interchangeably in the literature. Nevertheless, the terms of glycerine or glycerin commonly refers to a commercial solution of glycerol in water of which the main component is glycerol. Crude glycerol is 70–80% pure. Therefore, crude glycerol is often purified prior to commercial sale to 95.5–99% purity.

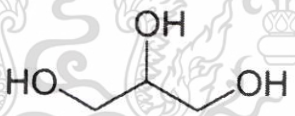

Figure 2.9 Structure of glycerol [69]

Glycerol is one of the most valuable and versatile and chemical substances. It is absolutely soluble in alcohols and water, is slightly soluble in many collective solvents such as dioxane and ether, but is insoluble in hydrocarbons. Glycerol has a specific gravity of 1.261 g mL^{-1}, a melting point of 18.2 °C and a boiling point of 290 °C under normal pressure, accompanied by decomposition. At low temperatures, glycerol may form crystals, which melt at 17.9 °C [69].

Physical and chemical properties of glycerol are shown in Table 2.10, which are applied in many thousands of commercial products. Actually, glycerol has over 1500 known end uses, involving applications as a processing aid ingredient or in cosmetics, foodstuffs, pharmaceutical formulations and personal care products. Additionally, glycerol is compatible with many other chemical materials, extremely stable under natural storage conditions, has no negative environmental effects and practically non-irritating in its various uses. Glycerol includes three hydrophilic hydroxyl groups, which are sensible for water and its hygroscopic nature. Glycerol has a highly flexible molecule forming both intra- and inter-molecular hydrogen bonds [69].

Table 2.10 Physicochemical properties of glycerol [69]

Information	Identification
Chemical formula	$C_3H_5(OH)_3$
Molecular weight	92.09 g mol^{-1}
Density	1.261 g cm^{-3}
Viscosity	1.5 Pa.s
Melting point	18.2 °C
Boiling point	290 °C
Flash point	160 °C
Surface tension	64.00 mNm^{-1}

2.10.2 Traditional Commercial Applications

Traditional commercial applications of glycerol, either as a raw material or as an additive, range from its use as a tobacco, food and drugs additive to the synthesis of alkyd resins, trinitroglycerine and polyurethanes. Presently, the amount of glycerol that reaches into technical applications is around 160000 tonnes and is expected to rise at an annual rate of 2.8% [69]. Chemical safety data of glycerol is shown in Table 2.11.

Table 2.11 Chemical safety data of glycerol [70]

Information	Identification
Preferred IUPAC name	Propane-1,2,3-Triol
Product Name	Glycerol
CAS No.	4740-78-7 and 5464-28-8
RTECS	JH8390000
NFPA	 NFPA Rating Health: 2 Flammability: 1 Reactivity: 0

2.11 Literature review

S. Sun *et al.* (2018) investigated the effects of different cross-linkers on the physicochemical properties of hydroxypropyl di-starch poly-hydroxy-alkanoate (PHA) composite films prepared by extrusion blowing. Four cross-linkers with multi-carboxyl or multi-hydroxyl structure—CA, adipic acid, boric acid and borax—were used. SEM images of the films crosslinked by CA, adipic acid, and borax showed that the films were more continuous and homogeneous than the film cross-linked with boric acid. The starch/PHA film cross-linked by boric acid showed a rough and discontinuous surface. Furthermore, the addition of cross-linkers to starch/ PHA blends significantly enhanced the tensile strength and elongation of the resulting films compared to the native film because of the stronger intermolecular interactions of between the cross-linkers, starch and PHA. The film cross-linked with boric acid exhibited the highest tensile strength, while the CA cross-linked film exhibited the highest elongation at break. Additionally, the result from thermogravimetric analysis (TGA) implied that thermal stability of the cross-linked films was greater than that of the native film [71].

L. Ren *et al.* (2017) examined the effects of cross-linking modification of starch nanocrystals (SNCs) with sodium hexametaphosphate (SHMP) and glutaraldehyde (GA) from waxy corn starch on the mechanical properties, degree of swelling and WVP of the resulting reinforced thermoplastic starch (TPS) nanocomposites. The data indicated that the degree of swelling decreased markedly after cross-linking, suggesting that the cross-linked modifications of SNCs did occur. Tensile strength and elongation at break for the TPS films reinforced with cross-linked SNCs were significantly increased as compared to the native TPS films. Cross-linking modifications changed the surface nature of SNCs and enhanced the dispersion of SNCs in water. Moreover, the WVP of cross-linked SNCs reinforced TPS films was lower than that of the native SNCs reinforced film. When SNCs was cross-linked with either SHMP or GA, some of the hydrophilic hydroxyl groups on the SNCs surface were substituted by more hydrophobic C=O groups, resulting in decreased WVP values [72].

H. Kim *et al.* (2017) cross-linked and heat-treated amorphous granular potato starch (AGPS). It was observed that the obtained cross-linked amorphous granular potato starch (CLAGPS) swelled to the same degree at all tested temperatures, implying that the cross-links between starch molecules successfully restricted its swelling. It was found that CLAGPS was apparently more viscous than AGPS, i.e., its resistance against a rapidly rotating spindle was increased, also implying a successful degree of cross-linking [73].

W. N. Gilfillan *et al.* (2016) examined the effectiveness of using aconitic acid (AA) as a cross-linking agent to improve the properties of starch-based films. Starch films were prepared with 0, 2, 5, 10 and 15 wt% AA (dry weight basis of starch). They presented that AA acted both as a cross-linking agent and a strong plasticizing agent. Five wt% AA starch films were the most effectively cross-linked and showed the lowest solubility (28 wt%) and reduced swelling capacity (three times lower than the native starch film). Elongation at break value for the film modified with 15 wt% AA also significant increased by approximately 35 times compared to that of the native starch film due to the plasticizing effect of AA. Furthermore, tensile strength was decreased: the film softened with an increasing content of AA. Thermal stability was improved for 0 to 15 wt% AA cross-linked films to approximately 350 to 370 °C [74].

C. Menzel *et al.* (2014) studied the effect of CA cross-linking on potato starch film. The results showed that the water solubility of the cross-linked films reduced with increasing CA content because the esterification chemically interconnected the starch network. Films cross-linked with 30wt% CA showed the highest gel content. The resistance to dissolution under these conditions might be due to high cross-linking density [75].

H. Li *et al.* (2013) studied the properties of unmodified and cross-linked chitosan/starch composite films with a glutaraldehyde cross-linking agent. SEM images of the composite films with different contents of glutaraldehyde showed that the surfaces were smooth, however the surface roughness increased with increasing glutaraldehyde content. Increasing content of glutaraldehyde brought about reduction in tensile strength. Using glutaraldehyde as a cross-linking agent caused brittleness, low compatibility and phase separation. In addition, the degree of swelling significantly decreased after cross-linking. Cross-linking caused the films to be more insoluble in water because of the ester linkages between the chitosan and starch molecules [76].

G. J. He *et al.* (2012) studied cross-linking potato starch films irradiated by UV in the presence of sodium benzoate as a photo-sensitizer (PHS). The cross-linking reaction was initiated by UV irradiation. The PHS content in the starch films was varied in the range of 0.2–1.0% (on dry starch basis). The native starch films were completely soluble when immersed in DMSO. The cross-linked potato starch films were formed as a three-dimensional network that limited its expansion. The water contact angle of the cross-linked potato starch film was found to increase, indicating that the cross-linking promoted the hydrophobic property. Starch films prepared with high PHS content (1.0% PHS) presented a slightly enhanced water contact angle compared with that of starch films with 0.2% PHS content because more radicals occurred with 1.0% PHS when exposed to UV irradiation and so denser networks were formed [77].

J.B. Olivato *et al.* (2012) studied the influence of CA, MA and TA on cassava starch/poly (butylene adipate co-terephthalate) blown films. A greater content of TA or CA (1.5wt%) resulted in a film with an enhanced elongation, decreased water vapor permeability and more homogeneous structure. A high content of CA or TA increased the film's tensile strength and reduced its elongation. This was a result of cross-linking where linkages between the backbones starch chains and the cross-linker restricted their mobility, in good agreement with the WVP results. Both CA and TA in combination with a hydrolysis agent acted as a better cross-linker than MA, producing a smoother and more uniform film that could be ascribed to proper esterification of the starch film [47].

T. G. Dastidar *et al.* (2012) studied the effects of cross-linking on the properties of cassava starch and potato starch. Native cassava starch and potato starch were chemically modified by cross-linking with malonic acid (MLA), and the effects of the chemical modification on their thermal and mechanical properties and swelling capacity under an aqueous condition were investigated as a function of the degree of cross-linking. It was found that the cross-linking decreased the solubility and swelling capacity of the starch, and the swelling capacity was precisely correlated with the degree of substitution. The swelling capacity decreased as the content of MLA increased because of higher degree of substitution as well as higher cross-linking density. WXRD patterns showed that the crystal structures of CS and PS as well as MLA were totally destroyed after gelatinization and the cross-linking process. After the curing step, Young's modulus of the cross-linked film was significantly increased, which could be ascribed to higher degree of cross-linking of PS after being cured. The degrees of cross-linking and esterification also increased with an increasing content of MLA [10].

N. Reddy *et al.* (2010) studied the effect of CA using as a cross-linker on corn starch-based film. CA interconnects backbone starch chains by forming an ester linkage. In their study, after the starch chains were cross-linked, their thermal stability and tensile strength of the resulting starch film enhanced while its solubility in water reduced. In addition, the cross-linked starch film exhibited higher strength than the native starch film. When soaked in formic acid, the film cross-linked with 5% citric acid lost 35% of its weight while the native starch film dissolved completely in 5 h at 50 °C. The cross-linked film had a slightly decreased water vapor permeability compared to the native film because its dense structure formed after cross-linking limited its swelling and molecular movement, leading to a decrease in water vapor permeability [7].

X. Ma *et al.* (2009) studied the effects of CA cross-linker on the thermal stability, mechanical properties and water vapor permeability of the film formed from pea starch and rice starch granules. They reported that substitution of CA with hydroxyl functional groups on starch chains could form a cross-linked starch. CA cross-linked pea starch (CAPS) and citric acid cross-linked rice starch (CARS) exhibited lower thermal stability than native starch. Moreover, the higher the CAPS or CARS content was, the greater the tensile strength of the thermoplastic starch (TPS) matrix. In addition, the storage modulus of the CAPS/TPS or CARS/ TPS composite was higher than that of native TPS. CAPS or CARS enhanced the intermolecular interaction of TPS. It was also observed that the water vapor permeability (WVP) value was noticeably decreased as CAPS or CARS content increased because their hydrophilic OH groups were substituted with hydrophobic ester groups [1].

S. Yoon *et al.* (2005) studied tensile strength, elongation at break and degree of swelling as well as solubility in water of the synthesized corn starch/PVA blend films prepared by using glycerol as a plasticizer and SA, MA and TA as cross-linkers. Elongation at break of the cross-linked films increased as the content of the cross-linkers increased. On the other hand, tensile strength of the cross-linked films decreased as the cross-linkers content increased due to hydrolysis of starch chains. The degree of swelling and solubility of the cross-linked starch/PVA blended films decreased rapidly with an increasing cross-linker content as a result of esterification between starch and PVA. The degree of swelling and solubility values of the MA and TA cross-linked films were higher than those of the SA cross-linked films because MA and TA are highly hydrophilic due to more hydroxyl groups in their molecular structure than in that of SA [8].

Chapter 3
Research methodology

3.1 Chemicals

1. Mung bean starch (MBS) (Food grade, Tongjan Co., Ltd.)

Table 3.1 chemical compositions of MBS [56]

Composition of MBS	Percentage by weight
Moisture	9.80
Crude protein	23.8
Crude lipid	1.22
Crude fiber	4.57
Ash	3.51
Carbohydrate	61
-Amylose	40
-Amylopectin	60

2. Basil seed mucilage (BSM) (Food grade, Raithip Co., Ltd.)

Table 3.2 Chemical composition of BSM [57]

Composition of BSM	Percentage by weight
Moisture	40
Protein	15.5-17.87
Lipid	18.3-19.60
Fiber	80
Ash	4.4-6.8
Carbohydrate -Amylose -Amylopectin	50 25 75

3. Tartaric acid (TA) (Food grade, Union Chemical Co., Ltd.)

Table 3.3 Information of TA

Information	Identification
Molecular weight	150.087 g/mol
Acidity (pKa)	pKa_1 = 2.89, pKa_2 = 4.40
Melting point	171-174 °C
Density	1.79 g/mL
Solubility in water	1.33 kg/L
Appearance	White power

4. Malic acid (MA) (Food grade, Union Chemical Co., Ltd.)

Table 3.4 Information of MA

Information	Identification
Molecular weight	134.09 g/mol
Acidity (pKa)	pKa_1 = 3.40, pKa_2 = 5.20
Melting point	175 °C
Density	1.609 g cm^{-3}
Solubility in water	558 g/L (at 20 °C)
Appearance	White powder

5. Succinic acid (SA) (Food grade, Union Chemical Co., Ltd.)

Table 3.5 Information of SA

Information	Identification
Molecular weight	118.09 g/mol
Acidity (pKa)	pKa_1 = 4.2, pKa_2 = 5.60
Melting point	184 °C
Density	1.56 g/cm^{-3}
Solubility in water	58 g/L (20 °C)
Appearance	White powder

7. Glycerol (Lab system, Co., Ltd.)
8. Dimethyl sulfoxide (DMSO) (AR grade, Co., Ltd.)
9. Distilled water (AR grade, Lab system, Co., Ltd.)

3.2 Equipment

1. Stirring rod
2. Magnetic bar
3. Beakers
4. Polypropylene tray (size 19.4x28 cm)
5. Thermometer
6. Hot air oven (MEMMERT, ULM 600/l, Germany)
7. Hotplate stirrer (IKA, C-MAG HS7, Germany)
8. Digital balance 4 digits (ITS, Thailand)
9. Digital balance 2 digits (ITS, Thailand)
10. Wire gauze
11. Fourier transforms infrared spectrometer (FT-IR) [Spectrum 200 GX spectrometer] [Perkin Elmer, USA]
12. Scanning Electron Microscopy (SEM) [LEO 1450 VP] [FEI, Quanta 250, USA]
13. X-ray Diffractometer (XRD) [D8 Advance] [Bruker, Madison, USA]
14. Universal testing Machine [LLYOD Instrument, LR5k, USA]
15. Thermogravimetric analyzer (TGA) [Perkin Elmer, Pyris 1, Massachusetts, USA]

Table 3.6 Flowchart of thesis research

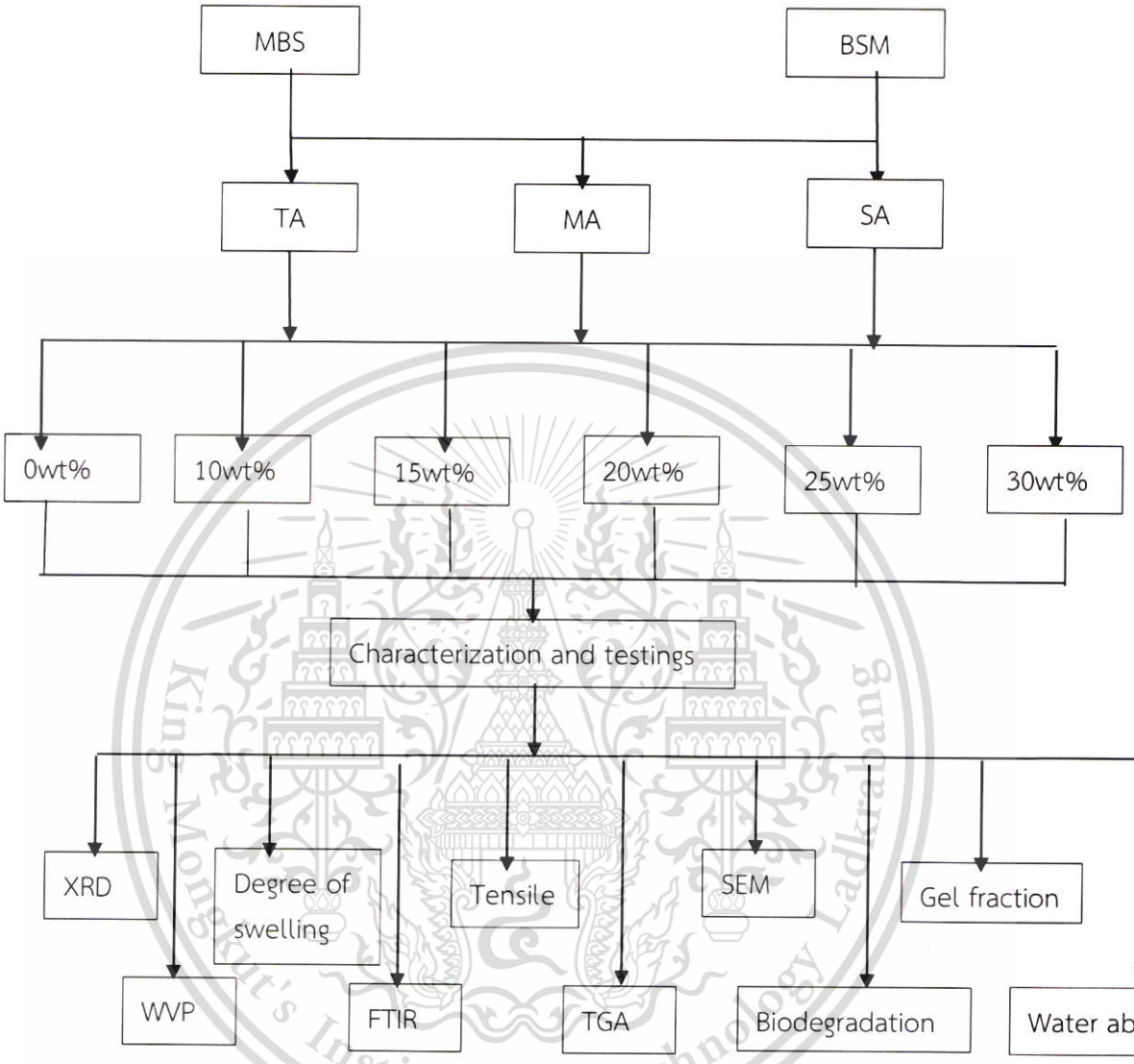

3.3 Procedures

3.3.1 Preparation of MBS films

1. Firstly, starch was gelatinized by mixing 7 g of starch with 70 ml water and the mixture was heated at 65 °C for 45 min with constant stirring.

2. For crosslinking the starch, different types and content of cross-linkers, i.e., 10, 15, 20, 25 and 30% w/w of TA, MA or SA (based on the initial dry weight of starch) were individually added to the pre-gelatinized starch (Table 3.8).

3. The solution was stirred constantly for 45 min at 60 °C with a magnetic stirrer.

4. After that, the mixture of starch was cast to form thin films of about 0.2 mm thickness on a polypropylene plate (PP).

5. The films were dried in an oven for 24 h at the temperature of 40 °C.

6. The starch films were further cured in a hot air oven at 150 °C for 10 min in order to complete the crosslinking process.

7. The cross-linked films were then thoroughly washed in water to remove leftover cross-linkers, i.e., they were completely soaked in distilled water for 8–10 h, which was changed twice. It was expected that the leftover cross-linkers molecules, which were highly soluble in water would leach out into water completely.

8. The washed films were air-dried in an oven at 40 °C for 24 hours and stored at 25°C and 60±2% relative humidity for 24 h before further characterization.

9. The dried films were peeled off the PP plates and stored in sealed polyethylene bags.

Table 3.7 Different types and acids contents of biodegradable MBS films.

Contents					
Starch	Water	Glycerol	Acids (%w/w of dry starch)		
MBS (g)	(g)	(%w/w)	TA (%w/w)	MA (%w/w)	SA (%w/w)
7	70	30	0	0	0
7	70	30	10	0	0
7	70	30	15	0	0
7	70	30	20	0	0
7	70	30	25	0	0
7	70	30	30	0	0
7	70	30	0	10	0
7	70	30	0	15	0
7	70	30	0	20	0
7	70	30	0	25	0
7	70	30	0	30	0
7	70	30	0	0	10
7	70	30	0	0	15
7	70	30	0	0	20
7	70	30	0	0	25
7	70	30	0	0	30

3.3.2 Preparation of BSM film

3.3.2.1 Preparation of BSM

1. For the extraction of BSM, 50 g of basil seeds was immersed in 2.5 l of distilled water and left to be swollen at the room temperature for 2 h.

2. After that, the swollen basil seeds were stirred with a rod paddle blender (IKA, Germany) at 1500 rpm for 1 min to scrub the mucilage layer off the basil seed surface.

3. The mucilage separated from the basil seeds still had some seed fragments, so it was passed through cheesecloth to remove the residue.

4. Mucilage was separately prepared for each experiment to ensure its freshness.

3.3.2.2 Preparation of BSM film

1. To prepare a film-forming solution, 70 g of BSM was heated in a beaker at 65 °C for 45 min under constant stirring at 450 rpm.

2. TA, MA and SA were used as cross-linkers at 10, 15, 20, 25 and 30% w/w (based on BSM weight). Each cross-linker with different contents was added to BSM solution.

3. The solution was stirred constantly for 45 min at 60 °C with a magnetic stirrer to form a homogeneous gel.

4. The BSM was then cast onto a PP plate and the film was dried in a hot air convection oven at 40 °C for 24 hours.

7. BSM film was further heated and cured in a hot air oven at 150 °C for 10 min in order to complete the crosslinking process.

8. The cross-linked films were then thoroughly washed in water to remove leftover cross-linkers, i.e., they were completely soaked in distilled water for 8–10 h, which was changed twice. It was expected that the leftover cross-linkers molecules, which were highly soluble in water would leach out into the water completely.

9. The washed films were air-dried in an oven at 40 °C for 24 hours and stored at 25°C and 60±2% (with a solution of saturated magnesium nitrate) relative humidity for 24 h before further characterization.

Table 3.9 Different types and acids contents of biodegradable BSM films.

Contents				
Type of polysaccharide	Glycerol (%w/w)	Acids (%w/w of BSM)		
BSM (g)		TA (%w/w)	MA (%w/w)	SA (%w/w)
70	30	0	0	0
70	30	10	0	0
70	30	15	0	0
70	30	20	0	0
70	30	25	0	0
70	30	30	0	0
70	30	0	10	0
70	30	0	15	0
70	30	0	20	0
70	30	0	25	0
70	30	0	30	0
70	30	0	0	10
70	30	0	0	15
70	30	0	0	20
70	30	0	0	25
70	30	0	0	30

3.4 Characterization

3.4.1 FTIR Spectroscopic

A sample was characterized by FTIR in transmission mode with a Spectrum 2000 GX spectrometer (Perkin Elmer, USA) and KBr disk technique. Absorption spectra were collected in the range of 4000 to 400 cm^{-1}. Twenty scans were taken at a resolution of 6 cm^{-1} and corrected against the background spectrum.

3.4.2 Swelling power

The swelling power of the native and cross-linked starch films in DMSO were determined by a modified method of Zhu *et al* [78]. Accurately weighed starch film was immersed in 25 mL DMSO at room temperature for 24 h. Then, the swollen film was washed with water and weighed (W_2).

The swelling ability was calculated as follows:

$$\text{Swelling power} = \frac{W_2 - W_1}{W_1} \times 100, \qquad (1)$$

where W_1 was the original weight of the sample, and W_2 was the weight of the film after it was immersed in DMSO for 24 hours.

3.4.3 Gel fraction

To determine gel fraction, 0.2 g of a film was soaked in 25 mL DMSO and stirred for 24 h at 25 °C. After that, the calculation of gel fraction of the insoluble part of the film was done after the film was washed thoroughly with water and dried at 80 °C and weighed (m_g) according to Eq. 2 below,

$$\text{Gel fraction} = \frac{M_g - M_b}{M_b} \times 100, \qquad (2)$$

where M_b was the dry weight of the film, and M_g was the weight of the film after it was immersed in DMSO for 24 h.

3.4.4 Water vapor permeability (WVP)

The WVP of a film was determined by an ASTM method E96. Semi-spherical test cups or permeation cells containing a dry desiccant (0% RH) were sealed with a film (the effective area of the film was 0.0036 m^2). The cups were then stored in a desiccator maintained at 75% RH with a saturated solution of sodium chloride. Water-vapor transport was determined from the weight gain. Changes in the weight of the permeation cells were recorded to the nearest 0.0001 g and plotted as a function of time. The values of water vapor permeability were calculated according to Eq. 3 below,

$$WVP = \frac{W \times X}{t \times A \times \Delta P} \quad (3)$$

where W/t was the slope of system weight gain vs. time (g/day); x was the film thickness (mm); A was the area of the exposed surface of the film (32.15 cm^2); and ΔP was the vapor pressure difference in mm Hg (1.333 $\times$ 10^2 Pa).

3.4.5 Water absorption

A sample was dried at 105 °C for 2 h and then kept at 75% RH (maintained by using a saturated solution of NaCl in a closed vessel) at a temperature of 25±2 °C prior to the determination. The amounts of water absorbed by a sample was determined as percentage of water absorption according to Eq. 4,

$$\text{Water absorption} = \frac{W_2 - W_1}{W_1} \times 100, \quad (4)$$

where W_2 and W_1 were the wet and dried weights of the sample, respectively.

3.4.6 Scanning Electron Microscopy (SEM)

Morphology of a film was determined using scanning electron microscope (FEI, Quanta 250, USA). Each sample was immersed into liquid nitrogen before being fractured then vacuum coated with a thin layer of gold to prevent accumulation of electrical charges.

3.4.7 X-ray diffractometry (XRD)

Wide-angle X-ray diffractograms of the starch films were taken by exposing a film sample (cut into approximately 30 mm × 30 mm rectangular pieces) to the X-ray beam. A specimen was tightly packed into the sample holder. X-ray diffraction pattern was recorded in the reflection mode and an angular range (2θ) of 5-60° at ambient temperature with a D8 Advance X-ray diffractometer (Bruker, Madison, U.S.A) operated at 40 kV and 35 mA with CuKα wavelength of 1.542 Å and radiation from the anode. The diffractometer was equipped with a 1° divergence slit, a 16 mm beam bask, a 0.2 mm receiving slit and a 1° scatter slit. The degree of bulk film crystallinity (Xc) was determined by the method described by Dai *et al.* [79],

$$X_c = \frac{A_c}{A_c + A_a} \times 100 \qquad (5)$$

where Ac refers to the sum of the crystallized peak areas above the amorphous area, and Aa refers to the amorphous area in the X-ray diffractogram.

3.4.8 Mechanical properties

Mechanical tests of the films were conducted according to ASTM D-638 at the temperature of 23±1 °C and relative humidity of 60±5%. The films were cut into rectangular pieces of 100mm × 15mm with a thickness of approximately 0.20 mm. They were, then, conditioned at 60% RH and a temperature of 25°C for 24 h before testing. The mechanical properties of the films were characterized by using a Lloyd LRX universal testing machine (UTM). Ten films were characterized to obtain the average values of stress at maximum load, Young's modulus and strain at maximum load.

3.4.9 TGA

Thermogravimetric (TGA) and derivative thermal gravimetric (DTG) analyses of a film was carried out by using thermogravimetric analyzer (Perkin Elmer, Pyris 1, Massachusetts, USA). A film was scanned from 50 °C to 700 °C at a rate of 10 °C/min in nitrogen atmosphere.

3.4.10 Biodegradability

A film with a dimension of 100 mm x 10 mm was buried under 10 cm of the soil at 10-15% moisture level in pots in a laboratory. The test was carried out over periods of 5 and 10 days. Then, the soil-buried samples were collected from the pots, gently cleaned by brushing and tested for its mechanical properties.

Chapter 4
Results and discussion

The molecular changes in polysaccharide of biodegradable films cross-linked and cured with different acids—TA, MA and SA—at different levels—10%, 15%, 20%, 25% and 30% were investigated. Related water permeability, thermal, mechanical, chemical and other physical properties of the films are explained according to the structural changes in the polysaccharide molecules.

Table 4.1 Abbreviations and symbols

No.	Abbreviations	Means
1	MBS	Mung bean starch film cross-linked with 0% acid
2	MBS10TA	Mung bean starch film cross-linked with 10% tartaric acid
3	MBS15TA	Mung bean starch film cross-linked with 15% tartaric acid
4	MBS20TA	Mung bean starch film cross-linked with 20% tartaric acid
5	MBS25TA	Mung bean starch film cross-linked with 25% tartaric acid
6	MBS30TA	Mung bean starch film cross-linked with 30% tartaric acid
7	MBS10MA	Mung bean starch film cross-linked with 10% malic acid
8	MBS15MA	Mung bean starch film cross-linked with 15% malic acid
9	MBS20MA	Mung bean starch film cross-linked with 20% malic acid
10	MBS25MA	Mung bean starch film cross-linked with 25% malic acid
11	MBS30MA	Mung bean starch film cross-linked with 30% malic acid
12	MBS10SA	Mung bean starch film cross-linked with 10% succinic acid
13	MBS15SA	Mung bean starch film cross-linked with 15% succinic acid
14	MBS20SA	Mung bean starch film cross-linked with 20% succinic acid
15	MBS25SA	Mung bean starch film cross-linked with 25% succinic acid
16	MBS30SA	Mung bean starch film cross-linked with 30% succinic acid
17	BSM	Basil seed mucilage film cross-linked with 0% acid
18	BSM10%TA	Basil seed mucilage film cross-linked with 10% tartaric acid
19	BSM15%TA	Basil seed mucilage film cross-linked with 15% tartaric acid
20	BSM20%TA	Basil seed mucilage film cross-linked with 20% tartaric acid

Table 4.1 Abbreviations and symbols (continue)

No.	Abbreviations	Means
21	BSM25%TA	Basil seed mucilage film cross-linked with 25% tartaric acid
22	BSM30%TA	Basil seed mucilage film cross-linked with 30% tartaric acid
23	BSM10%MA	Basil seed mucilage film cross-linked with 10% malic acid
24	BSM15%MA	Basil seed mucilage film cross-linked with 15% malic acid
25	BSM20%MA	Basil seed mucilage film cross-linked with 20% malic acid
26	BSM25%MA	Basil seed mucilage film cross-linked with 25% malic acid
27	BSM30%MA	Basil seed mucilage film cross-linked with 30% malic acid
28	BSM10%SA	Basil seed mucilage film cross-linked with 10% succinic acid
29	BSM15%SA	Basil seed mucilage film cross-linked with 15% succinic acid
30	BSM20%SA	Basil seed mucilage film cross-linked with 20% succinic acid
31	BSM25%SA	Basil seed mucilage film cross-linked with 25% succinic acid
32	BSM30%SA	Basil seed mucilage film cross-linked with 30% succinic acid

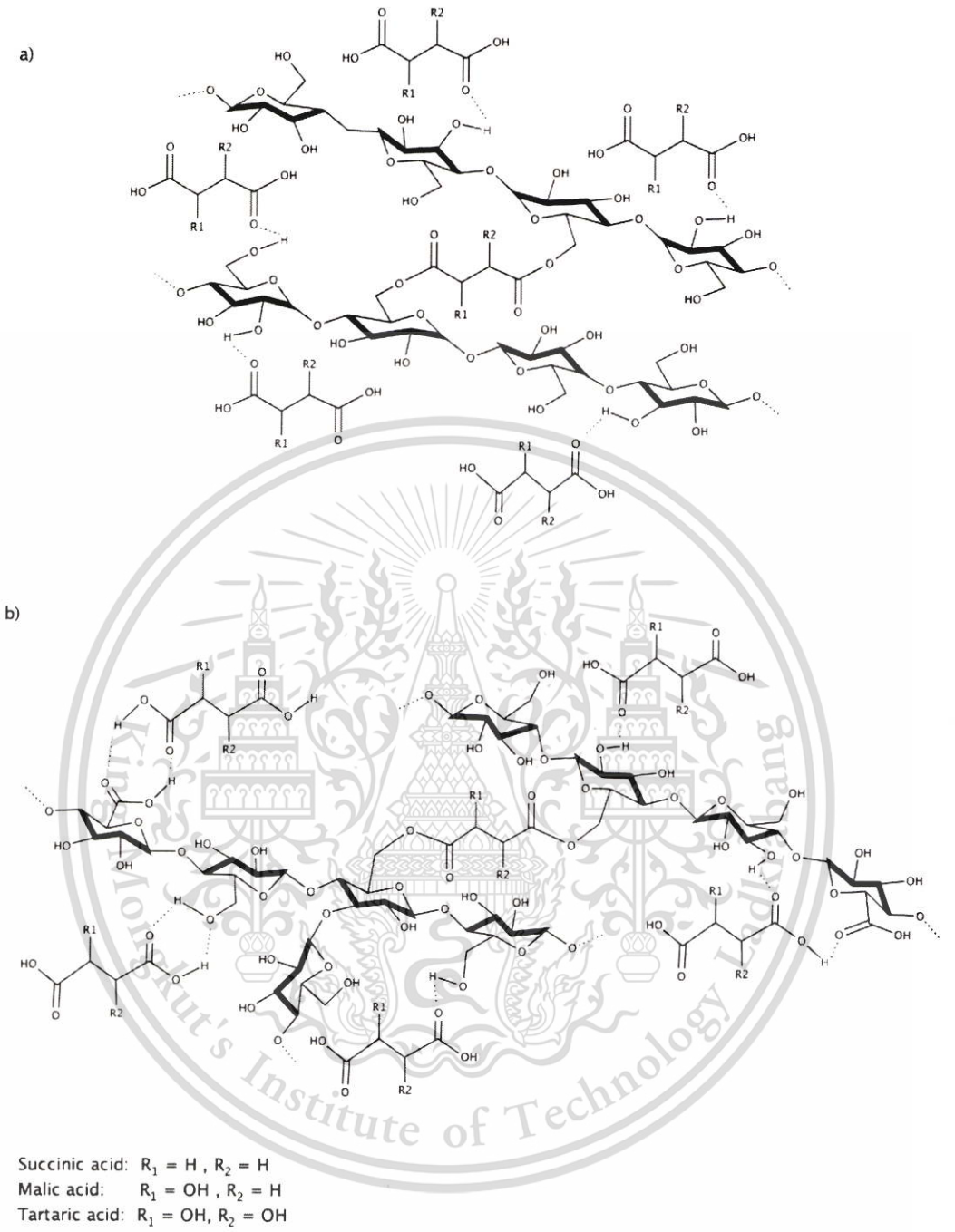

Figure 4.1 Chemical structure of (a) MBS and (b) BSM film cross-linked by TA, MA or SA

The chemical structure of MBS and BSM cross-linked by TA, MA and SA films is presented in Figure 4.1. The di-carboxylic acids (TA, MA or SA) can react with the hydroxyl groups of MBS and BSM via esterification. Because of steric hindrance of 2 hydroxyl groups of TA and 1 hydroxyl group of MA, the TA or MA carboxyl groups could not link to the BSM hydroxyl groups as easily as SA which lacks a hydroxyl group, so as the number of hydroxyl groups increased, steric hindrance of the cross-

linkers also increased. Moreover, hydrogen bonding could form between OH group of starch and acid cross-linkers. Further, both esterification and acid hydrolysis of MBS or BSM backbone chain occur. The acidity of the cross-linkers increased in the sequence of TA > MA > SA. Solution pH values were SA 4.0, MA 3.0, TA 2.5 and native MBS 4.5. Moreover, pH values of 4.0, 3.0 and 2.5 were found for BSM solution without acid, with SA and with MA, respectively.

4.1 Fourier-transform infrared spectroscopy (FT-IR)

FT-IR is used to identify the structure and functional groups of different films. Fundamentally, an IR spectrum shows absorption peaks corresponding to the vibrations of different bonds: this enables the identification of the bonds in a functional group. The environment (i.e. neighboring bonds or H-bonds) shifts the basic bond frequency and enables identical of completed functional groups. The positions of characteristic bands are summarized in correlation tables displayed below.

Table 4.2 Structural-assignment for FT-IR spectrum of modified bio-based film cross-linked by different acids

Wave number (cm^{-1})	Characteristic band
3200-3600 (V)	O-H stretching
2800-3000 (m→s)	Alkanes C-H stretching
1735-1750 (s)	Ester C=O stretching
1600-1630 (s)	Bounded water
1445-1485 (m)	O-H bending
1000-1300 (s)	C-O-C stretching
1000-1200 (s)	C-O-H bending
900-940 (s)	C-H out-of-plane bending
800-860 (s)	C-H out-of-plane bending
735-770 (s)	C-H out-of-plane bending

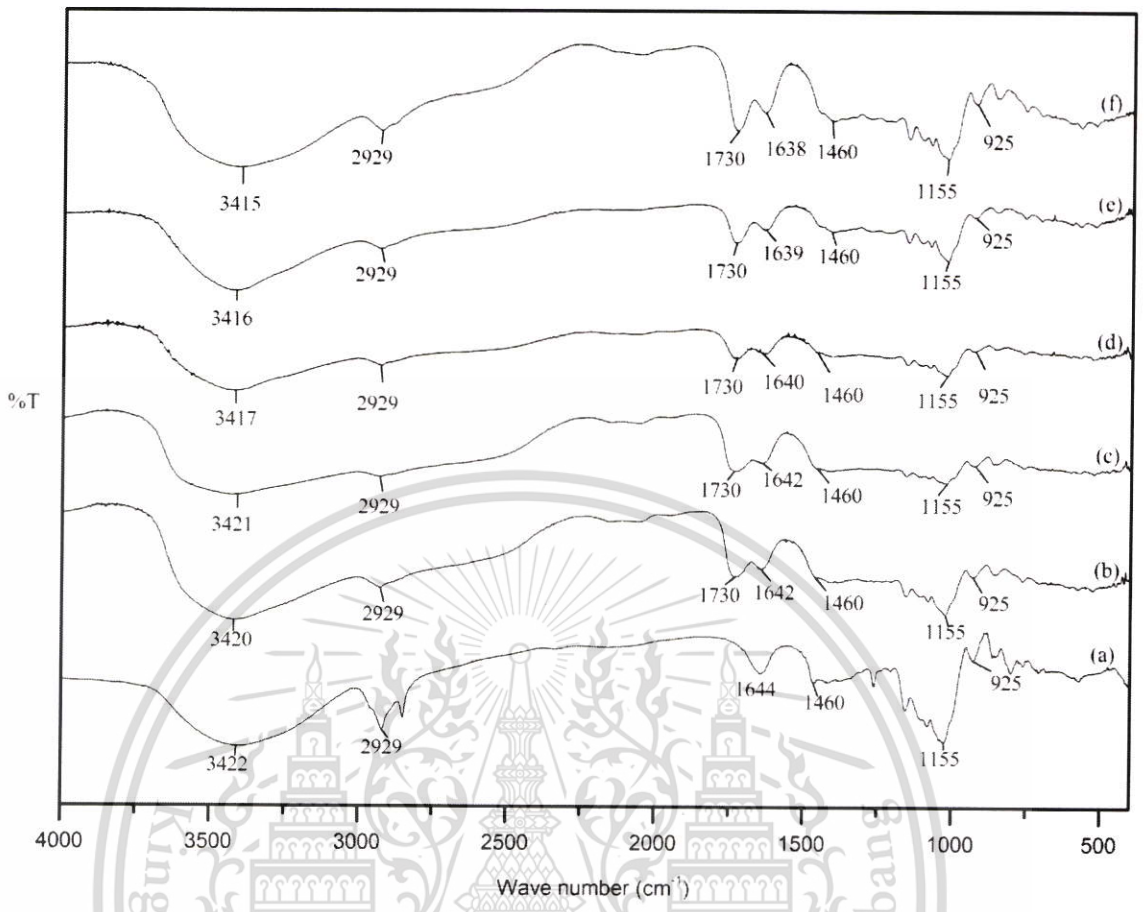

Figure 4.2 IR spectra of MBS film cross-linked by different contents of TA (a) MBS, (b) MBS10TA, (c) MBS15TA, (d) MBS20TA, (e) MBS25TA and (f) MBS30TA

It can be observed in the FT-IR spectrum (Figure 4.1) that the O-H stretching peak appears as a very broad peak at 3500-3300 cm^{-1}, while the aliphatic C-H stretching peak appears as a sharp peak at 3000-2800 cm^{-1}. The peak at 1640 cm^{-1} is assigned to the water adsorbed by starch molecules. All starch films have two C-O stretching absorption peaks (C-O-C and C-O-H) between 1200-1000 and 927-800 cm^{-1}, the fingerprint region. The peaks at 1080 and 1020 cm^{-1} are attributed to the glucopyranose ring O-C stretching vibration [1, 76] All types of cross-linked MBS films exhibited a similar IR peak pattern.

The only difference in the spectra of native MBS and different cross-linked MBS films is the carbonyl (C=O) peak of ester bonds in all cross-linked MBS films at 1730 cm^{-1}. Furthermore, a gradual increase in intensity of the peak at 1730 cm^{-1} was observed as the TA content increased. This suggests an increase in the number of formed ester bonds as the TA content increased [10]. In addition, the presence of ester linkages was confirmed by gel fraction (Table 4.5). It was observed that MBS was absolutely soluble in DMSO. However, gel fractions of different MBS films

increased with increasing TA content. This can be associated with the higher degree of cross-linking. In addition, the O-H stretching (3500-3300 cm^{-1}) peaks of the films cross-linked with TA shifted to lower wavenumbers, which suggests intermolecular interactions between the hydroxyl groups of MBS and TA molecules, resulting in an increase of the intermolecular hydrogen bonds [79]. Shenglin Sun *et al.* reported similar results for hydroxypropyl distarch phosphate/polyhydroxyalkanoate composite films cross-linked by citric acid, adipic acid, borax, and boric acid [71]. They reported that the infrared absorption peak of the O-H bonds shifted to lower wave numbers with the addition of a cross-linking agent because the interactions between the cross-linking agent and starch chain probably increased the number of the intermolecular hydrogen bonds.

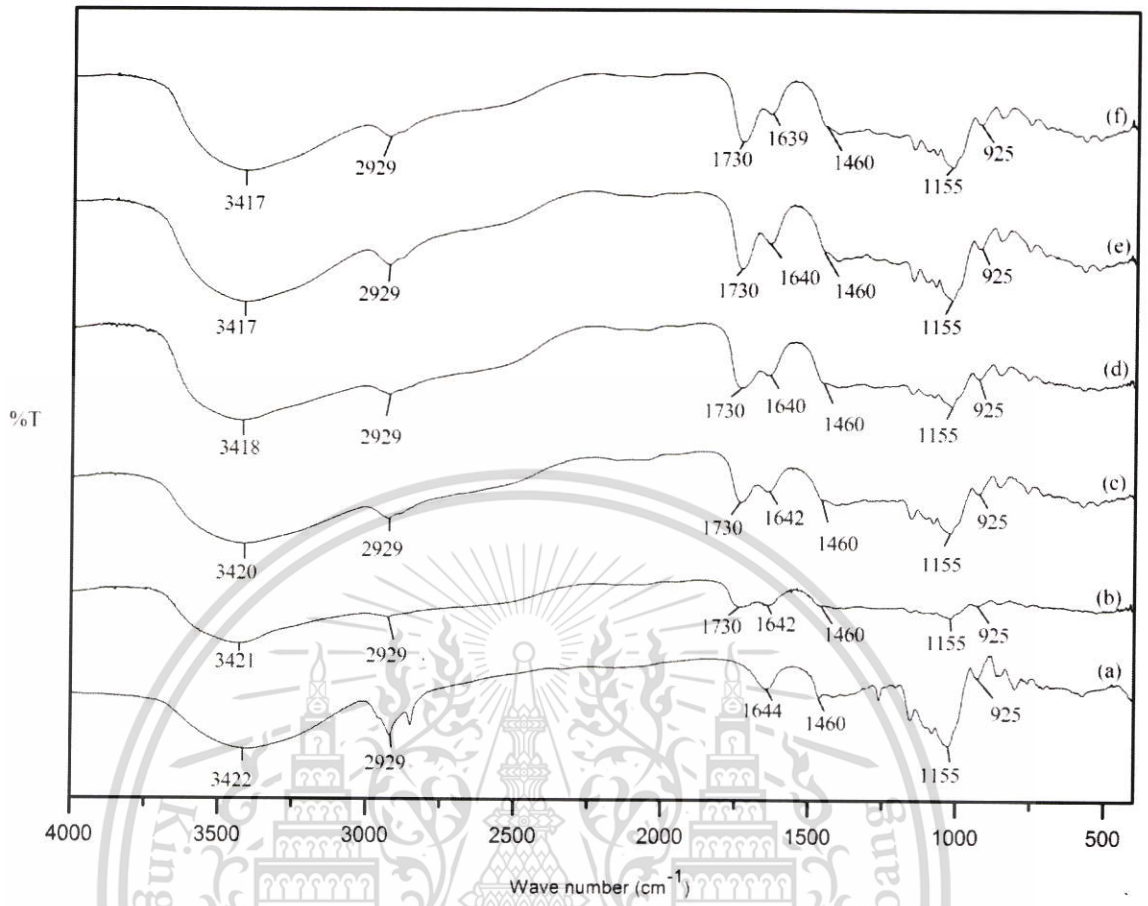

Figure 4.3 IR spectra of MBS film cross-linked by different contents of MA (a) MBS, (b) MBS10MA, (c) MBS15MA, (d) MBS20MA, (e) MBS25MA and (f) MBS30MA

It was observed that all MBS films cross-linked with MA exhibited a similar IR peak pattern (Figure 4.3). Moreover, the C-H stretching peak shifted to a lower wave number with the addition of MA. This data further confirms that the interactions between hydroxyl groups of MBS and MA were via intermolecular hydrogen bonding [79]. New ester linkages were formed in cross-linked MBS films, indicating that C=O bonds were formed from the carbonyl groups of MA interacting with hydroxyl group of starch molecules by the cross-linking reaction. Additionally, the C=O characteristic peaks of cross-linked MBS films gradually increased with increasing MA content [10].

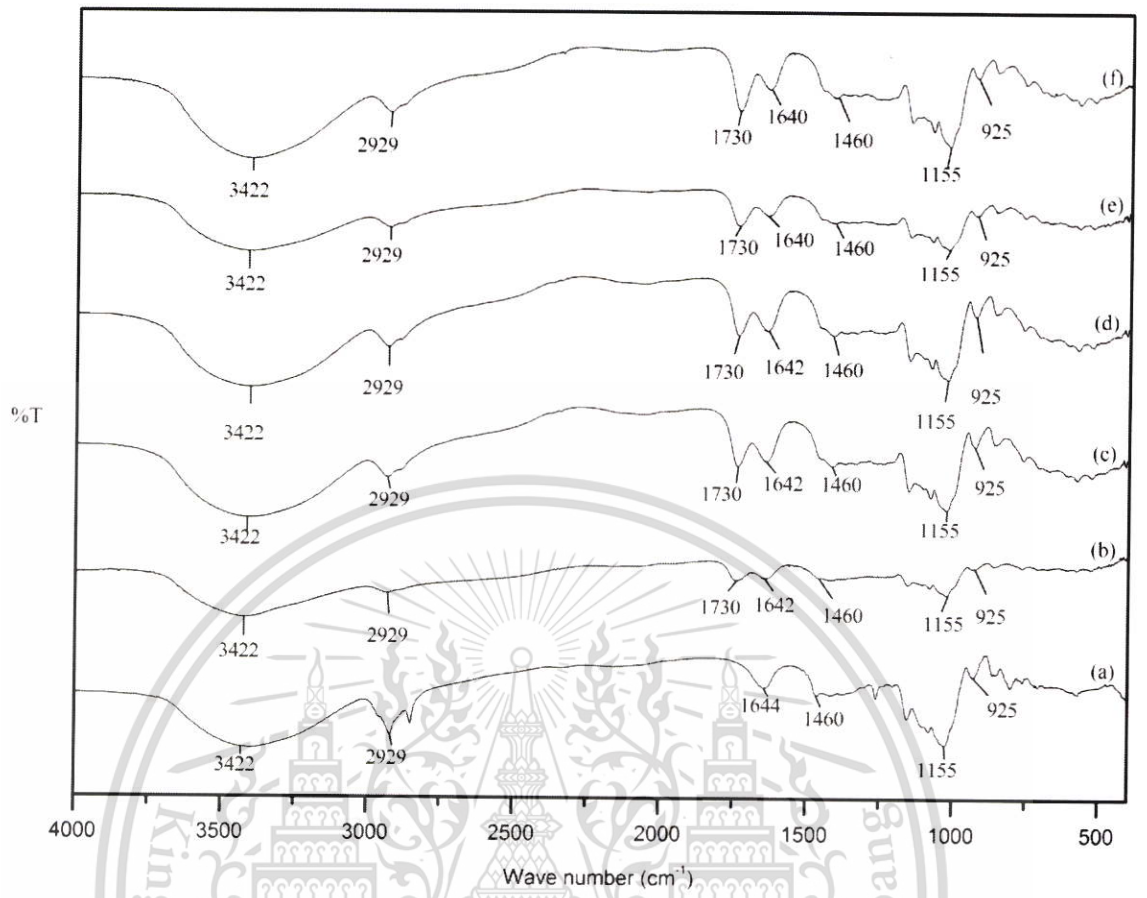

Figure 4.4 IR spectra of MBS film cross-linked by different contents of SA (a) MBS, (b) MBS10SA, (c) MBS15SA, (d) MBS20SA, (e) MBS25SA and (f) MBS30SA

All films exhibited a similar peak pattern (Figure 4.4), except for the additional peak in the spectrum of cross-linked MBS film at 1730 cm^{-1}. The peak at 1730 cm^{-1} is attributed to ester formation. The presence of the carbonyl (C=O) peak confirms the ester linkages between SA and MBS [10].

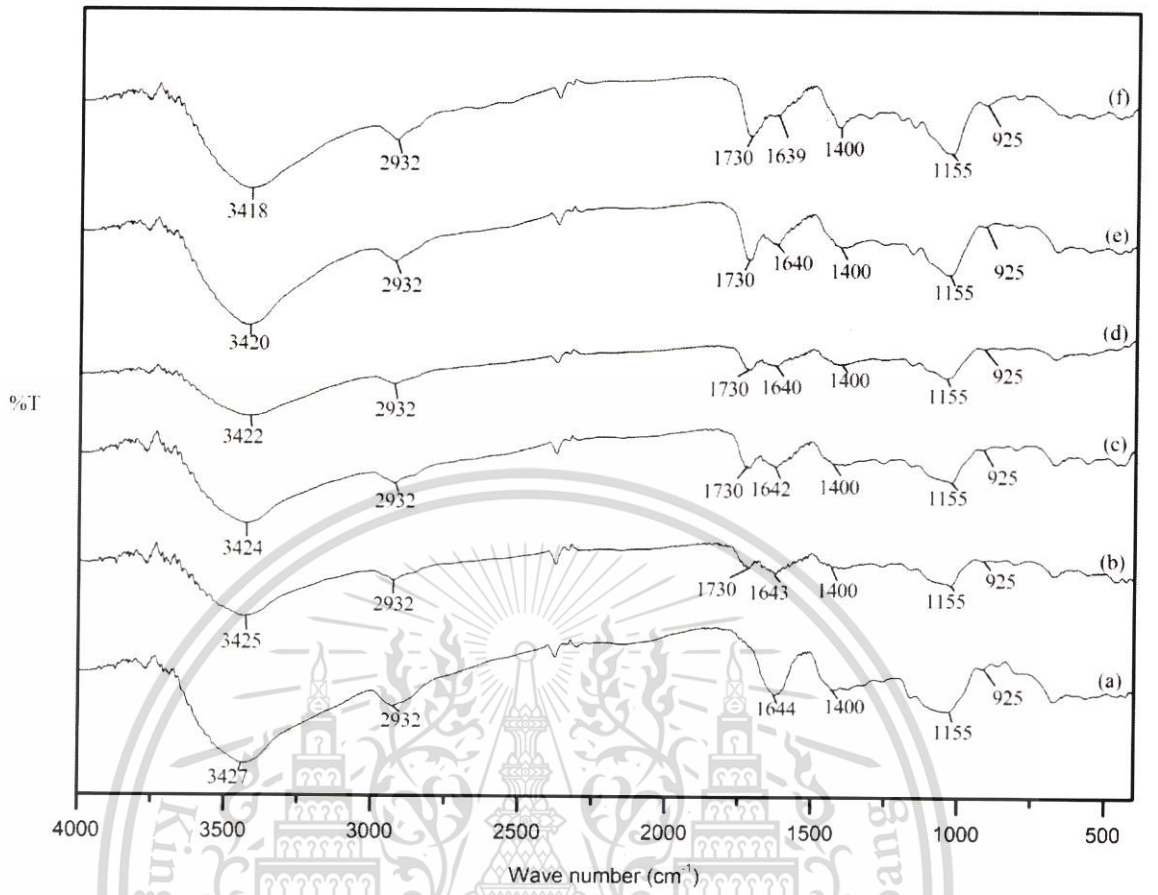

Figure 4.5 IR spectra of BSM film cross-linked by different contents of TA (a) BSM, (b) BSM10TA, (c) BSM15TA, (d) BSM20TA, (e) BSM25TA and (f) BSM30TA

The 1400 cm^{-1} peak (Figure 4.5), attributable to C-OO symmetric and C-OO asymmetric stretching, confirms the presence of uronic acid [62]. The 1630-1600 cm^{-1} band shows the presence of free carboxylate groups [80]. The spectra of BSM and MBS were essentially identical, with a small difference at 1400 cm^{-1}.

Moreover, the IR spectra revealed one additional band at ~1730 cm^{-1} attributed to the C=O groups in the cross-linked BSM films, showing that the ester carbonyl group from TA replaced the hydroxyl groups in the polysaccharide chains [10]. Additionally, a new 1730 cm^{-1}peak gradually increased as the TA content increased. Comparing between the spectra of native BSM and TA cross-linked BSM films, the 3500-3300 cm^{-1} O-H stretching bands shifted toward a lower range, indicative of an interaction between BSM and TA, most likely hydrogen bonding.

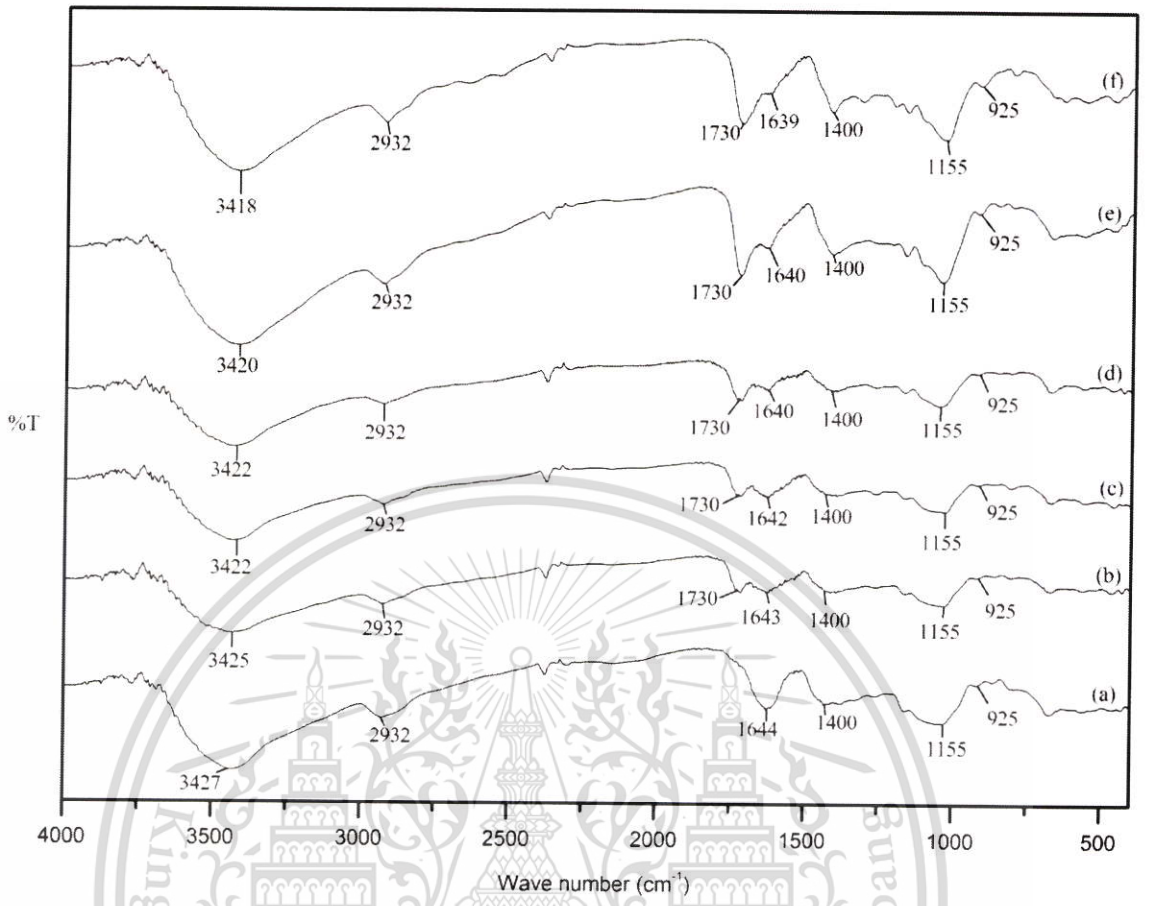

Figure 4.6 IR spectra of BSM film cross-linked by different contents of MA (a) BSM, (b) BSM10MA, (c) BSM15MA, (d) BSM20MA, (e) BSM25MA and (f) BSM30MA

In addition to the peaks in the spectrum of native BSM, there were new peaks at the 1730 cm^{-1} band intensity gradually increased as the content of MA in the BSM film increased (Figure 4.6). The FT-IR spectrum demonstrated that the structure of BSM contained a new ester bond formed after cross-linking. Moreover, the characteristic 3500-3300 cm^{-1} bands shifted toward a lower range along with increasing MA content, indicating occurrences of hydrogen bonding in BSM films.

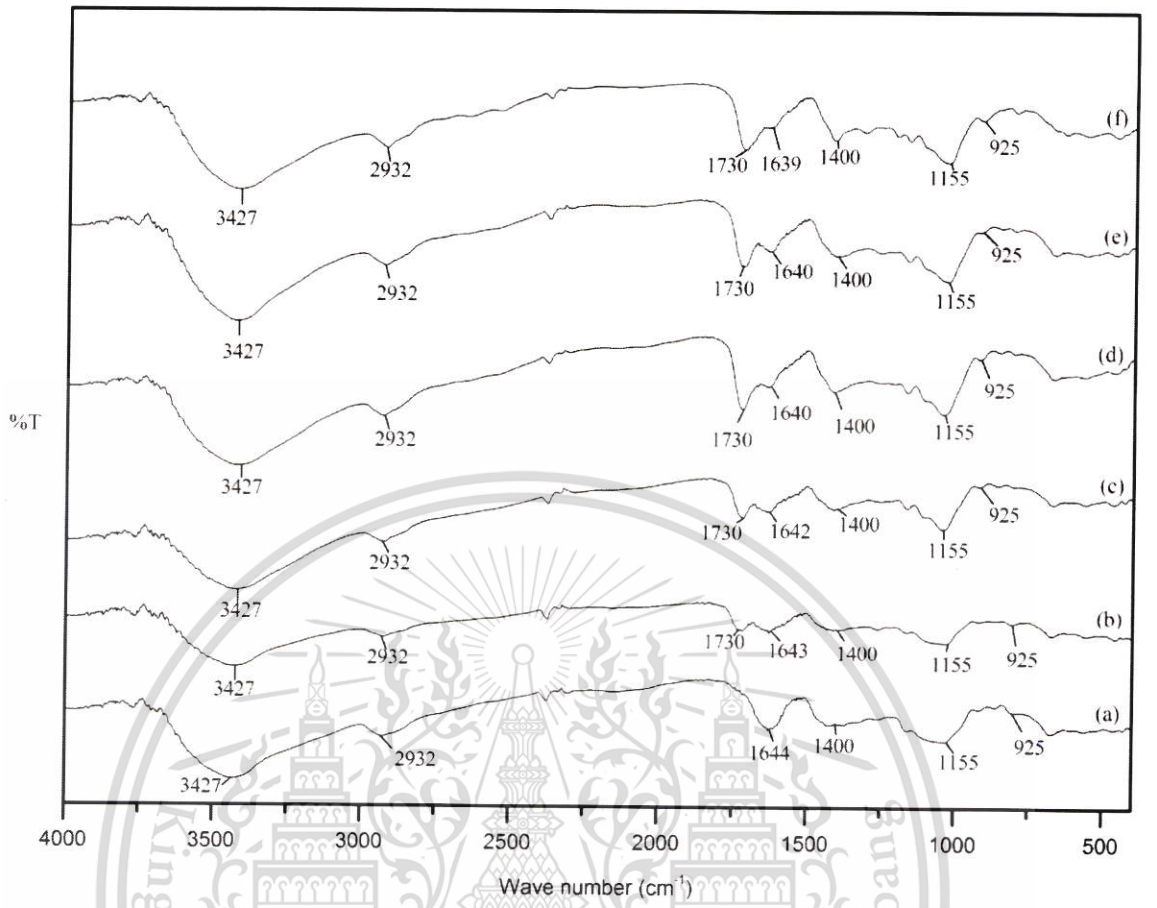

Figure 4.7 IR spectra of BSM film cross-linked by different contents of SA (a) BSM, (b) BSM10SA, (c) BSM15SA, (d) BSM20SA, (e) BSM25SA and (f) BSM30SA

Compared to the peaks in the spectrum of native BSM, a new characteristic ~1730 cm^{-1} absorption band and the gradual increase in its intensity as SA was added were observed in the spectra of cross-linked BSM films, confirming the formation of C=O group by the cross-linking process (Figure 4.7).

4.2 X-ray Diffraction (XRD)

X-ray diffraction was used to determine the crystalline structure of the different biodegradable films cross-linked by TA, MA and SA. X-ray powder diffraction patterns were determined with an X-ray diffractometer under the following conditions: CuKα (40 kV, 50 mA) radiation source, 10 to 80°angle of diffraction.

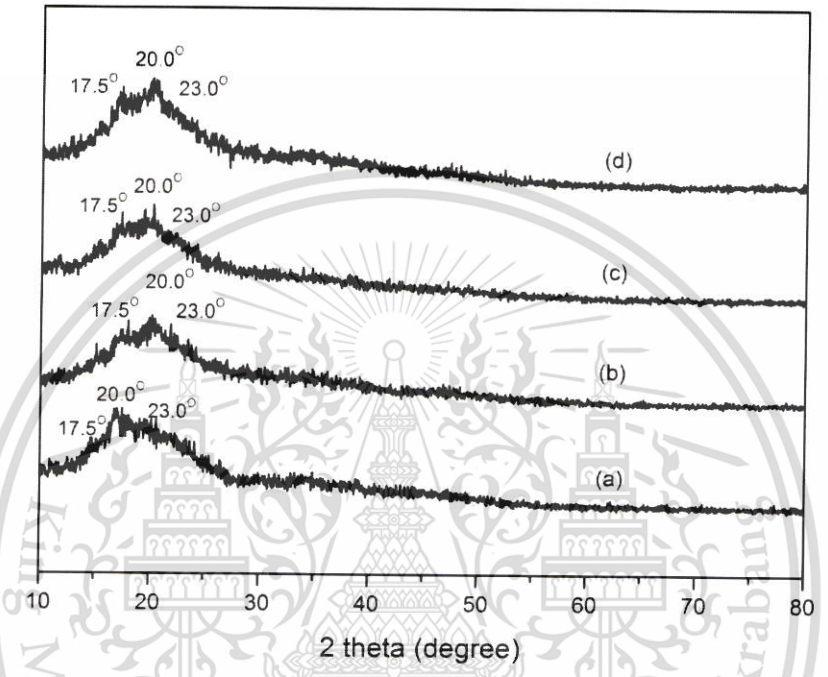

Figure 4. 8 X-ray diffraction patterns of different MBS film cross-linked by TA (a) MBS, (b) MBS10TA, (c) MBS20TA and (d) MBS30TA

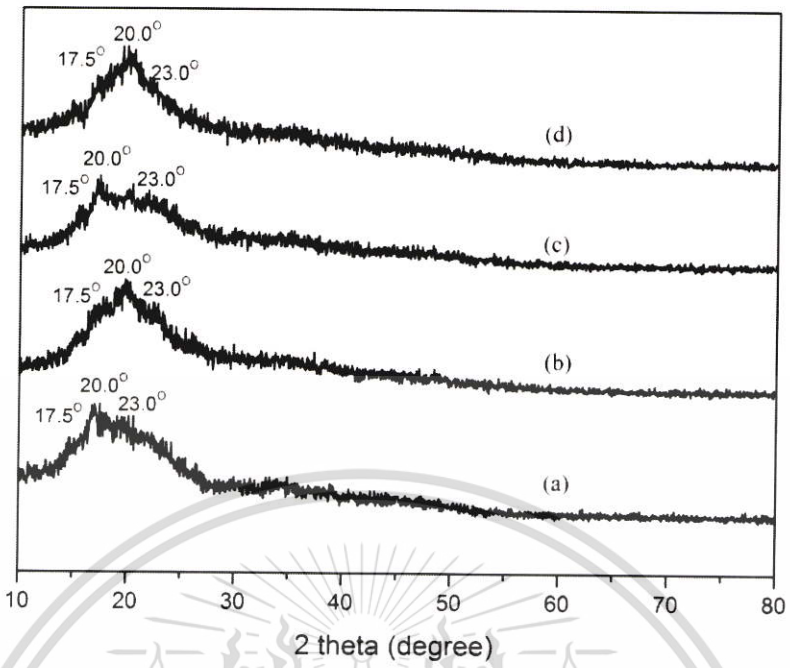

Figure 4. 9 X-ray diffraction patterns of different MBS film cross-linked by MA (a) MBS, (b) MBS10MA, (c) MBS20MA and (d) MBS30MA

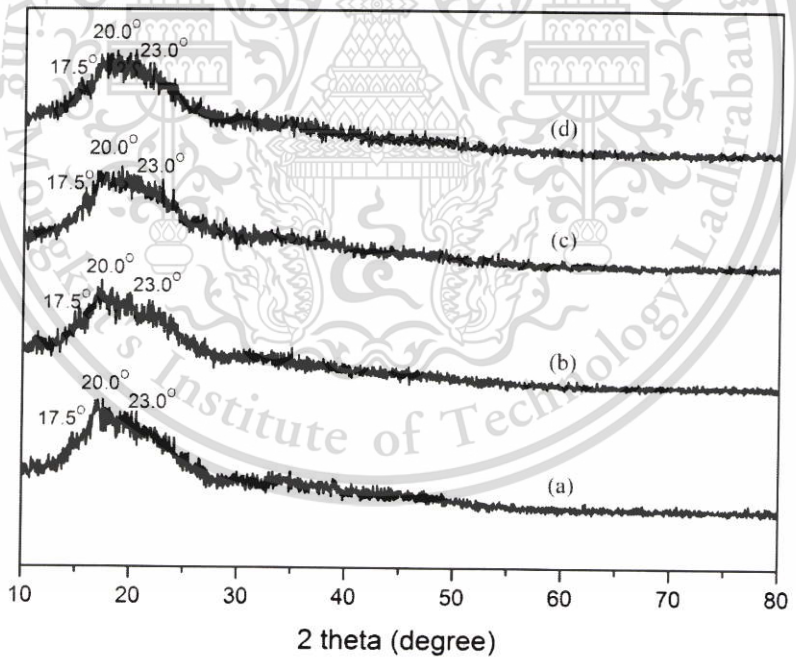

Figure 4.10 X-ray diffraction patterns of different MBS film cross-linked by SA (a) MBS, (b) MBS10SA, (c) MBS20SA and (d) MBS30SA

It was observed from Figures 4.8-4.10 that the native MBS and different cross-linked MBS films showed similar crystal peaks at 2θ of 17.5°, 20.0° and 23.0°. The native and different cross-linked MBS films showed a typical C-type XRD pattern of legume starch. The XRD patterns in Figures 4.8-4.10 indicate that the crystal structure of the native MBS film was disrupted after plasticization and cross-linking process. The disruption of the crystal structure was due to the higher exposure of hydroxyl groups of MBS molecules to TA molecules. Furthermore, the replacement of the OH groups on the MBS molecules with the C=O groups from TA molecules restricted inter- and intra-molecular hydrogen bonding and absolutely prevented formation of crystal structure. Compared to native MBS film, the degree of crystallinity of cross-linked MBS films tended to be lower. A similar result was observed by Bruni GP *et al.* who cross-linked wheat starch with sodium trimetaphosphate and found less formation of crystalline regions in the wheat starch film [81]. The lower degree of crystallinity in the cross-linked MBS films compared to that in the native MBS film was due to the high acidity of the cross-linkers that enhanced hydrolysis of MBS backbone chains.

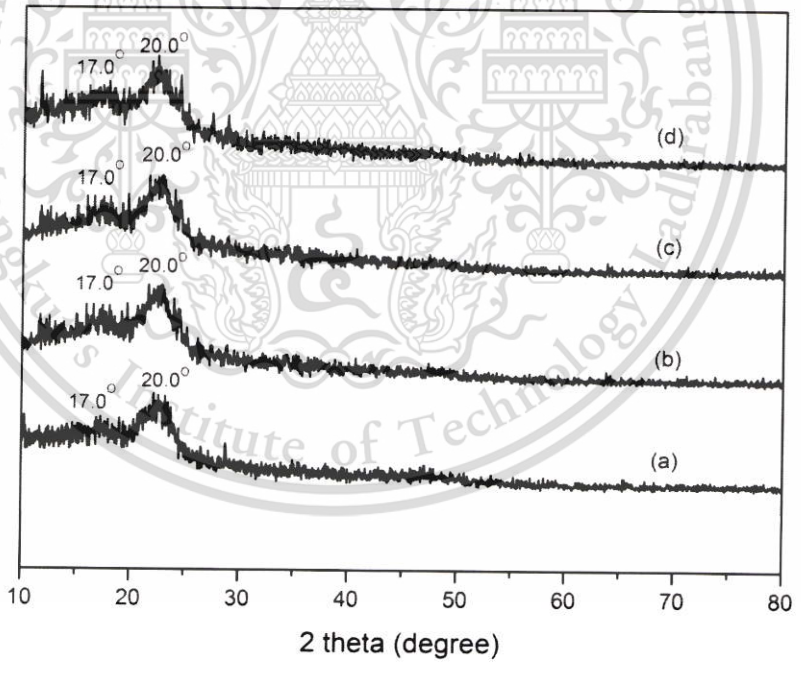

Figure 4. 11 X-ray diffraction patterns of different BSM film cross-linked by TA **(a)** BSM, **(b)** BSM10TA, **(c)** BSM20TA and **(d)** BSM30TA

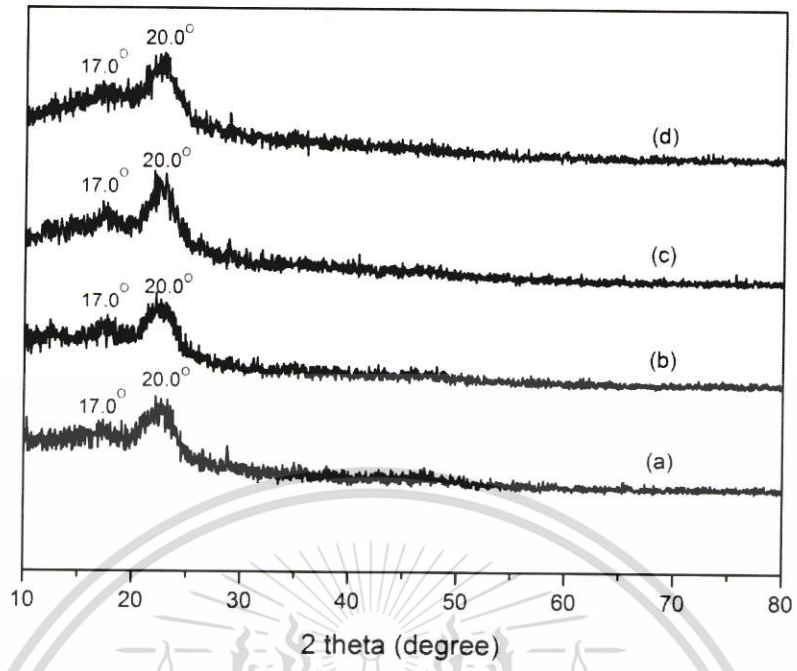

Figure 4.12 X-ray diffraction patterns of different BSM film cross-linked by MA (a) BSM, (b) BSM10MA, (c) BSM20MA and (d) BSM30MA

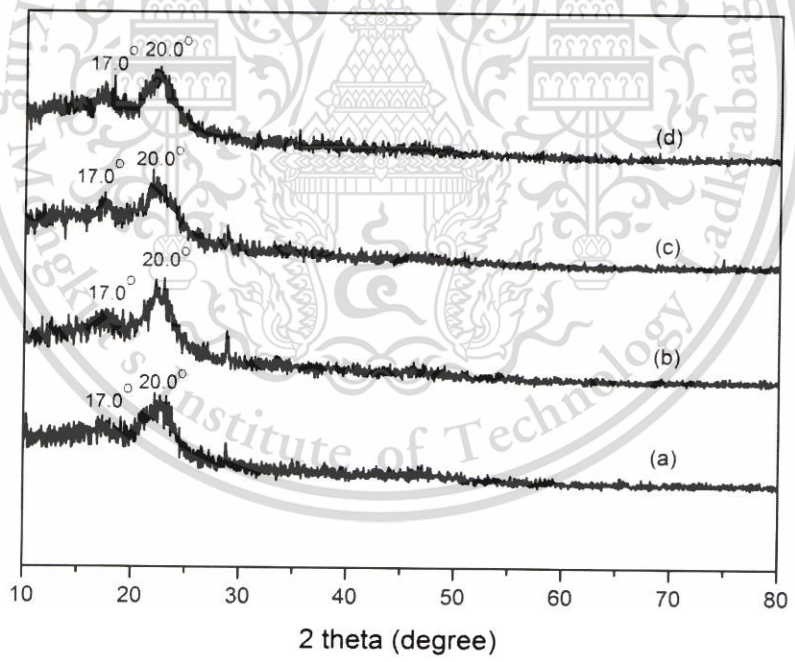

Figure 4.13 X-ray diffraction patterns of different BSM film cross-linked by SA (a) BSM, (b) BSM10SA, (c) BSM20SA and (d) BSM30SA

It was also observed from Figures 4.11-4.13 that broad peak at $2\theta \approx 17.0$ and 20.0° were recorded for BSM films which indicated a dominant crystal structure. A similar pattern was reported for BSM [6]. Cross-linked BSM films had more amorphous regions than native BSM film due to cross-linking. After the cross-linking

process, the BSM molecules of the cross-linked BSM films could not be re-crystallized because the cross-linking molecules had replaced their hydroxyl groups. Moreover, the high acidity of the cross-linking acids provided efficient hydrolysis of BSM backbone chains. Therefore, the degree of crystallinity of cross-linked BSM films tended to be lower.

Table 4.3 Degree of cryatallinity of various native and biodegradable MBS and BSM films cross-linked by different contents of TA, MA and SA

Samples	Degree of crystallinity **(%)**	Samples	Degree of crystallinity **(%)**
MBS	61.50±0.04	BSM	46.5±0.04
MBS10TA	49.08±0.05	BSM10TA	41.4±0.07
MBS20TA	45.08±0.06	BSM20TA	34.1±0.08
MBS30TA	42.08±0.04	BSM30TA	28.0±0.06
MBS10MA	50.75±0.02	BSM10MA	43.2±0.04
MBS20MA	48.08±0.03	BSM20MA	38.3±0.05
MBS30MA	46.42±0.02	BSM30MA	34.3±0.03
MBS10SA	54.75±0.04	BSM10SA	45.7±0.03
MBS20SA	53.58±0.03	BSM20SA	43.3±0.07
MBS30SA	52.73±0.02	BSM30SA	40.0±0.05

The degrees of crystallinity of native and different cross-linked biodegradable BSM films are also shown in Table 4.3. The addition of TA, MA and SA resulted in a decrease in the degree of crystallinity attributable to the replacement of hydroxyl group by carboxylic group via the cross-linking process [10]. Additionally, the substitution of the hydroxyl groups on the polysaccharide molecules by the covalent ester groups interrupted hydrogen bonding, and so the molecules could not rearrange themselves into a perfect crystal structure. Moreover, the decrease in the degree of crystallinity was due to an induced acid hydrolysis. According to C. Menzel *et al.*, films containing CA showed a lower degree of crystallinity, which was probably due to strong hydrolysis of starch backbone chains [75].

Table 4.3 shows that native MBS presented a higher degree of crystallinity than BSM because MBS contained higher amylose content of 60%, compared to 45% of BSM. Amylose content strongly influences properties of these starches. It is one of the controlling factors of the barrier and mechanical properties of bio-based films. This is because linear structure of amylose contains more hydrogen bonding than branched structure of amylopectin. Moreover, long and linear backbone amylose chains of MBS are packed closer together than highly branched chain of the lower amylose content of BSM. These tightly packed MBS chains promote formation of a cohesive film network, resulting in a higher degree of crystallinity as compared to BSM [4].

A comparison of the degrees of crystallinity of TA-, MA- and SA- cross-linked films showed that the highest to lowest degree among them were SA > MA > TA. In addition, the degree of crystallinity of the films prepared with TA was the lowest compared to those prepared with MA and SA. This is because of the highest acidity of TA provided the strongest hydrolysis, resulting in lowest degree of crystallinity. Moreover, the steric effect of the 2-hydroxyl groups of TA caused a lower degree of crystallinity.

4.3 Scanning electron microscopy (SEM)

The morphology of the native and different cross-linked films was observed by SEM at 3000x magnifications.

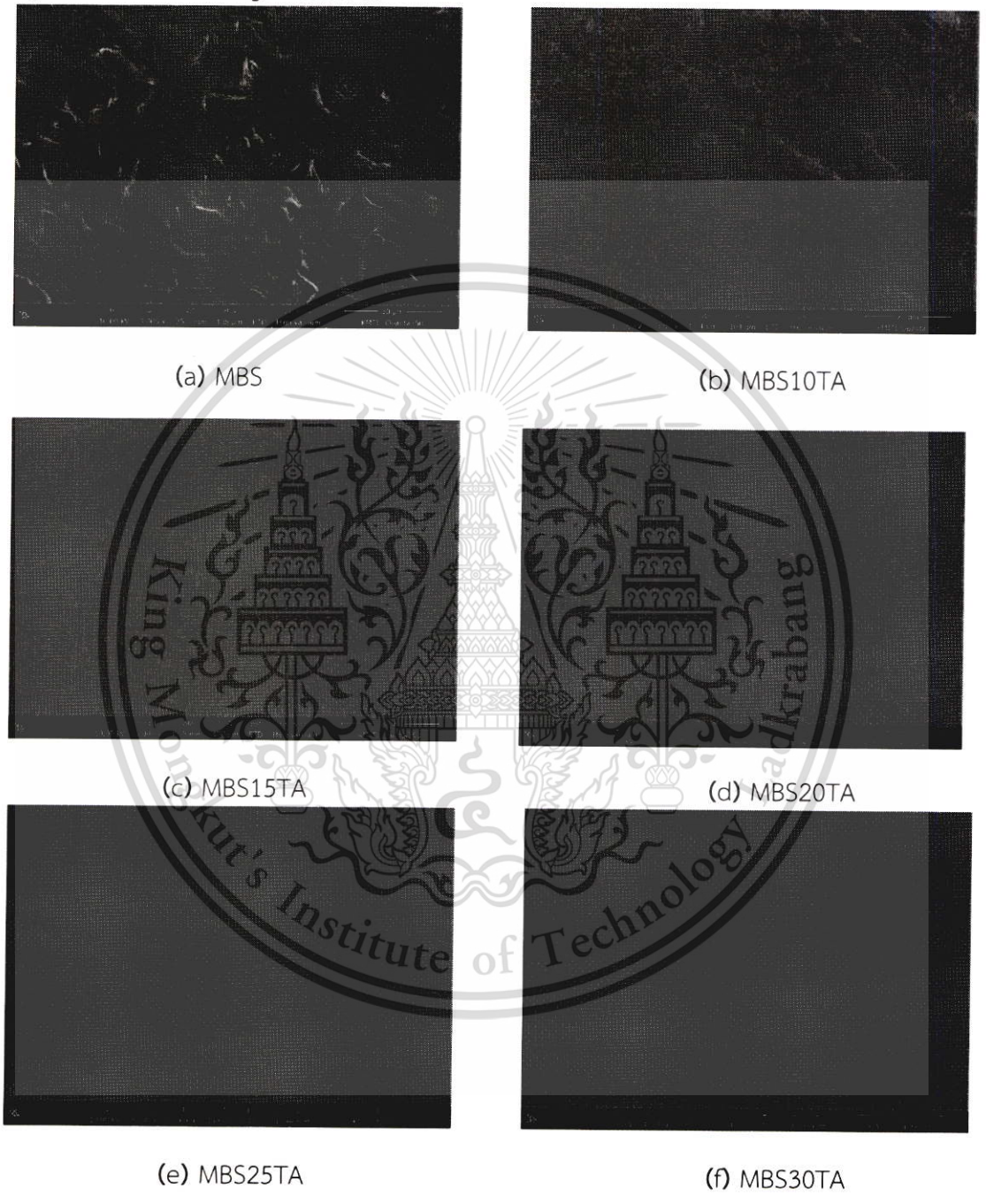

Figure 4.14 Fractured surfaces of native and different cross-linked MBS films with TA (a) MBS, (b) MBS10TA, (c) MBS15TA, (d) MBS20TA, (e) MBS25TA and (f) MBS30TA

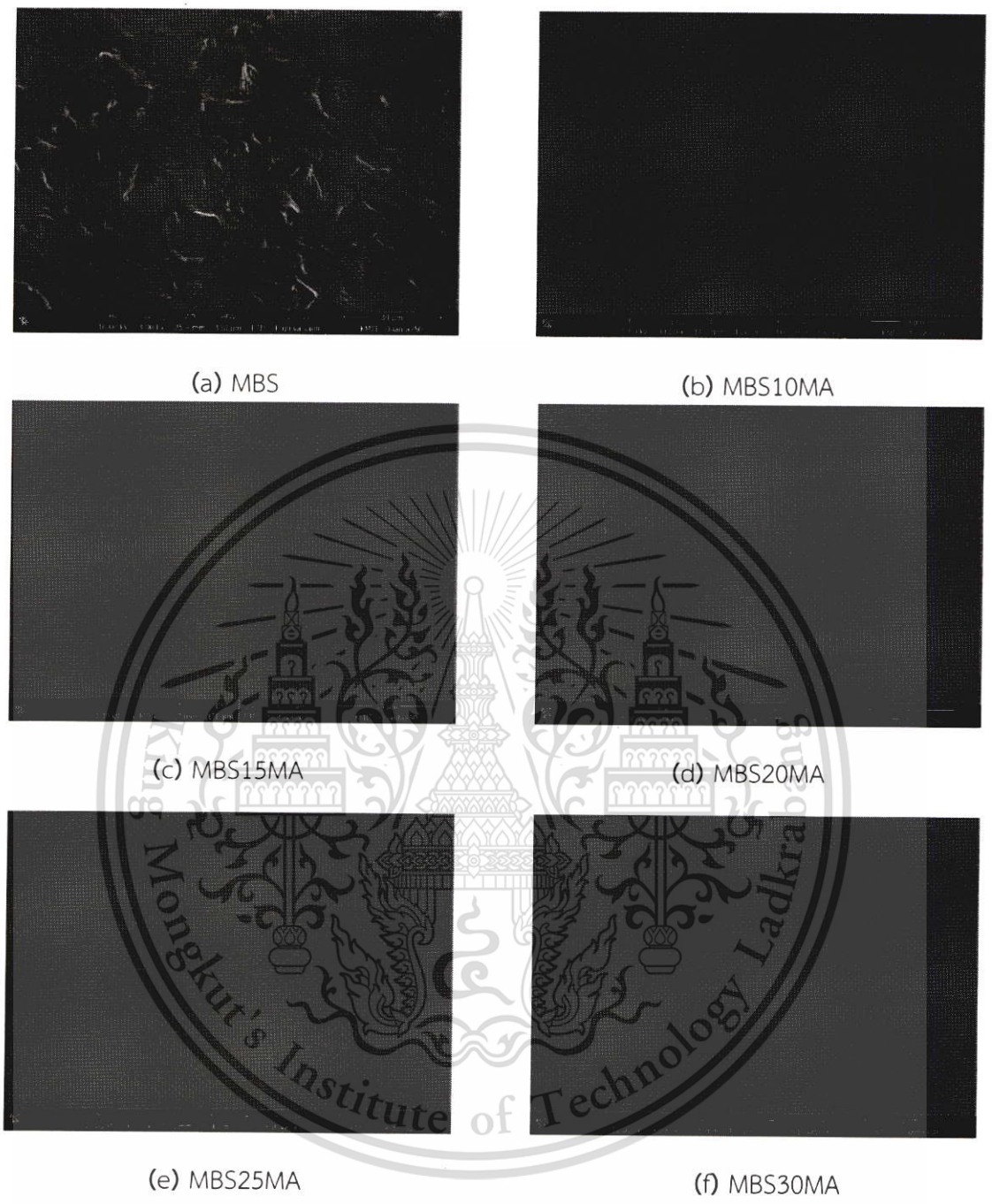

Figure 4.15 Fractured surfaces of native and different cross-linked MBS films with MA (a) MBS (b) MBS10MA, (c) MBS15MA, (d) MBS20MA, (e) MBS25MA and (f) MBS30MA

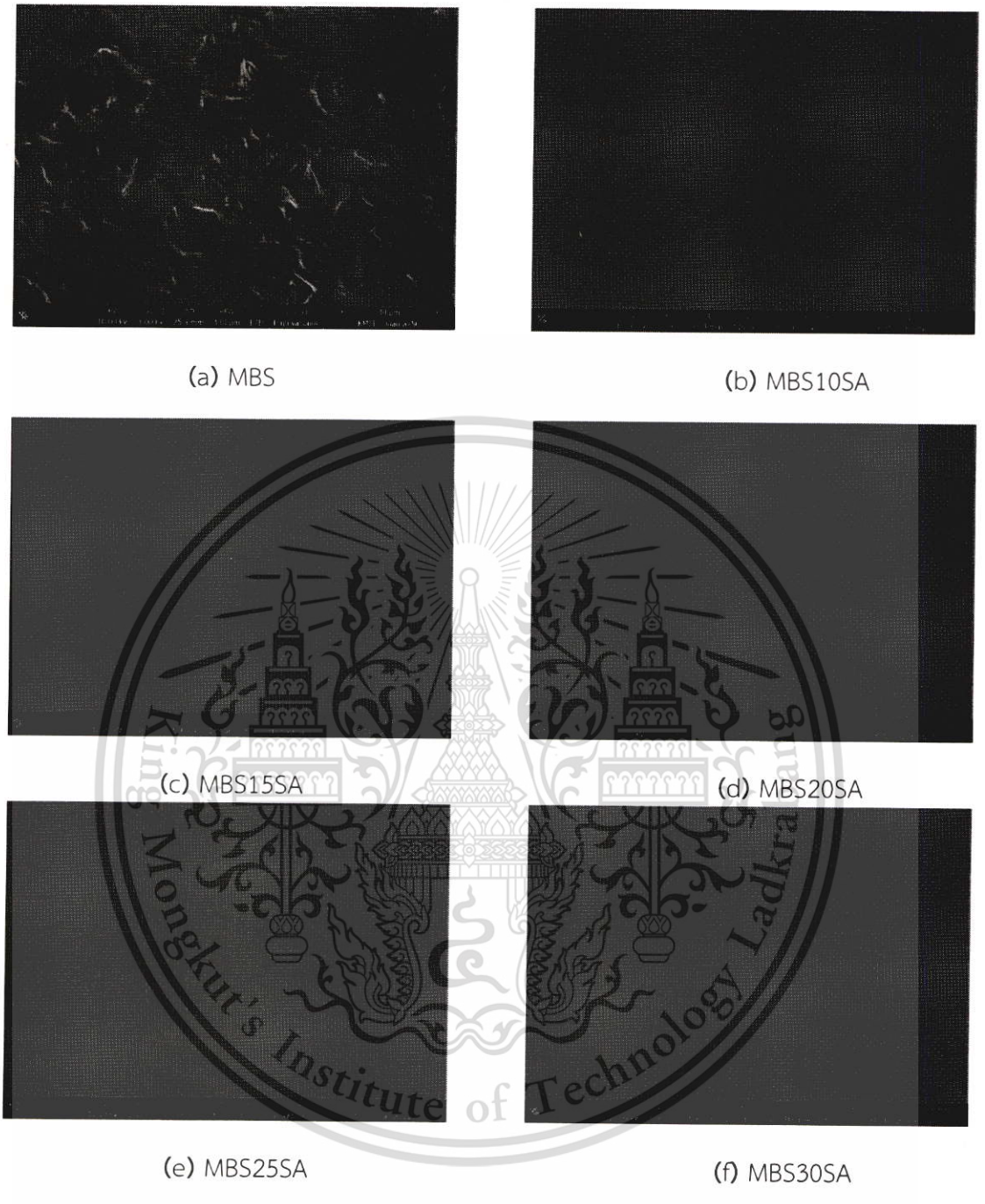

Figure 4.16 Fractured surfaces of native and different cross-linked MBS films with SA **(a)** MBS, **(b)** MBS10SA, **(c)** MBS15SA, **(d)** MBS20SA, **(e)** MBS25SA and **(f)** MBS30SA

SEM images show the morphology of different films: in Figures 4.14-4.16. In gelatinization, glycerol and water molecules penetrated into starch granules, and replaced starch inter- and intra- molecular hydrogen bonds between starch chain and disintegrated starch granules. The destruction of starch granules helped to expose the hydroxyl groups of the starch molecules, which, in turn, ensured better reaction with TA, MA and SA molecules.

With TA, MA and SA in the films, they were more homogeneous and continuous than the native film. The smoother cross-section surface of cross linked films is produced by acid hydrolysis of the glycosidic linkage of starch backbone chains, allowing water molecules to penetrate more easily into starch granules and breaking them down.

All cross-linked films showed similar morphology. N. Reddy *et al.* demonstrated that corn starch films with CA showed more homogeneous morphology than that of the native film [7]. SEM images also confirm FT-IR results (Figures 4.1 - 4.6), in which the O-H stretching vibration, ~3500–3200 cm^{-1}, shifted to lower frequency, due to hydrogen bonding between hydroxyl groups of acids and starch molecules, indicating strong interaction between the acids and starch in the films.

In addition, the cross-section micrograph of native BSM (Figure 4.17 (a)) displayed a rough surface. However, the cross-linked BSM films (Figure 4.17-4.19 (b)-(e) illustrated homogenous and continuous morphology without pores or cracks. Furthermore, the homogenous and continuous morphology of cross-linked BSM film may be caused by the partial chain scission from the acid hydrolysis reaction. Moreover, the increase in cross-linkers content resulted in the smoother surface.

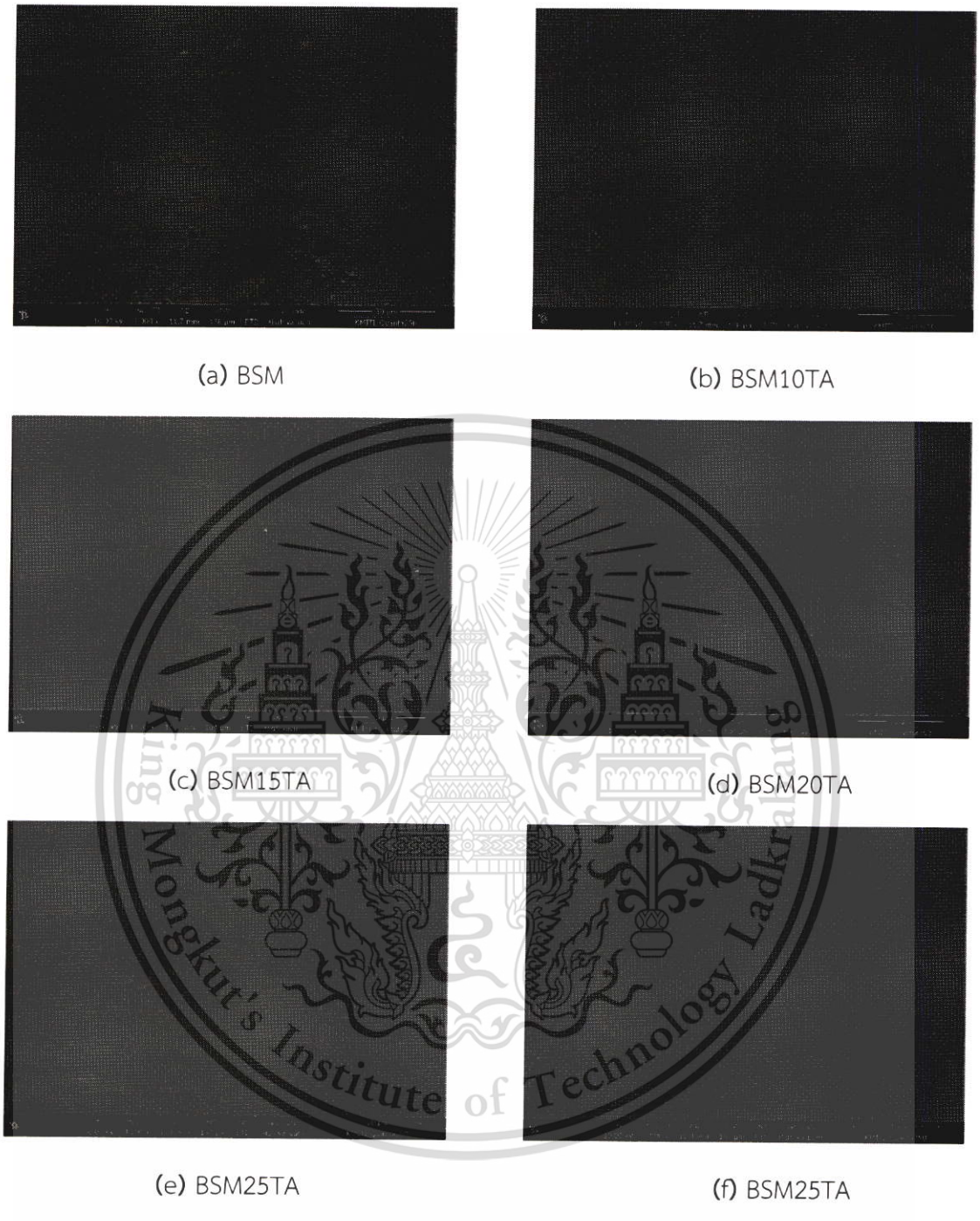

Figure 4.17 Fractured surfaces of native and different cross-linked BSM films with TA (a) BSM, (b) BSM10TA, (c) BSM15TA, (d) BSM20TA, (e) BSM25TA and (f) BSM30TA

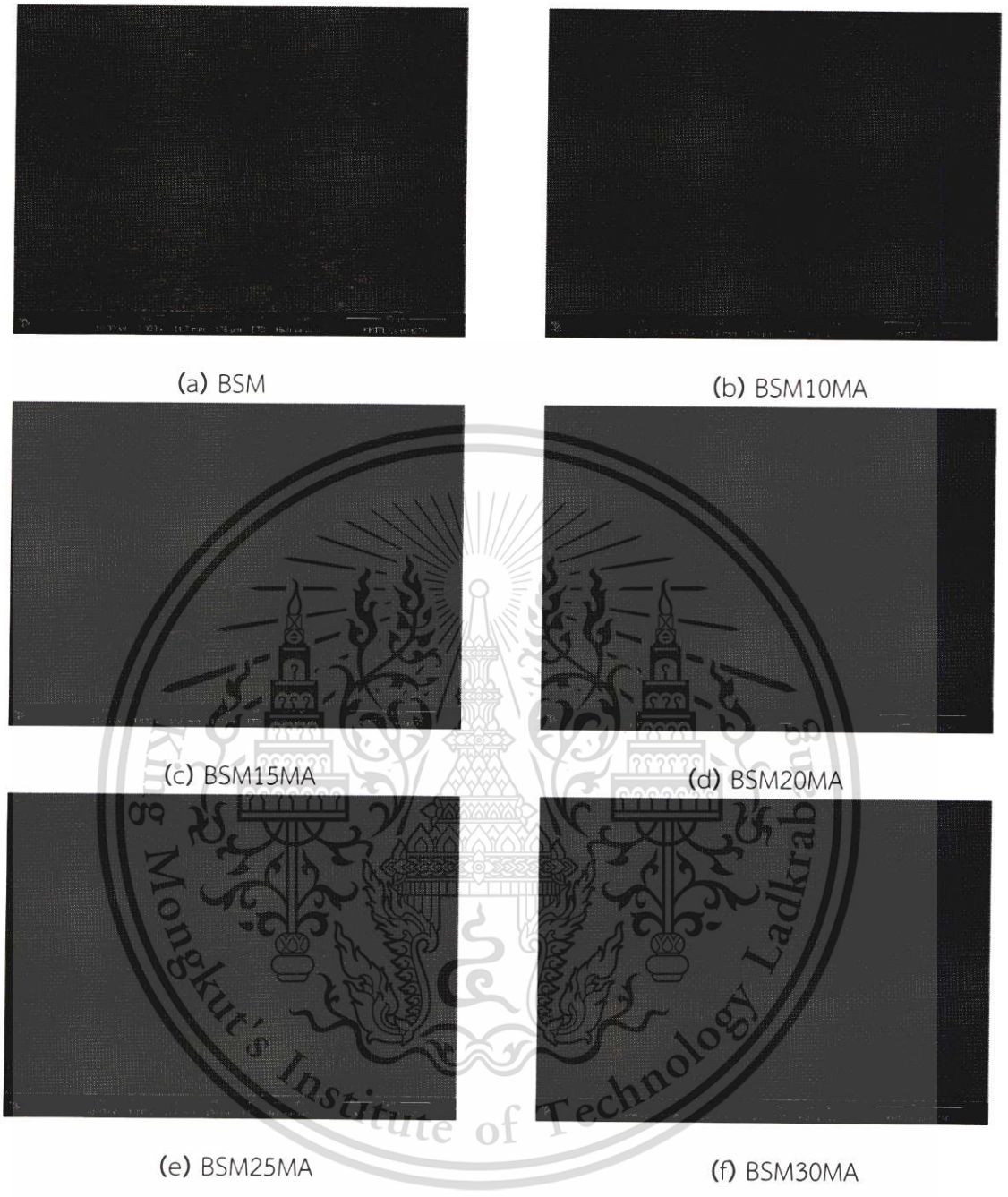

Figure 4.18 Fractured surfaces of native and different cross-linked BSM films with MA (a) BSM (b) BSM10MA, (c) BSM15MA, (d) BSM20MA, (e) BSM25MA and (f) BSM30MA

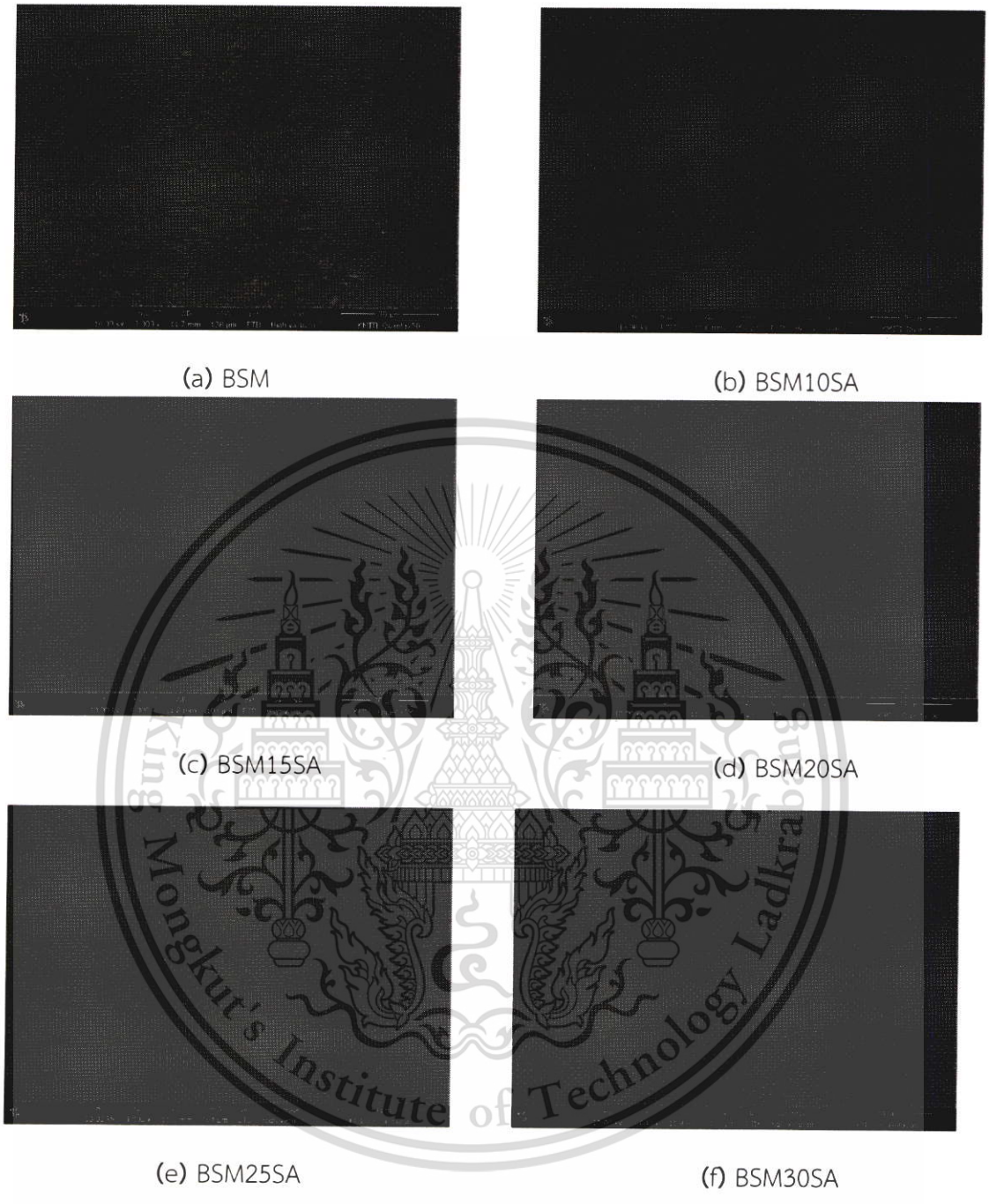

Figure 4.19 Fractured surfaces of native and different cross-linked BSM films with SA **(a)** BSM **(b)** BSM10SA, **(c)** BSM15SA, **(d)** BSM20SA, **(e)** BSM25SA and **(f)** BSM30SA

4.4 Swelling power

The native MBS, BSM and different cross-linked films were determined swelling power at the soaking period of 0, 1, 2, 3, 4, 5, 6 and 72 hours.

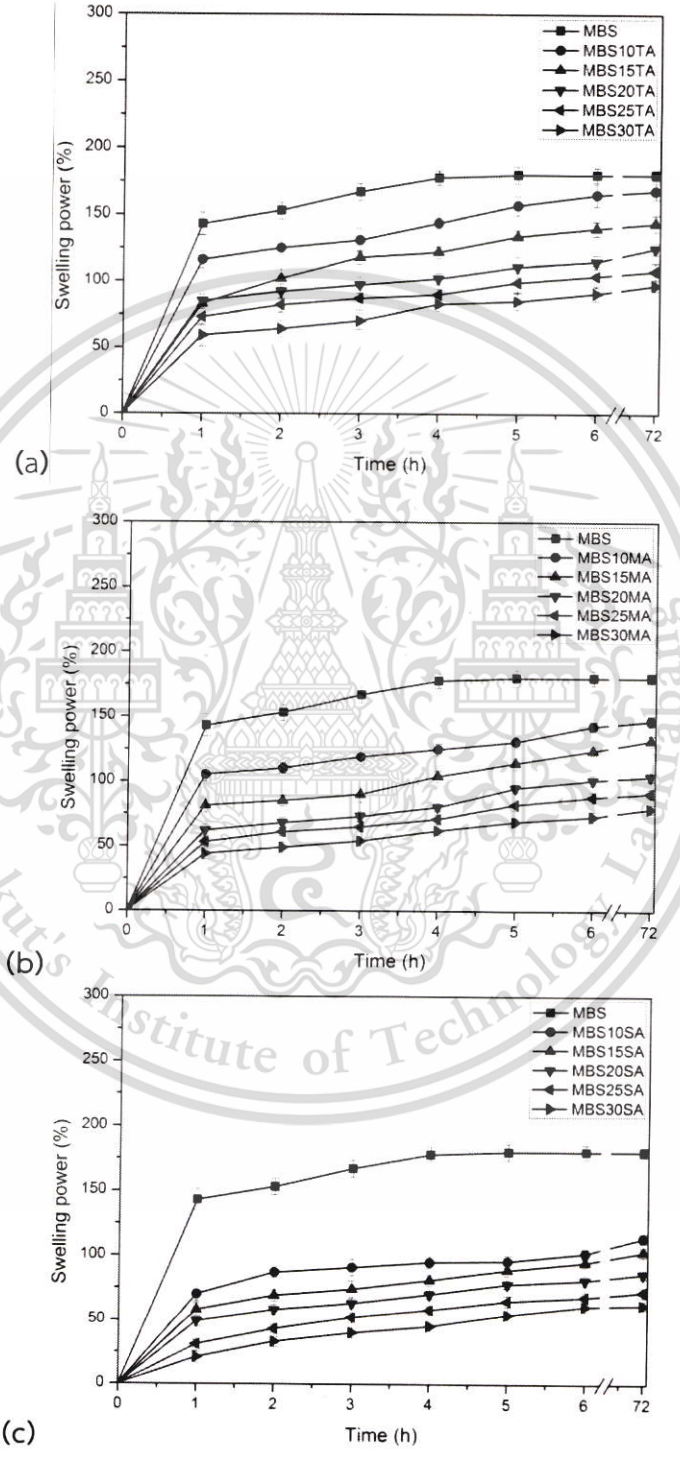

Figure 4.20 Swelling power of different native and cross-linked MBS films with **(a)** TA, **(b)** MA and **(c)** SA

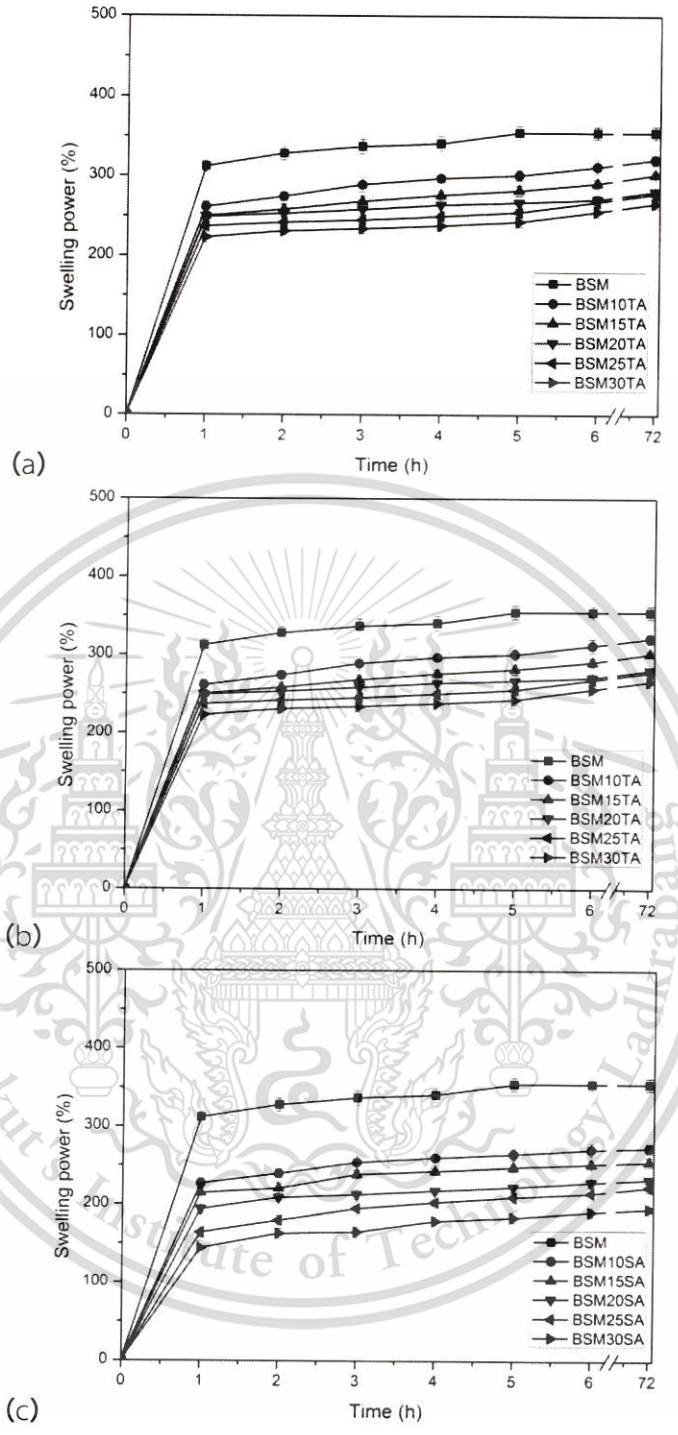

Figure 4.21 Swelling power of different native and cross-linked BSM films with **(a)** TA, **(b)** MA and **(c)** SA

Figures 4.20-4.21 show swelling power *vs* different lengths of time for both native and cross-linked films. Both native films showed the highest swelling power due to its hydrophilic nature. However, the incorporation of cross-linkers caused the decrease in the swelling power. This is because of increasing in the hydrophobicity by ester bond formation and cross-linking, which hindered the penetration of water into the polysaccharide molecular network.

Furthermore, greatly decrease of swelling power was observed as the contents of TA, MA and SA increased. This could be because there were an increase in the number of ester linkage with the increase TA, MA and SA content. Additionally, the results were related to FT-IR spectra that O-H stretching peaks of different cross-linked film, which shifted toward to lower wavenumbers due to new hydrogen bond formation.

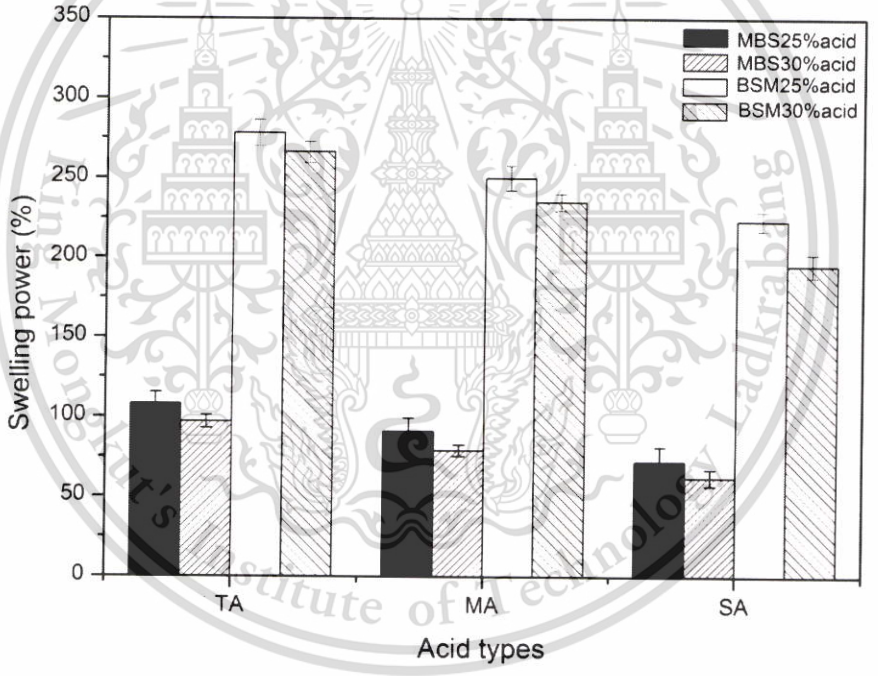

Figure 4.22 Swelling power of native and different cross-linked MBS and BSM films cross-linked by 30% of TA, MA and SA at the soaking period 72 hours

The swelling power of films cross-linked with acids of different types was markedly different (Figure 4.22). The TA cross-linked films showed the highest swelling power, followed by MA and SA cross-linked films. This is because the highest acidity of TA resulted in the strongest hydrolysis of glycosidic linkage, leading to a high hydrophilic property. In addition, a higher swelling power of films prepared with TA could arise from the steric hindrance from the presence of two-hydroxyl groups in TA that reduced the degree of cross-linking, as shown in Table 4.3. It can

be observed from Figure 4.22 that, at the same content, the addition of SA led to a lower swelling power than that of MA, suggesting that more ester linkages could form with the addition of SA.

The degree of amylose content also influences the reactivity of MBS and BSM. High amylose MBS content led to a more rigid structure that has been claimed to provide higher tensile and barrier properties [4]. MBS has high amylose content and a highly compact structure, which limits the swelling power [4]. Therefore, the swelling power of high amylose MBS films was lower than those of moderate amylose BSM films.

Furthermore, it was observed that all BSM films showed a higher swelling power than all cross-linked MBS films under the same conditions of cross-linking acid type and content. BSM structure has been reported to comprise of two major fractions of glucomannan (43%). The structure has a high ratio of glucose to mannose at 10:2 [58]. Glucomannan which is an acidic polysaccharide containing many carboxylic groups (-COOH) has a pK_a value of 3.0 [82]. These carboxylic groups strongly affected the swelling property of BSM films, i.e., the presence of many carboxylic groups in BSM made it more hydrophilic than MBS. This is because of the electrostatic repulsion between highly negatively charged of carboxylate groups in BSM molecules. Therefore, various cross-linked BSM films showed a higher swelling power as compared to MBS cross-linked films.

4.5 Water absorption

Water absorption of the various films was determined after the film was conditioned at 99±2% RH at room temperature.

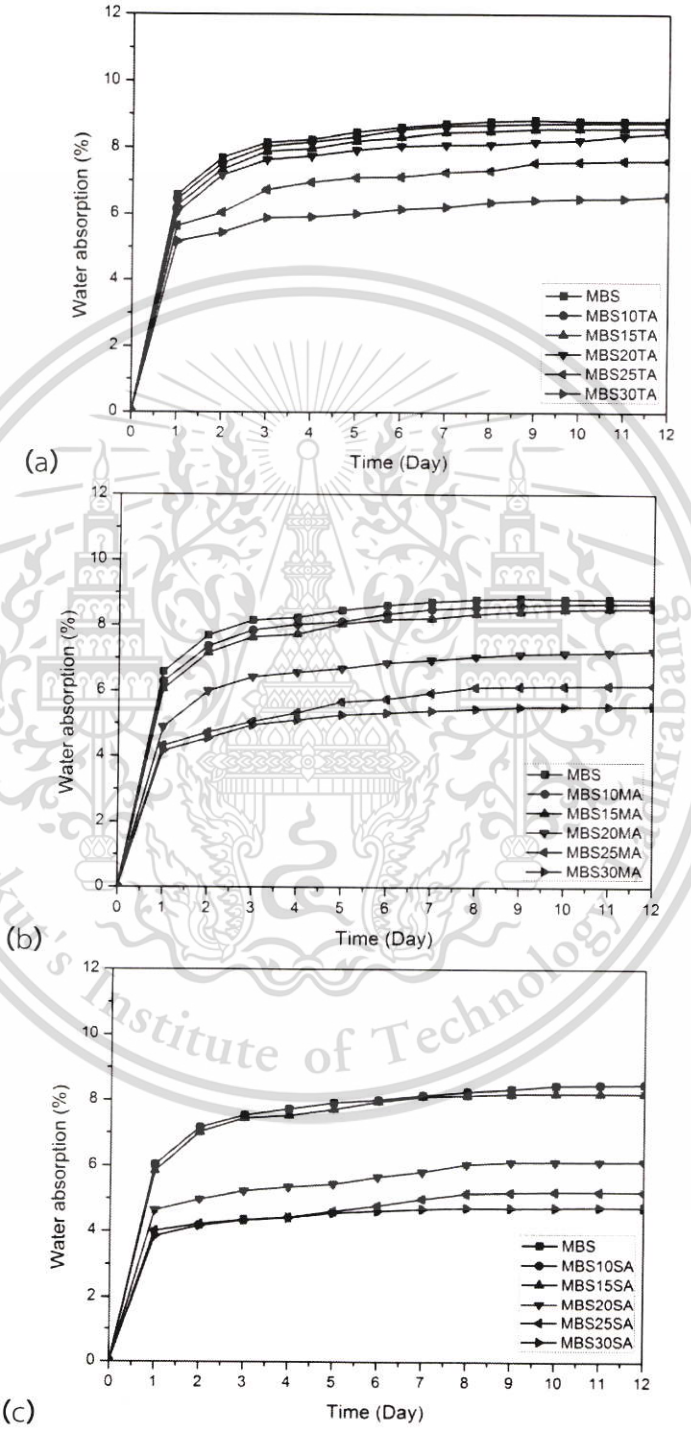

Figure 4.23 Water absorption of different native and cross-linked MBS films with **(a)** TA, **(b)** MA and **(c)** SA

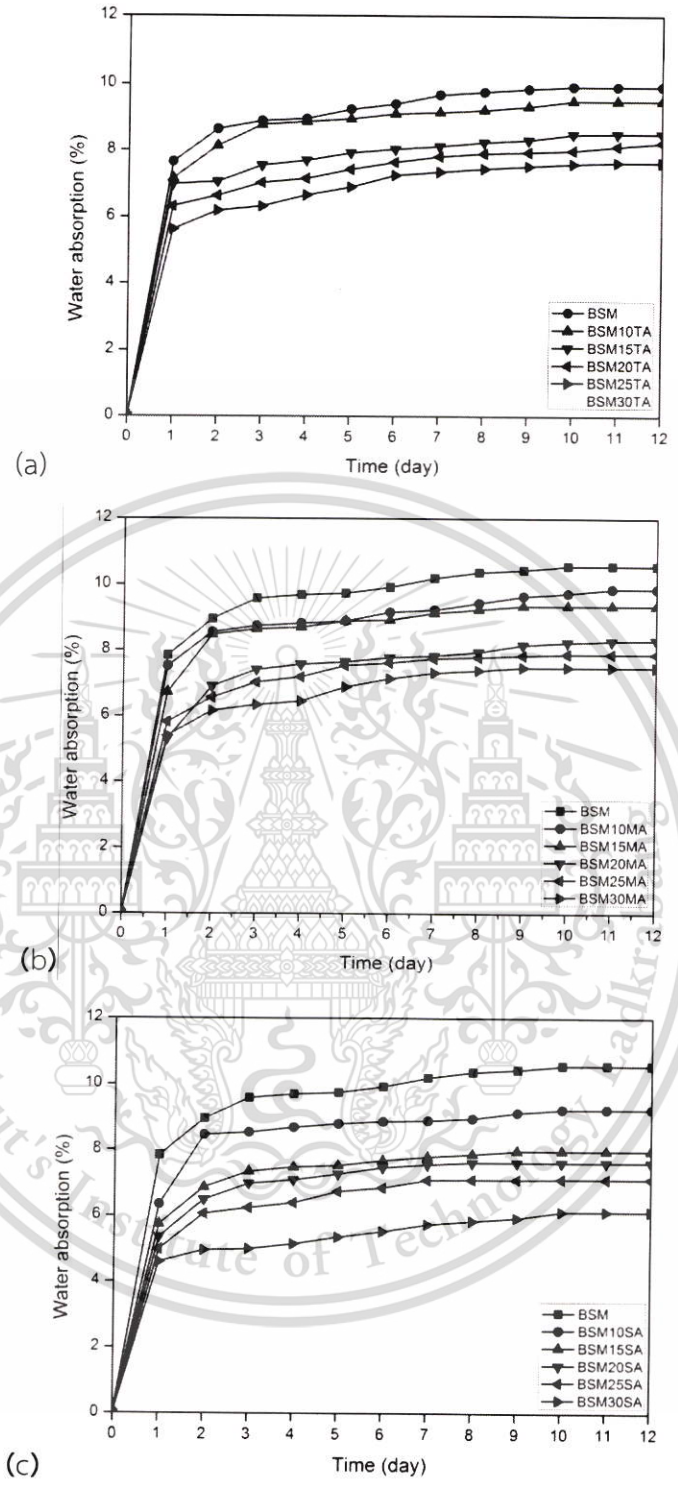

Figure 4.24 Water absorption of different native and cross-linked BSM films with **(a)** TA, **(b)** MA and **(c)** SA

As shown in Figures 4.23-4.24, both native MBS and BSM show the highest water absorption due to the hydrophilic nature of the polysaccharides. All cross-linked films showed the significantly less water absorption than the native MBS and BSM films. Cross-linking created a three-dimensional polymeric structure, which was stabilized via both hydrogen bonding and newly generated ester linkages, resulting in lower water absorption. Moreover, water absorption decreased as the density of cross linkers increased. Cross-linking strengthens the polysaccharides network, reducing the absorption of water and does not allow it to swell.

This agreed with Olsson *et al.*, who reported that the potato starch film cross-linked by CA noticeably decreased water absorption [84]. Kaewtatip *et al.* used cross-linked starch (Distarch phosphate) to improve the properties of thermoplastic starch (TPS)/cross-linked starch composites; they also found that cross-linking led to a significant loss of ability to absorb water [84].

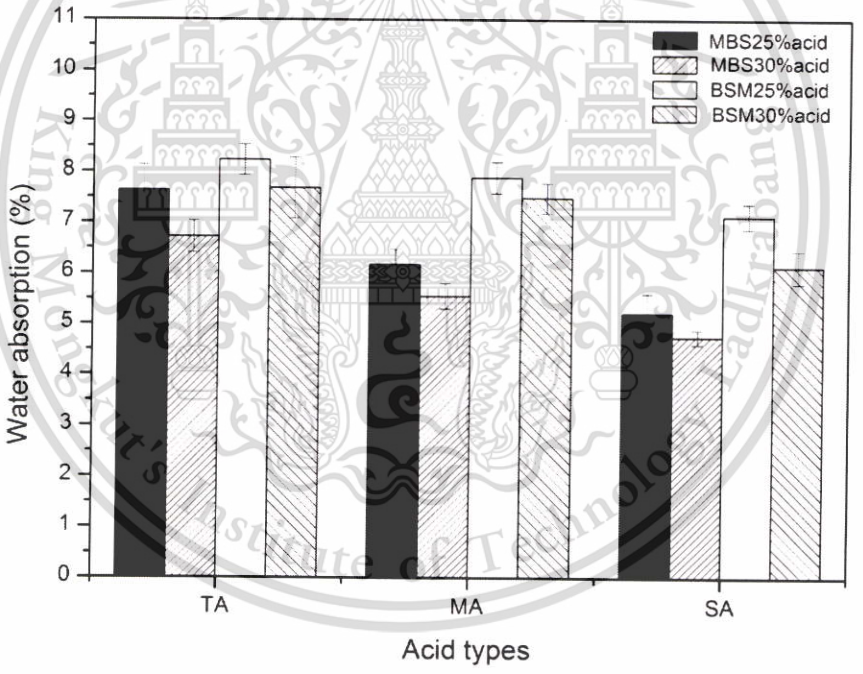

Figure 4.25 Water absorption of different native and cross-linked MBS and BSM films with 30**%** of TA, MA and SA at the period of 12 days

It was observed from Figure 4.25 that the water absorption capacities of the three types of films cross-linked with different acids could be ranked in the following order: films prepared with SA < MA < TA. Films cross-linked with TA showed the highest water absorption, compared to films cross-linked with MA and SA at similar content. This is because of the highest acidity of TA causing more hydrolysis of polysaccharide backbone chains, resulting in its more hydrophilic property. Moreover,

the steric hindrance from the two-hydroxyl groups in TA caused a lower degree of cross-linking, leading to a more hydrophilic property. It can be observed in Figure 4.38 that the addition of SA led to a lower water absorption capacity than that from the addition of MA, suggesting that more ester bridges were formed when SA was added.

MBS with greater amylose content tended to have a lower water absorption capacity. This may be attributed to an increase in starch polymer chain association at higher amylose content, resulting in a denser film matrix. Diffusion of water molecules in MBS film matrix might be more difficult as the matrix was more compact with a stronger cohesive force between the starch chains, causing a lower water absorption capacity as compared to BSM films.

Furthermore, all cross-linked BSM films prepared with the same acid type and content exhibited higher water absorption capacities than those of all cross-linked MBS films. BSM is an acidic polysaccharide because it contains uronic acid functional groups that affect its water absorption capacity. Uronic acid contains many carboxylic acid functional groups that can form solubilizing H-bonds with water. Carboxylic acid interacts more strongly with water compared to other organic compounds **[86]**. Therefore, the presence of many carboxylic groups in the BSM structure showed made it more hydrophilic than the cross-linked MBS films.

4.6 WVP

Circular test cups containing desiccant (0% RH) were sealed with film. The film was stored in a desiccator maintained at 75% RH with saturated NaCl. Water-vapor transport was determined from the weight gain.

Table 4.4 WVP of MBS and BSM films cross-linked by TA, MA or SA

Samples	WVP ($g.mm/m^2.day.kPa$)	Samples	WVP ($g.mm/m^2.day.kPa$)
MBS	4.03±0.04	BSM	3.38±0.07
MBS10TA	3.70±0.06	BSM10TA	3.35±0.06
MBS15TA	3.03±0.08	BSM15TA	3.31±0.07
MBS20TA	2.83±0.05	BSM20TA	3.23±0.04
MBS25TA	2.46±0.04	BSM25TA	3.06±0.09
MBS30TA	2.37±0.06	BSM30TA	2.69±0.06
MBS10MA	3.62±0.07	BSM10MA	3.30±0.04
MBS15MA	2.91±0.06	BSM15MA	3.22±0.07
MBS20MA	2.58±0.03	BSM20MA	2.79±0.05
MBS25MA	2.07±0.08	BSM25MA	2.34±0.08
MBS30MA	1.44±0.06	BSM30MA	1.62±0.03
MBS10SA	2.54±0.03	BSM10SA	2.95±0.05
MBS15SA	2.06±0.08	BSM15SA	2.74±0.07
MBS20SA	1.03±0.07	BSM20SA	2.25±0.06
MBS25SA	0.81±0.09	BSM25SA	1.76±0.03
MBS30SA	0.56±0.0	BSM30SA	1.04±0.05

The highest WVP was observed for the both native films, due to the abundance of hydroxyl groups in the polysaccharide molecules. All the cross-linked films showed lower WVP than both native films. The incorporation of cross-linkers causes a rise formation of hydrophobic C=O groups in BSM film by ester bond via cross-linking process, causing the difficulty for diffusion of water vapor molecules. Moreover, the formation of a dense networked structure after cross-linking inhibits absorption of water and also restricts the movement of molecules, causing the difficulty for diffusion of water vapor permeability.

The WVP of all TA cross-linked films tended to be the highest followed by those of MA and SA cross-linked BSM films. This is because TA was the strongest acid among these three acids. It caused the highest hydrolysis of backbone chains, leading to a more hydrophilic property. In addition, the higher WVP of TA cross-linked films could arise from the steric hindrance from the two-hydroxyl groups in TA that favored a lower degree of cross-linking. It can be observed from Table 4.4 that the addition of SA to polysaccharides led to a lower WVP of all produced films than the addition of MA, suggesting that more esterification and cross-linking occurred with the addition of SA and the results also correlated to the swelling power (Figure 4.20-4.21) and water absorption (Figure 4.23-4.24). This result agrees with a result of a study by Olsson E. *et al*. They reported that the water vapor barrier property of a potato starch film was improved by cross-linked with CA [83]. It should be noted that the WVP results are closely related to the swelling power results (Figure 4.22).

MBS films exhibited lower WVP values as compared to all BSM films prepared with the same acid type and content. MBS films with higher amylose content commonly a show higher barrier property than lower amylose content films. The high adjacency of starch chains from high amylose content per unit area led to formation of a dense structure, which consequently improved the WVP of MBS films. Therefore, diffusion of water molecules was more difficult in a more compact MBS film matrix due to a higher degree of cohesive force between MBS starch chains, hence causing lower WVP values as compared to BSM films.

Furthermore, all cross-linked BSM films exhibited higher WVP values as compared to all MBS films prepared with the same acid type and content. This is because BSM is a more hydrophilic acidic polysaccharide. The presence of uronic acid in the BSM structure provides BSM films with a higher hydrophilic property than all MBS films. These WVP results also correlated to the swelling power and water absorption (Figure 4.22 and 4.25, respectively).

4.7. Gel fraction

The insoluble part of each film cross-linked by TA, MA or SA was quantified by gel fraction method. Gel fraction measurements of native and cross-linked films are shown in Table 4.5. No gel content was detected in both native films subjected to DMSO due to its hydrophilic character. The increase in gel fraction for the cross-linked film showed stability compared to the both native film. From Table 4.5, it was clear that the gel fraction increased with increasing cross-linkers content. Cross-linking enhanced stability between polysaccharide molecules and enhanced the integrity of the film due to the additional ester bonds; and therefore, hydrophobic properties of cross-linked film increased.

Table 4.5 Gel fraction of MBS and BSM films cross-linked by TA, MA or SA

Samples	Gel fraction (%)	Samples	Gel fraction (%)
MBS	0	BSM	0
MBS10TA	29.60±0.04	BSM10TA	22.23±0.06
MBS15TA	44.13±0.05	BSM15TA	38.26±0.04
MBS20TA	65.50±0.03	BSM20TA	51.55±0.07
MBS25TA	76.40±0.06	BSM25TA	62.18±0.05
MBS30TA	87.25±0.07	BSM30TA	79.57±0.09
MBS10MA	38.81±0.05	BSM10MA	29.69±0.04
MBS15MA	50.47±0.04	BSM15MA	41.35±0.06
MBS20MA	79.17±0.03	BSM20MA	65.91±0.07
MBS25MA	83.41±0.05	BSM25MA	78.46±0.04
MBS30MA	92.30±0.07	BSM30MA	92.69±0.08
MBS10SA	44.87±0.04	BSM10SA	39.65±0.05
MBS15SA	69.85±0.09	BSM15SA	59.51±0.08
MBS20SA	88.79±0.06	BSM20SA	75.95±0.07
MBS25SA	90.20±0.04	BSM25SA	87.83±0.06
MBS30SA	98.05±0.03	BSM30SA	95.14±0.02

As expected, film, cross-linked with SA, showed the highest gel fraction, resulting from the higher degree of cross-linking. The increase in gel fraction of different cross-linkers also related to the results from the swelling power (Figure 4.22), water absorption (Figure 4.25) and WVP (Table 4.4).

All MBS films had higher gel fractions compared to those from BSM films prepared with the same acid type and content. Films with higher amylose content generally possess a higher barrier property than low amylose content films [4]. These gel fraction results were consistent with the high degree of crystallinity of all cross-linked MSB films (Table 4.3), indicating that a high degree of crystallinity could improve the barrier property and amount of gel fraction.

Moreover, BSM films showed lower gel fractions as compared to those from MBS films prepared with the same acid type and content. BSM contains uronic acid, which makes it more polar. The lower gel fraction of cross-linked BSM films is highly dependent on its ionic strength, which is higher when more carboxylate groups are present [85]. The highly expanded conformation of BSM in water is related to the electrostatic repulsion of negatively charged side chains, which is responsible for its high solubility in water and lower gel fraction.

4.8 Mechanical properties

Young's modulus, stress at maximum load and strain at maximum load of various films are summarized in Figures 4.26 - 4.27. It can be observed that both native films showed a higher stress at maximum load and Young's modulus but a lower strain at maximum load than those cross-linked films. This is due to excessive hydrogen bonds among polysaccharide molecules.

On the contrary, cross-linked films by TA, MA or SA exhibited a lower stress at maximum load and Young's modulus than their native films. Consequently, their strain at maximum load was significantly increased, like that for aconitic acid cross-linked potato starch film reported in [10]. This could be because the acid cross-linker reacted with hydroxyl groups in polysaccharide molecules and formed ester linkages that were more difficult to break. The mechanical property results also confirmed the decrease in the degree of crystallinity shown in Table 4.3. Moreover, it can be observed that cross-linked films by 30% TA, MA or SA showed a lower stress at maximum load and Young's modulus than films cross-linked by 10, 15, 20 and 25 wt% TA, MA or SA. As a result, the increase in strain at maximum load was obtained. This is because there is more excessive of cross-linking bridges, resulting in lower chain stiffness and higher extendibility. This result also agrees with that from Reddy N et al. who reported that a high CA content caused by excessive cross-linking led to a decrease in tensile strength [49].

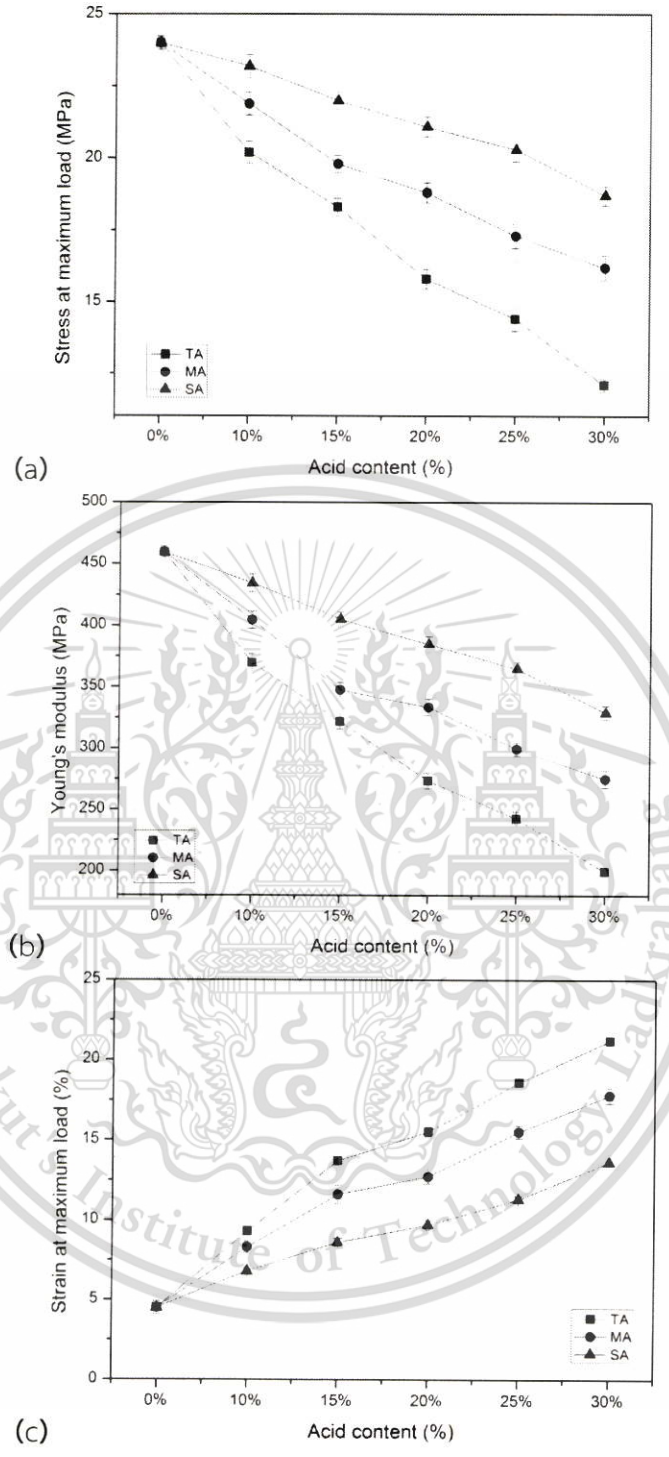

Figure 4.26 Mechanical properties of different MBS films cross-linked with TA, MA and SA **(a)** stress at maximum load, **(b)** Young's modulus and **(c)** strain at maximum load

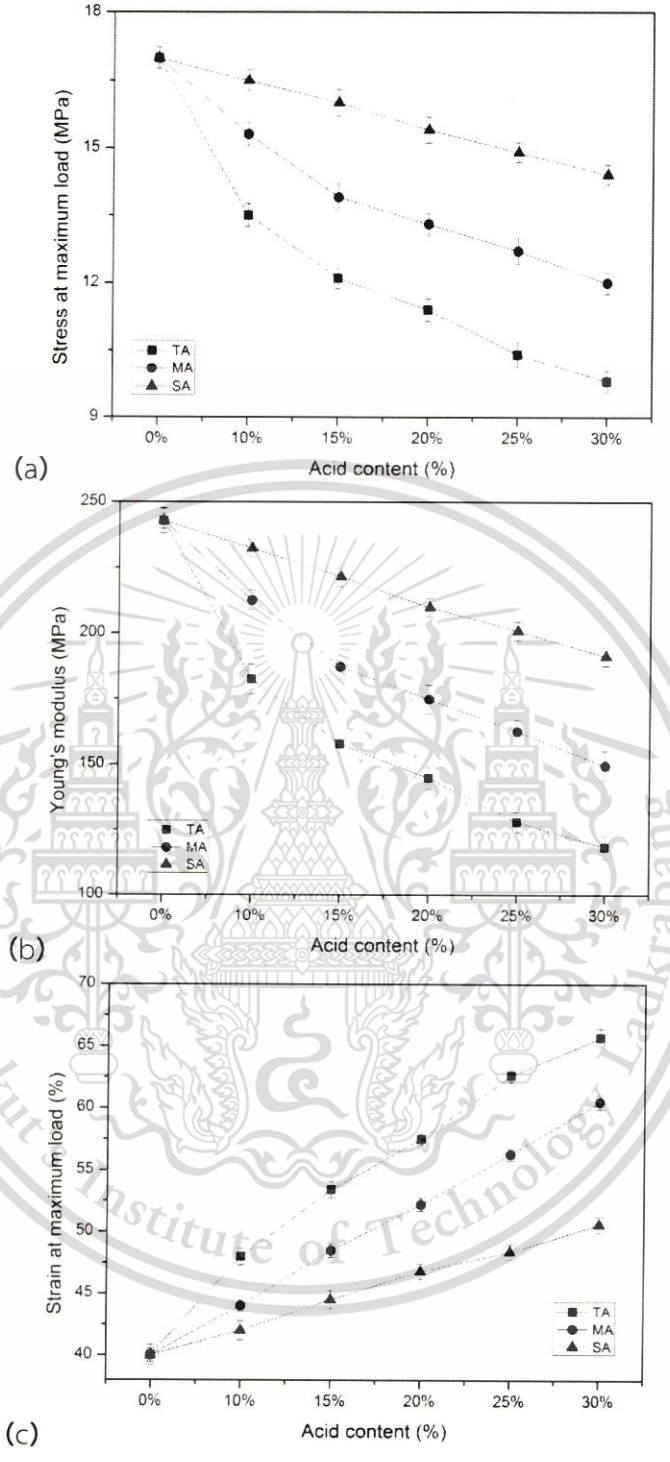

Figure 4.27 Mechanical properties of different BSM films cross-linked with TA, MA and SA (d) stress at maximum load, (e) Young's modulus and (f) strain at maximum load

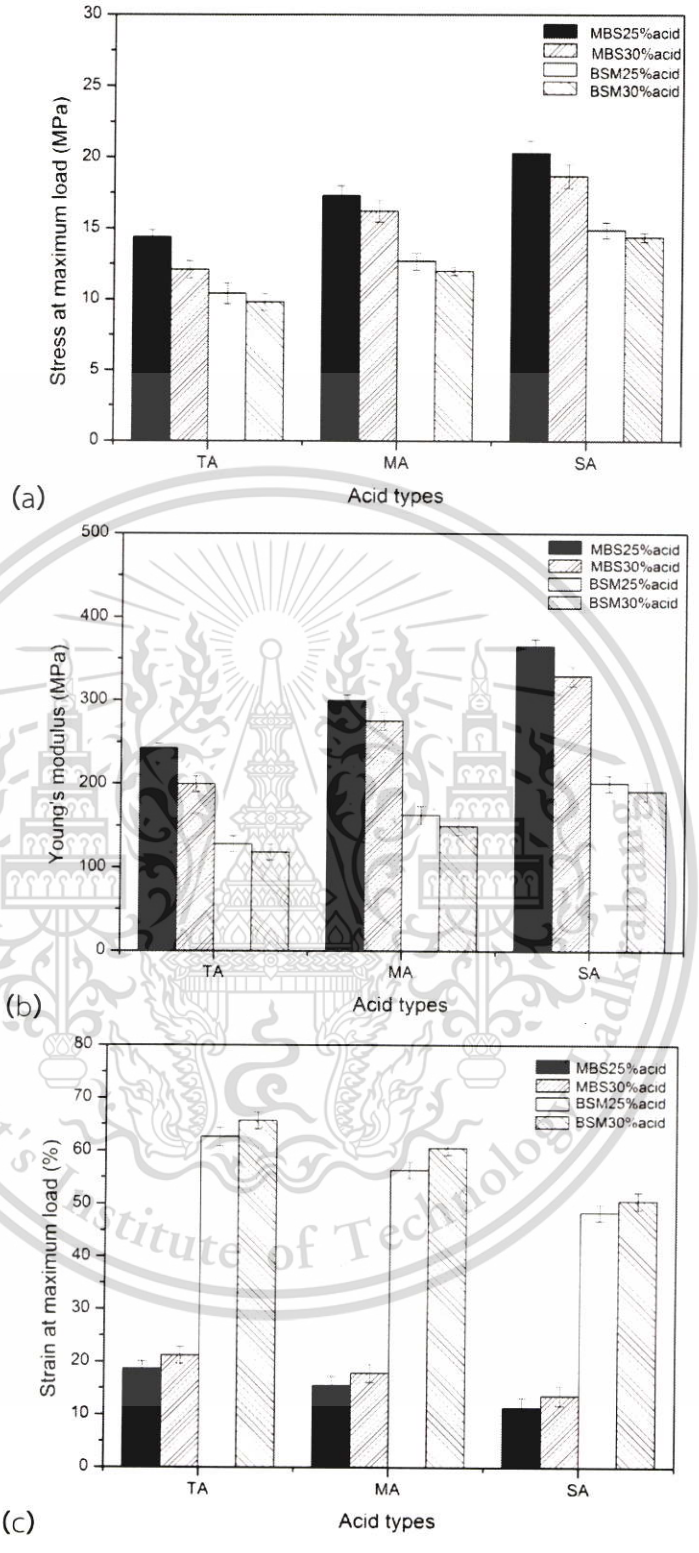

Figure 4.28 Mechanical properties of different MBS and BSM films cross-linked with TA, MA and SA **(a)** stress at maximum load, **(b)** Young's modulus and **(c)** strain at maximum load

Regarding films cross-linked by TA, MA and SA, the results (Figure 4.28) suggested that films cross-linked by SA exhibited the highest stress at maximum load and Young's modulus hence the lowest strain at maximum load. This is because of the highest degree of crystallinity of SA cross-linked films as confirmed by XRD (Table 4.3), gel fraction (Table 4.5) and swelling power (Figure 4.22). Moreover, the highest acidity of TA resulted in more hydrolyzed polysaccharide molecules and led to the lowest tensile strength and highest strain at maximum load of films prepared with it than those prepared with MA or SA. Similar trends have been reported for corn starch/PVA blend films cross-linked with MA and SA [8]. In addition, the values of stress at maximum load and Young's modulus of cross-linked MBS and BSM films with MA and SA are competitive to that of commercial LDPE film [86].

Moreover, due to the high amylose content of MBS films, their strength and stiffness were expected to be high and observed to be so compared to those of BSM films. This is due to extensive hydrogen bonding among MBS molecules. Amylose-rich MBS films were stronger than BSM films prepared with the same acid type and content.

Furthermore, the uronic acid functional group has a strong affinity for water molecules, allowing BSM films to easily form hydrogen bonds with water and retain it. Therefore, BSM films exhibited an enhanced strain at maximum load when compared with that of MBS films prepared with the same acid type and content.

4.9 Soil burial test

Before the test, films were buried about 10 cm under the surface of 10-15% moisture soil over a period of 5 and 10 days.

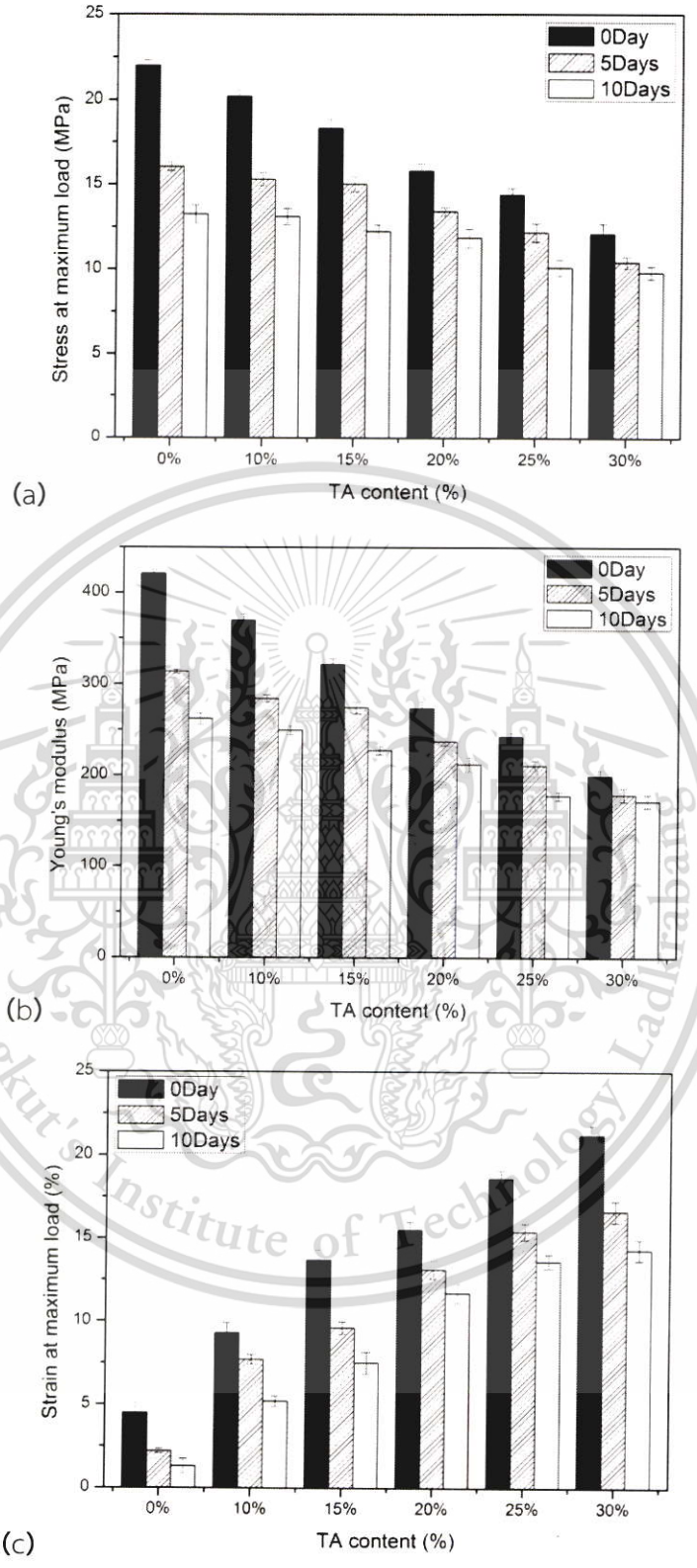

Figure 4.29 Mechanical properties after biodegradation in soil of different MBS films cross-linked by TA **(a)** stress at maximum load, **(b)** Young's modulus and **(c)** strain at maximum load

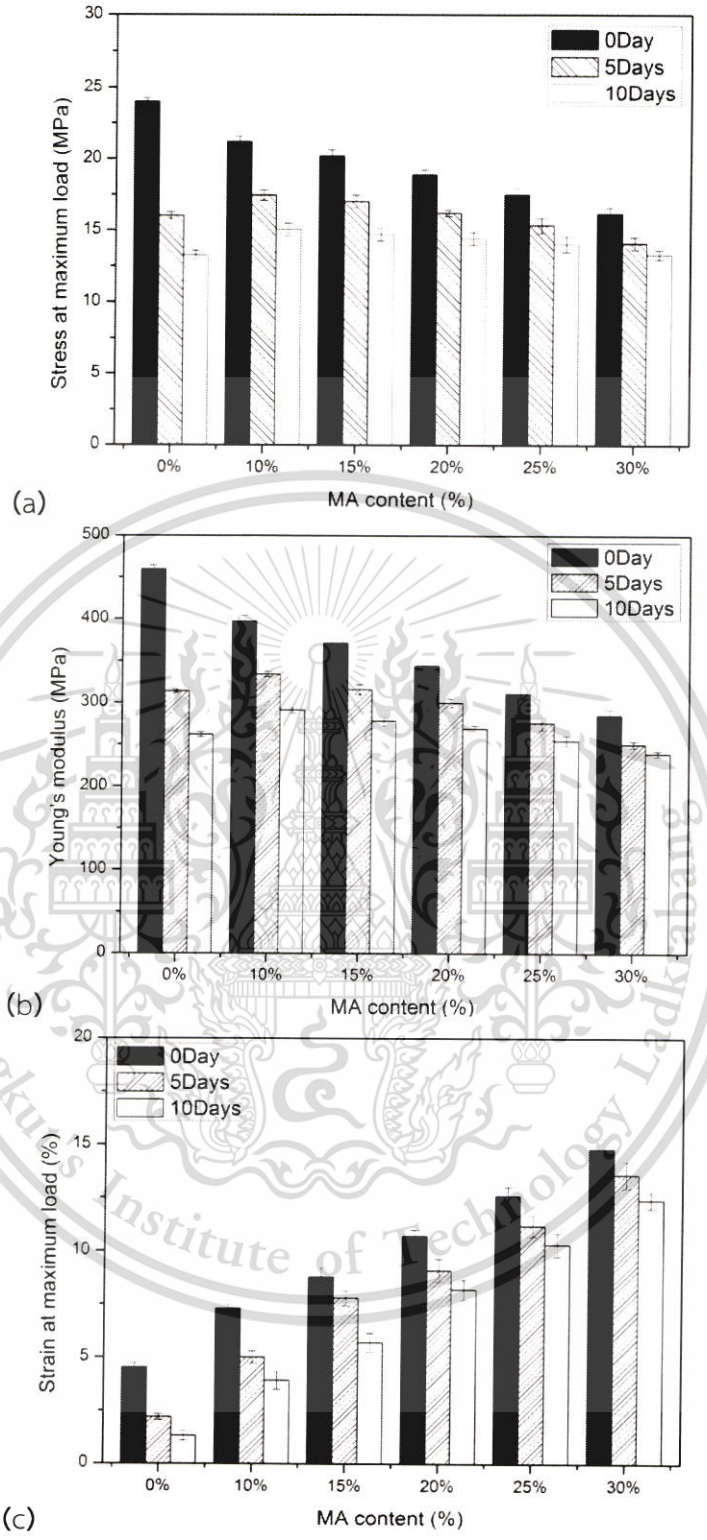

Figure 4.30 Mechanical properties after biodegradation in soil of different MBS films cross-linked by MA **(a)** stress at maximum load, **(b)** Young's modulus and **(c)** strain at maximum load

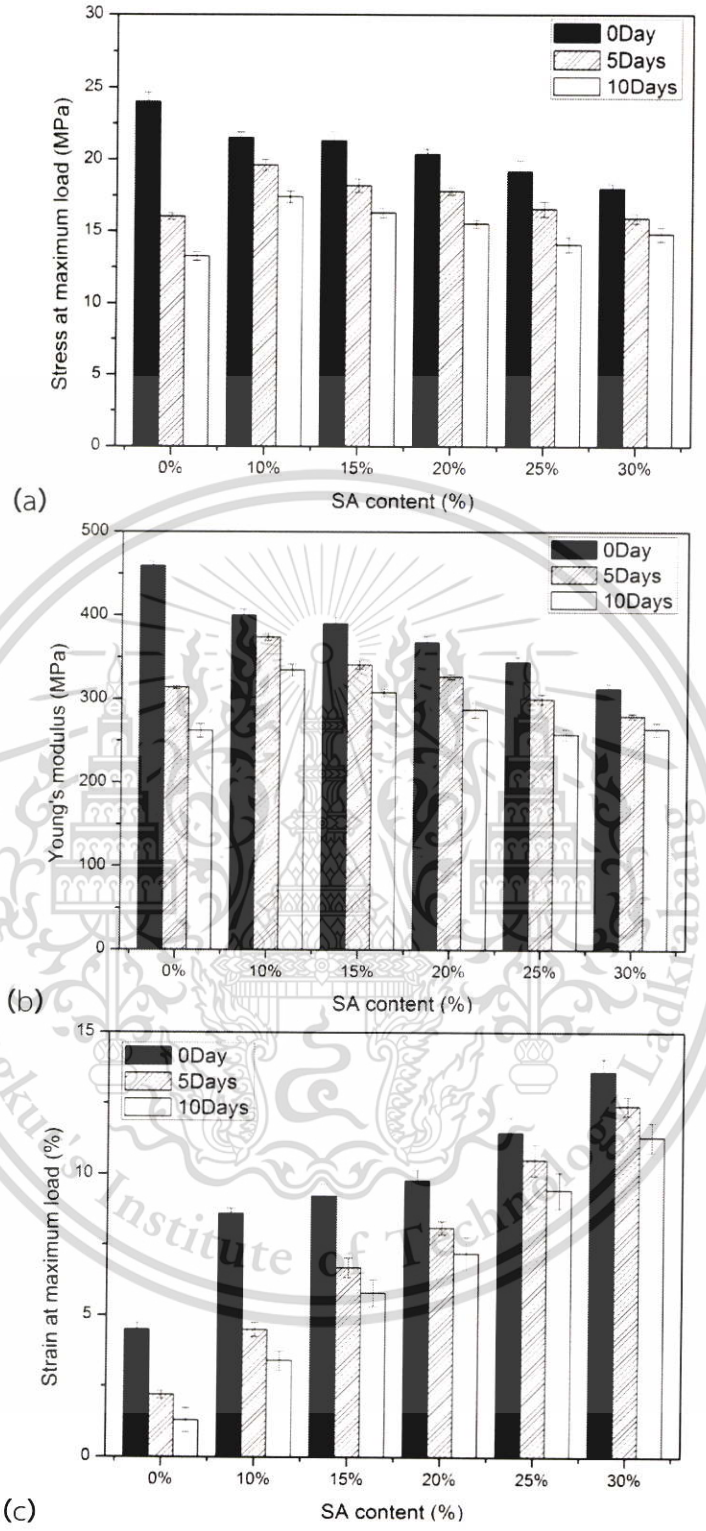

Figure 4.31 Mechanical properties after biodegradation in soil of different MBS films cross-linked by SA **(a)** stress at maximum load, **(b)** Young's modulus and **(c)** strain at maximum load

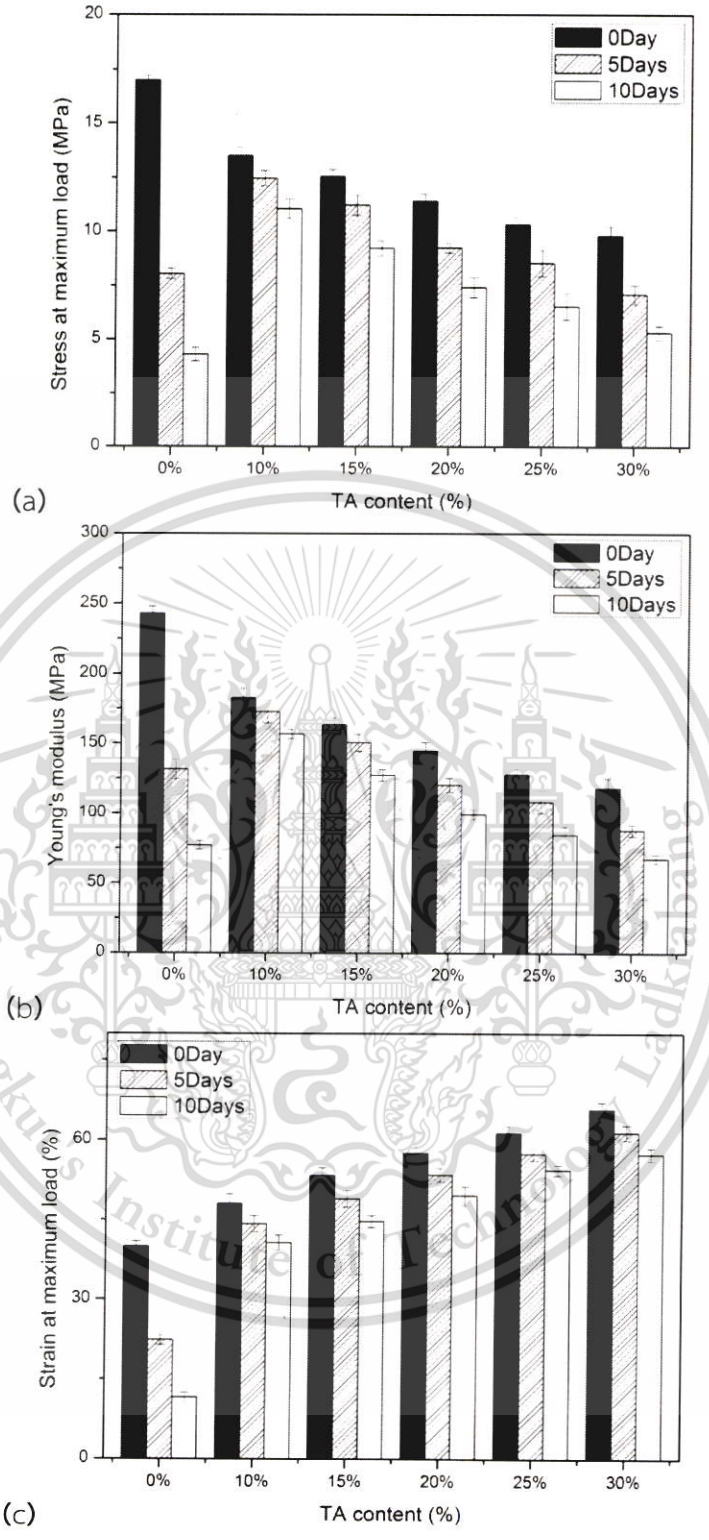

Figure 4.32 Mechanical properties after biodegradation in soil of different BSM films cross-linked by TA **(a)** stress at maximum load, **(b)** Young's modulus and **(c)** strain at maximum load

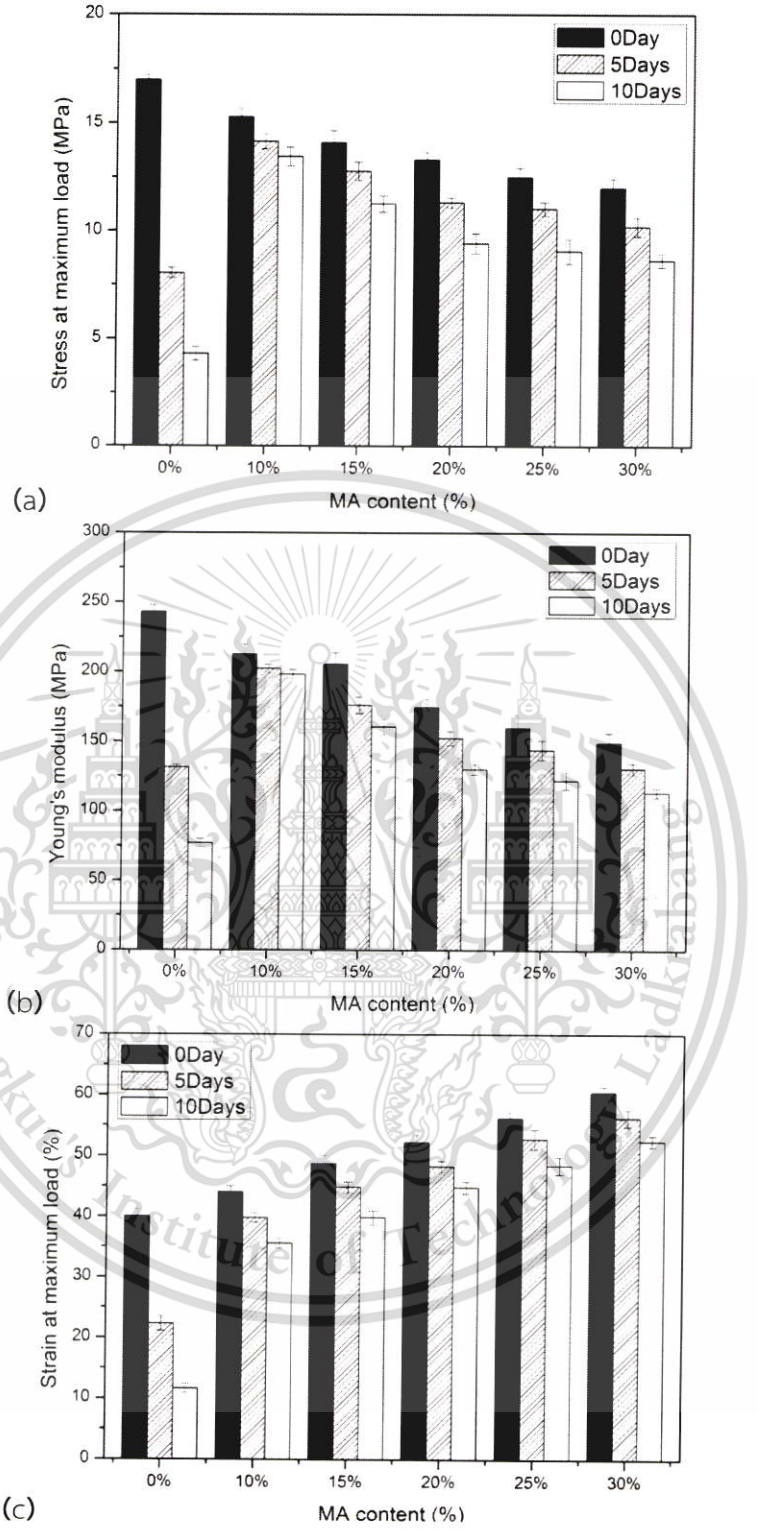

Figure 4.33 Mechanical properties after biodegradation in soil of different BSM films cross-linked by MA (a) stress at maximum load, (b) Young's modulus and (c) strain at maximum load

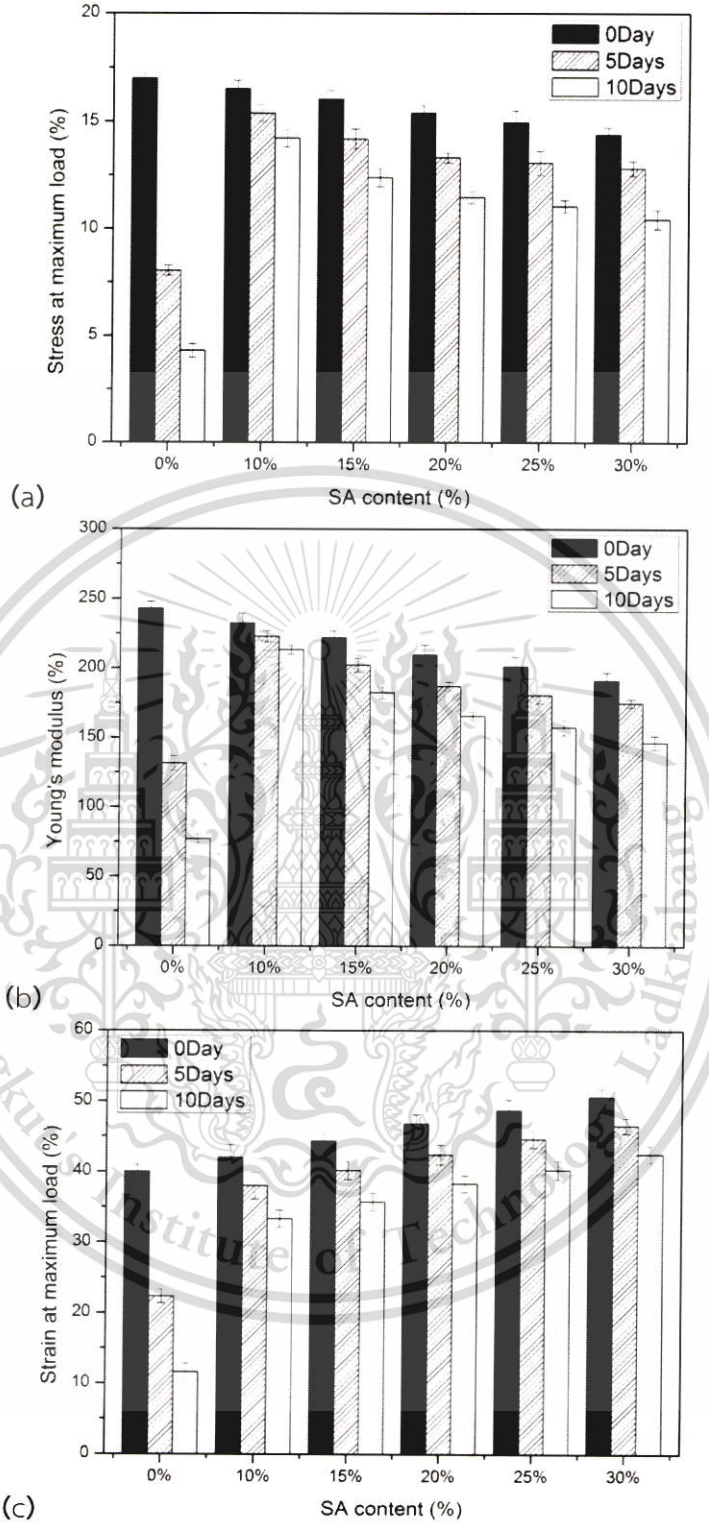

Figure 4.34 Mechanical properties after biodegradation in soil of different BSM films cross-linked by SA (a) stress at maximum load, (b) Young's modulus and (c) strain at maximum load

Figures 4.29 - 4.34 show the tensile properties of various native and cross-linked films before and after biodegradation in the soil burial test. After having been buried, every film sample showed a significant drop in its stress at maximum load from absorption of moisture from the soil and hydrolysis of the polysaccharide chains as well as biodegradation by microorganisms in the soil [88].

In addition, a film cross-linked with TA exhibited the lowest strength and elasticity compared to those cross-linked with MA and SA in this order at the same percentage of acid content after buried. This implies that the rapid degradation of polysaccharide chains was mainly due to acid hydrolysis since TA has a higher acidity than MA and SA and in part due to the lowest crystallinity of the film cross-linked with TA (Table 4.3) among the three types of cross-linked films tested.

It was observed from the Figure 4.49 that film with higher amylose content commonly provides a higher water barrier than a film with lower amylose content. After soil burial test, the high amylose content of MBS made its cross-linked counterpart provide a higher stress at maximum load and Young's modulus as well as a lower strain at maximum load compared to those provided by BSM. Amylose-rich MBS film was stronger than BSM films because of more numerous hydrogen bonds among MBS molecules.

In addition, uronic acid functional groups in BSM give it a strong affinity for water molecules in the soil, allowing the film to easily retain water and form hydrogen bonds, leading to more rapid biodegradation. These results are consistent with the higher WVP and swelling power of BSM film shown in Table 4.4 and Figure 4.26, respectively.

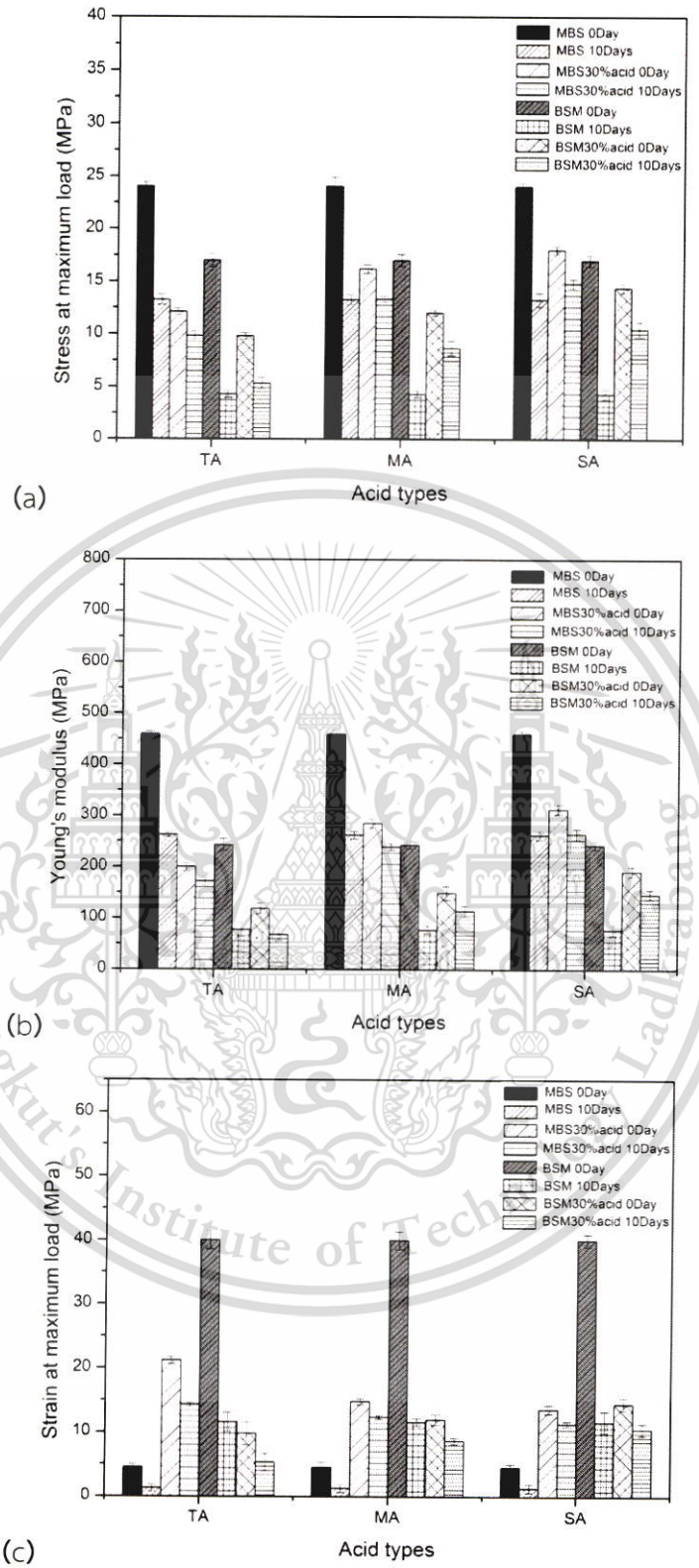

Figure 4.35 Mechanical properties after biodegradation in soil of different MBS and BSM films cross-linked by TA, MA or SA **(a)** stress at maximum load, **(b)** Young's modulus and **(c)** strain at maximum load

4.10 TGA

Thermogravimetric (TGA) and derivative thermal gravimetric (DTG) analyses used a thermogravimetric analyzer. Film was scanned from 50 °C to 700 °C at a 10 °C/min in a nitrogen atmosphere to characterize thermal stability and degradation temperature.

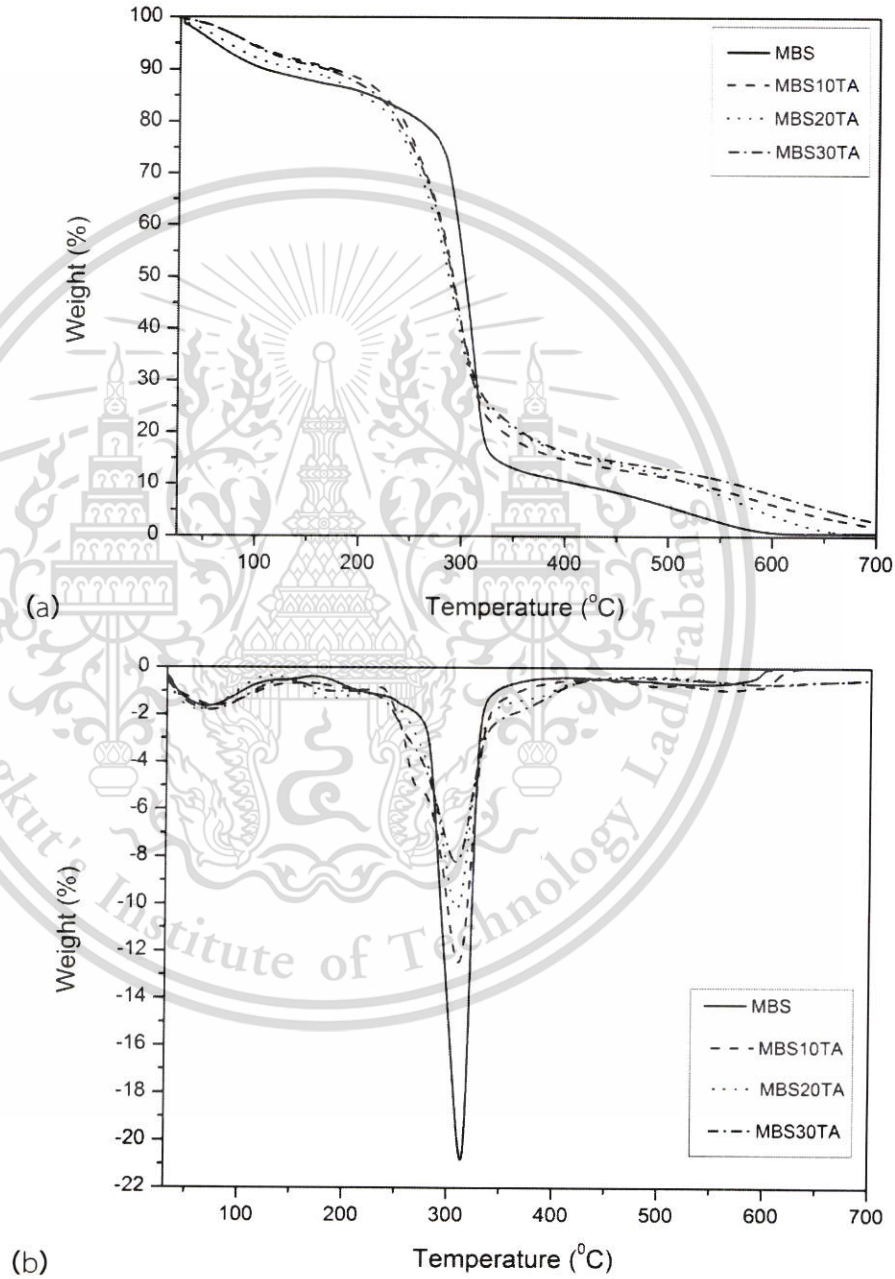

Figure 4.36 (a) TGA and (b) DTG thermograms of different modified MBS films by TA

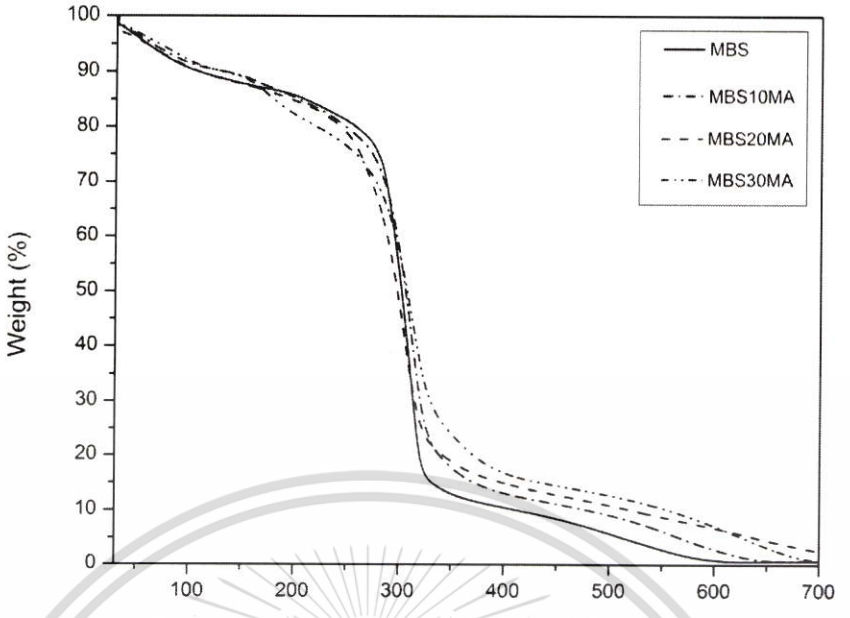

(c)

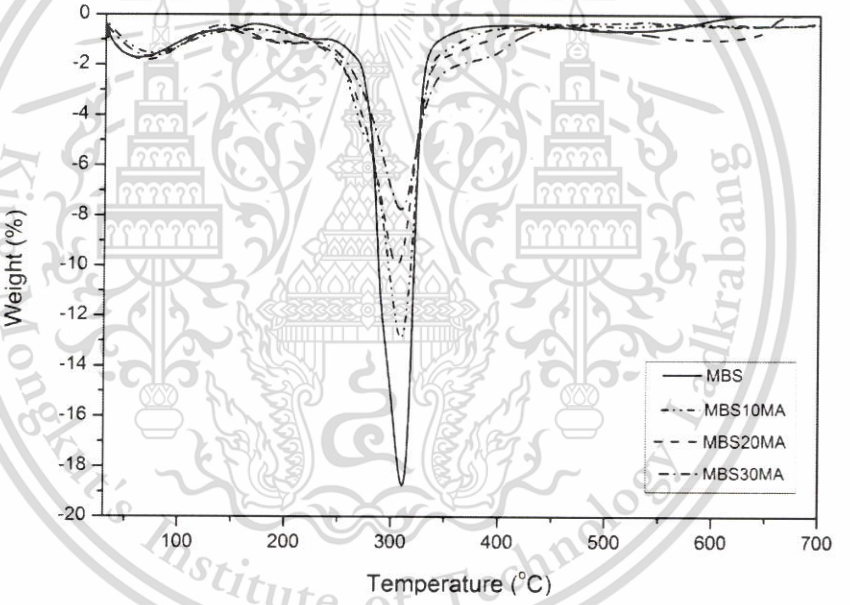

(d)

Figure 4.37 (c) TGA and (d) DTG thermograms of different modified MBS films by MA

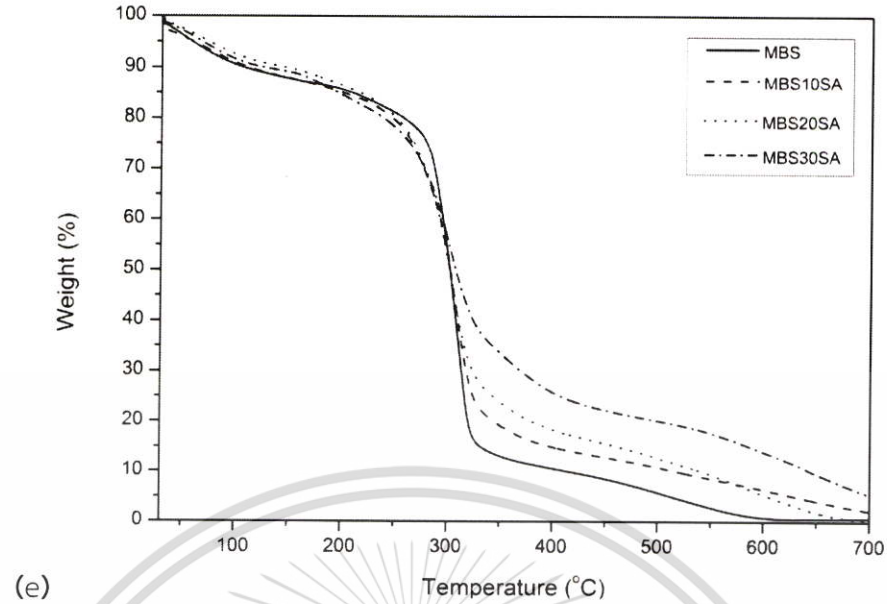

(e)

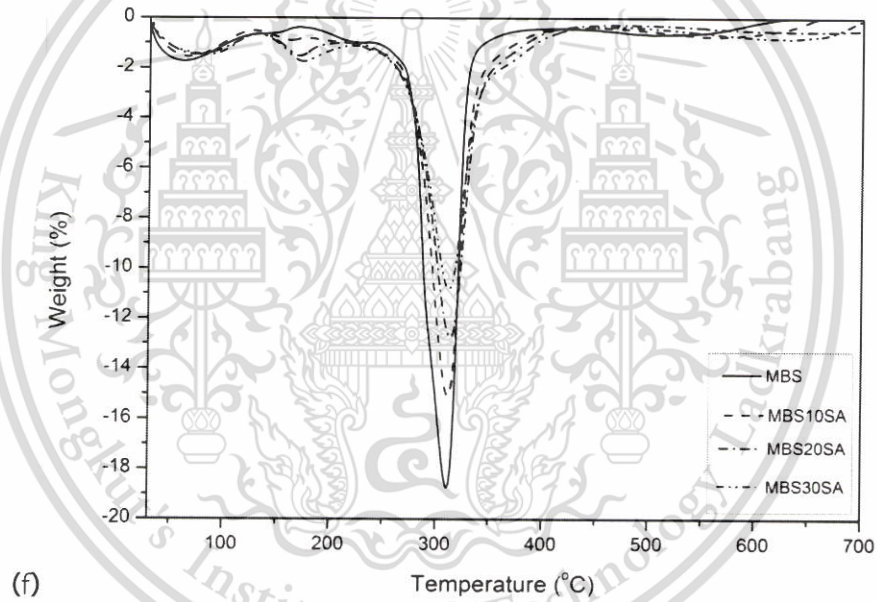

(f)

Figure 4.38 (e) TGA and (f) DTG thermograms of different modified MBS films by SA

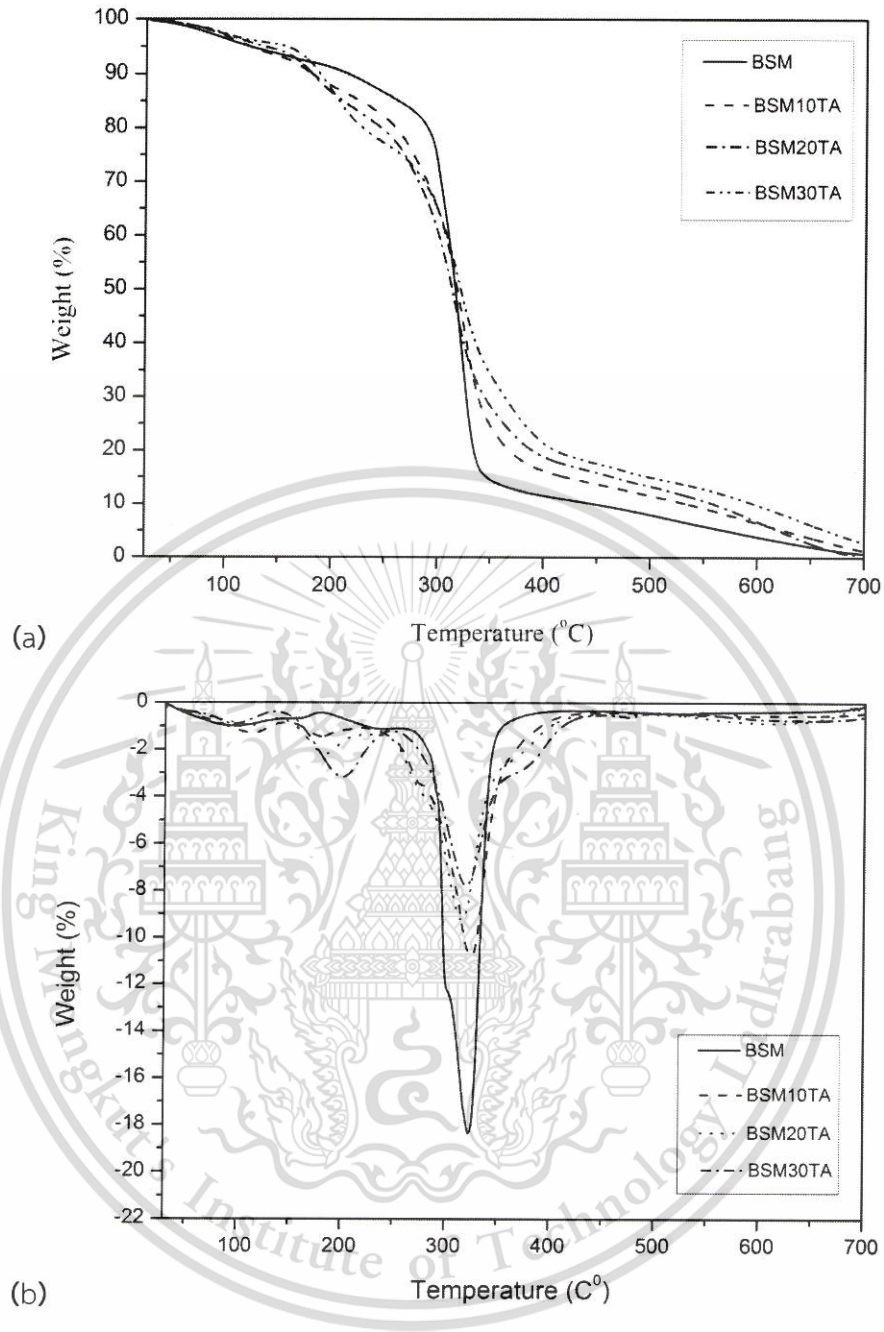

Figure 4.39 (a) TGA and (b) DTG thermograms of different modified BSM films by TA

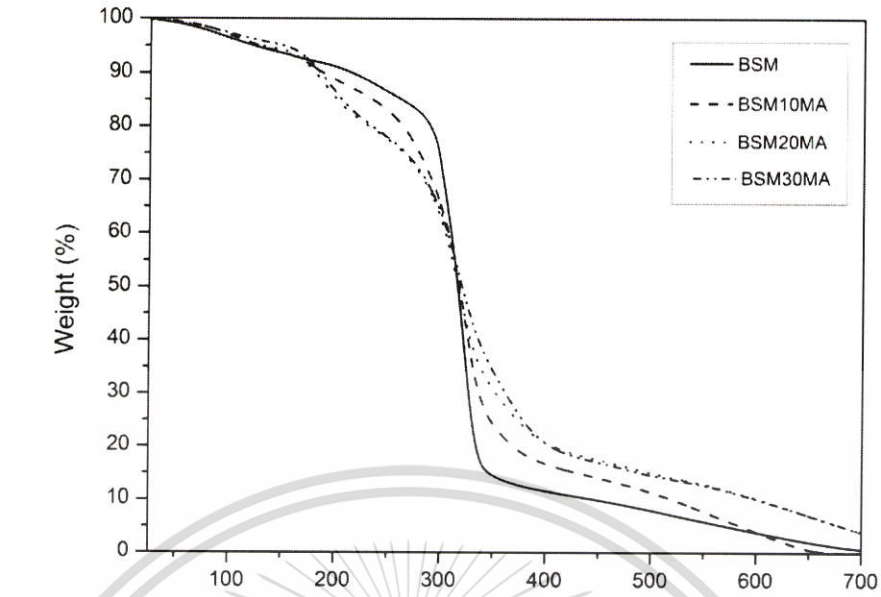

(c)

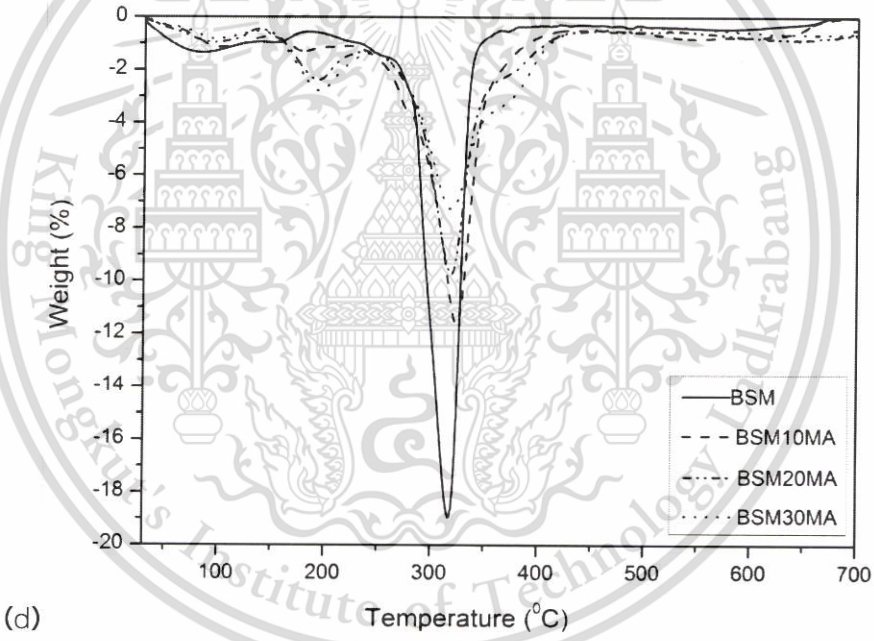

(d)

Figure 4.40 (c) TGA and (d) DTG thermograms of different modified BSM films by MA

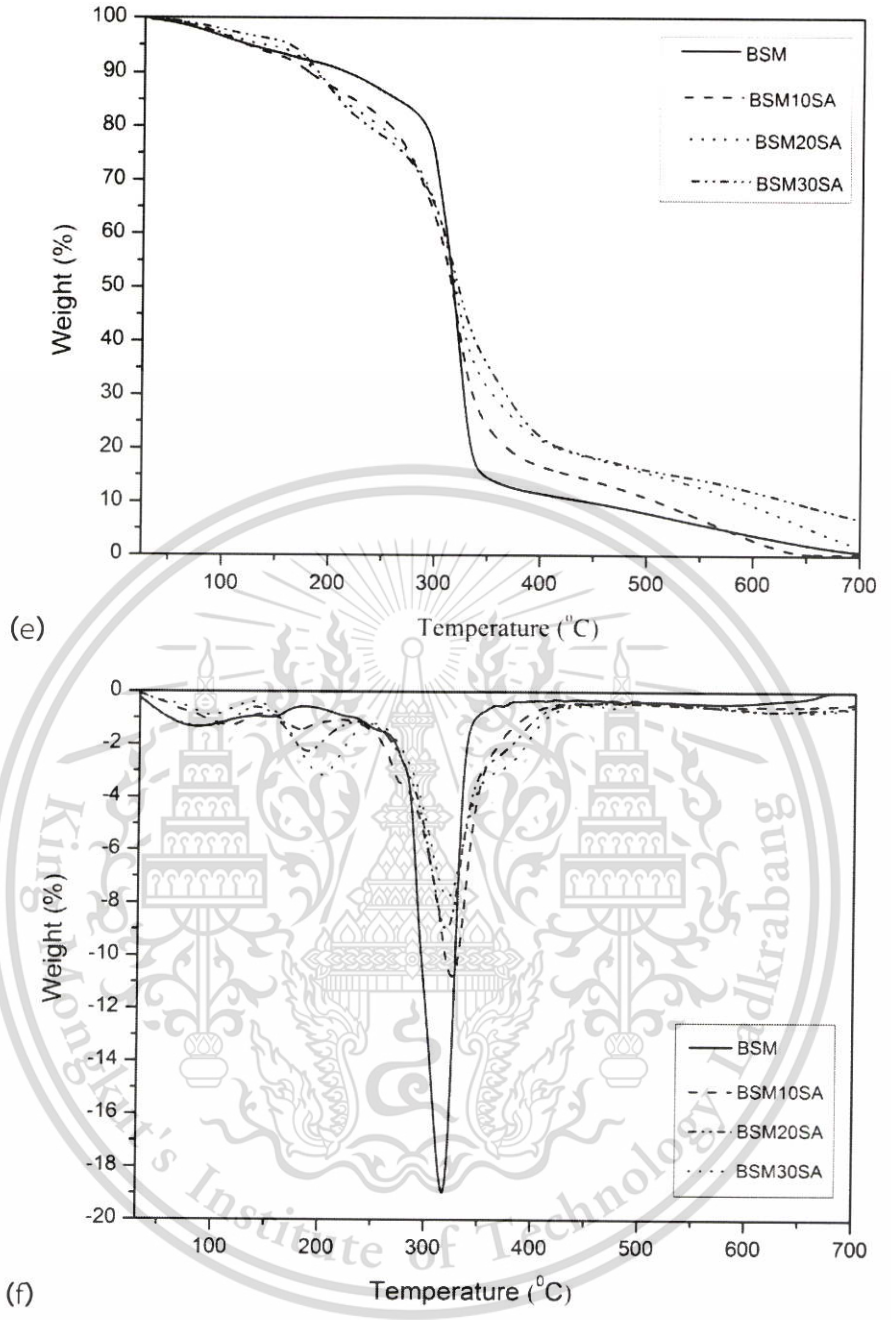

Figure 4.41 (e) TGA and (f) DTG thermograms of different modified BSM films by SA

Table 4.6 Decomposition temperatures and residual weight percentage of different native and cross-linked films obtained from TG and DTG thermograms

Samples	Thermal decomposition temperature (°C)					Residues (%)
	Zone 1 (Water)	Zone 2 (Glycerol)	Zone 3 (Hydrolyzed starch)	Zone 4 (Starch)	Zone 5 (Cross-linked starch)	600 °C
MBS	**72.6**	**172.4**	-	**305.4**	-	**0**
MBS10TA	72.4	175.3	262.4	310.9	366.1	3.3
MBS20TA	67.3	177.1	264.1	311.2	368.4	7.2
MBS30TA	70.1	179.4	260.5	311.4	372.8	10.1
MBS10MA	74.1	185.3	272.2	308.4	365.3	5.2
MBS20MA	68.2	186.2	274.5	309.8	370.4	8.4
MBS30MA	70.7	183.6	277.1	317.9	382.3	12.1
MBS10SA	65.5	184.4	-	311.6	370.2	6.5
MBS20SA	68.1	184.1	-	313.2	376.1	9.5
MBS30SA	74.3	187.9	-	325.8	388.6	16.0
BSM	**70.2**	**170.5**	-	**302.9**	-	**0**
BSM10TA	73.1	176.2	263.0	308.8	364.9	5.5
BSM20TA	71.4	176.5	262.5	305.1	369.4	7.8
BSM30TA	68.8	187.7	260.4	310.6	373.5	10.4
BSM10MA	72.4	191.3	262.3	306.3	366.8	4.8
BSM20MA	71.1	189.2	263.5	310.4	371.2	8.0
BSM30MA	70.7	189.6	262.8	317.2	381.4	11.9
BSM10SA	78.4	192.3	-	310.3	369.8	4.7
BSM20SA	81.2	189.6	-	312.9	375.5	8.3
BSM30SA	84.3	188.7	-	325.2	380.9	14.4

TGA and DTG thermograms of native and cross-linked films are presented in Figure 4.36-4.41 and Table 4.6. The first stage corresponds to water evaporation which occurred at about 70-80 °C; the second stage at approximately 180 °C is associated with degradation of the glycerol-rich phase. In addition, all cross-linked film showed a third stage decomposition at 260 °C, due to decomposition of hydrolyzed polysaccharide molecules thus the molecular weight and thermal resistance of the polysaccharide film was reduced [74].

The main degradation stage at 300 °C is assigned to thermal degradation of polysaccharide backbone [87]. Furthermore, another thermal degradation step for TA, MA and SA cross-linked films was observed at 370 °C [74]. This is attributed to formation of stronger ester bonds between the acids and polysaccharide chains. Moreover, this behavior shows that the temperature of the main degradation step (step 4) of cross-linked films clearly increased compared to those of the native films. This may be because TA, MA and SA enhanced the intermolecular interactions between the polysaccharide backbone chains by cross-linking them, which strengthened the covalent network, resulting in the increase in thermal degradation temperature of the cross-linked films.

By comparison, cross-linked films also exhibited a higher residual weight percentage (step 5), which can be explained by the effect of extensive cross-linking between the acids and polysaccharide chains. It should be noted that SA cross-linked films exhibited the highest residual weight percentage and thermal degradation temperature among cross-linked films, which suggests that SA was able to create the highest degree of cross-linking in a film. The results clearly correspond to the swelling power (Figure 4.22), water absorption (Figure 4.25), WVP (Table 4.4) and gel fraction (Table 4.5). In addition, there was no significant difference in the thermal degradation temperature of MBS and BSM due to the similarity of their chemical structures.

Chapter 5

Conclusion and suggestions

5.1 Conclusion

The molecular changes in polysaccharide of biodegradable films cross-linked with different acids—TA, MA and SA—at different levels—10%, 15%, 20%, 25% and 30% were investigated. After testing and characterization, conclusions are exhibited as follows.

1. FT-IR spectra showed new ester linkages. This could be confirmed by the presence of carbonyl (C=O) peak at 1730 cm^{-1} in cross-linked film. In addition, the O-H stretching (3500-3300 cm^{-1}) peaks of the cross-linked films also shifted to lower wavenumbers.

2. From XRD spectra, the addition of TA, MA and SA resulted in the decrease of degree of crystallinity, as compared to both native films. Moreover, the degree of crystallinity of both SA cross-linked films was the highest, followed by MA- and TA-cross-linked films. Additionally, it can be seen that the MBS showed higher degree of crystallinity compared to BSM films.

3. From SEM micrograph, the incorporation of TA, MA and SA produced smoother in MBS and BSM films, more homogeneous and continuous than those of both native films. Moreover, the different cross-linked films do not showed appreciable difference in morphology by the use of various acids types and acid contents.

4. Both native films showed the highest swelling power compared to those cross-linked films. However, the addition of TA, MA and SA caused the decrease the swelling power. In addition, the increasing contents of the cross-linker tended to decrease swelling power. Additionally, the swelling power of TA cross-linked films showed the highest, descending followed by MA and SA cross-linked films, respectively. Moreover, cross-linked MBS films presented lower swelling power than cross-linked BSM films.

5. Water absorption of all cross-linked film was lower than those of native films. TA cross-linked films showed the highest water absorption followed by MA and SA cross-linked films, respectively. Cross-linked MBS films presented lower water absorption as compared to cross-linked BSM films. The lowest water absorption was found in MBS30SA, while the highest was observed for BSM10TA.

6. WVP values of cross-linked MBS and BSM films with TA, MA and SA were lower compared to both native films. Moreover, the increase of the acid cross-linkers content tended to decrease WVP values. WVP values of all cross-linked MBS films were lower than cross-linked BSM films. The lowest WVP value was clearly observed in MBS30SA.

7. From gel fraction, there was no gel content detectable in both native films subjected to DMSO. Gel fraction of all cross-linked films was clearly increased with the increasing of cross-linker content. Cross-linked BSM films presented lower gel fraction than cross-linked MBS films. BSM10TA showed the lowest gel fraction among various cross-linked films.

8. Cross-linked films exhibited slightly lower stress at maximum load and Young's modulus than both native films. Consequently, strain at maximum load was significantly increased. Comparison between TA, MA and SA, the films cross-linked by SA illustrated higher stress at maximum load and Young's modulus; and subsequently, lower strain at maximum load than that by TA and MA. Moreover, cross-linked MBS film showed higher stress at maximum load and Young's modulus but lower strain at maximum load as compared to cross-linked BSM films.

9. The resulted presented that both native and all cross-linked films showed biodegradability. Both native films degraded faster than all cross-linked films. Cross-linked films with SA degraded at a slower rate as compared to cross-linked film with MA and SA, respectively. Moreover, BSM film cross-linked with TA showed the quickest biodegradation.

10. By comparison, various cross-linked films exhibited both higher thermal degradation temperature and higher residual weight percentage than MBS and BSM native films. In addition, both SA cross-linked films presented the maximum of thermal degradation (387 °C) and residual weight percentage than those of MA and TA cross-linked films.

11. It was concluded that cross-linked MBS film with 30% SA showed the greatest overall properties than those of the cross-linked films. MBS film cross-linked with 30% SA exhibited the lowest degree of swelling, water absorption and WVP as well as the highest gel fraction, good tensile properties including elongation and strength.

5.2 Suggestions

-It would be interesting to study on the preparation of MBS and BSM by cross-linking with the mixer of two or three types of the acids.

-It would be interesting to investigate the effect of mucilage from other polysaccharides i.e. *Dracocephalum moldavica* seed mucilage for producing a new biodegradable film.

-It is of interesting to study the preparation of a natural-based to other application i.e. hydrogel sponge and wound dressing because basil seed mucilage has effective swelling and water holding properties.

-Study the use of inorganic antibacterial materials for example ZnO nano-particles to improve antibacterial activity and mechanical properties of MBS and BSM films.

References

[1] Ma, X., Chang, P.R., Yu, J., Stumborg, M. 2009. "Properties of biodegradable citric acid-modified granular starch/thermoplastic pea starch composites." Carbohydrate Polymers 75: 1–8.

[2] Hooverl, R., Li, Y.X., Hynes, G. and Senanayake, N. 2003. "Physicochemical characterization of mung bean starch." Food Hydrocolloids Vo. 11 no. 4: 401-408.

[3] Kim S.H., Lee B.H., Baik M.Y., Joo M.H., and Yoo S.H. 2007. "Chemical structure and physical properties of mung bean starches isolated from 5 domestic cultivars." Institute of Food Technologists Vol. 72: 9-18.

[4] Rompothia O., Pradipasena P., Tananuwonga K, Somwangthanaroj A., Janjarasskula T. 2017. "Development of non-water soluble, ductile mung bean starch based edible film with oxygen barrier and heat sealability." Carbohydrate Polymers 157: 748–756.

[5] Luchese C.L., Garrido T., Spada J.C., Tessaro I.C., Caba K. 2018. "Development and characterization of cassava starch films incorporated with blueberry pomace." International Journal of Biological Macromolecules 106: 834–839.

[6] Kurd F, Fathi M, Shekarchizadeh H. 2017. "Basil seed mucilage as a new source for electrospinning: Production and physicochemical characterization." International Journal of Biological Macromolecules 95: 689–695.

[7] Reddy N., Yang T. 2010. "Citric acid cross-linking of starch films." Food Chemistry 118: 702–711.

[8] Yoon S.D., Chough S.H., Park H.R. 2005. "Effects of additives with different functional groups on the physical properties of starch/PVA blend film." Applied Polymer Science 100: 3733–3740.

[9] Shen L., Xu H., Kong L., Yang Y. 2015. "Non-Toxic Crosslinking of Starch Using Polycarboxylic Acids: Kinetic Study and Quantitative Correlation of Mechanical Properties and Crosslinking Degrees." Polymer Environment 23: 588–594.

[10] Dastidara T.G., Netravalib A.N. 2012. "'Green' crosslinking of native starches with malonic acid and their properties." Carbohydrate Polymers 90: 1620–1628.

[11] Majzoobi M., Beparva P., Farahnaky A., Badii F. 2014. "Effects of malic acid and citric acid on the functional properties of native and cross-linked wheat." Starch/Stärke 66: 491–495.

[12] Yeng C.M., Husseinsyah S., Ting S.S. 2015. "A compara-tive study of different crosslinking agent-modified chitosan/corn cob biocomposite films" Polymer. Bull. 72: 791–808.

[13] Yeng C.M., Salmah H., Sam S.T. 2013. Chitosan/corn cob biocomposite films by cross-linking with glutaraldehyde. Bioresources 8: 2910–2923.

[14] Muller R.J. 2010. "Biodegradability of Polymers: Regulations and Methods for Testing" Gesellschaft fur, Biotechnologische Forschung mbH, Braunschweig, Germany 48: 365-374.

[15] Guilbert, S. 2000. "Potential of the protein based biomaterials for the industry." Paper presented at The Food Biopack Conference. Copenhagen. Denmark. 72: 755-764

[16] Vilpoux O. and Avérous, L. 2004. "Use and Potentialities of Latin American Starchy Tubers." Starch-based plastics. Technology 74: 521–553.

[17] Koch K., Johansson D., Johansson K., Svegmark, K. 2014. "Material properties and molecular aspects of highly acetylated starch-based films." Journal of Renewable Materials, *2(2):* 134-144.

[18] Vikman M., Itävaara M., Poutanen K. 2004. "Measurement of the biodegradation of starch-based materials by enzymatic methods and composting." Journal Environment Polymer Degradation 3: 23-29.

[19] Takeda, Y., Hizukuri, S., Takeda, C., Suzuki, A. 2003. "Structures of branched molecules of amyloses of various origins, and molar fractions of branched and unbranched molecules." Carbohydrate Research 165: 139 -147.

[20] Hizukuri, S.; Takeda, Y.; Yasuda, M.; Suzuki, A. 2002. "Multi-branched nature of amylose and the action of debranching enzymes." Carbohydrate Research *94:* 205-212.

[21] Young A.H. 2006. "Fractionation of starch, in Starch: Chemistry and Technology." (Ed. R.L. Whistler, J.N. Bemiller, E.F. Passchall), Academic Press, Inc., London, UK.

[22] Whistler R.L, Daniel J.R. 2005. Starch, in *Kirk Othmer Encyclopedia of Chemical Technology Volume 22, Fifth Edition* (Ed. A. Seidel), John Wiley & Sons, Inc., Hoboken, USA.

[23] Imberty A, Chanzy H., Pérez S., Bulèon A., Tran V. 2004. "The double-helical nature of the crystalline part of A-starch." Journal of Molecular Biology 201: 365-370.

[24] Imberty, A., Buléon A., Tran V., Péerez S. 2001 "Recent Advances in Knowledge of Starch Structure." *Starch/Staerke* 43: 375.

[25] Colonna P., Buleon A., Lemaguer M, Mercier C. 2005. "Pisum sativum and vicia faba carbohydrates: Part IV — Granular structure of wrinkled pea starch" Carbohydrate Polymers 2: 43.

[26] Zobel H.F. 2002 "Molecules to Granules: A Comprehensive Starch Review." *Starch/Staerke 40*, 44.

[27] Gernat C., Krist D., Radosta S., Anger H., Damaschun G. 2007. "Crystalline Parts of Three Different Conformations Detected in Native and Enzymatically Degraded Starches." *Starch/Staerke 45:* 309.

[28] Buléon A., Colonna P., Planchot V., Ball S. 2004 "Starch granules: structure and biosynthesis." International Journal of Biological Macromolecules *23*; 85.

[29] Kainuma K., French D. 2003. "Naegeli amylodextrin and its relationship to starch granule structure. II. Role of water in crystallization of B-starch." Biopolymers 11: 2241.

[30] Mizukami H., Takeda Y., Hizukuri S. 2005. "The structure of the hot-water soluble components in the starch granules of new Japanese rice cultivars." Carbohydrate Polymers *38:* 329.

[31] Bizot H., Bail L., Leroux B., Davy J., Roger P., Buleon A. 2006. "Calorimetric evaluation of the glass transition in hydrated, linear and branched polyanhydroglucose compounds." Carbohydrate Polymers *32:* 33.

[32] Hulleman S.H.D., Helbert W., Chanzy H. 2001. "Single crystals of V amylose complexed with glycerol." International Journal of Biological Macromolecules 18: 115.

[33] Gaudin S., Lourdin D., Forssell P.M., Colonna P. 2007. "Antiplasticisation and oxygen permeability of starch–sorbitol films." Carbohydrate Polymers *43:* 33.

[34] Miles M.J., Morris V.J., Ring, S.G. 2000. "Gelation of amylose." Carbohydrate Research *135:* 257.

[35] Gidley M.J. 2006. "Molecular mechanisms underlying amylose aggregation and gelation." Macromolecules 22: 351.

[36] Gidley, M. J., Bulpin, P. V. "Aggregation of amylose in aqueous systems: the effect of chain length on phase behavior and aggregation kinetics." *Macromolecules* 1989, *22*, 341.

[37] Sagar A.D., Merrill E.W. 2003. "Properties of fatty acid esters of starch." Journal of Applied Polymer Science 58: 1647-1656.

[38] Kavlani N 2012. "Various Techniques for the Modification of Starch and the Applications of its Derivatives." International Research Journal of Pharmacy. 28: 366-372

[39] Singh J., Kaur L., McCarthy O.J. 2007. "Factors influencing the physico- chemical, morphological, thermal and rheological properties of some chemically modified starches for food applications"--A review. Food Hydrocolloids, 21: 1-22.

[40] Ashogbon A.O., Akintayo E.T. 2014. "Recent trend in the physical and chemical modification of starches from different botanical sources." A review. Starch-Stärke, 66: 41-57.

[41] Kavlani N. 2012. "Various Techniques for the Modification of Starch and the Applications of its Derivatives." International Research Journal of Pharmacy. 55: 33-46.

[42] Kaur B., Ariffin F., Bhat R., Karim A.A. 2012. "Progress in starch modification in the last decade.: Food Hydrocolloids. 26: 398-404.

[43] Olsson E., Hedenqvist M.S., Johansson C., Järnström L. 2013. "Influence of citric acid and curing on water sorption, diffusion and permeability of starch films." Carbohydrate Polymers, 94(2): 765-772.

[44] Ghanbarzadeh B., Almasi H., Entezami, A.A. 2011. "Improving the barrier and mechanical properties of corn starch-based edible films: Effect of citric acid and carboxymethyl cellulose." Industrial Crops and Products, 33(1): 229-235.

[45] Yeng C.M., Husseinsyah S., Ting S.S. 2015. "A comparative study of different crosslinking agent-modified chitosan/corn cob biocomposite films." Polymer Bull. 72:791–808.

[46] Gramera R.E., Heerema J., Parrish F.W. 2002. "Distribution and Structural Form of Phospahte Ester Groups in Commercial Starch Phosphates." Cereal Chemistry, 43: 104-111.

[47] Dastidar G.T., Netravali, A.N. 2012. "'Green' crosslinking of native starches with malonic acid and their properties." Carbohydrate Polymers, 90(4): 1620-1628.

[48] Olivato J.B., Grossmann M.V.E., Bilck A.P., Yamashita F. 2012. "Effect of organic acids as additives on the performance of thermoplastic starch/polyester blown films." Carbohydrate Polymers, 90(1): 159-164.

[49] Reddy N., Yang, Y. 2010. "Citric acid cross-linking of starch films." Food Chemistry, 118(3): 702-711.

[50] Wang S., Ren J, Li W, Sun R, Liu S. 2014. "Properties of polyvinyl alcohol/xylan composite films with citric acid." Carbohydrate Polymers 103: 94–99.

[51] Hirashima M., Takahashi R., Nishinari K. 2005. "Effects of adding acids before and after gelatinization on the viscoelasticity of cornstarch pastes." Food Hydrocolloids, 19(5): 909-914.

[52] Wing R.E. 2007. "Starch Citrate: Preparation and Ion Exchange Properties." Starch -Stärke, 48(7-8): 275-279.

[53] Murakami T., Siripin S., Wadisirisuk P., Boonkerd N., Yoneyama T., Yokoyama T., Imai H. 2005. "The nitrogen fixing ability of mung bean *(Ocimum basilicum* L.*)*." Chiang Mai, Thailand. 187-198.

[54] Engel R.W. 2005. "The importance of legumes as a protein source in Asian diets." in Proceedings of the 1st international mung bean symposium, Los Banos, Philippines. 35-39.

[55] Adsule R.N., Kadam S.S., Salunkhe D.K., Adsule R.N., Kadam S.S., Salunkhe D.K. 2005. "Chemistry and technology of green gram *(Vigna radiata [L.] Wilczek)."* Critical Reviews in Food Science & Nutrition. 25:73-105.

[56] Barakoti L., Bains, K. 2007. "Effect of household processing on the in vitro bioavailability of iron in mung bean *(Ocimum basilicum* L.*)."* Food and Nutrition Bulletin. 28:18-22.

[57] Yousif A.N., Scaman C.H., Durance T.D., Girard B. 2004 "Flavor volatiles and physical properties of vacuum-microwave and air-dried sweet basil *(Ocimum basilicum* L.*)."* Journal of Agricultural Food Chemistry, 47: 4777–4781.

[58] Razavi S.M.A., Mortazavi S.A., Matia-Merino L., Hosseini-Parvar S.H., Motamedzadegan A., Khanipour E. 2009. "Optimization study of gum extraction from Basil seeds *(Ocimum basilicum* L.*)."* International Journal of Food Science and Technology, 44: 1755–1762.

[59] Li B., Xie B., Kennedy J.F. 2006 "Studies on the molecular chain morphology of konjac glucomannan." Carbohydrate Polymers, 64: 510–515.

[60] Hosseini-Parvar S.H., Matia-Merino L., Goh, K.K.T., Razavi S.M.A., Mortazavi S.A. 2010. "Steady shear flow behavior of gum extracted from *Ocimum basilicum* L. seed: Effect of concentration and temperature." Journal of Food Engineering 101: 236–243.

[61] Mirhosseini H., Amid, B.T. 2012. "A review study on chemical composition and molecular structure of newly plant gum exudates and seed gums." Food Research International, 46: 387–396.

[62] Naji-Tabasi S., Razavi S., Mohebbi M., Malaekeh-Nikouei, B. 2016a. "Evaluation of physicochemical, rheological, functional and bioactivity properties of basil seed gum fractions and preparation of basil seed gum nanoparticles as a carrier of glutathione." Ph.D. Dissertation. Iran: Ferdowsi University of Mashhad.

[63] LabChem performance through chemistry Tartaric Acid Safety Data Sheet according to Federal Register / Vol. 77, No. 58 / Revision date: 05/15/2018 Supersedes: 05/15/2018 Version: 1.1 http://www.labchem.com/tools/msds/msds/LC25940.pdf

[64] Majzoobi M, Beparva P, Farahnaky A, Badii F. 2014. "Effects of malic acid and citric acid on the functional properties of native and cross-linked wheat starches." WILEY-VCH Verlag GmbH & Co. KGaA, Weinheim Starch 66: 491–495.

[65] LabChem performance through chemistry Malic Acid Safety Data Sheet according to Federal Register / Revision date: 03/02/2018 Supersedes: 03/02/2018 Version: 1.1 http://datasheets.scbt.com/sc-257687.pdf

[66] Okino S, Noburyu R, Suda M, Jojima T, Inui M, Yukawa H.2008 "An efficient succinic acid production process in a metabolically engineered." Corynebacterium glutamicum strain. Appl Microbiol Biotechnol 81(34):59–64.

[67] Fisher Scientific, Material safety data sheet succinic acid, MSDS# 22125, Revision Date18-Jan-2018, https://www.nanotech.ucsb.edu/wiki/images/c/c5/SuccinicAcid99%25MSDS.pdf

[68] McHugh T.H., Krochta J.M. 2009. "Sorbitol- vs glycerol-plasticized whey protein edible films: integrated oxygen permeability and tensile property evaluation." Journal of Agricultural and Food Chemistry, 42: 841-845.

[69] Chelli R., Procacci P., Cardini G., Califano S. 2009. "Glycerol condensed phases. Part II: A molecular dynamics study of the conformational structure and hydrogen bonding." Physical Chemistry. 1: 879.

[70] Material Safety Data Sheet Glycerol, Reagent ACS, MSDS# 96129, https://westliberty.edu/health-and-safety/files/2012/08/Glycerol-Reagent-ACS.pdf

[71] Shenglin S., Pengfei L., Na J., Hanxue H., Haizhou D. 2018. "Effects of various cross-linking agents on the physicochemical properties of starch/PHA composite films produced by extrusion blowing." Food Hydrocolloids 77: 964-975

[72] Lili R., Youjia F., Yanjiao C., Man J., Jin T., Jiang Z. 2017. "Performance improvement of starch films reinforced with starch nanocrystals (SNCs) modified by cross-linking." Starch/Stärke, 69: 1600025

[73] Kim H.Y., Oh S.M., Bae J.E., Yeom J.H., Kim B.Y., Kim H.S., Baik M.Y. 2017. "Preparation and characterization of amorphous granular potato starches (AGPS) and cross-linked amorphous granular potato starches (CLAGPS)." Carbohydrate Polymers 178: 41–47.

[74] Gilfillan W.N., Doherty W. 2016. "Starch composites with aconitic acid." Carbohydrate Polymers 141: 60–67.

[75] Menzel C. 2014. "Starch structures and their usefulness in the production of packagingmaterials" Faculty of Natural Resources and Agricultural Sciences Department of Food Science Uppsala Acta Universitatis agriculturae Sueciae 2014:90

[76] Li H, Gao X., Wang T., Zhang X., Tong Z. 2013. "Comparison of chitosan/starch composite film properties before and after cross-linking." International Journal of Biological Macromolecules 52: 275–279.

[77] He J.G., Liu Q., Thompson M.R. 2012. "Characterization of structure and properties of thermoplastic potato starch film surface cross-linked by UV irradiation." WILEY-VCH Verlag GmbH & Co. KGaA, Weinheim 65: 304–311.

[78] Zhu, J. F., Zhang, G. H., & Lai, Z. C. 2007. "Synthesis and characterization of maize starch acetates and its biodegradable film." Polymer-Plastics Technology and Engineering, 46(10–12): 1135–1141.

[79] Parvin, F., Khan, M. A., Saadat, A. H. M., Khan, M. A. H., Islam, J. M. M., Ahmed, M., *et al.* (2011). Preparation and characterization of gamma irradiated sugar containing starch/poly (vinyl alcohol)-based blend films. Journal of polymers and the environment 19(4): 1013-1022.

[80] Karazhiyan, H., Razavi, S., Phillips, G. O., Fang, Y., Al-Assaf, S., & Nishinari, K. (2011). Physicochemical aspects of hydrocolloid extract from the seeds of Lepidium sativum. International Journal of Food Science & Technology, 46, 1066-1072.

[81] Bruni GP, Oliveira JP, Halal SLME, Flores WH, Gundel A, Miranda MZ, Dias ARG, and Zavareze ER (2018). "Phosphorylated and cross-linked wheat starches in the presence of polyethylene oxide and their application in biocomposite films." Starch/Stärke 170-192

[82] Du, J., Dai, J., Liu, J. L., Dankovich, T. (2006). Novel pH-sensitive polyelectrolyte carboxymethyl konjac glucomannan-chitosan beads as drug carriers. Reactive & Functional Polymers, 66:1055–1061.

[83] Erik Olsson, Carolin Menzel, Caisa Johansson, Roger Andersson, Kristine Koch, Lars Järnström (2013) "The effect of pH on hydrolysis, cross-linking and barrier properties of starch barriers containing citric acid" Carbohydrate Polymers 98:1505–1513

[84] Kaewta Kaewtatip, Jariya Thongmee (2013) "The effects of cross-linked starch on the properties of thermoplastic starch." Materials and Design 45:586–589

[85] Jack DeRuiter. "Carboxylic Acid Structure and Chemistry: Part 1 Principles of Drug" Action 1, Spring 2005, Carboxylic Acids Part 1

[86] Seyed Ahmad Attaran, Azman Hassan, Mat Uzir Wahit (2015) "Effects of ENR and OMMT on barrier and tensile properties of LDPE nanocomposite film." Iran Polym J 24:367–378

[87] Yeng, C. M., Husseinsyah, S., Ting, S. S. (2015). A comparative study of different crosslinking agent-modified chitosan/corn cob biocomposite films. Polymer Bulletin, 72(4), 791-808

[88] Wang H, Wei D, Zheng A, Xiao H (2015) Soil burial biodegradation of antimicrobial biodegradable PBAT films. Polymer Degradation and Stability 116:14-22

Appendix A

Appendix A

FT-IR

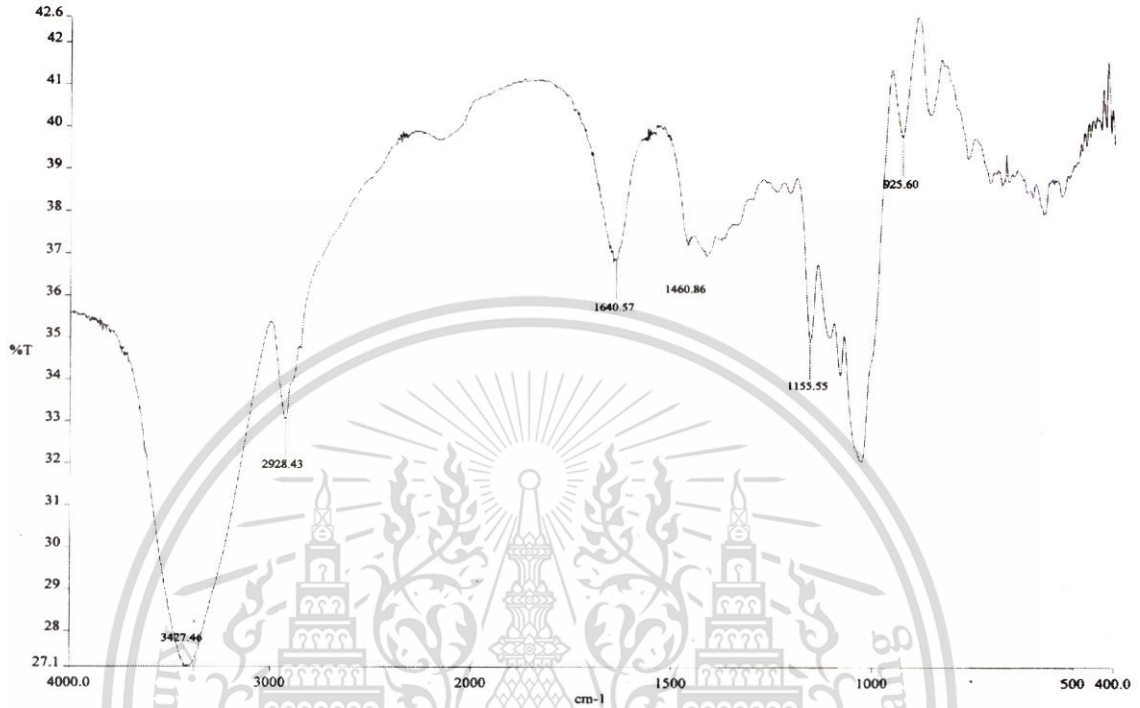

Figure A1 FT-IR spectra of native MBS films

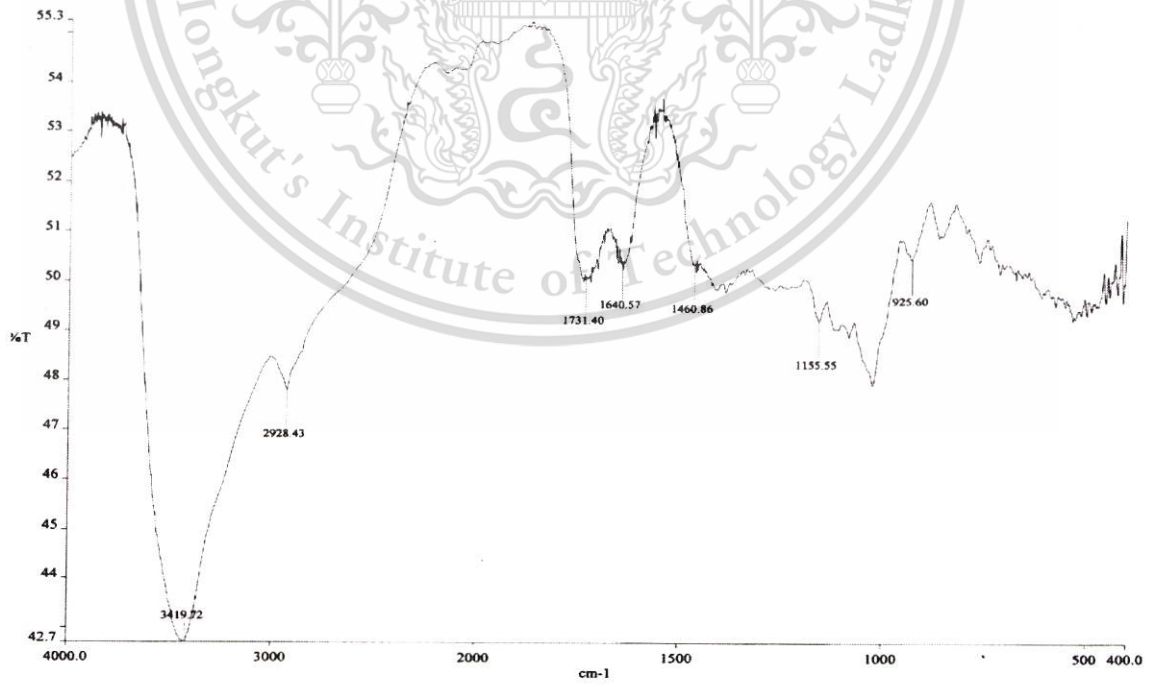

Figure A2 FT-IR spectra of MBS films cross-linked by of 10%TA

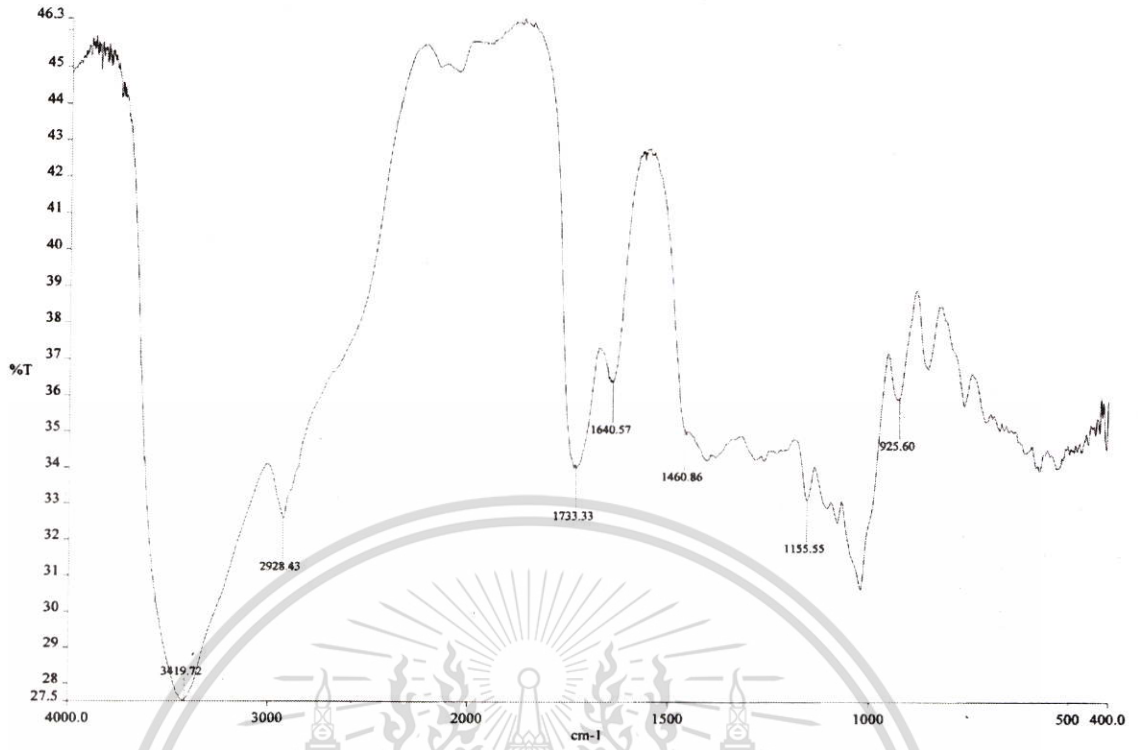

Figure A3 FT-IR spectra of MBS films cross-linked by of 15%TA

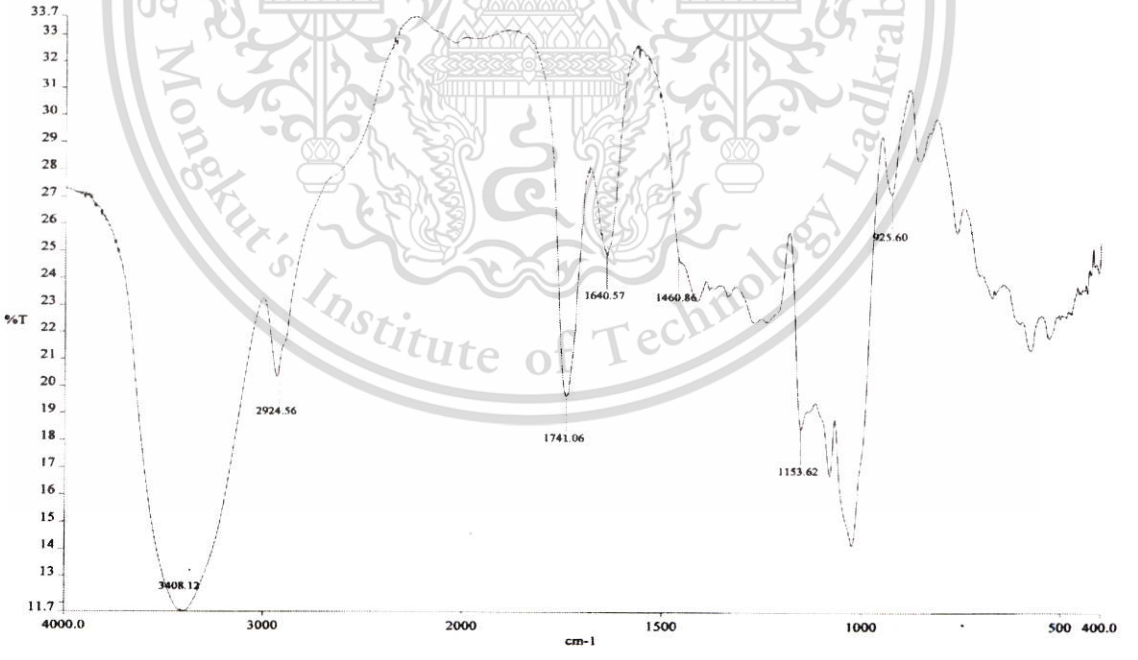

Figure A4 FT-IR spectra of MBS films cross-linked by of 20%TA

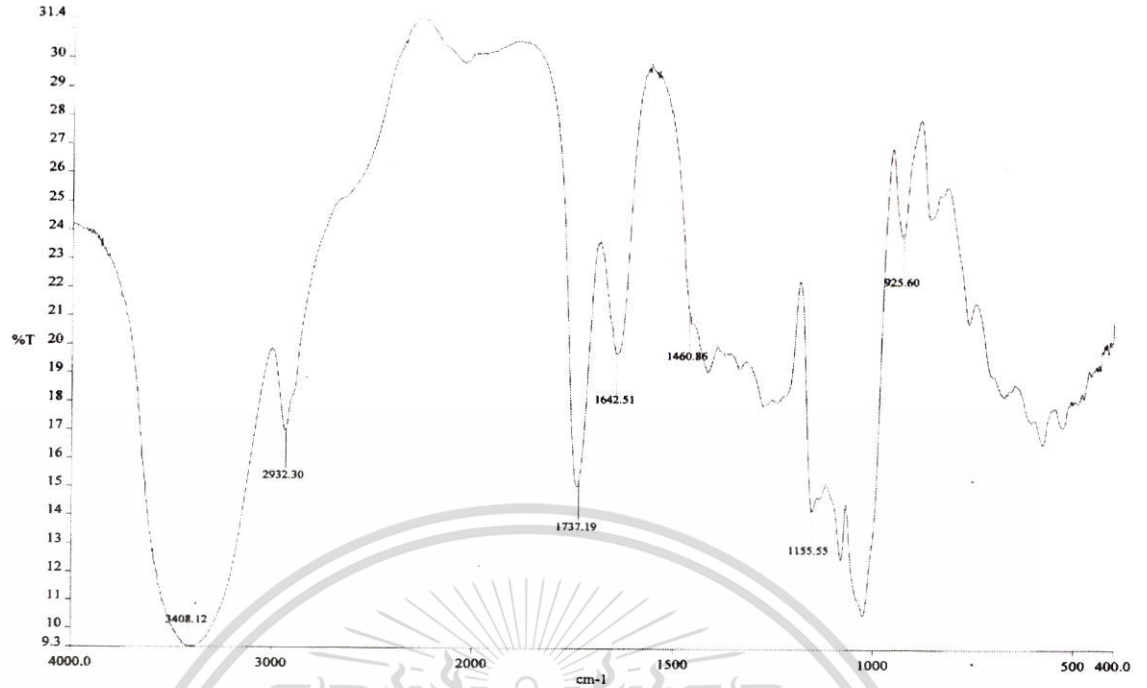

Figure A5 FT-IR spectra of MBS films cross-linked by of 25%TA

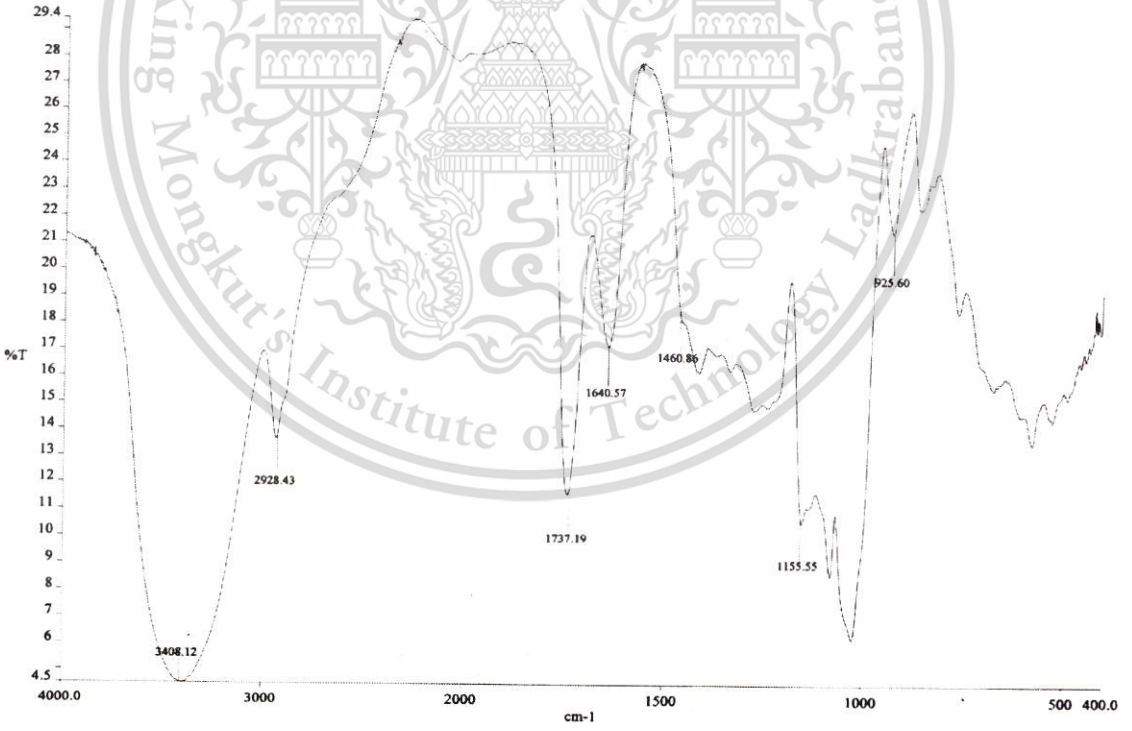

Figure A6 FT-IR spectra of MBS films cross-linked by of 30%TA

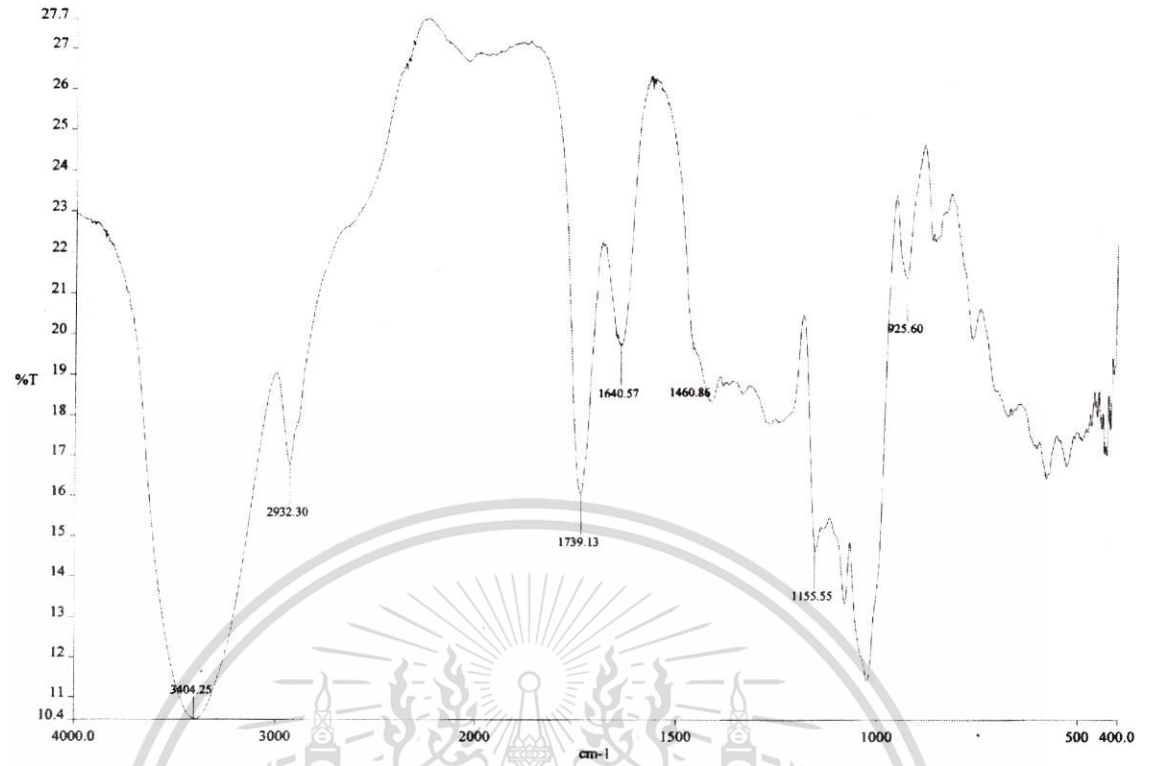

Figure A7 FT-IR spectra of MBS films cross-linked by of 10%MA

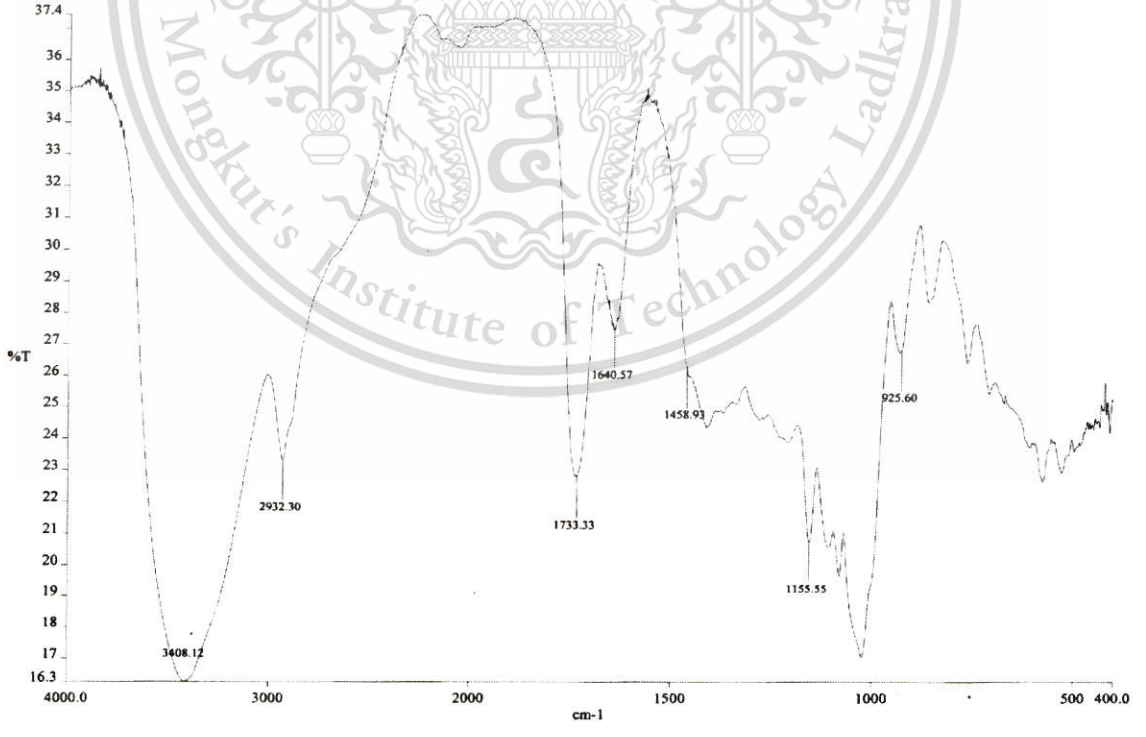

Figure A8 FT-IR spectra of MBS films cross-linked by of 15%MA

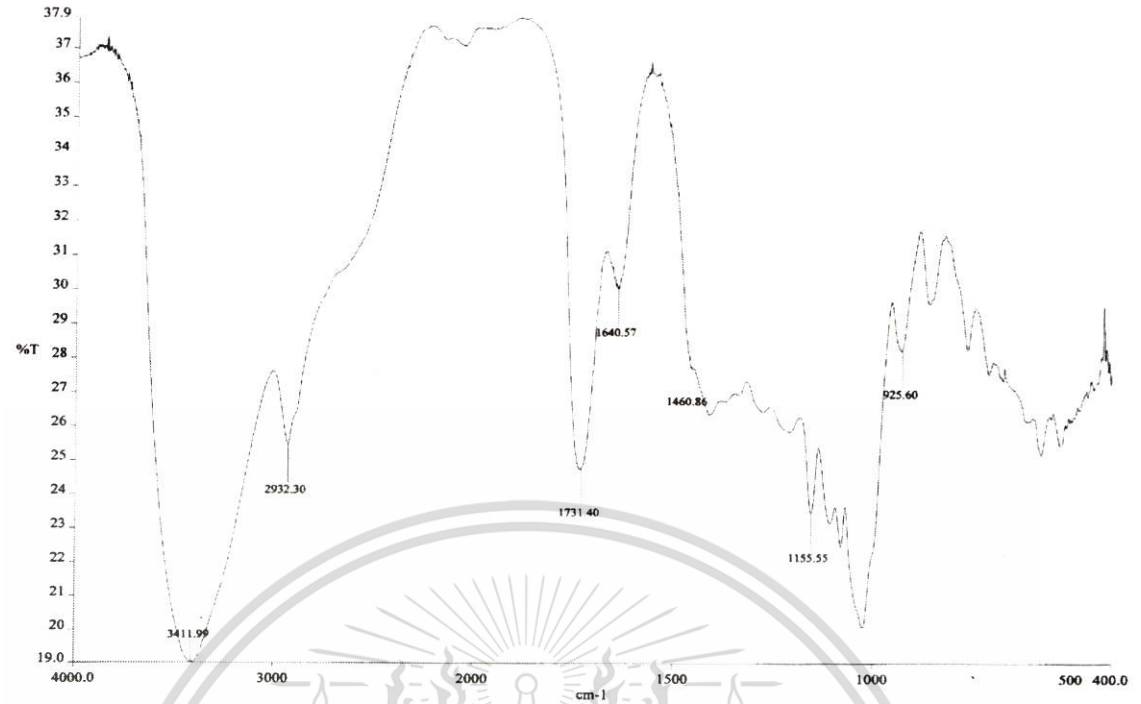

Figure A9 FT-IR spectra of MBS films cross-linked by of 20%MA

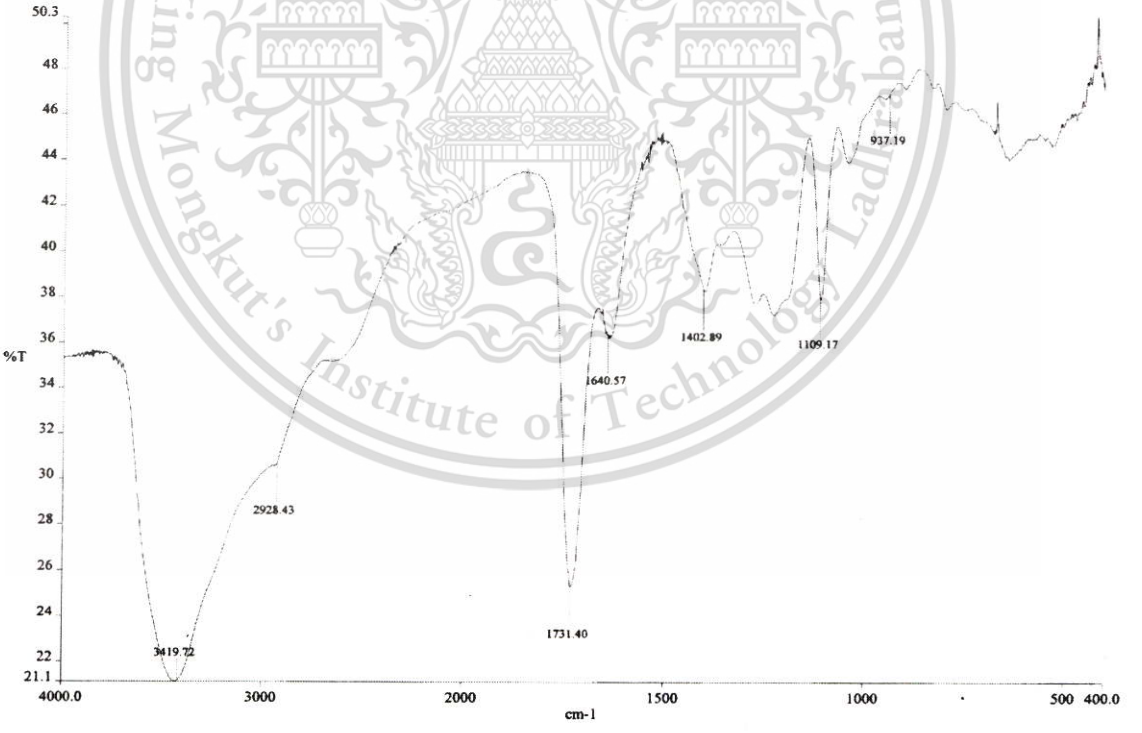

Figure A10 FT-IR spectra of MBS films cross-linked by of 25%MA

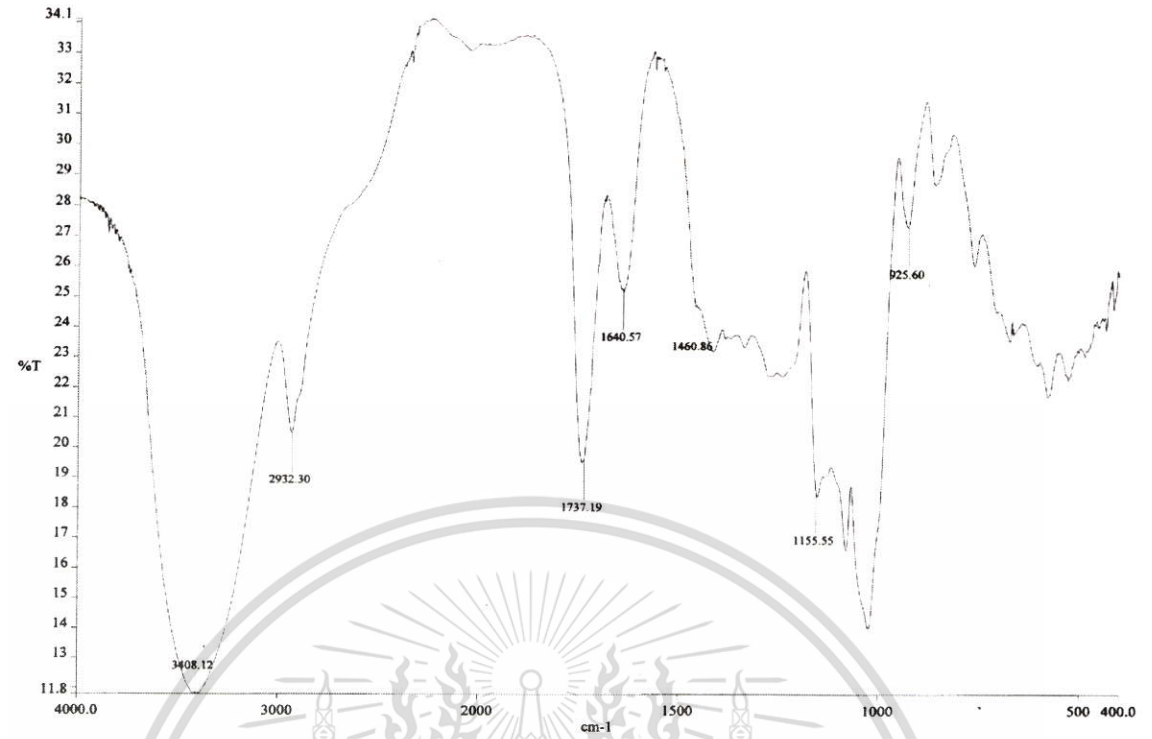

Figure A11 FT-IR spectra of MBS films cross-linked by of 30%MA

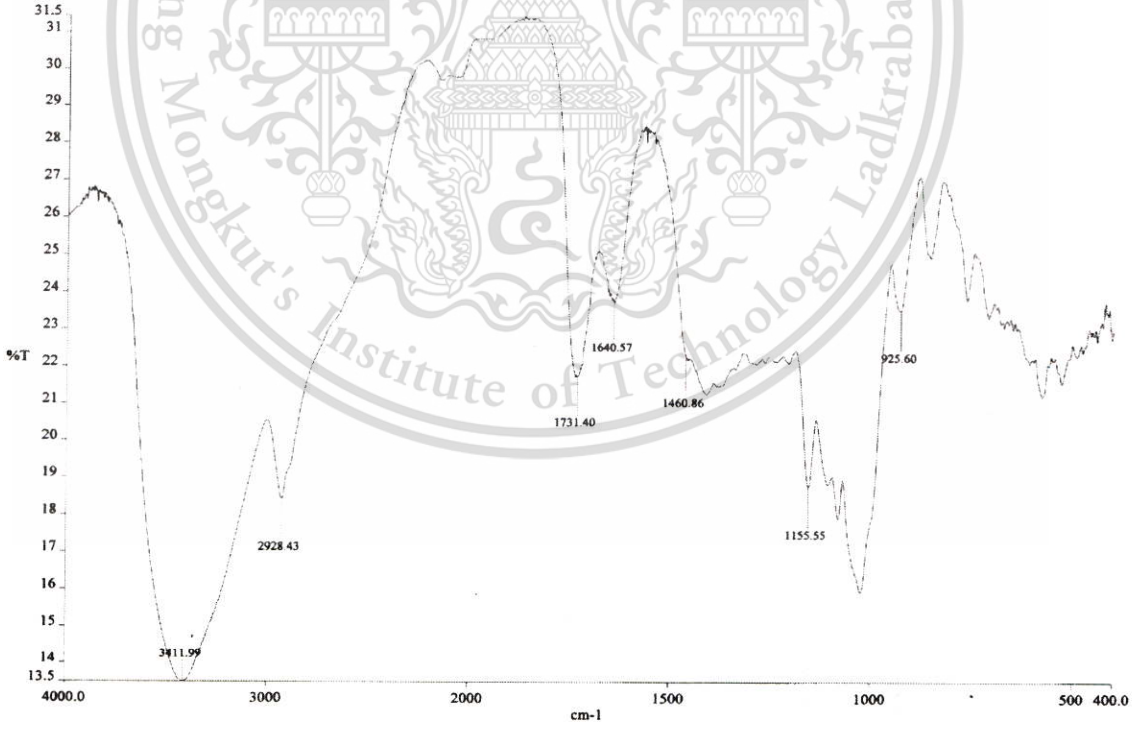

Figure A12 FT-IR spectra of MBS films cross-linked by of 10%SA

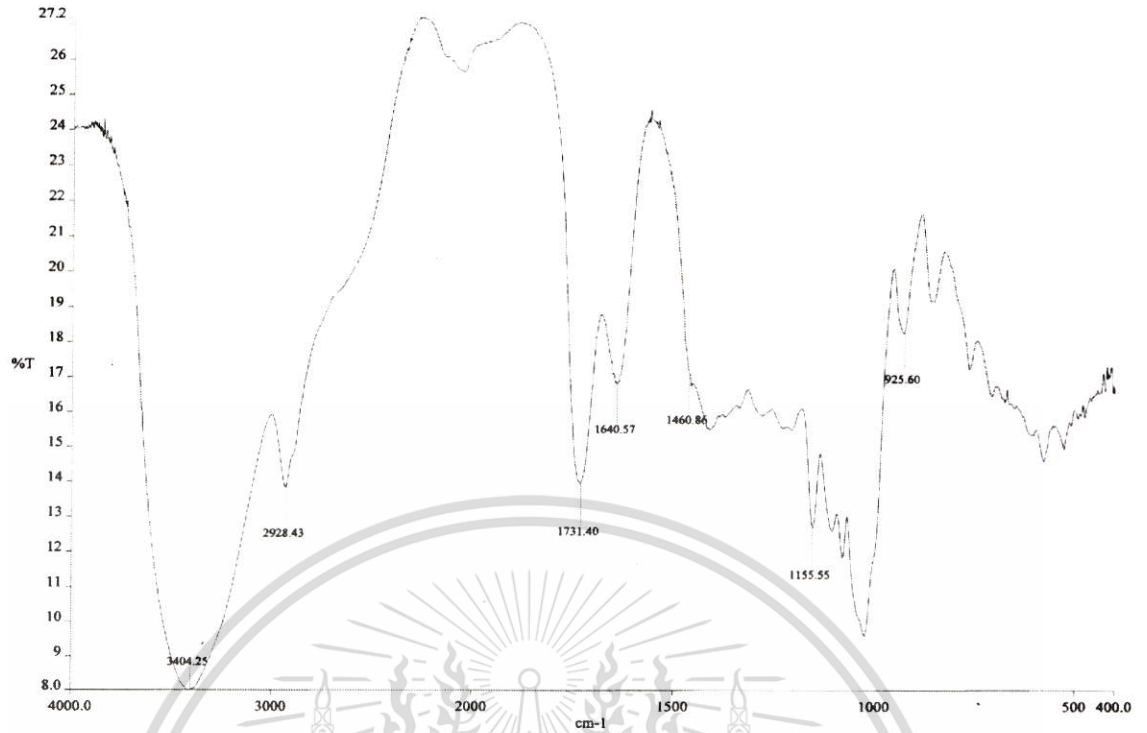

Figure A13 FT-IR spectra of MBS films cross-linked by of 15%SA

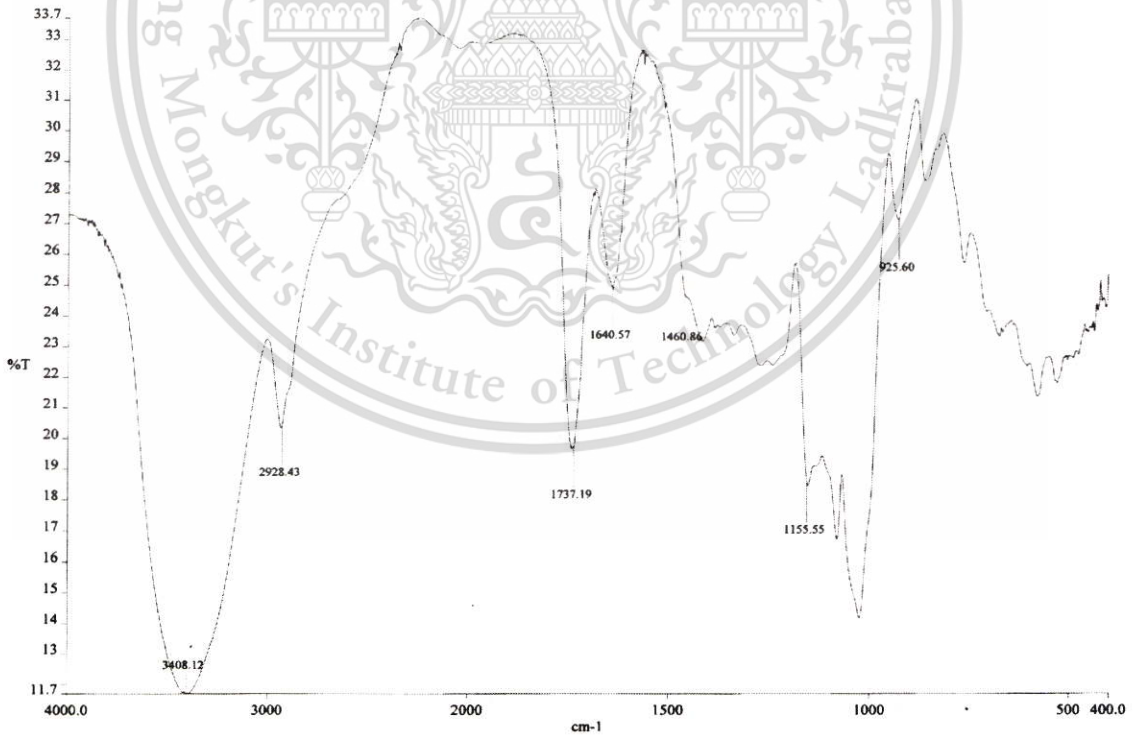

Figure A14 FT-IR spectra of MBS films cross-linked by of 20%SA

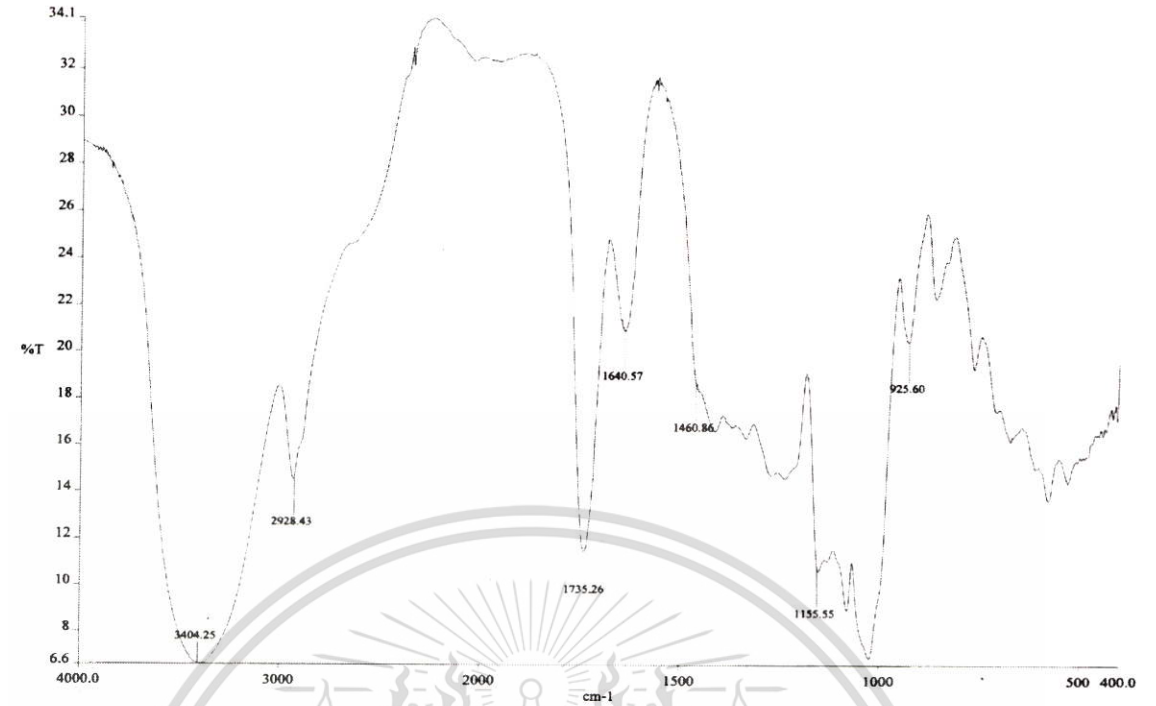

Figure A15 FT-IR spectra of MBS films cross-linked by of 25%SA

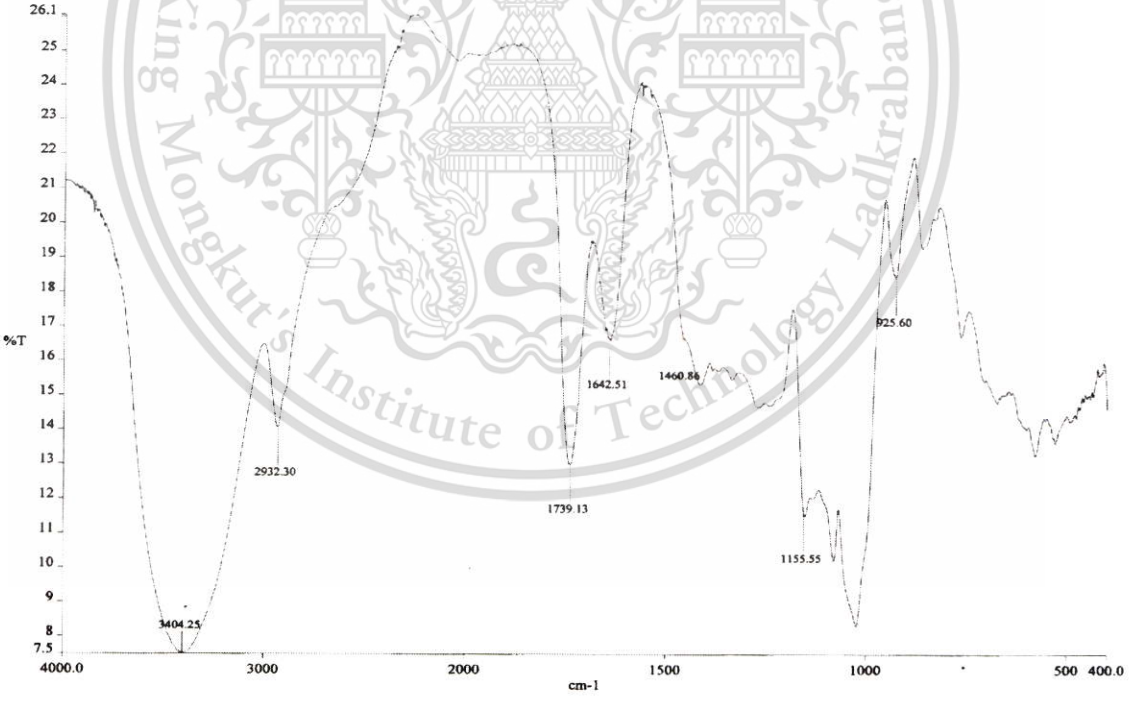

Figure A16 FT-IR spectra of MBS films cross-linked by of 30%SA

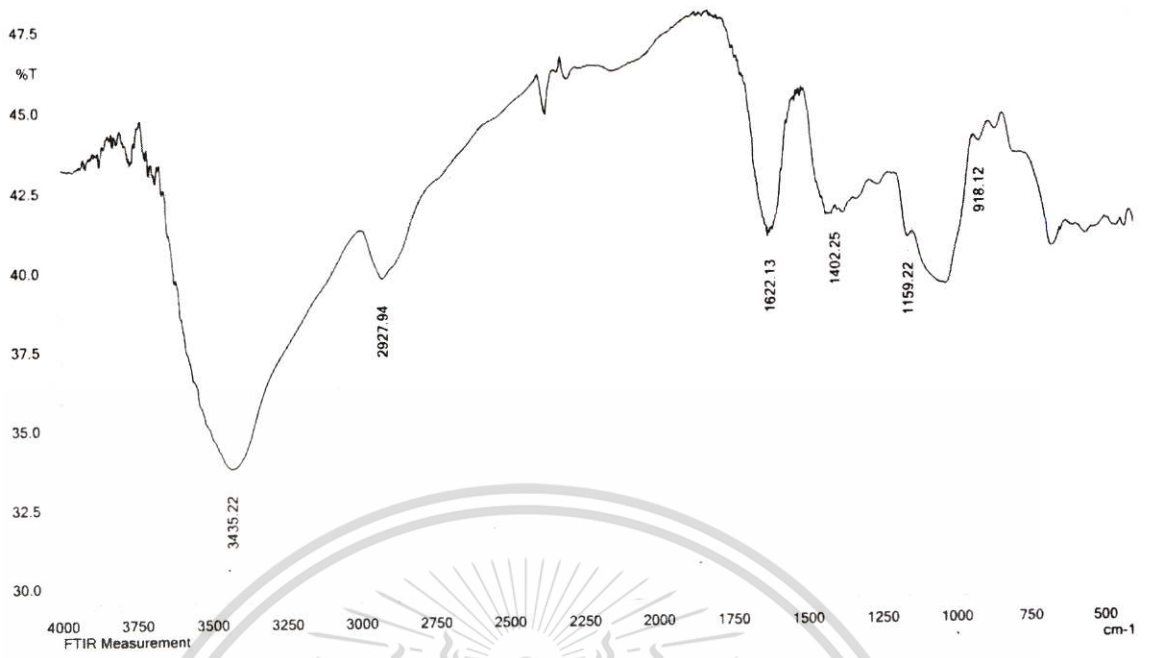

Figure A17 FT-IR spectra of native BSM films

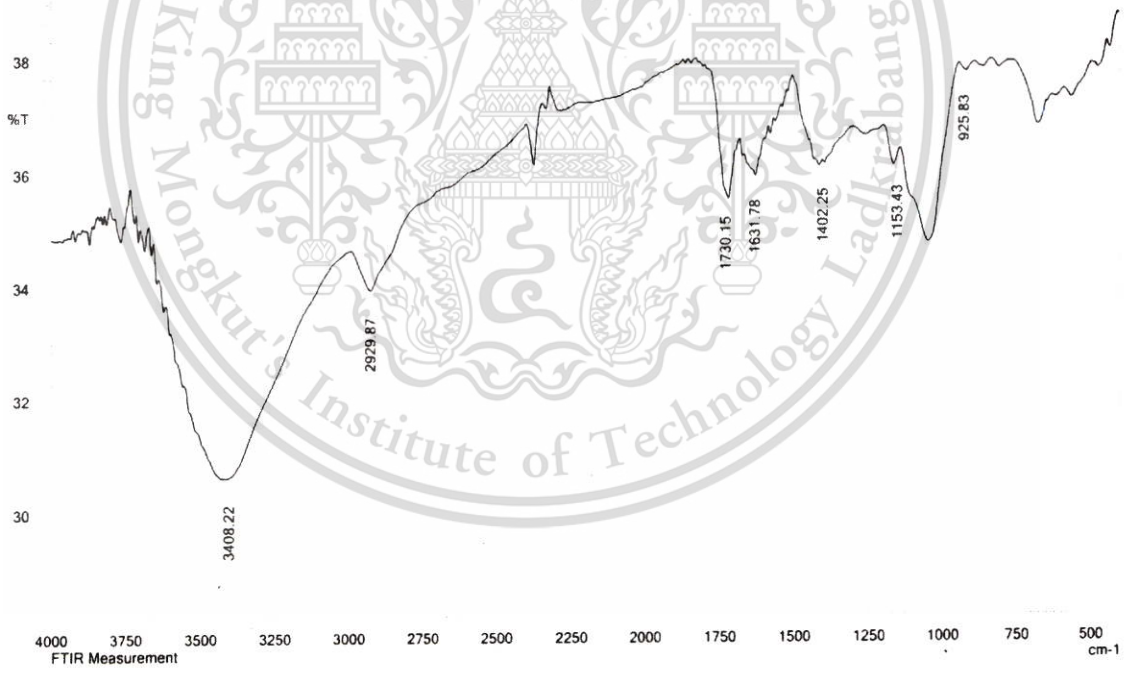

Figure A18 FT-IR spectra of BSM films cross-linked by of 10%TA

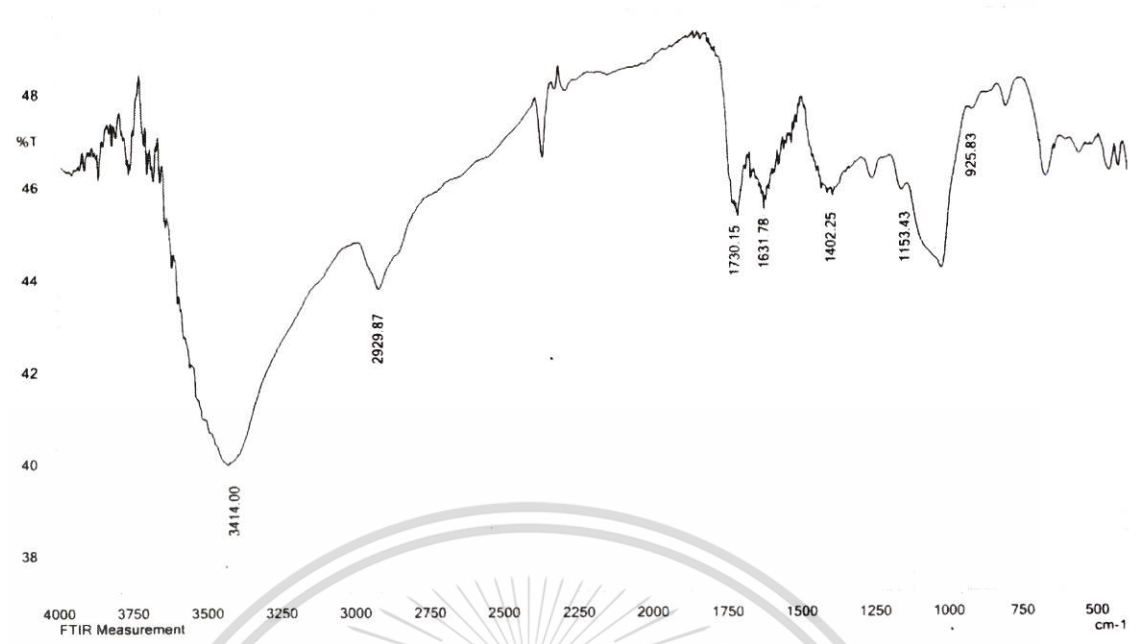

Figure A19 FT-IR spectra of BSM films cross-linked by of 15%TA

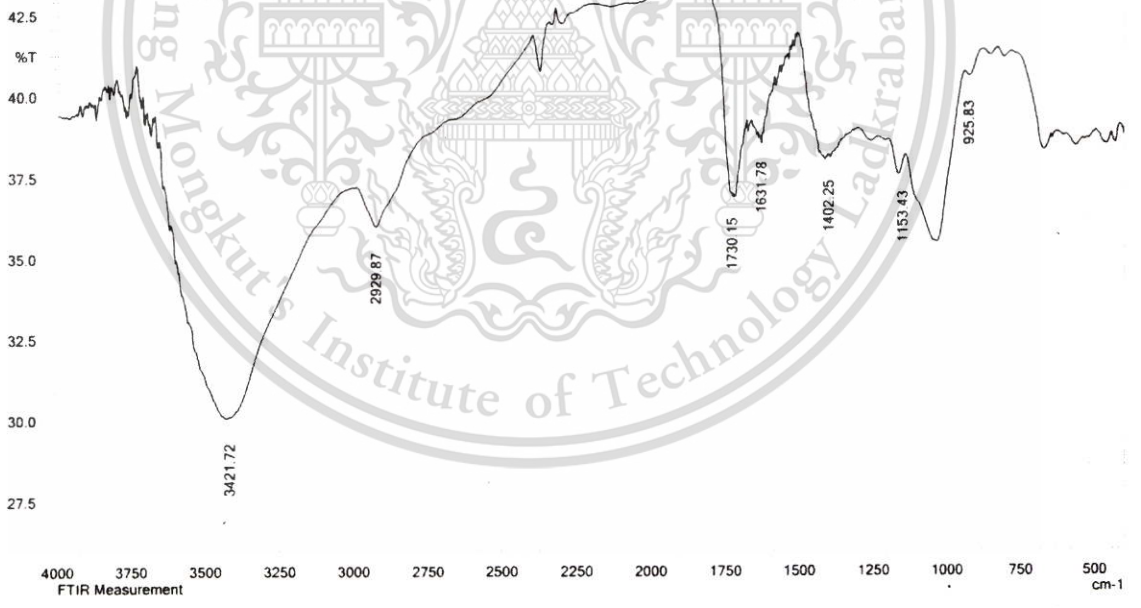

Figure A20 FT-IR spectra of BSM films cross-linked by of 20%TA

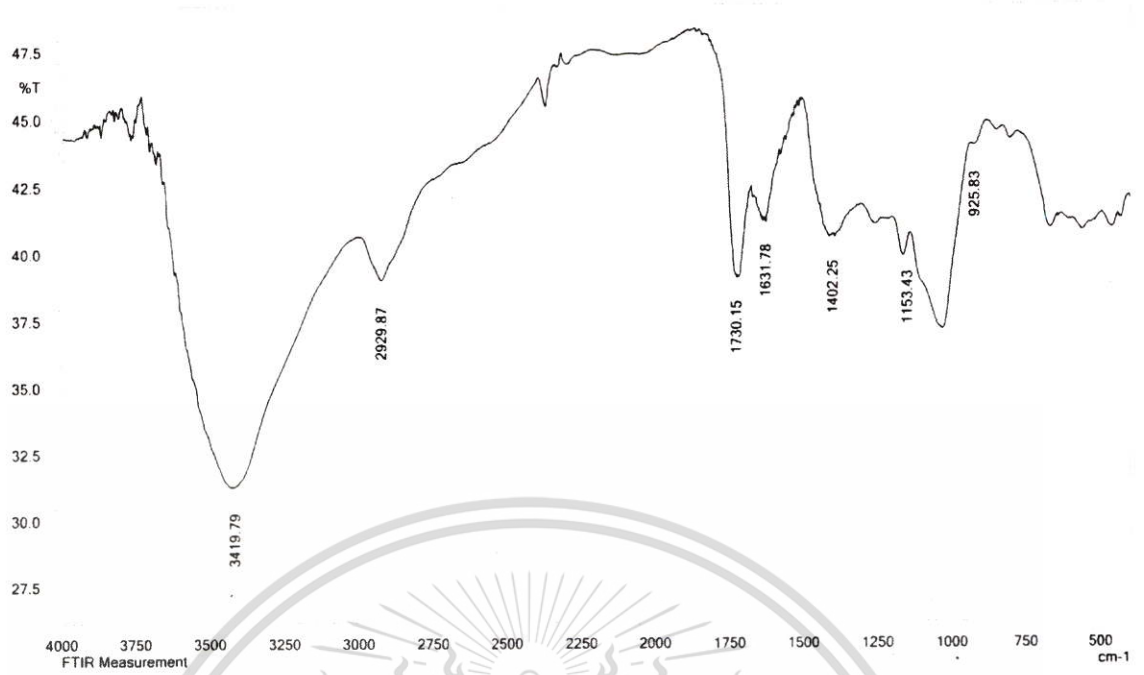

Figure A21 FT-IR spectra of BSM films cross-linked by of 25%TA

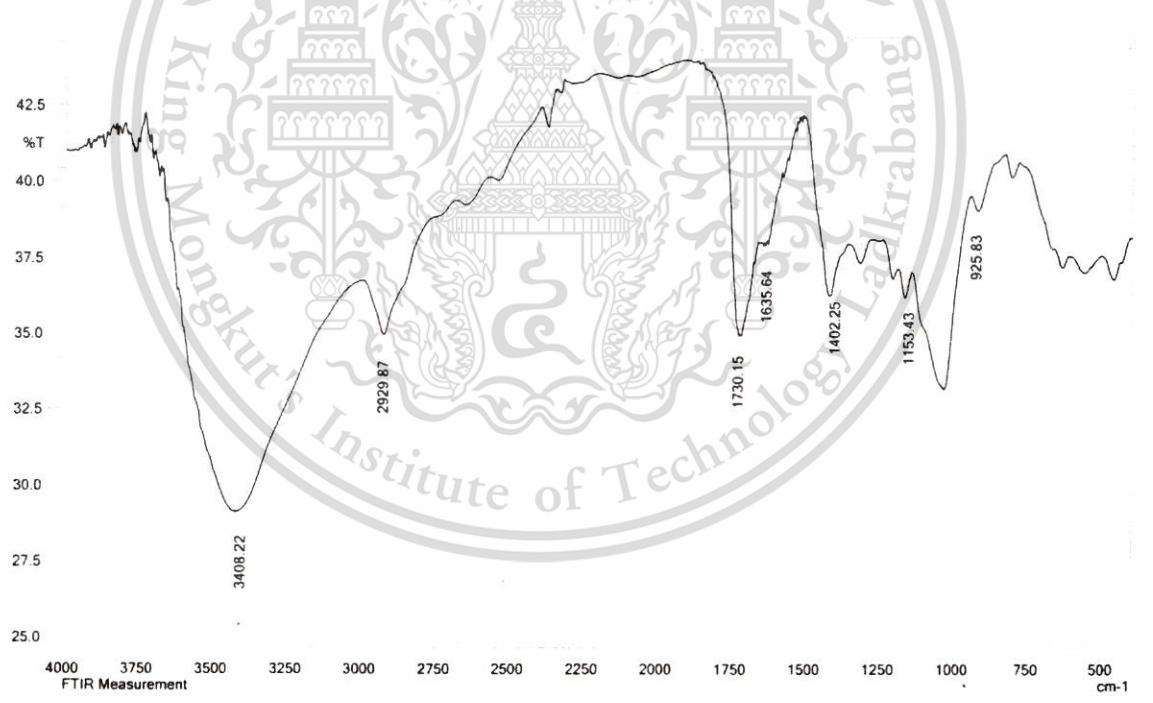

Figure A22 FT-IR spectra of BSM films cross-linked by of 30%TA

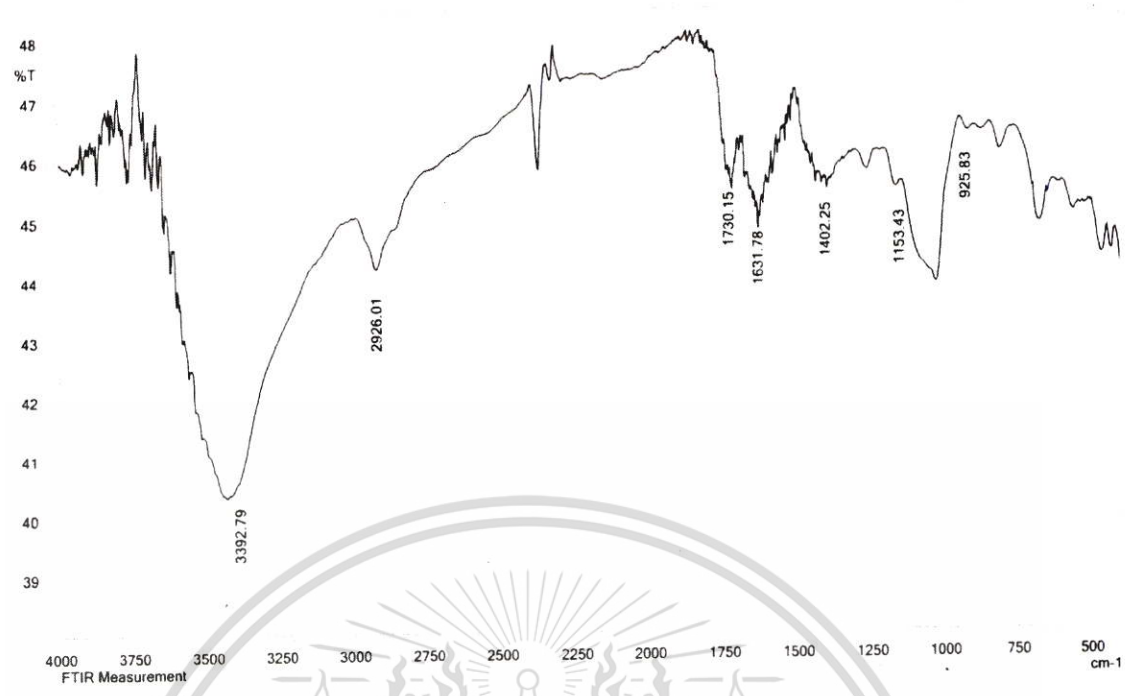

Figure A23 FT-IR spectra of BSM films cross-linked by of 10%MA

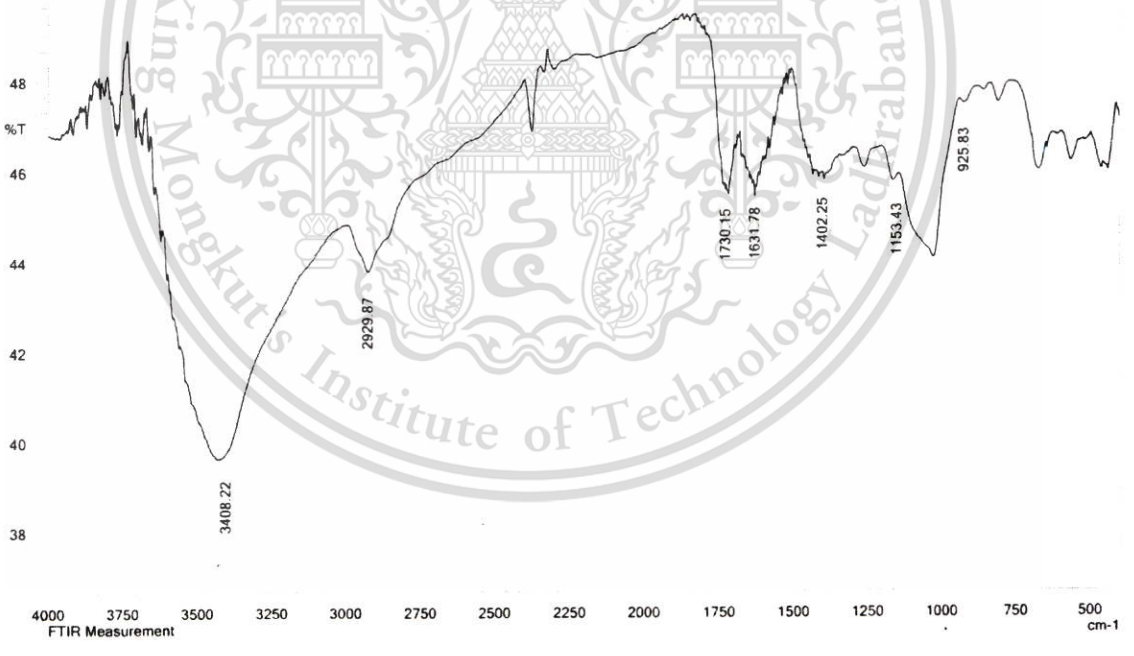

Figure A24 FT-IR spectra of BSM films cross-linked by of 15%MA

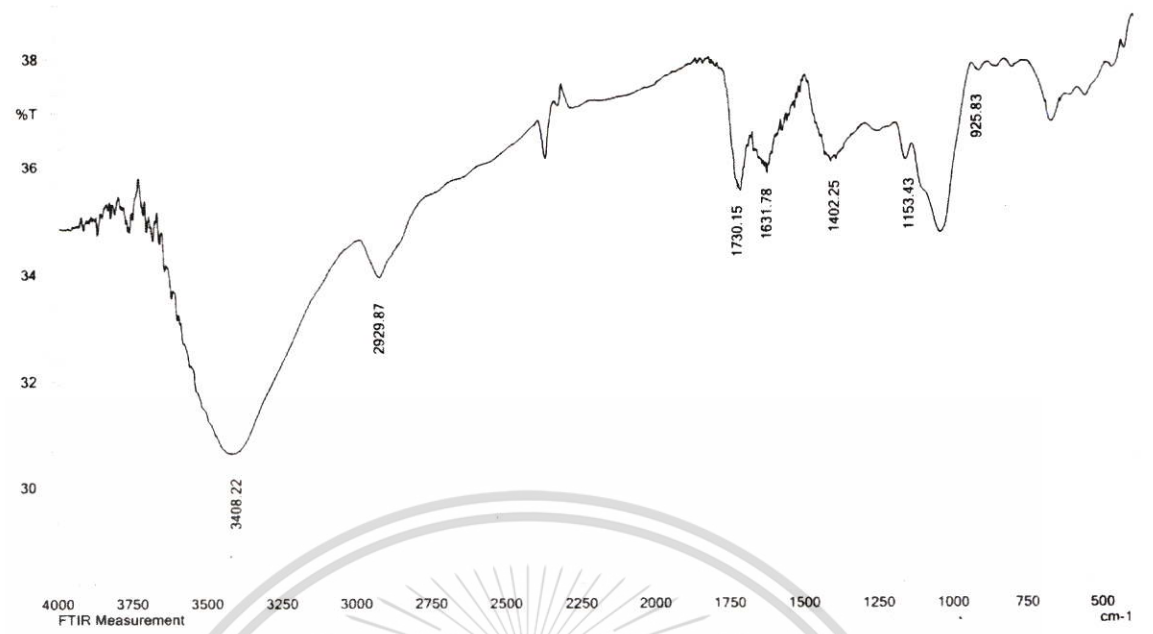

Figure A25 FT-IR spectra of BSM films cross-linked by of 20%MA

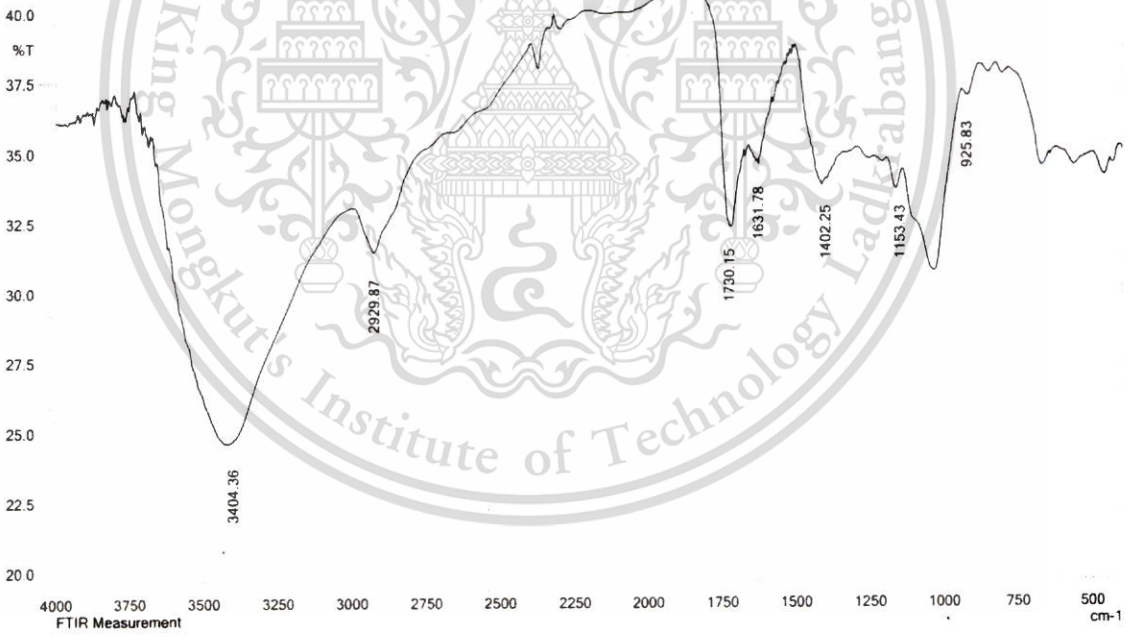

Figure A26 FT-IR spectra of BSM films cross-linked by of 25%MA

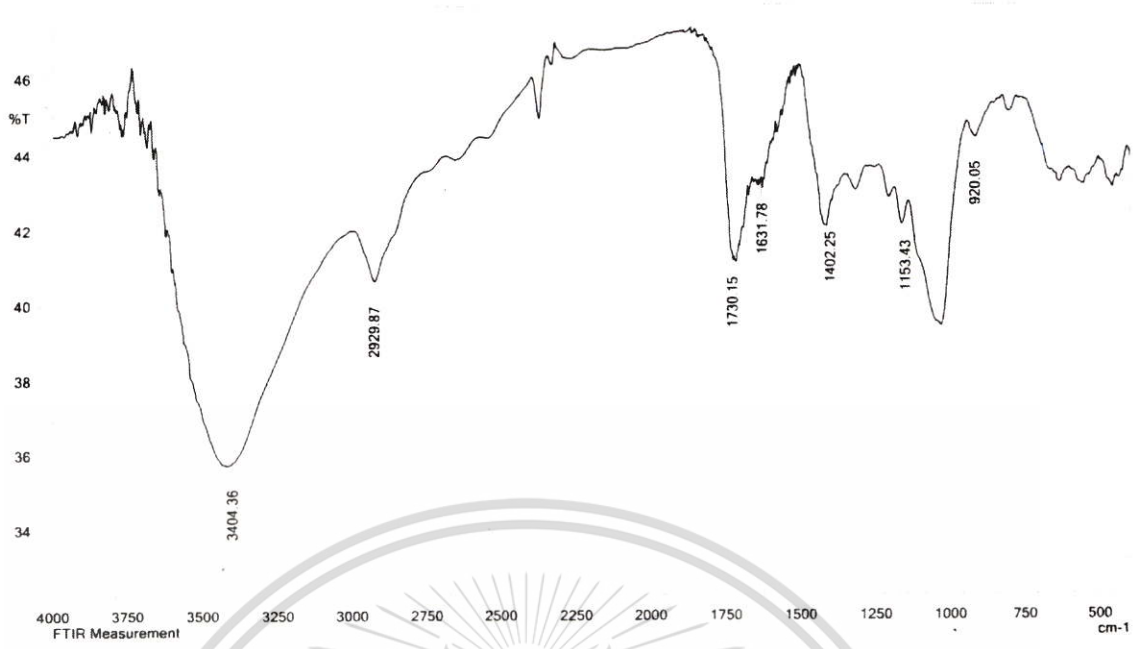

Figure A27 FT-IR spectra of BSM films cross-linked by of 30%MA

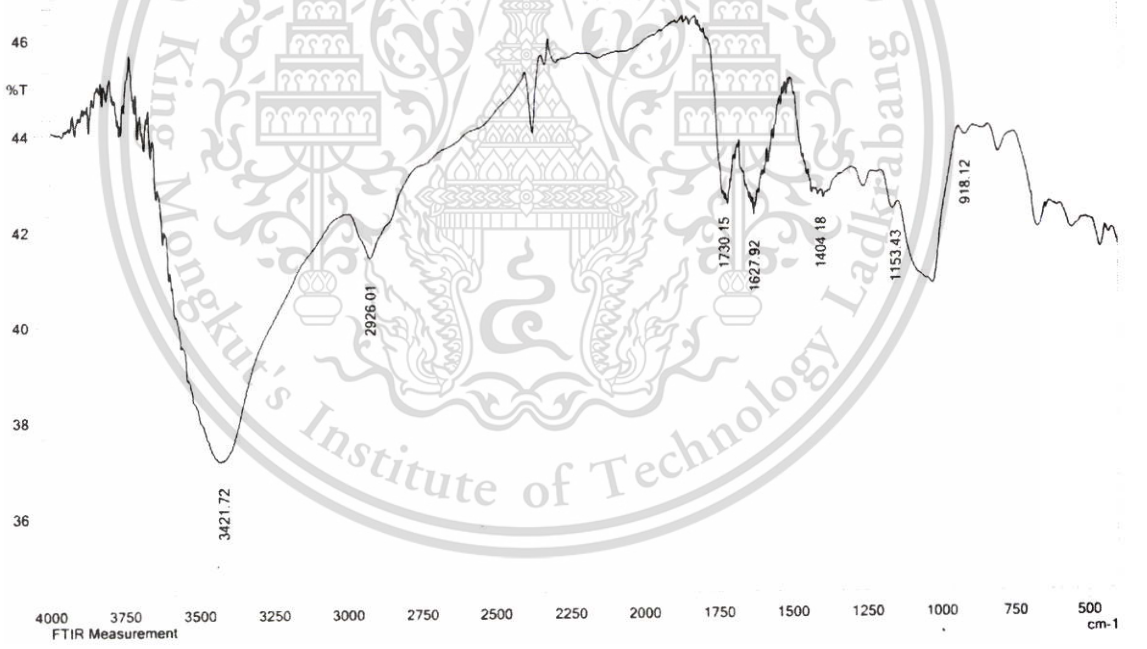

Figure A28 FT-IR spectra of BSM films cross-linked by of 10%SA

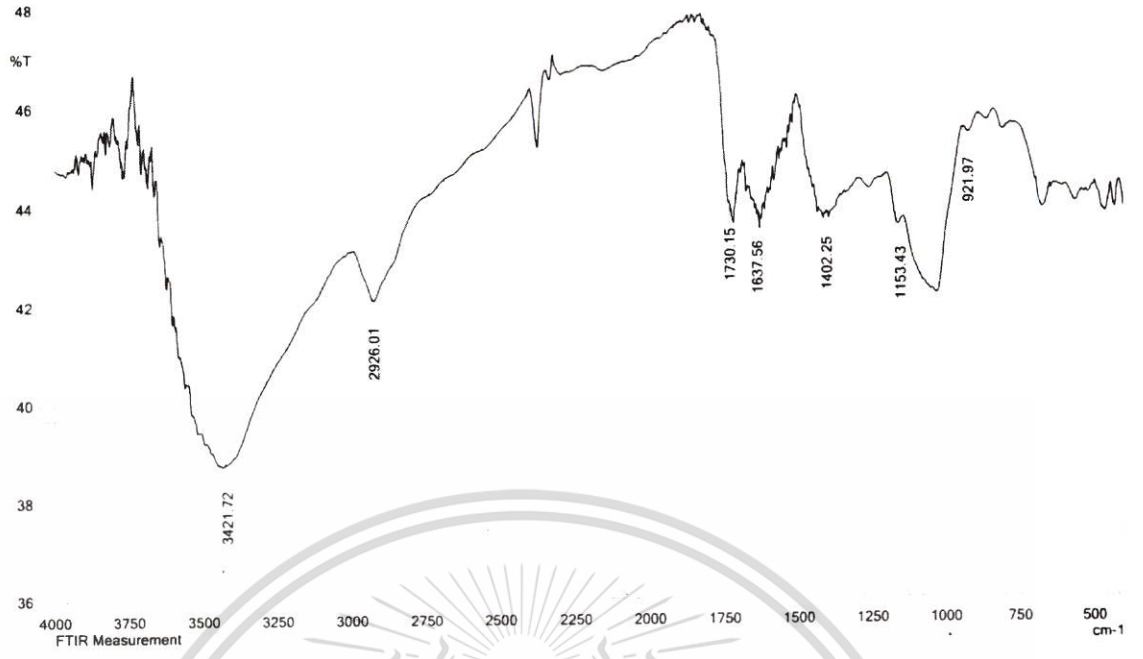

Figure A28 FT-IR spectra of BSM films cross-linked by of 15%SA

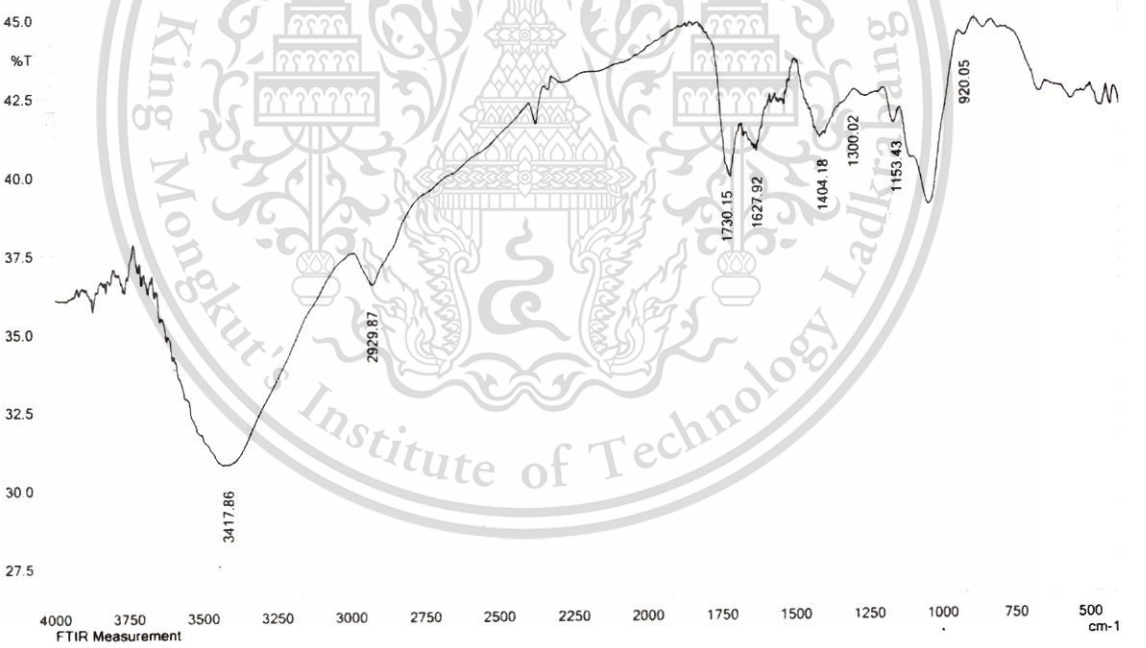

Figure A29 FT-IR spectra of BSM films cross-linked by of 20%SA

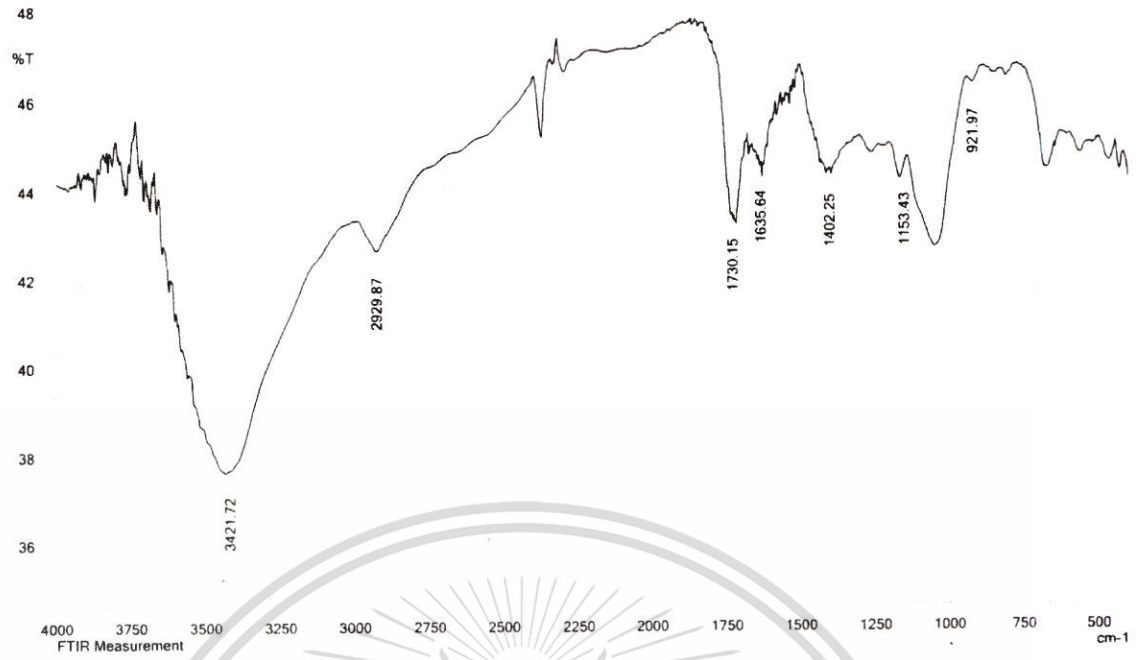

Figure A30 FT-IR spectra of BSM films cross-linked by of 25%SA

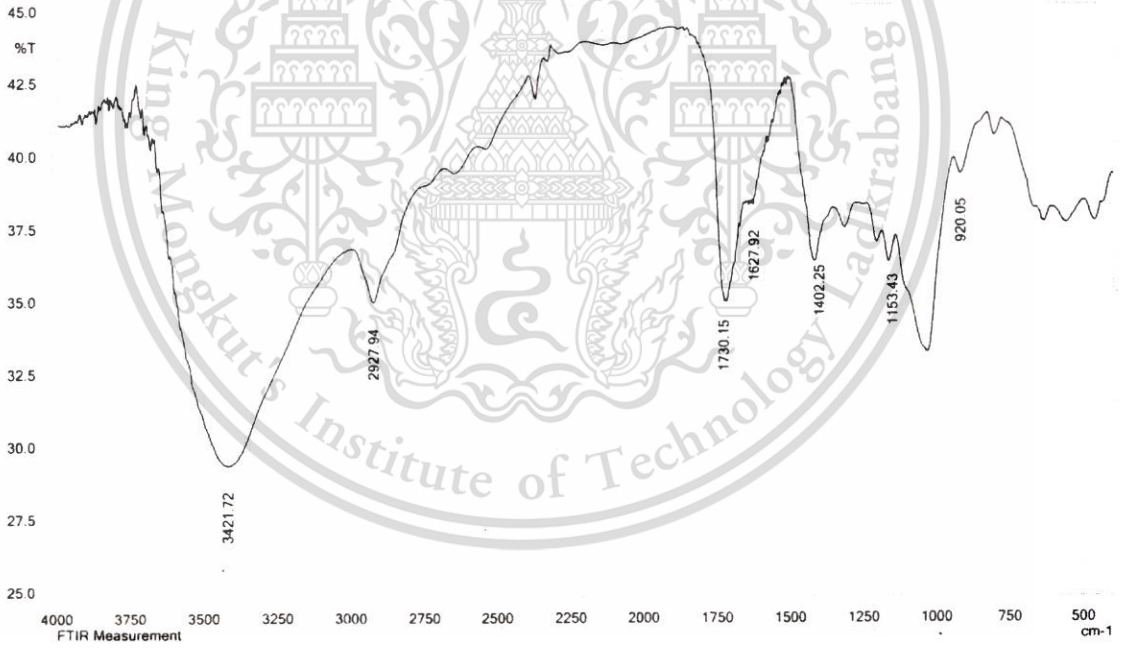

Figure A31 FT-IR spectra of BSM films cross-linked by of 30%SA

Appendix B

Appendix B

X-ray diffraction (XRD)

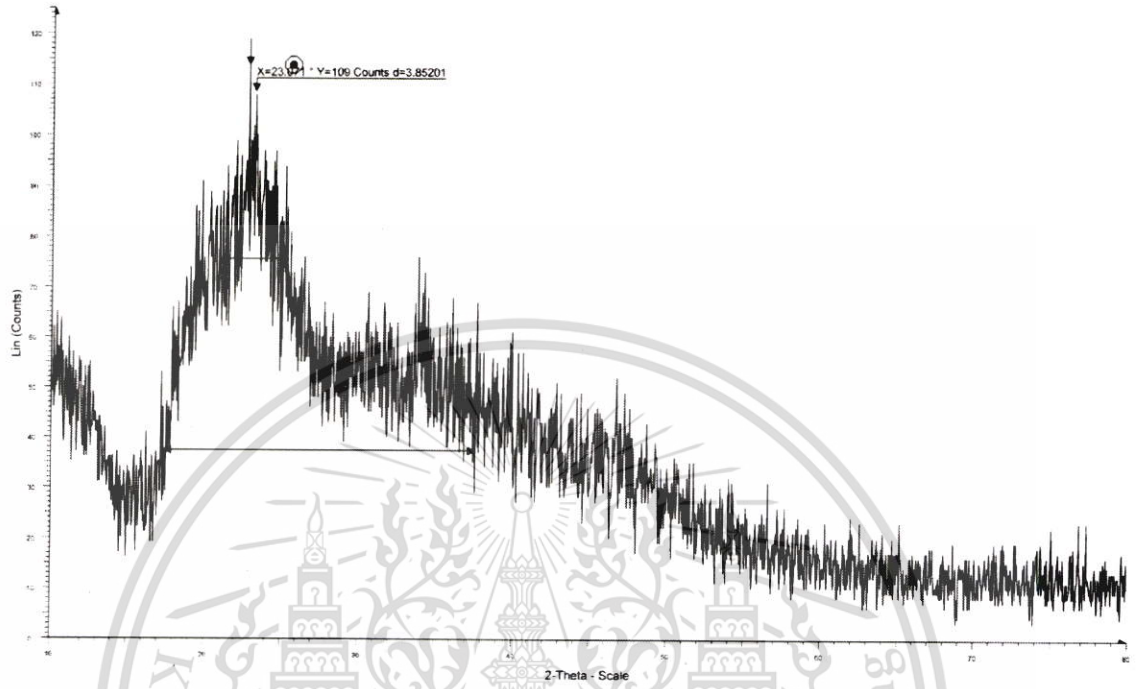

Figure B1 X-ray diffractogram of native MBS film

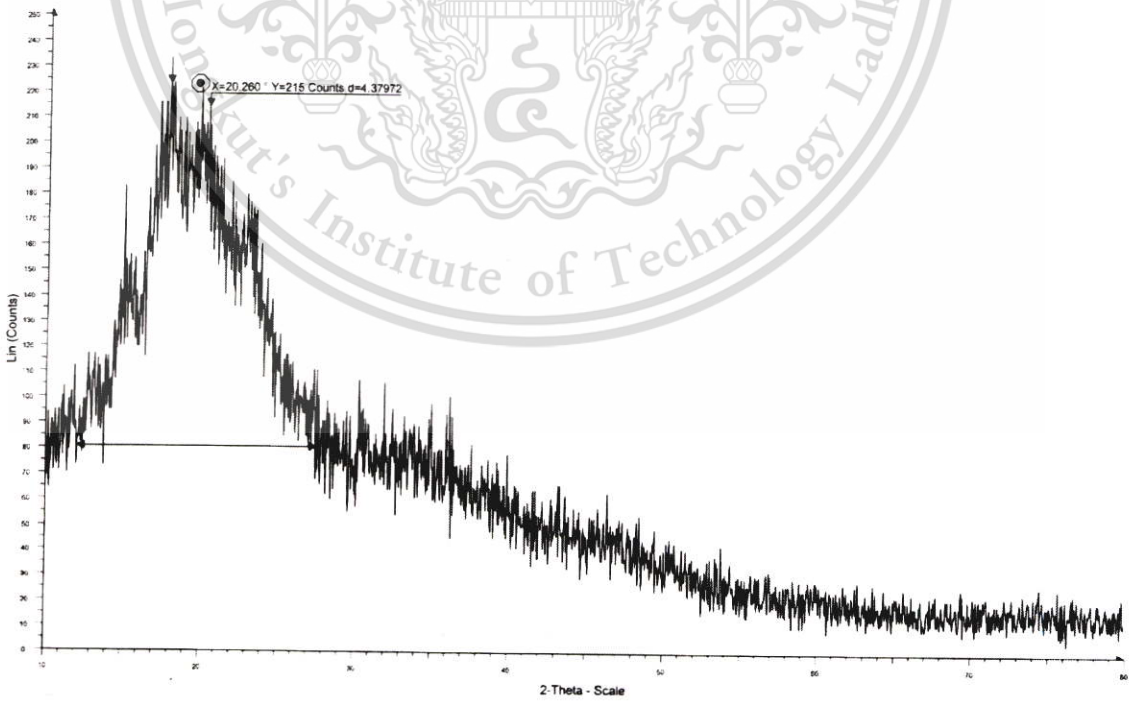

Figure B2 X-ray diffractogram of MBS film cross-linked by 10%TA

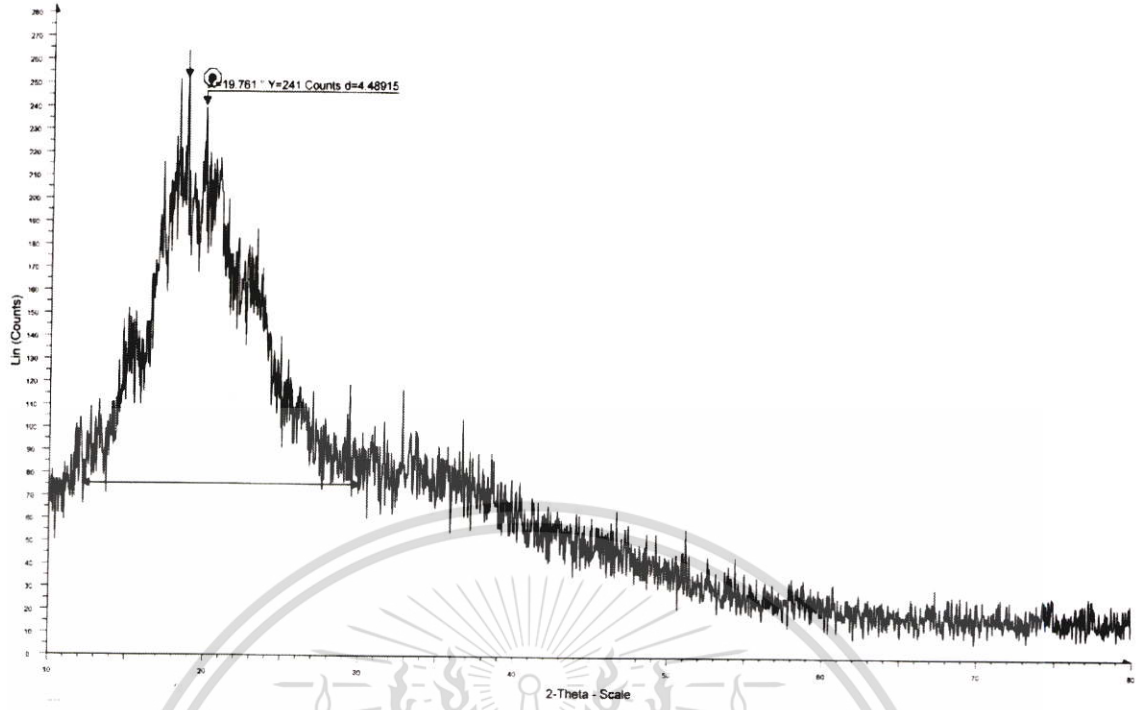

Figure B3 X-ray diffractogram of MBS film cross-linked by 20%TA

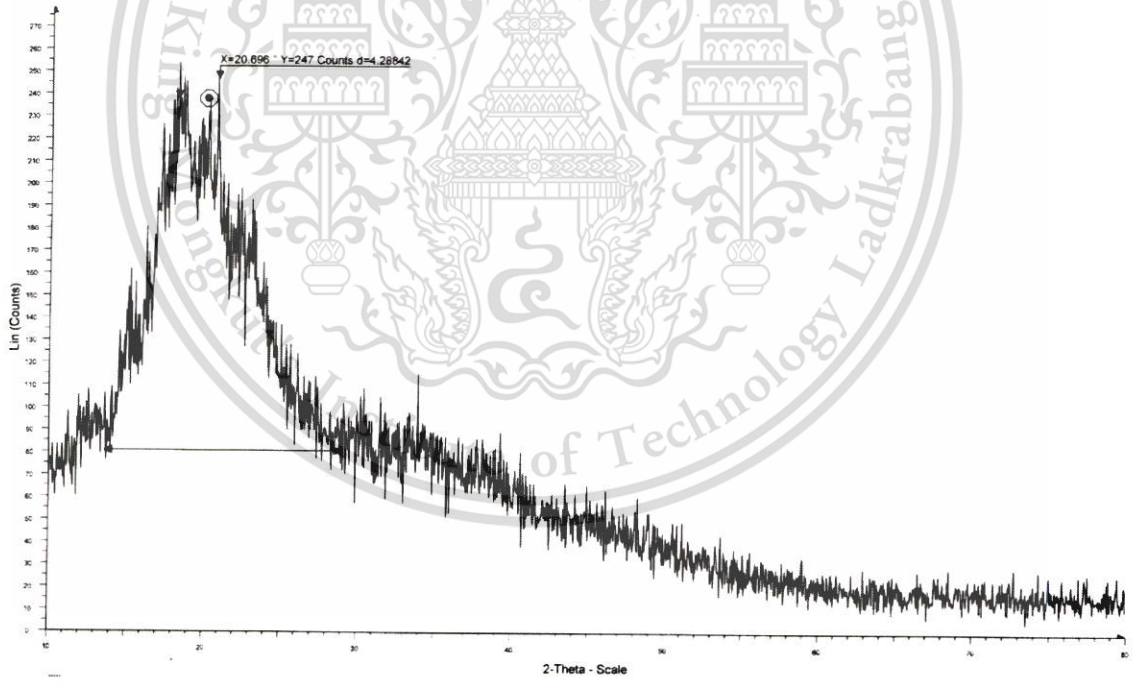

Figure B4 X-ray diffractogram of MBS film cross-linked by 30%TA

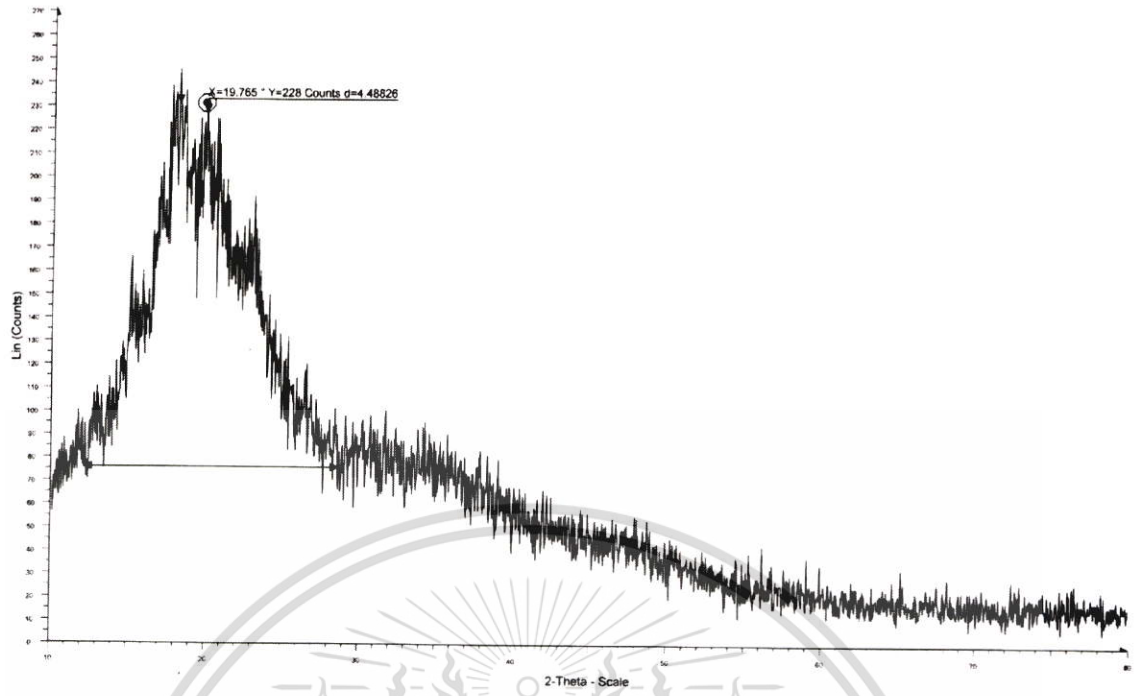

Figure B5 X-ray diffractogram of MBS film cross-linked by 10%MA

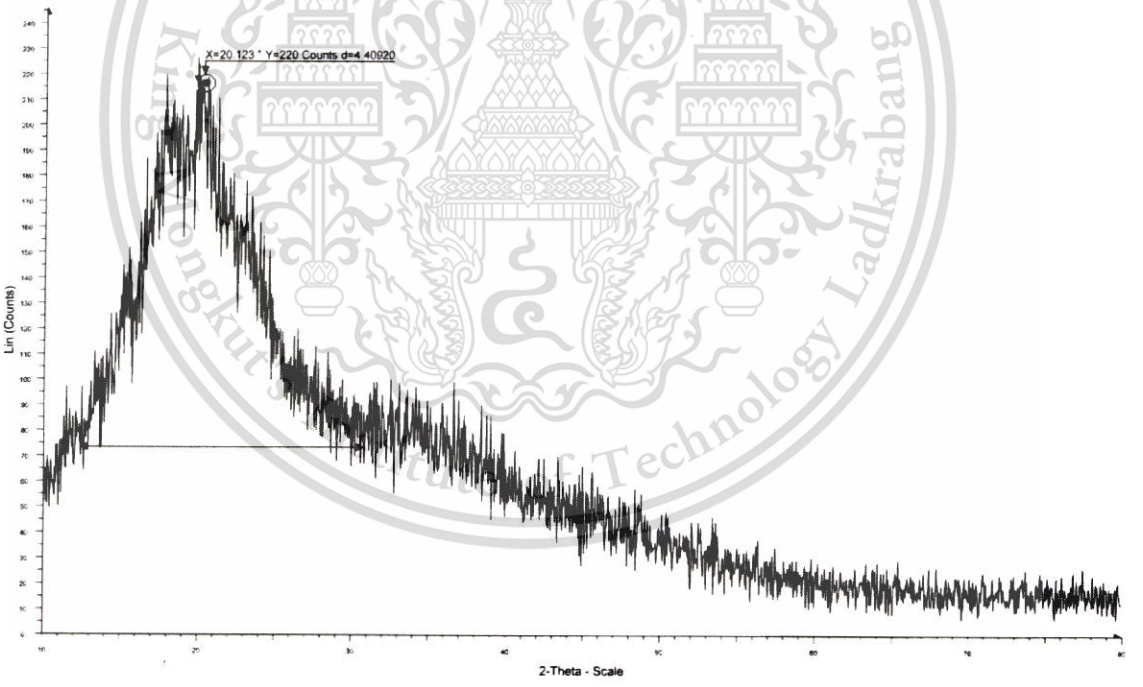

Figure B6 X-ray diffractogram of MBS film cross-linked by 20%MA

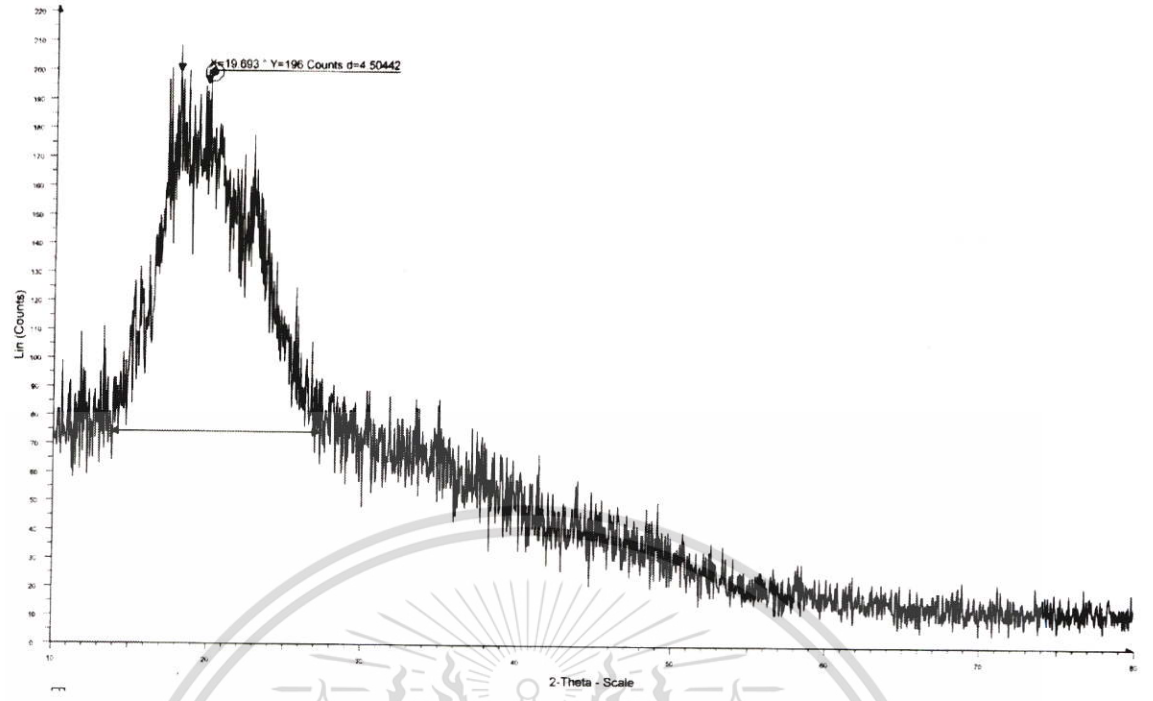

Figure B7 X-ray diffractogram of MBS film cross-linked by 30%MA

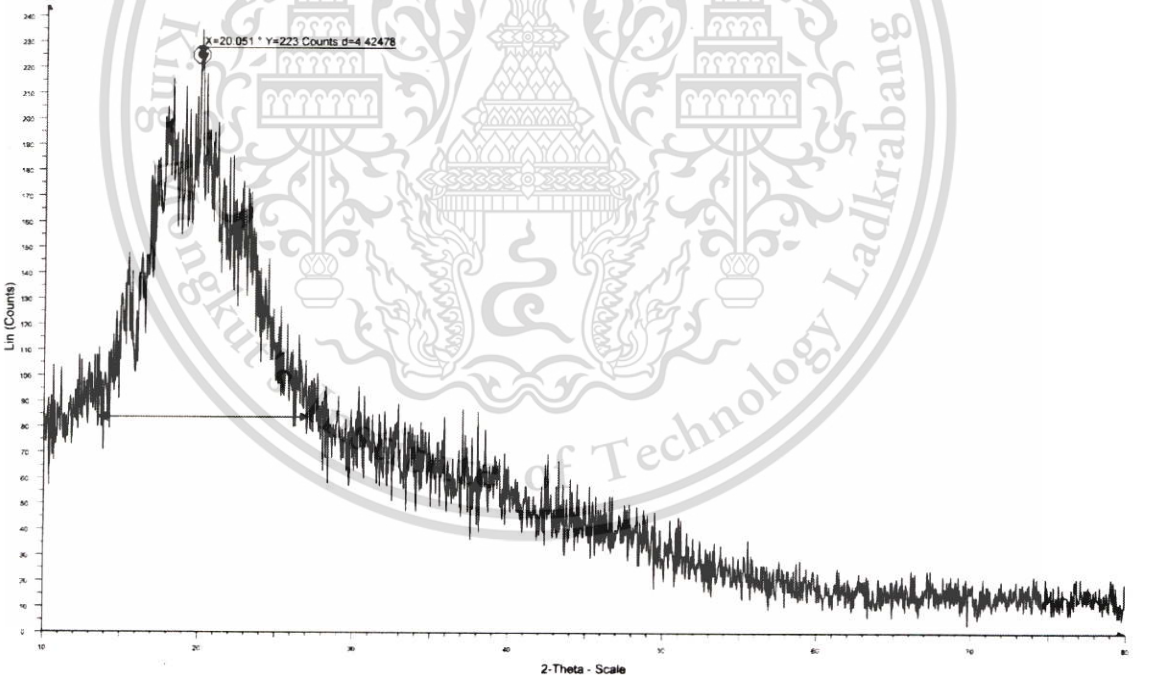

Figure B8 X-ray diffractogram of MBS film cross-linked by 10%SA

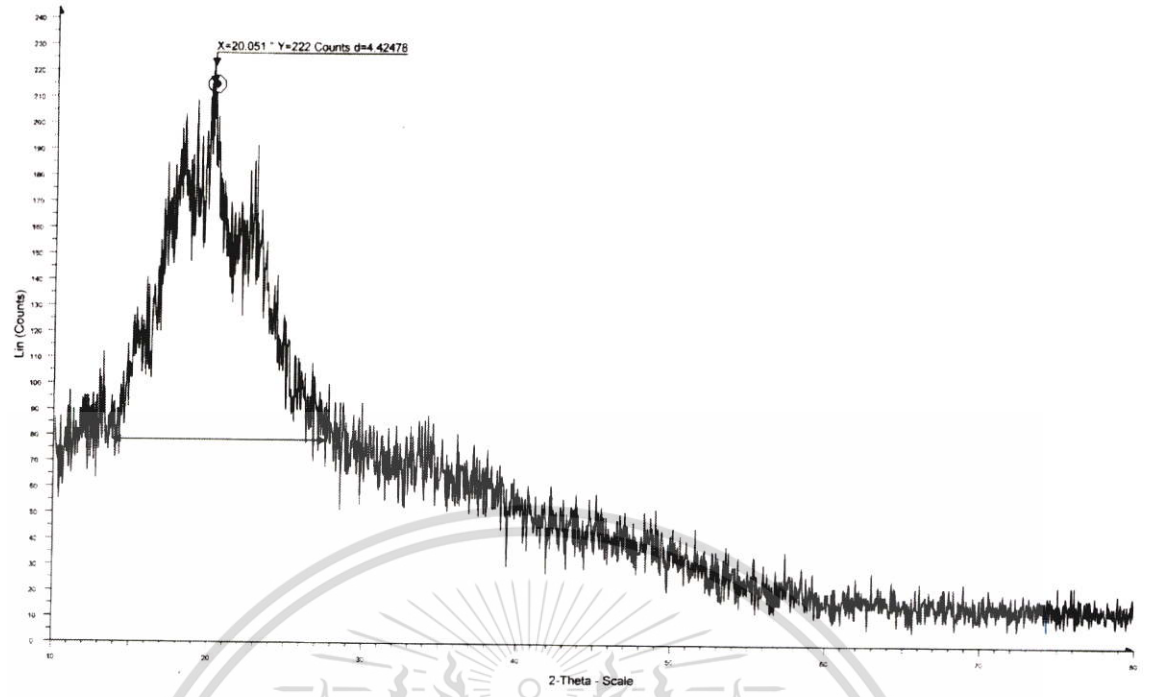

Figure B9 X-ray diffractogram of MBS film cross-linked by 20%SA

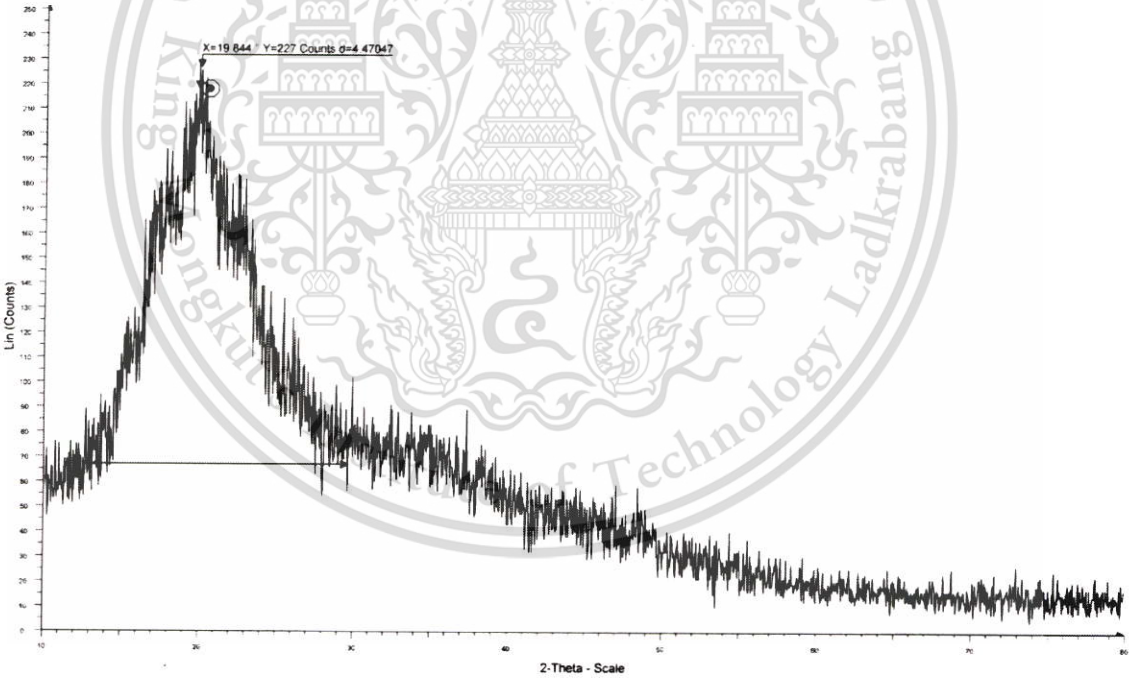

Figure B10 X-ray diffractogram of MBS film cross-linked by 30%SA

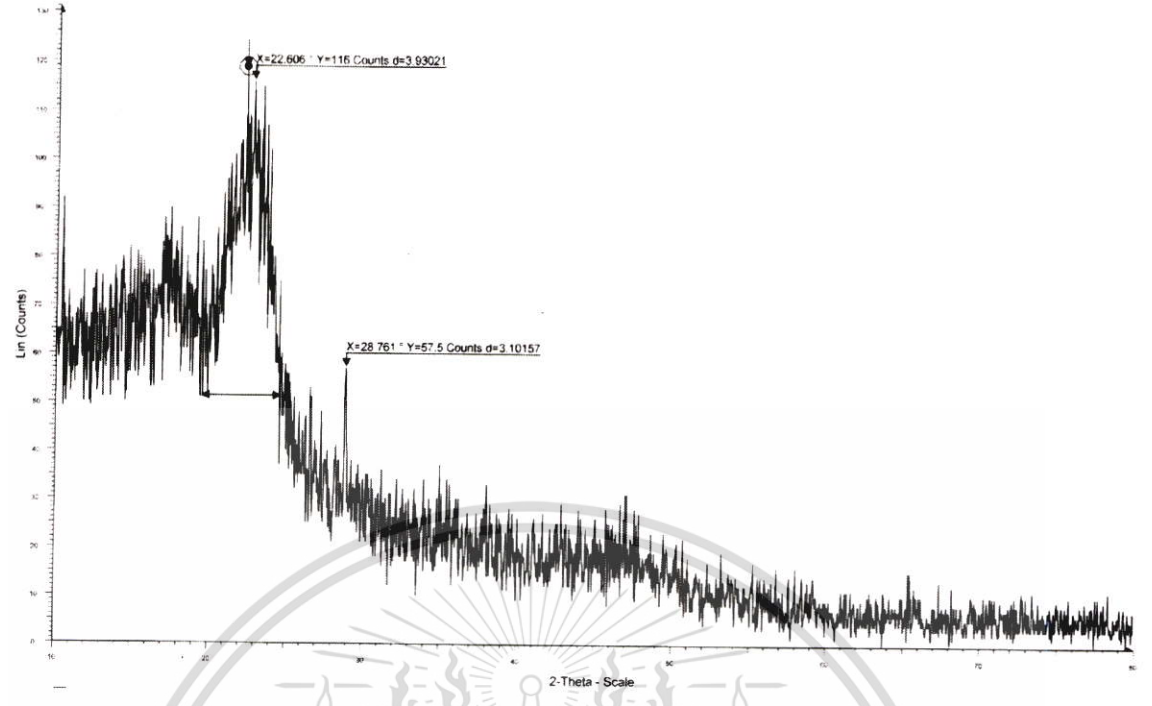

Figure B11 X-ray diffractogram of native BSM film

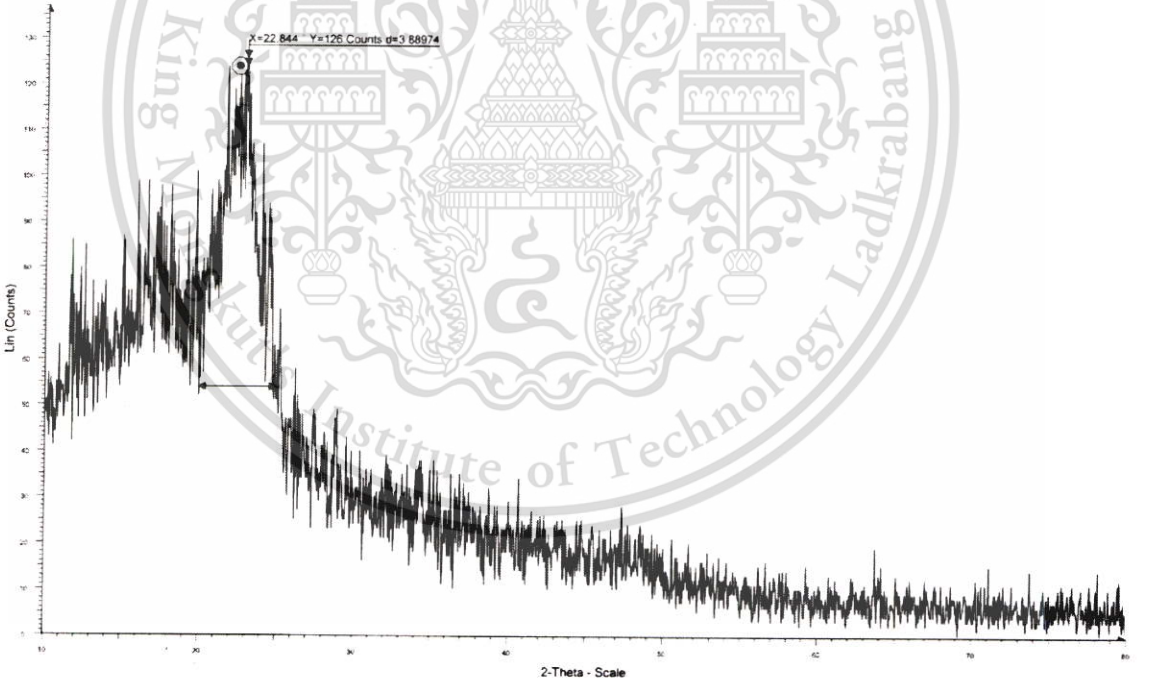

Figure B12 X-ray diffractogram of BSM film cross-linked by 10%TA

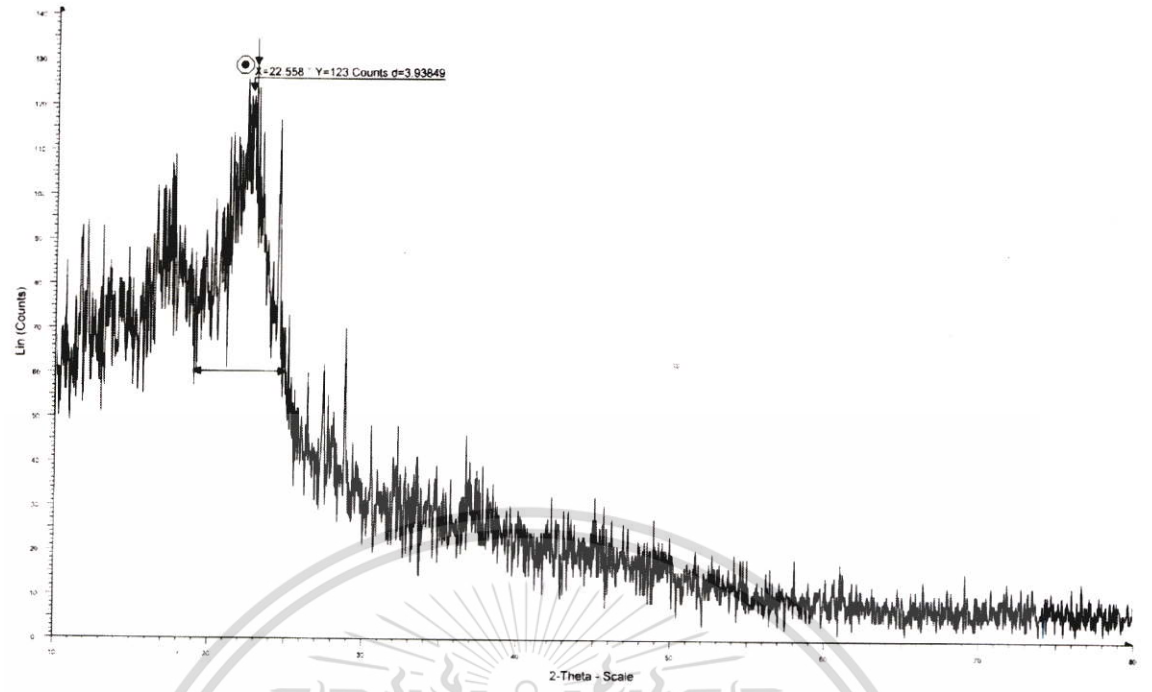

Figure B13 X-ray diffractogram of BSM film cross-linked by 20%TA

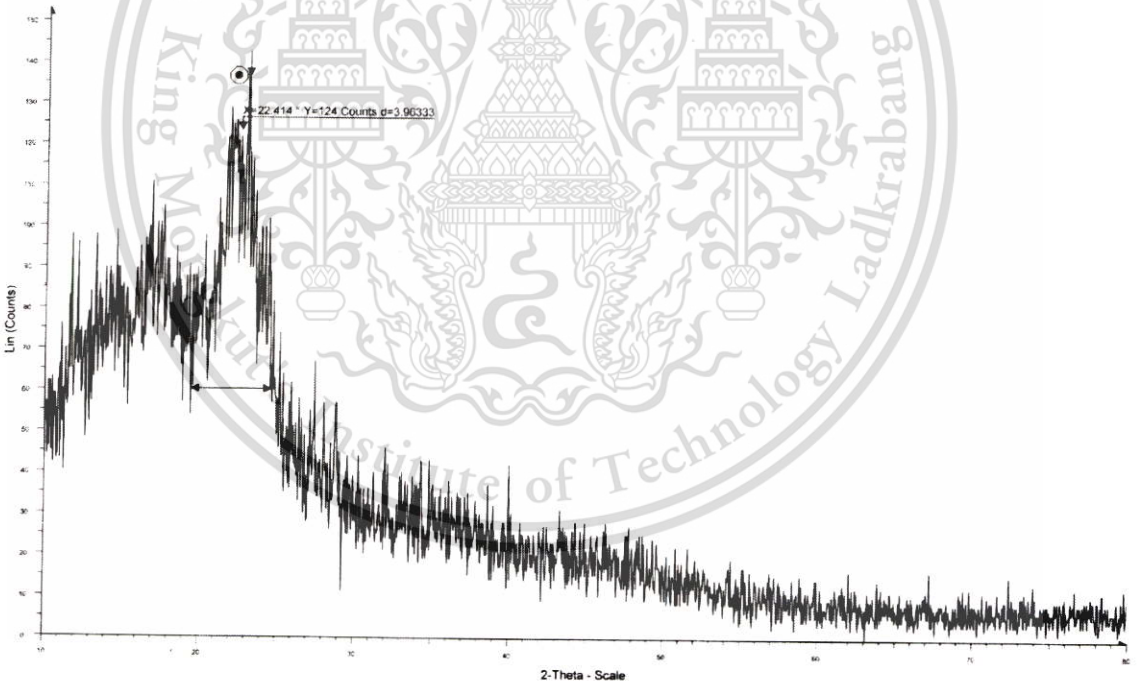

Figure B14 X-ray diffractogram of BSM film cross-linked by 30%TA

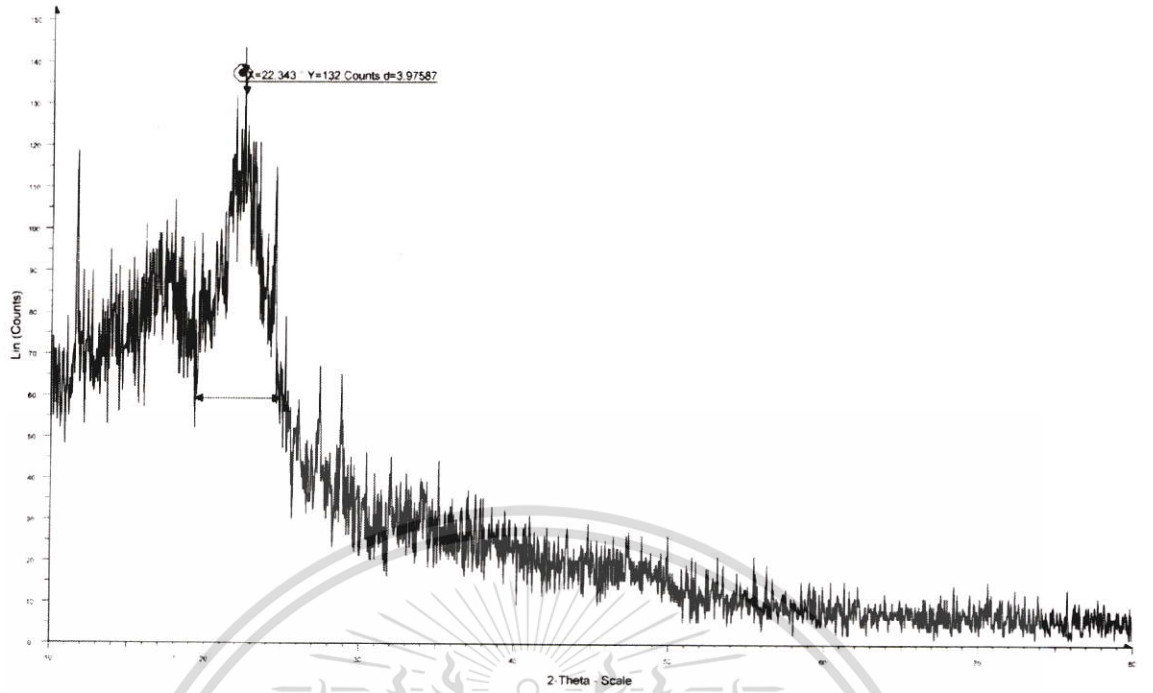

Figure B15 X-ray diffractogram of BSM film cross-linked by 10%MA

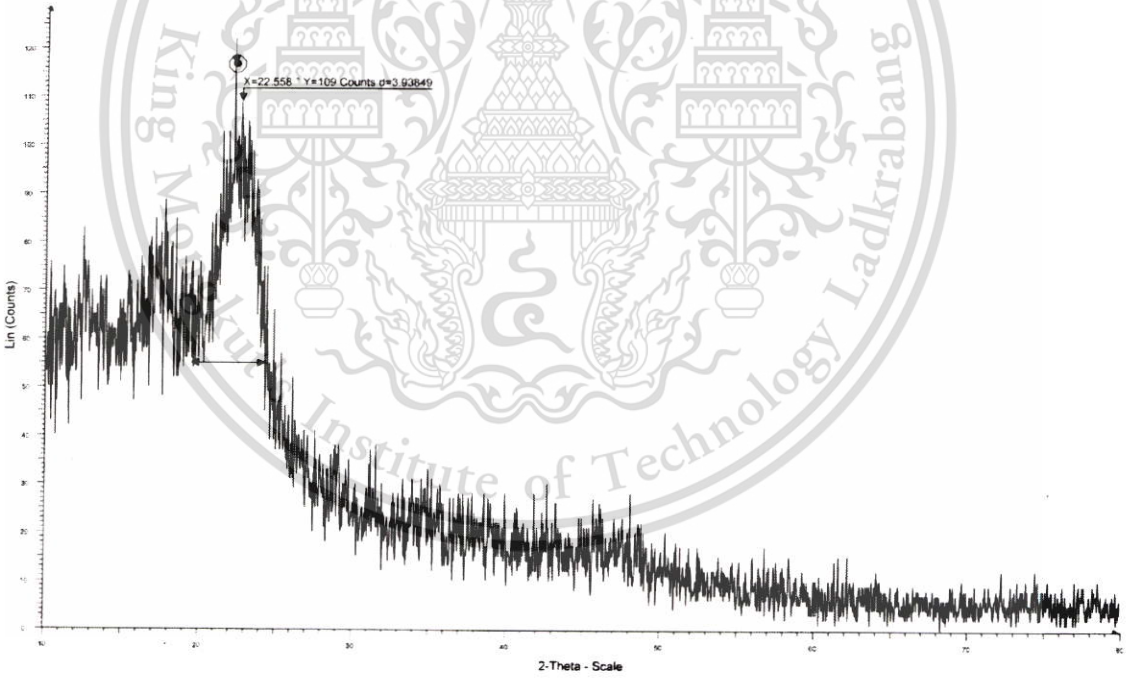

Figure B16 X-ray diffractogram of BSM film cross-linked by 20%MA

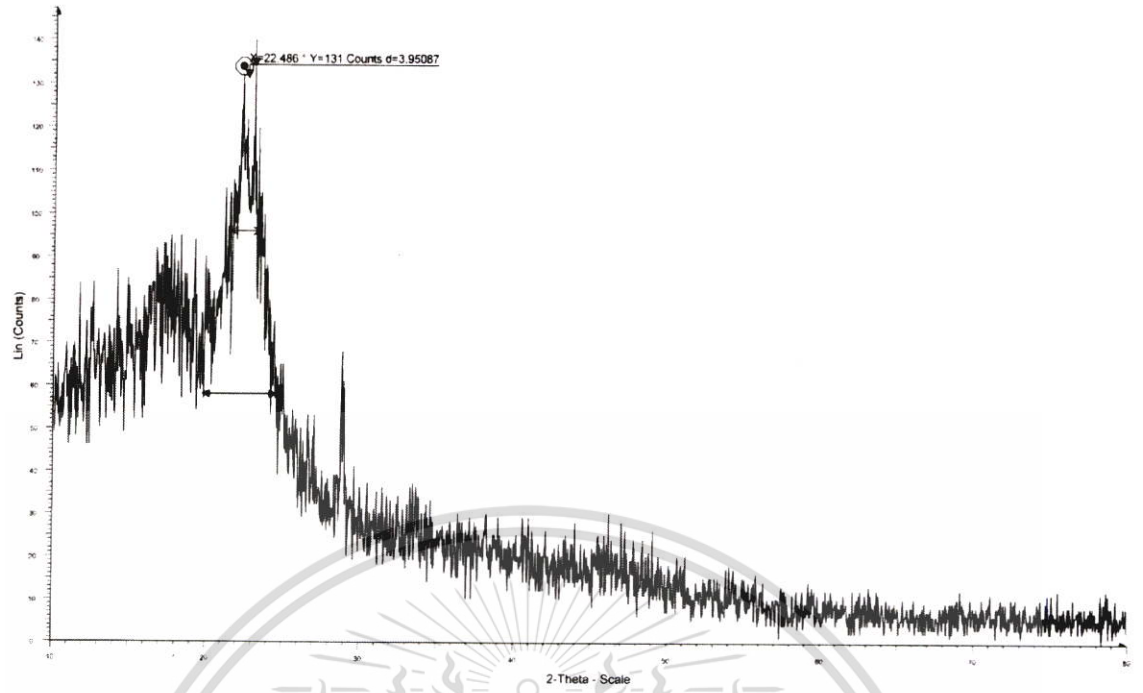

Figure B16 X-ray diffractogram of BSM film cross-linked by 30%MA

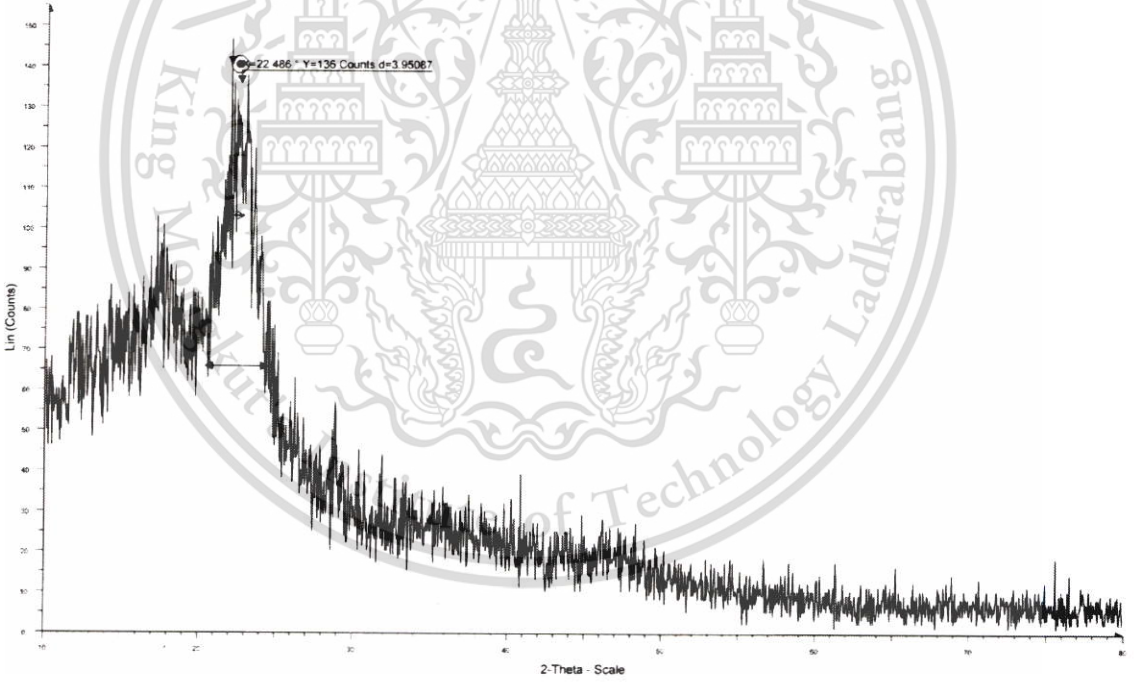

Figure B16 X-ray diffractogram of BSM film cross-linked by 10%SA

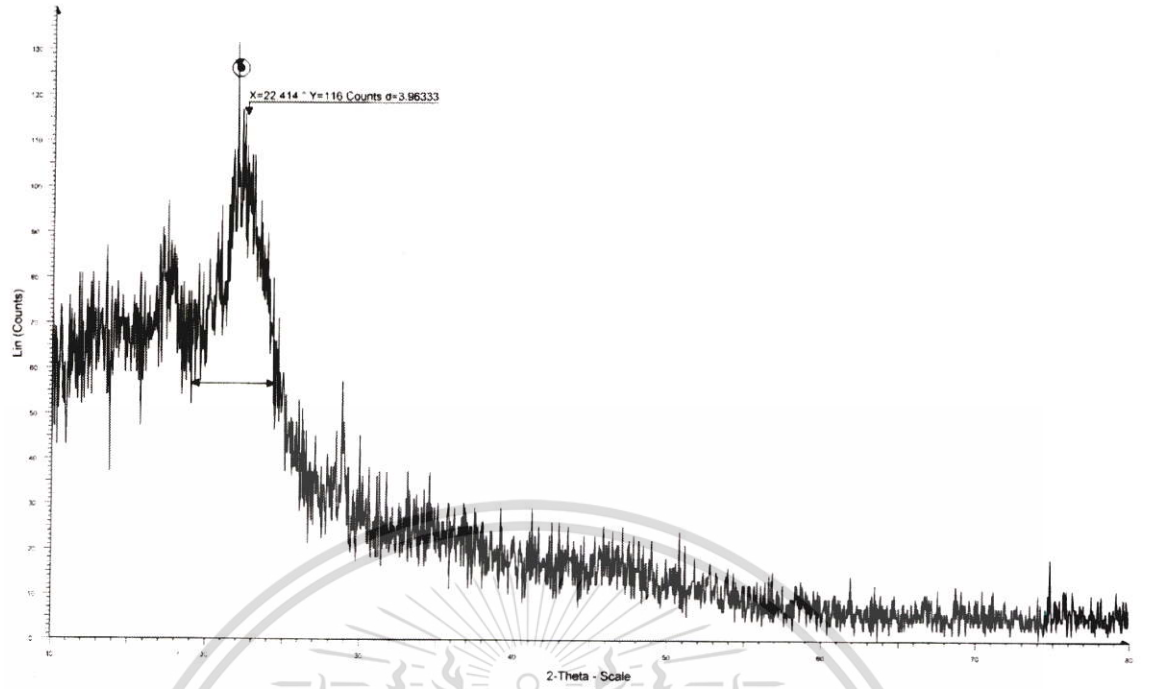

Figure B17 X-ray diffractogram of BSM film cross-linked by 20%SA

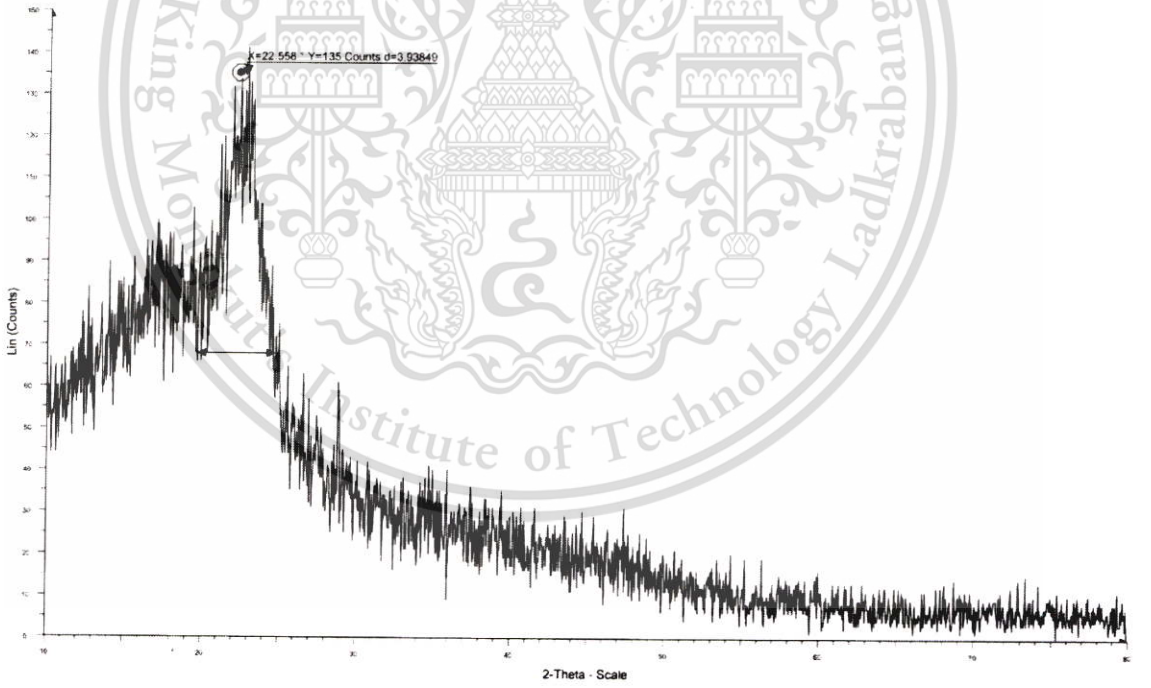

Figure B18 X-ray diffractogram of BSM film cross-linked by 30%SA

Appendix C

Appendix C

Thermogravimetric analysis (TGA)

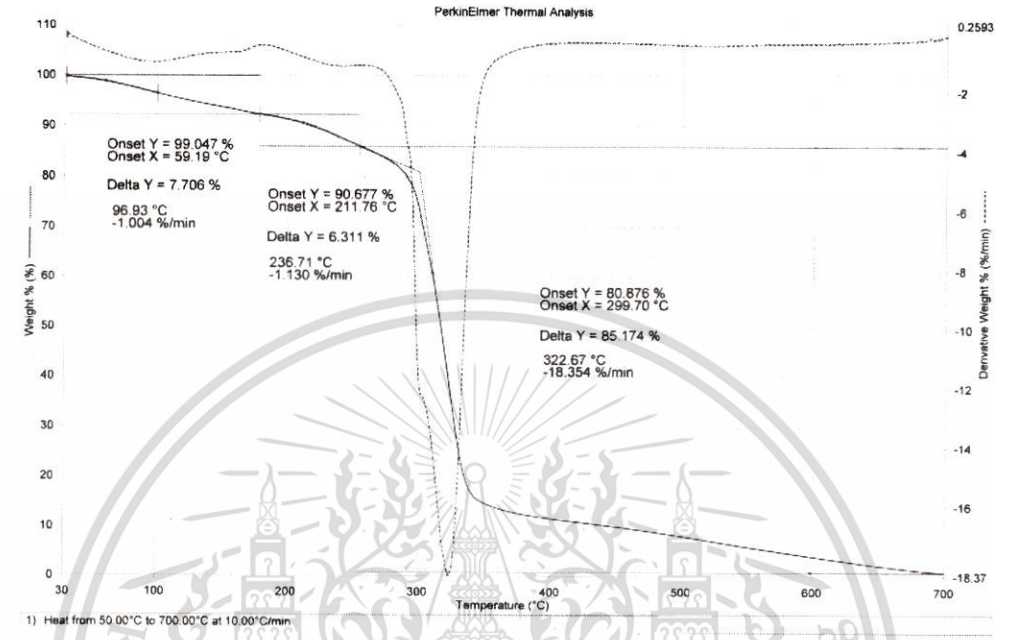

Figure C1 TGA and DTG thermograms of native MBS films

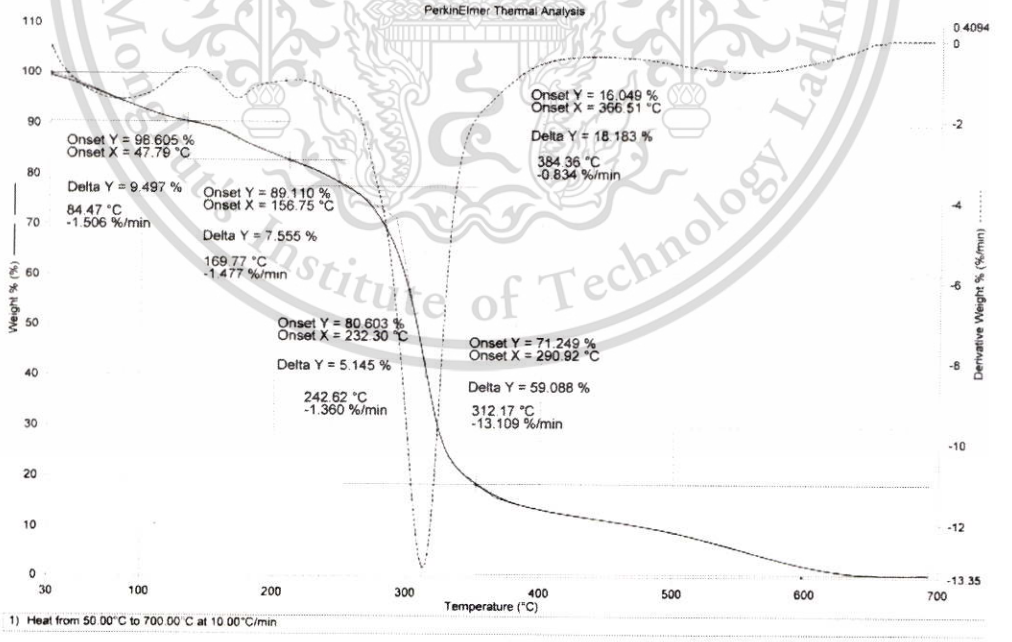

Figure C2 TGA and DTG thermograms of MBS films cross-linked by 10%TA

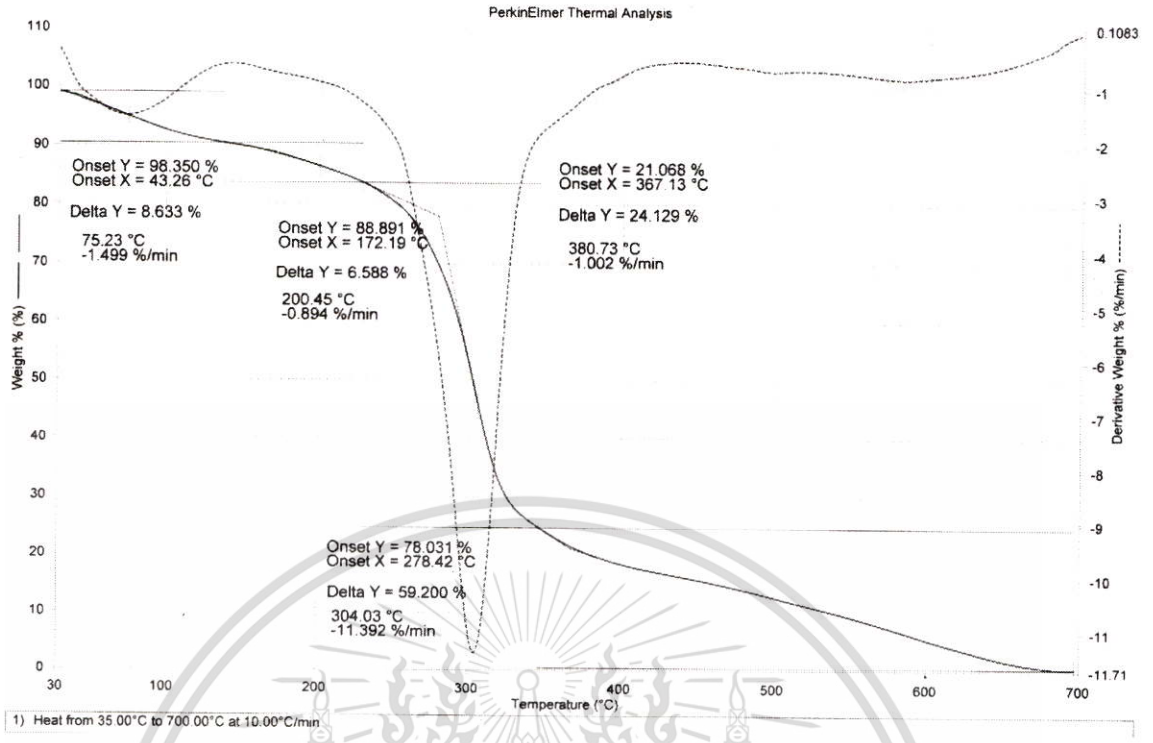

Figure C3 TGA and DTG thermograms of MBS films cross-linked by 20%TA

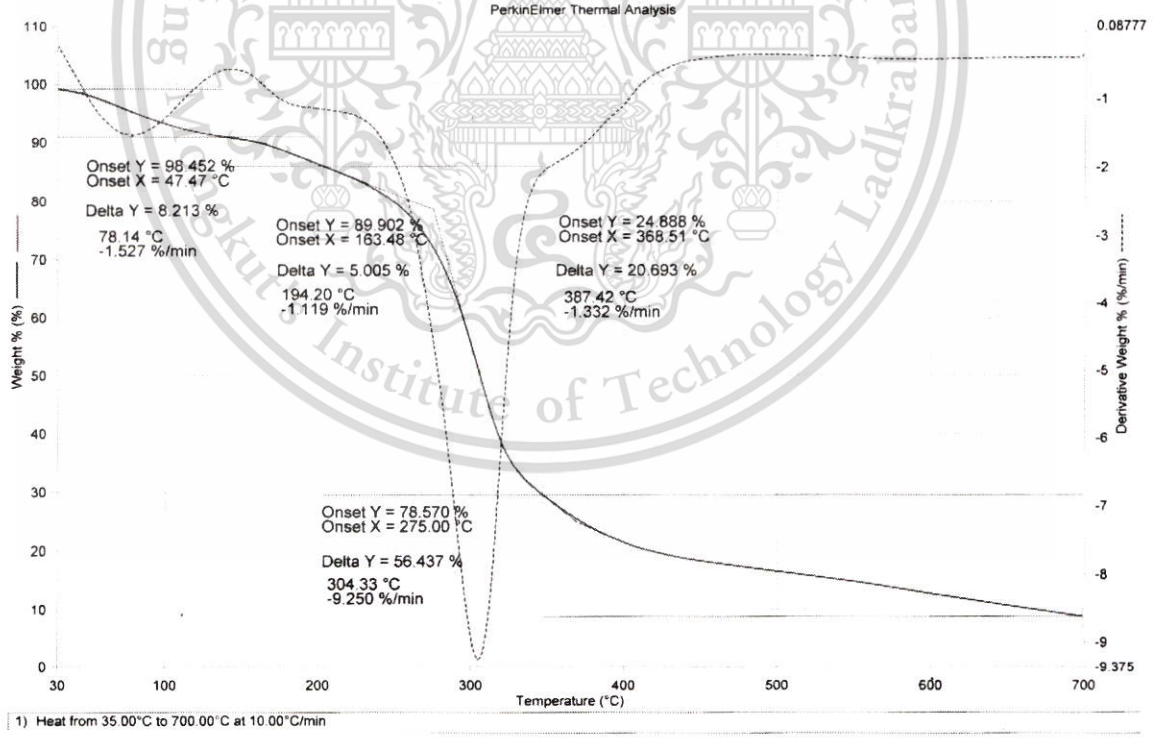

Figure C4 TGA and DTG thermograms of MBS films cross-linked by 30%TA

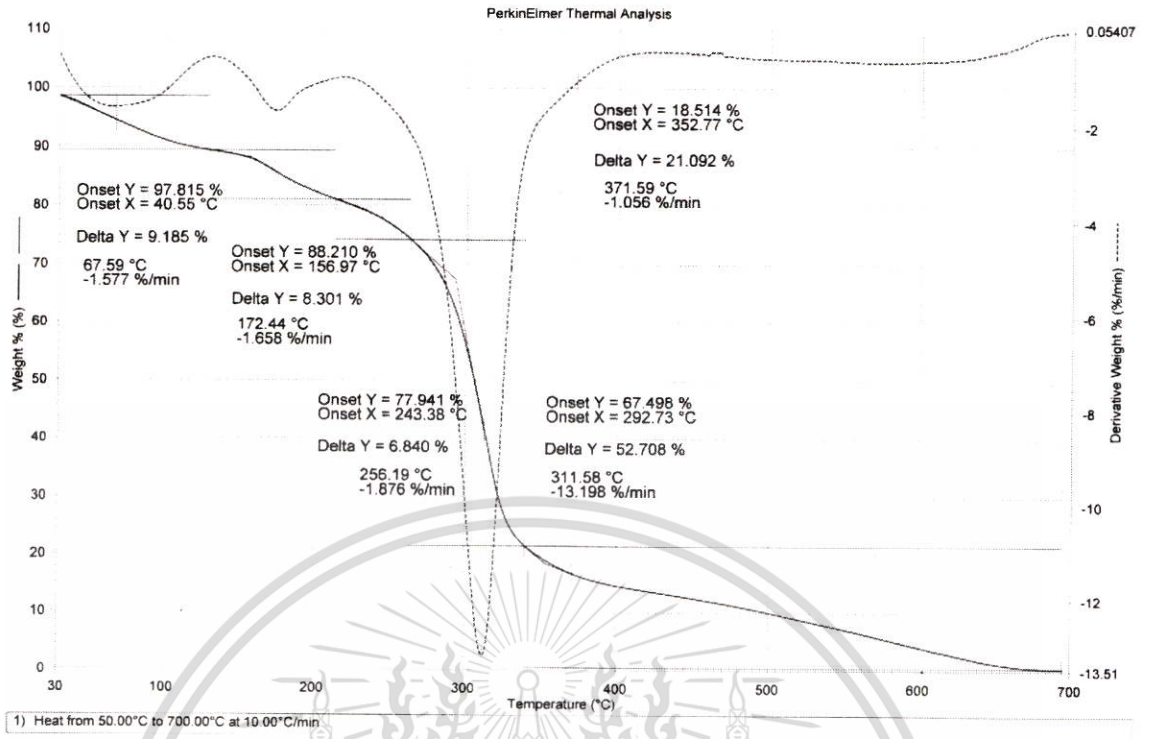

Figure C5 TGA and DTG thermograms of MBS films cross-linked by 10%MA

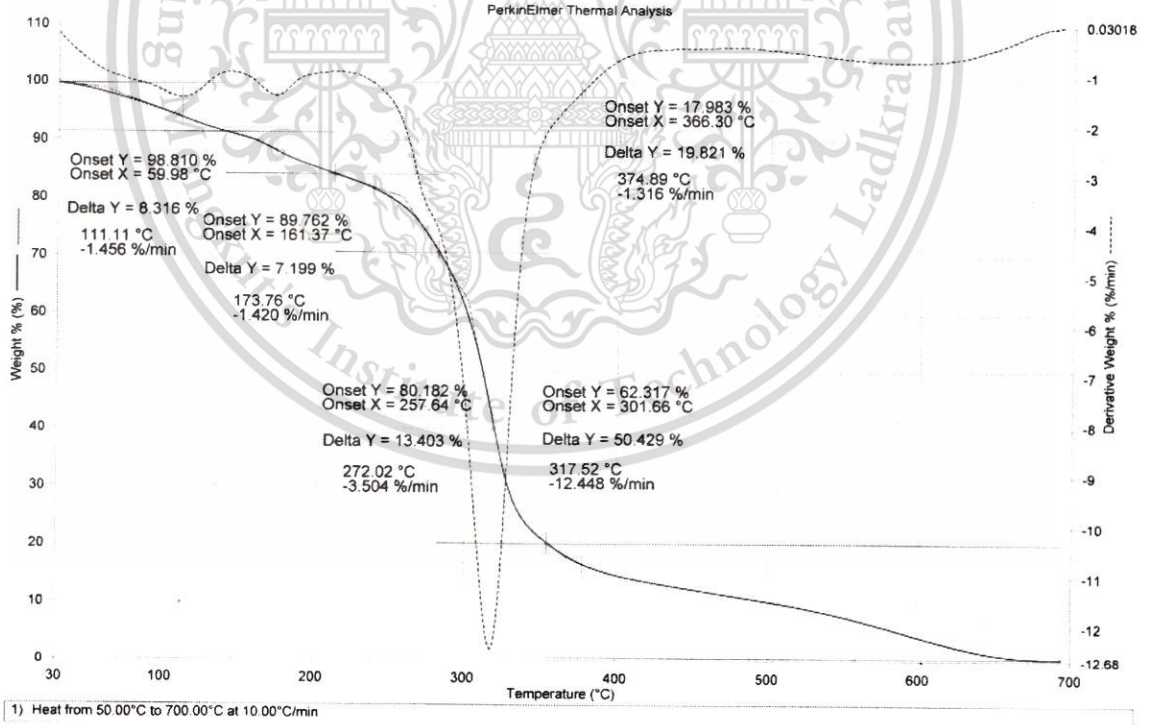

Figure C6 TGA and DTG thermograms of MBS films cross-linked by 20%MA

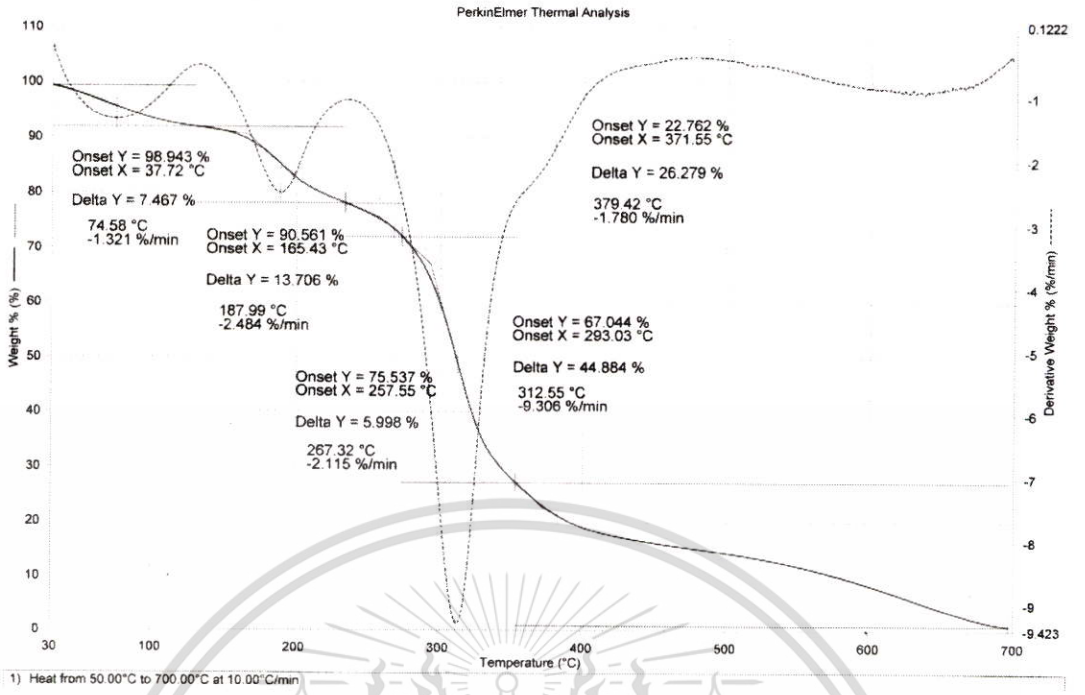

Figure C7 TGA and DTG thermograms of MBS films cross-linked by 30%MA

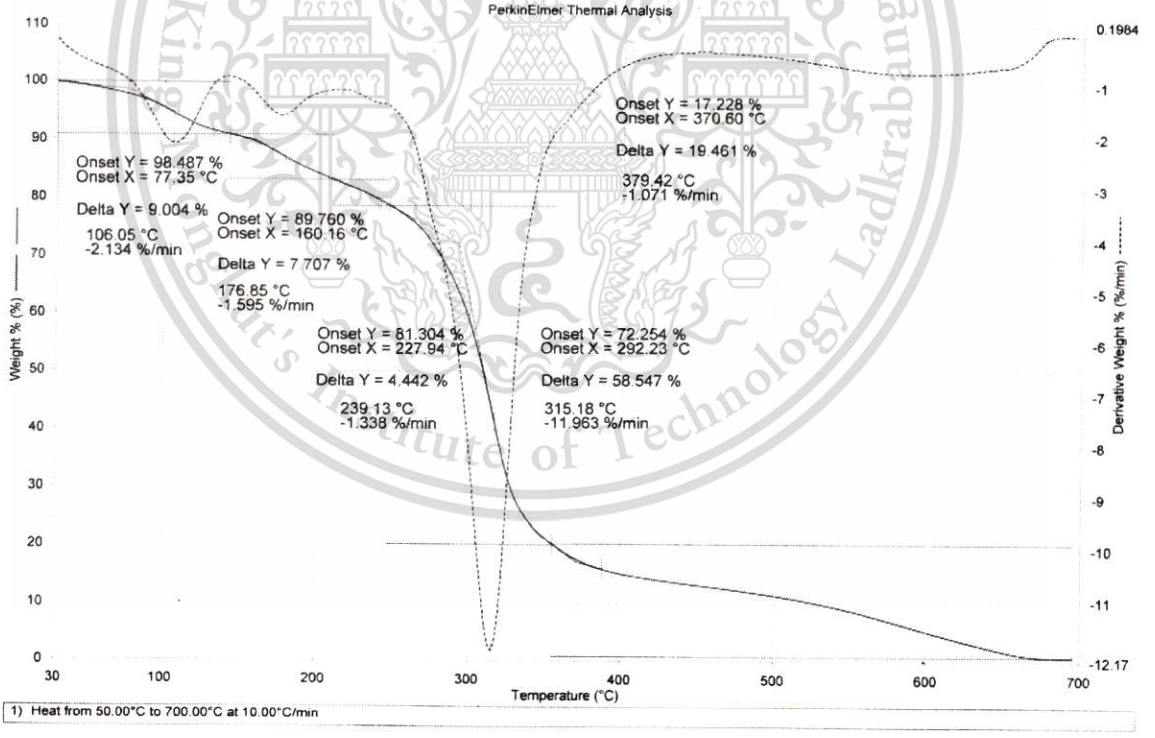

Figure C8 TGA and DTG thermograms of MBS films cross-linked by 10%SA

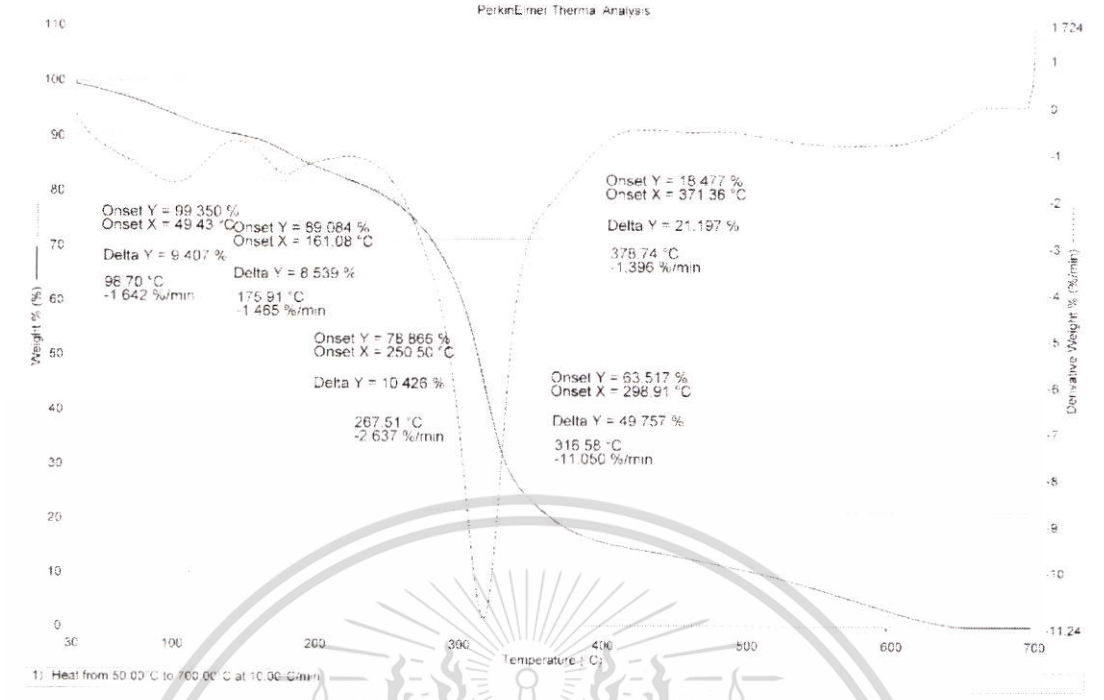

Figure C9 TGA and DTG thermograms of MBS films cross-linked by 20%SA

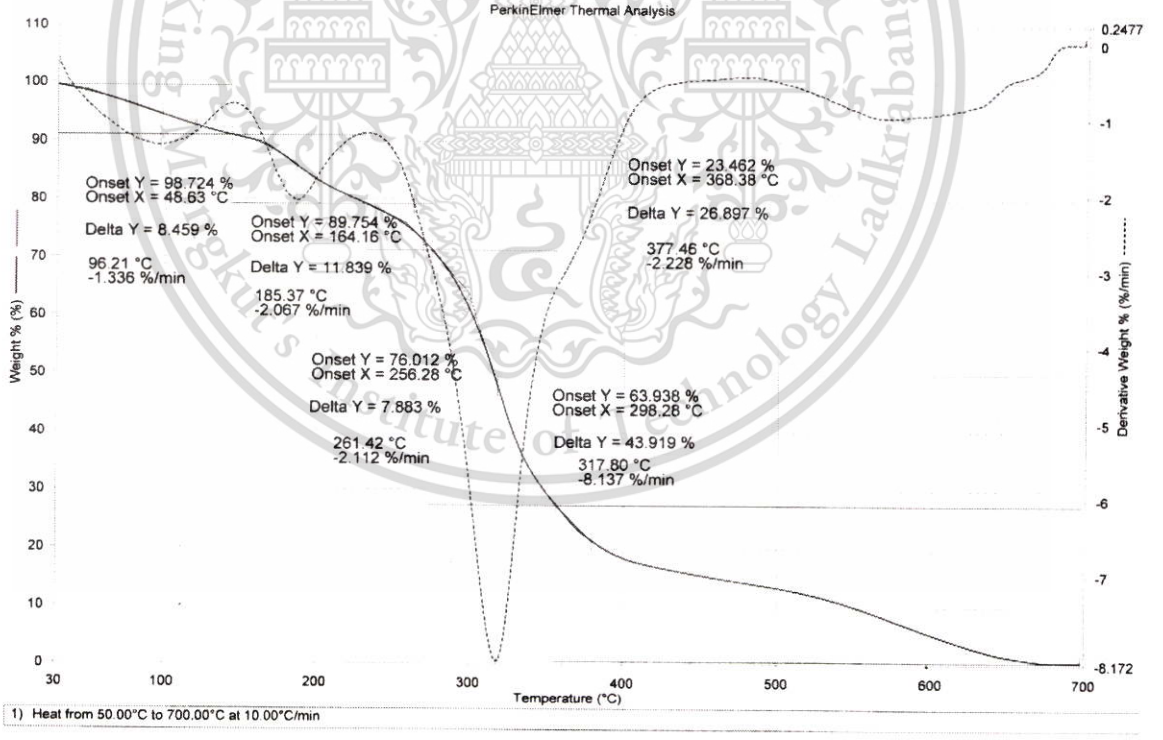

Figure C10 TGA and DTG thermograms of MBS films cross-linked by 30%SA

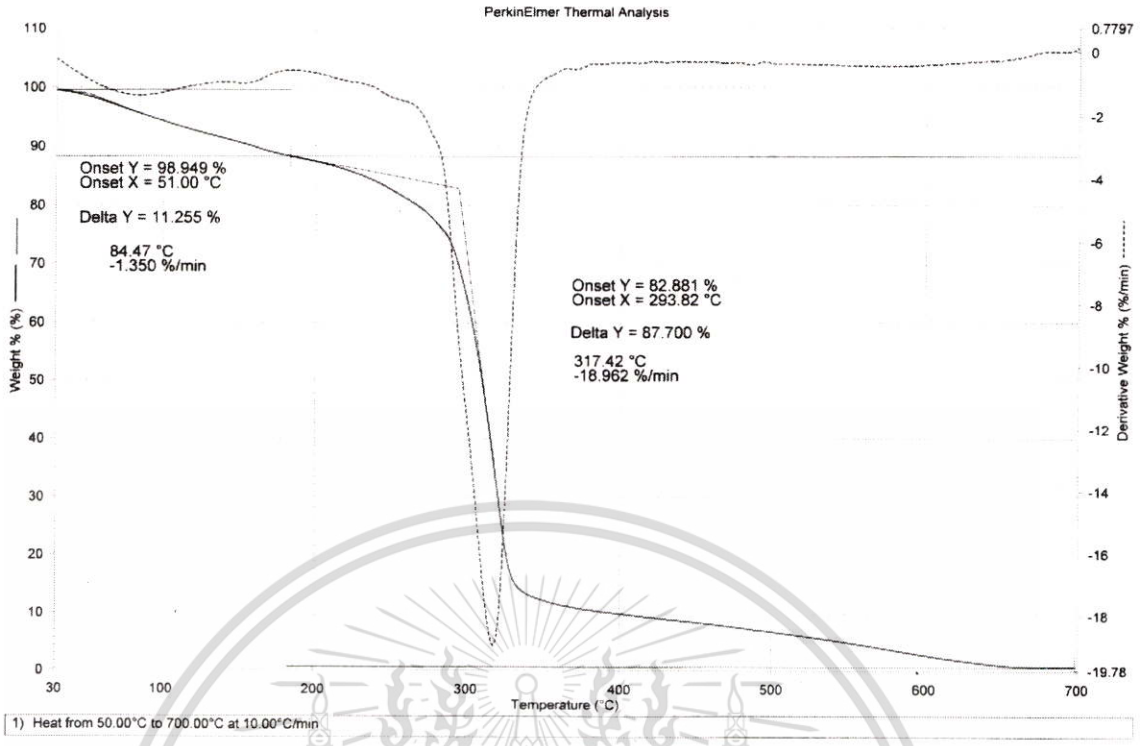

Figure C11 TGA and DTG thermograms of native BSM films

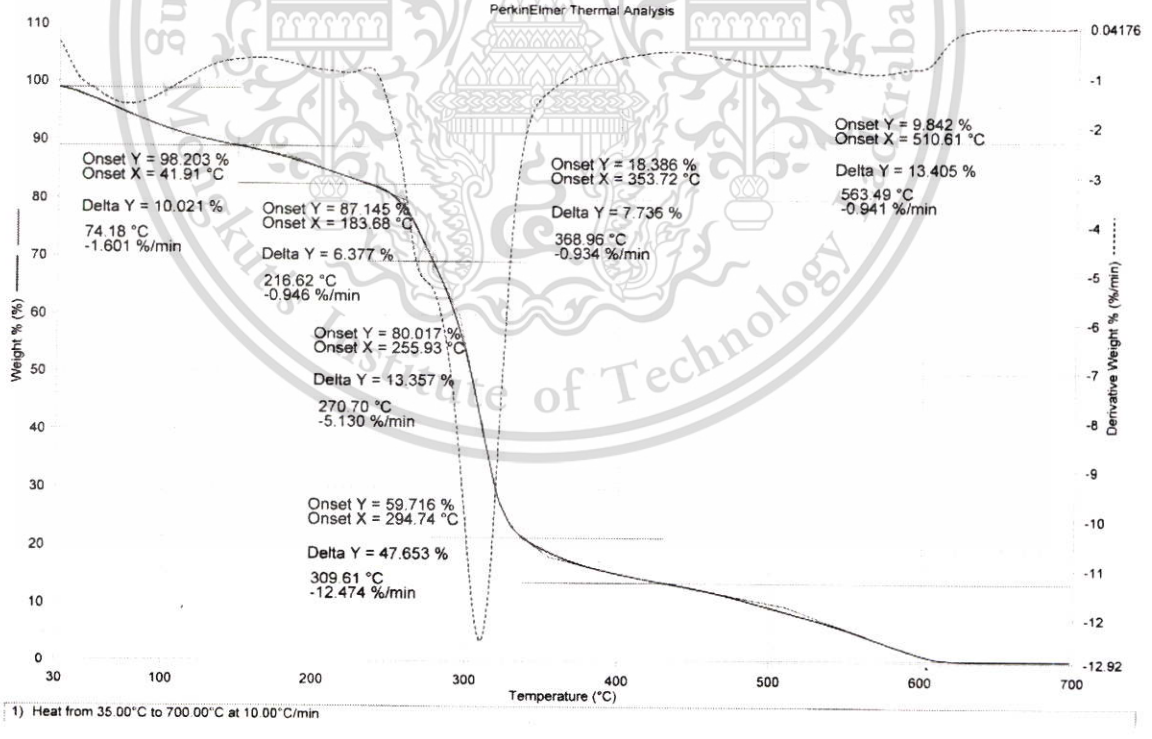

Figure C12 TGA and DTG thermograms of BSM films cross-linked by 10%TA

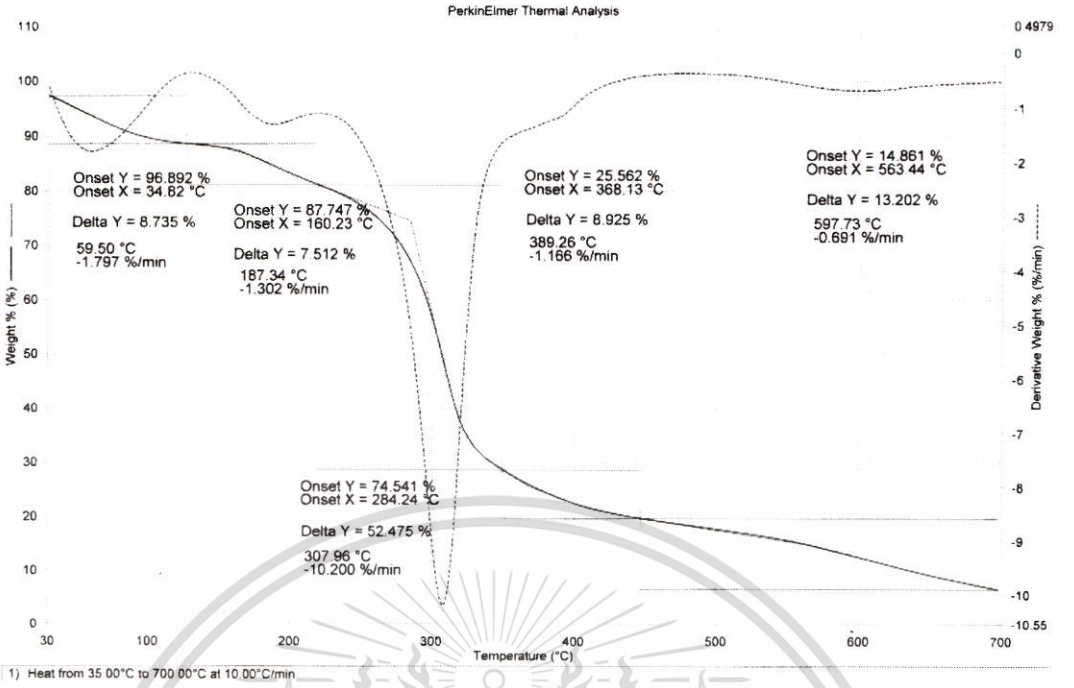

Figure C13 TGA and DTG thermograms of BSM films cross-linked by 20%TA

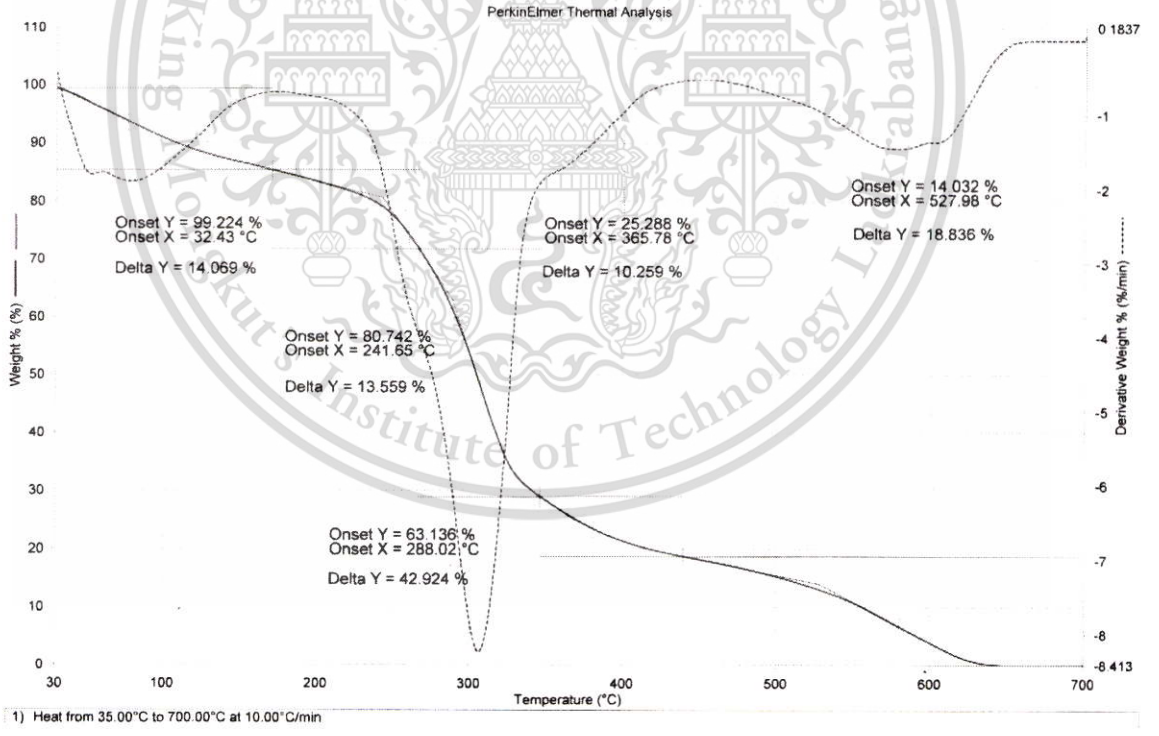

Figure C14 TGA and DTG thermograms of BSM films cross-linked by 30%TA

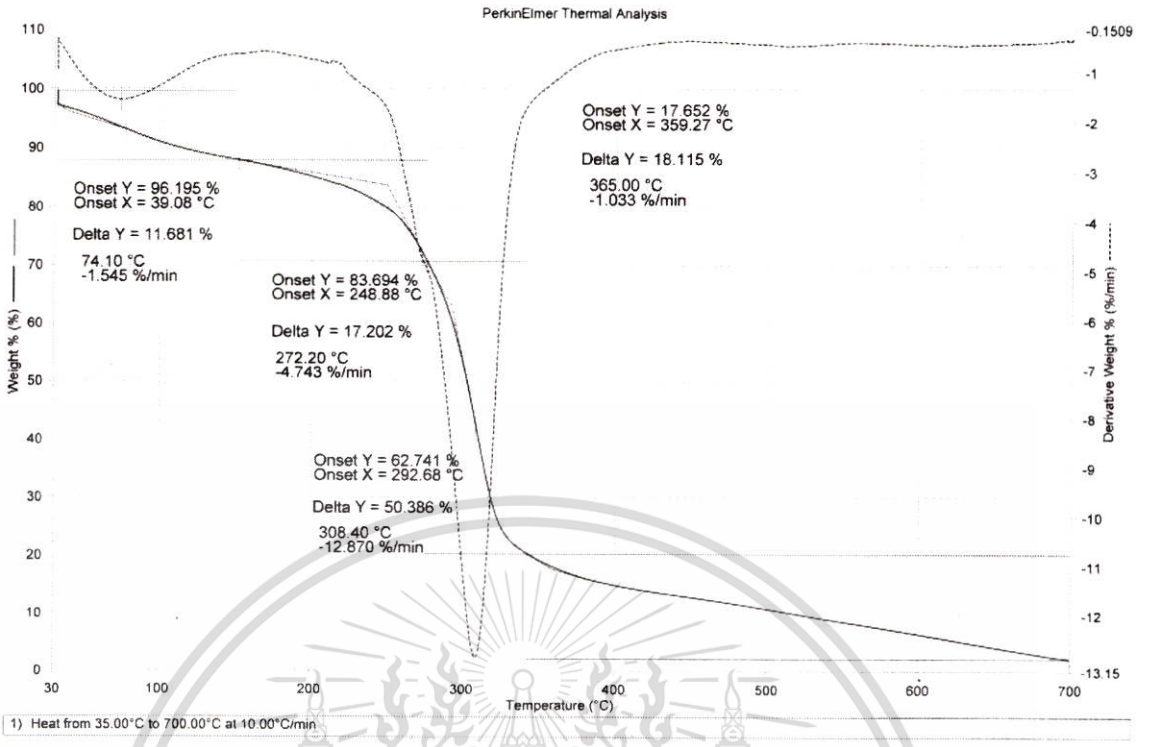

Figure C14 TGA and DTG thermograms of BSM films cross-linked by 10%MA

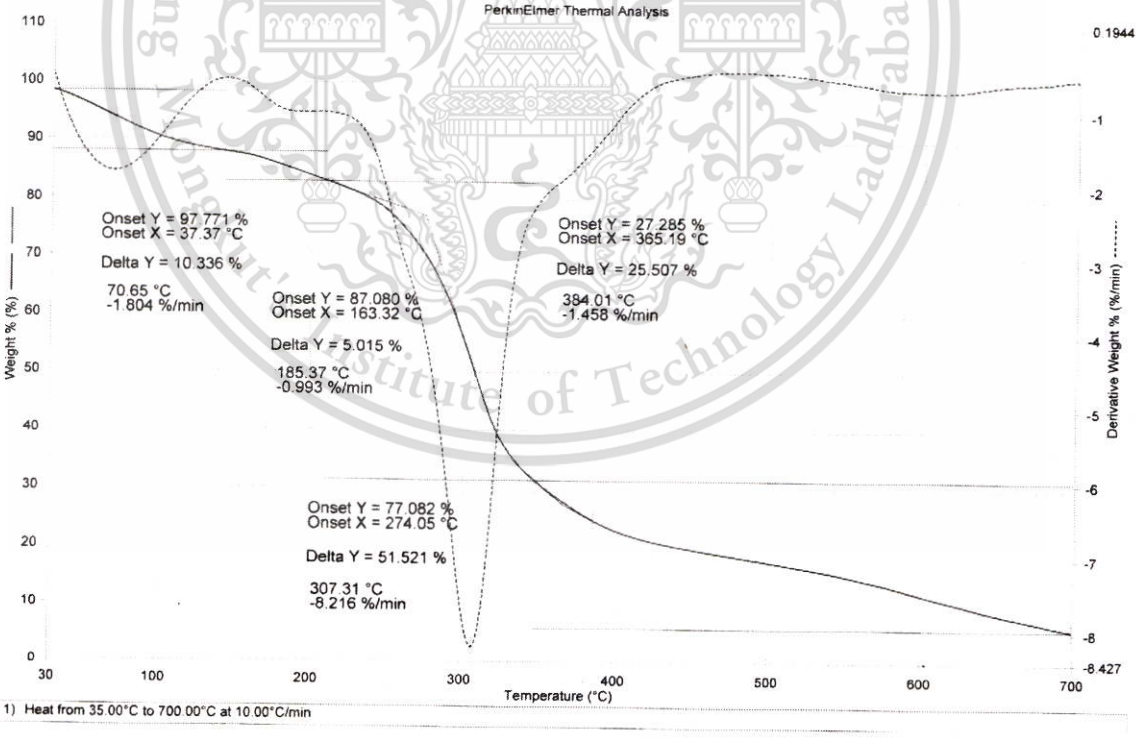

Figure C14 TGA and DTG thermograms of BSM films cross-linked by 20%MA

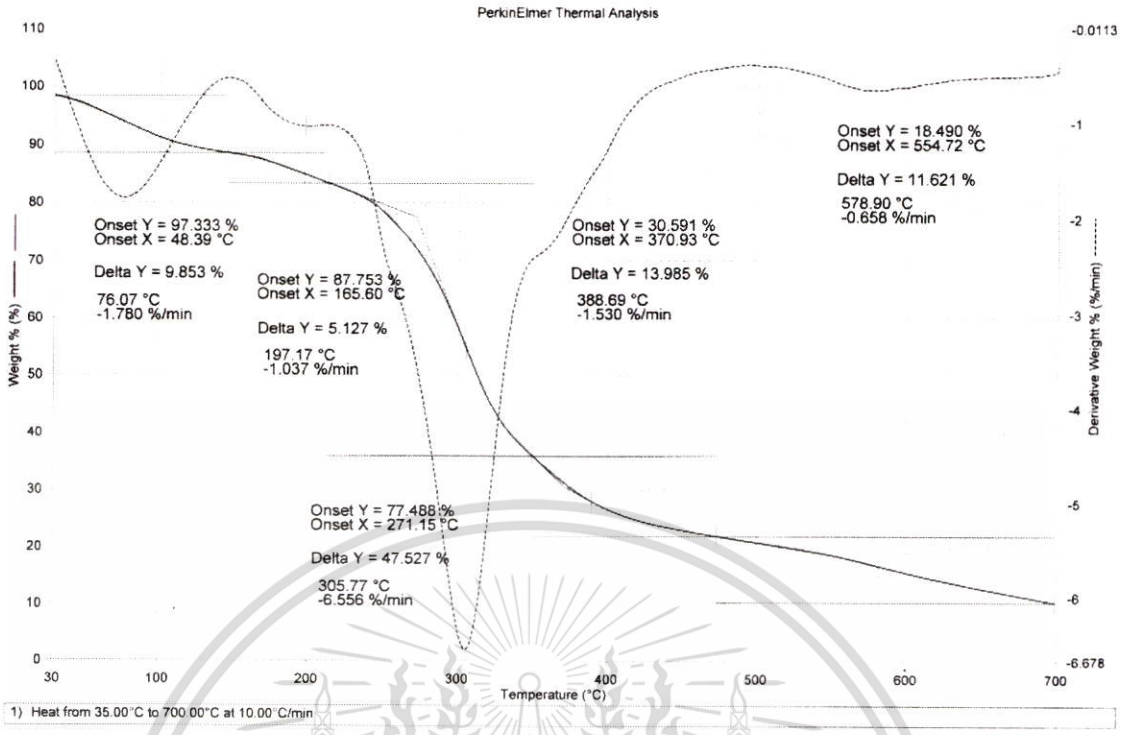

Figure C14 TGA and DTG thermograms of BSM films cross-linked by 30%MA

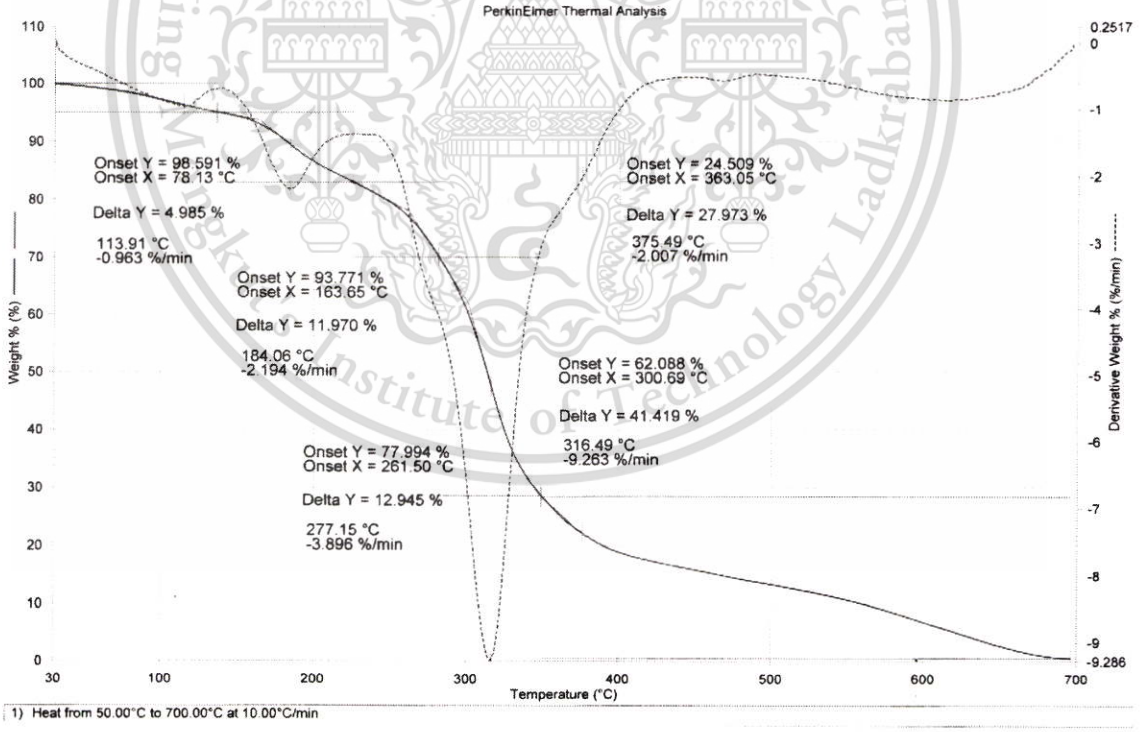

Figure C15 TGA and DTG thermograms of BSM films cross-linked by 10%SA

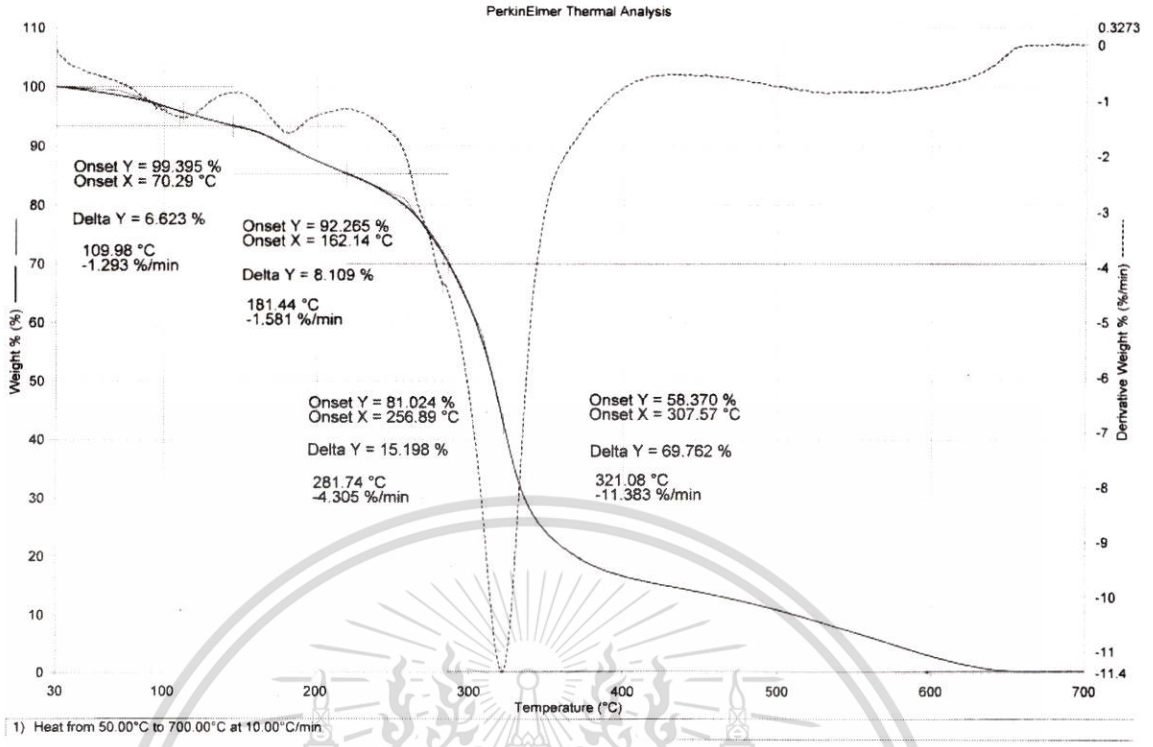

Figure C16 TGA and DTG thermograms of BSM films cross-linked by 20%SA

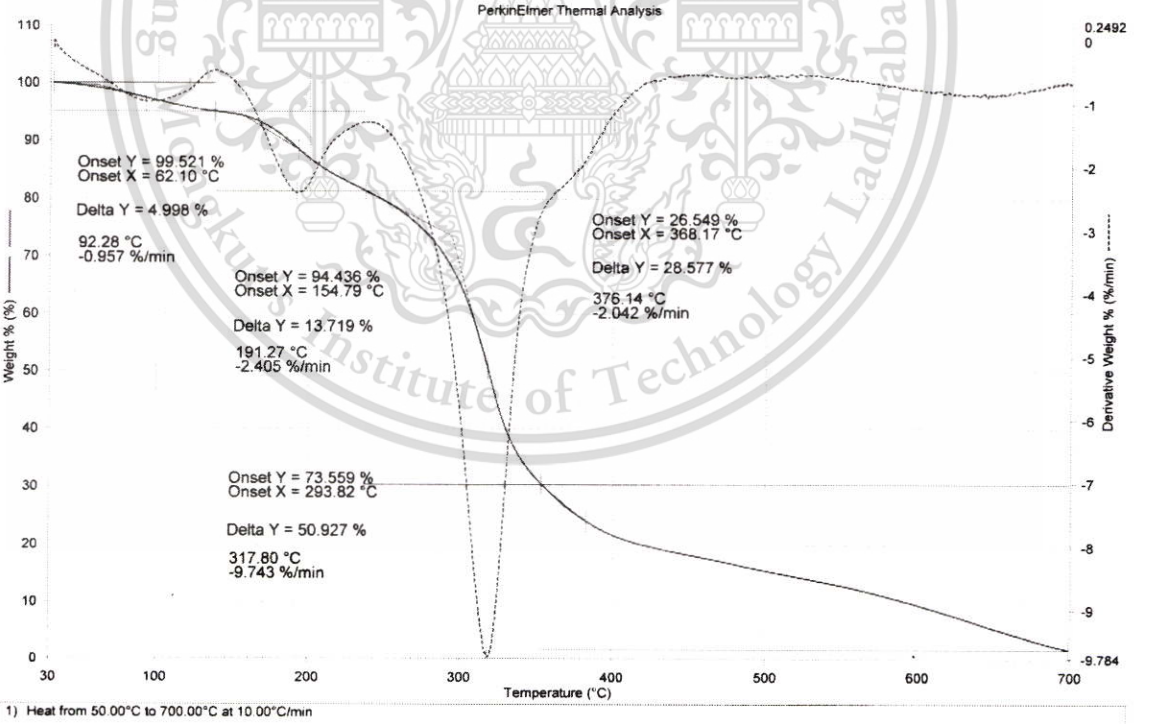

Figure C17 TGA and DTG thermograms of BSM films cross-linked by 30%SA

Appendix D

Appendix D

Soil burial test

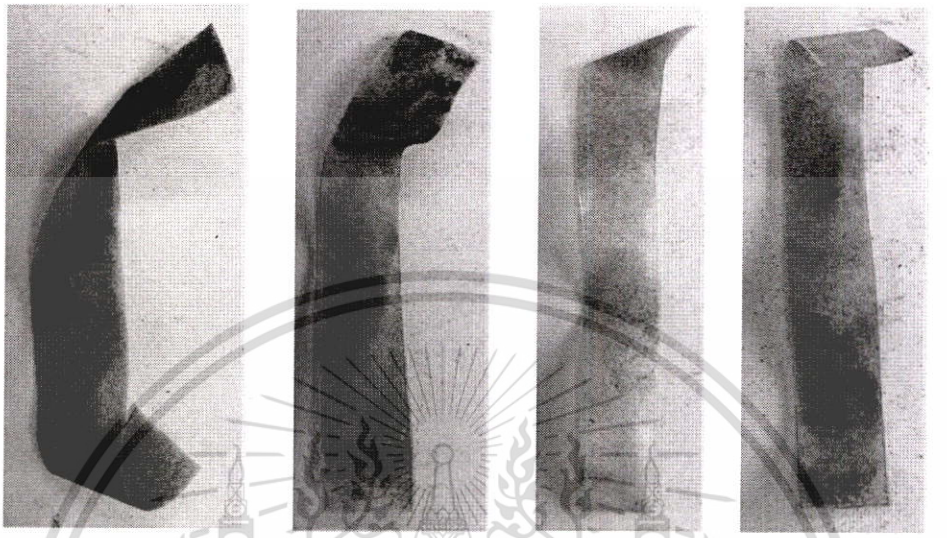

(1) BSM (2) BSM10TA (3) BSM15TA (4) BSM20TA

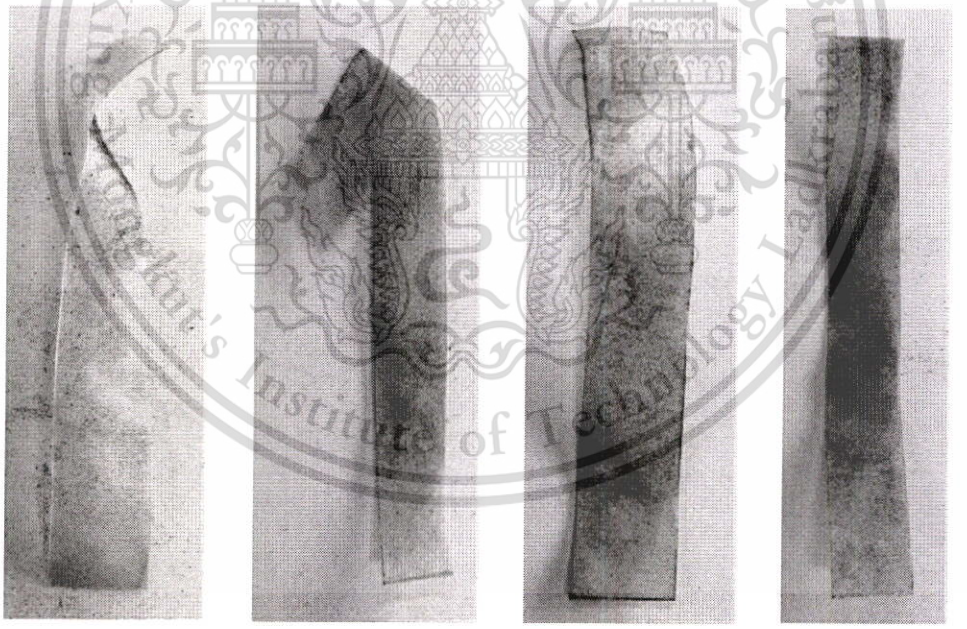

(5) BSM25TA (6) BSM30TA (7) BSM10MA (8) BSM15MA

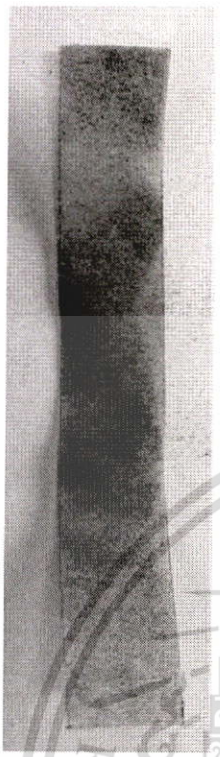

(9) BSM20MA

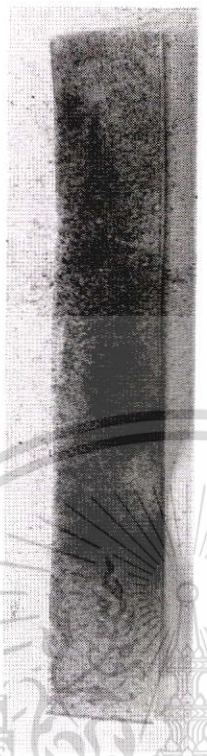

(10) BSM25MA

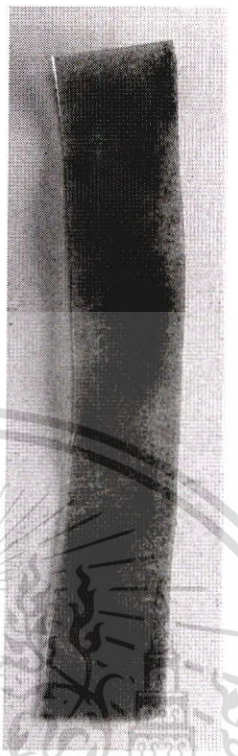

(11) BSM30MA

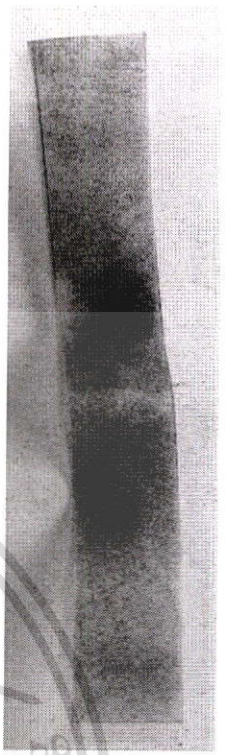

(12) BSM10SA

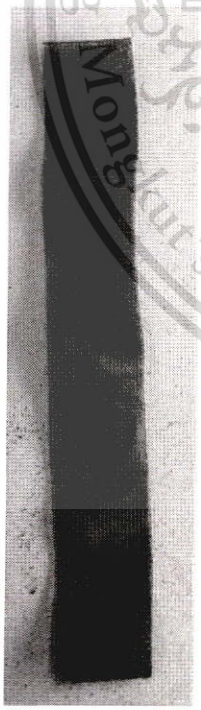

(13) BSM15SA

(14) BSM20SA

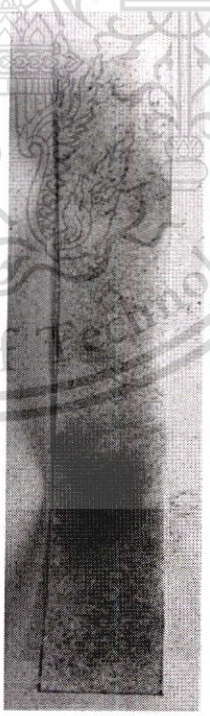

(15) BSM25SA

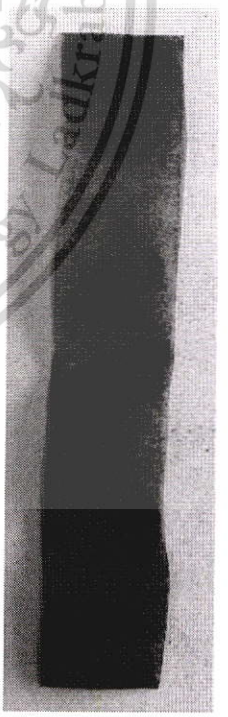

(16) BSM30SA

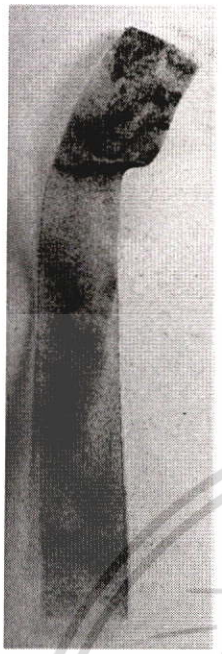

(17) MBS

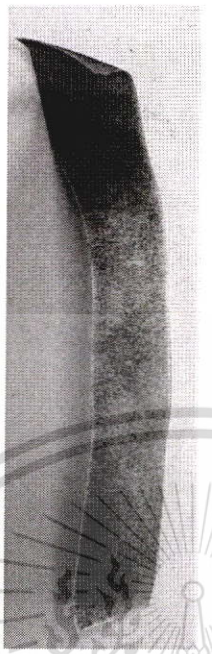

(18) MBS10TA

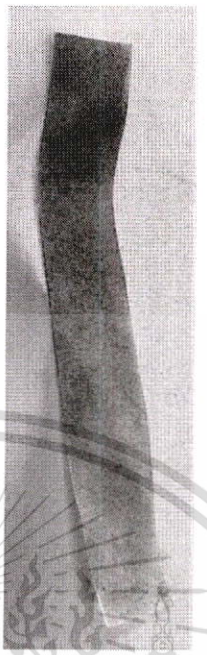

(19) MBS15TA

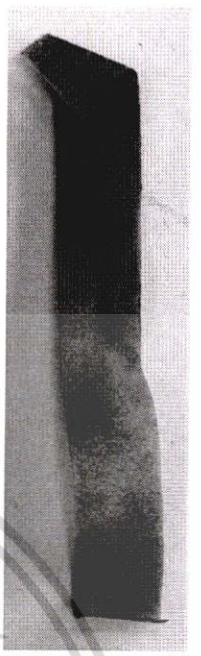

(20) MBS20TA

(21) MBS25TA

(22) MBS30TA

(23) MBS10MA

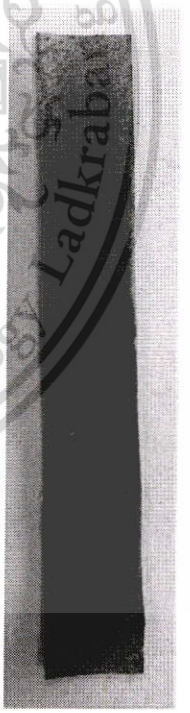

(24) MBS15MA

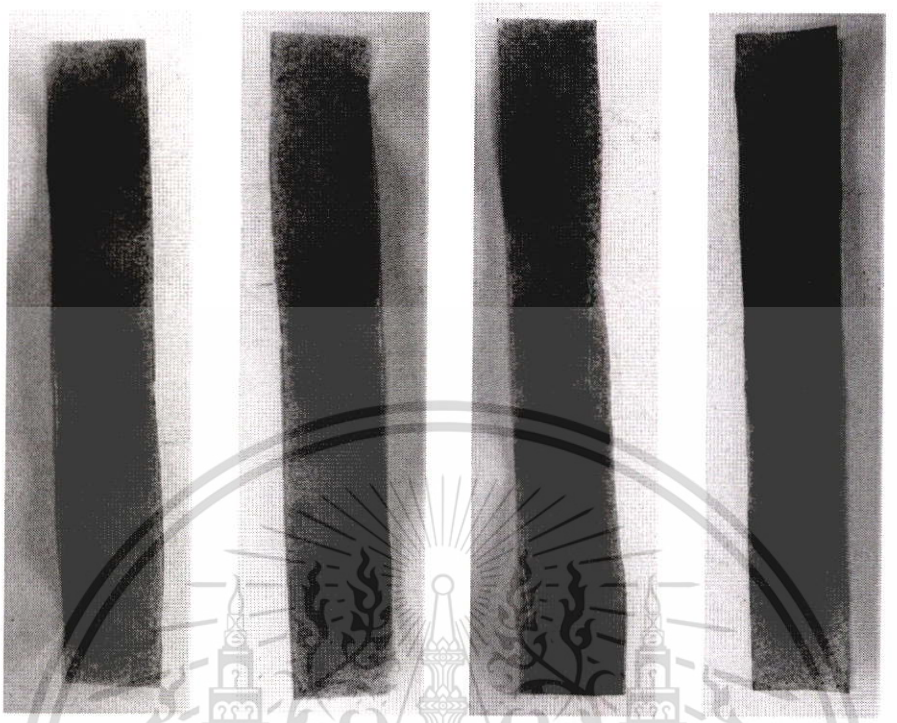

(25) MBS20MA (26) MBS25MA (27) MBS30MA (28) MBS10SA

(29) MBS15SA (30) MBS20SA (31) MBS25SA (32) MBS30SA

Appendix E

Appendix E

Swelling power

Table E.1 Swelling power of different native and cross-linked MBS and BSM films with TA, MA and SA

Time (h)	Swelling power (%)								
	MBS	MBS10TA	MBS15TA	MBS20TA	MBS25TA	MBS30TA	MBS10MA	MBS15MA	MBS20MA
0	0	0	0	0	0	0	0	0	0
1	143±1.32	116±1.77	83±1.55	85±1.91	73±1.24	59±1.52	105±1.12	81±1.22	62±1.44
2	153±1.82	125±1.66	102±1.76	92±1.68	82±1.09	64±1.47	110±1.46	85±1.19	68±1.23
3	167±1.14	131±1.29	118±1.03	97±1.11	87±1.44	70±1.88	119±1.58	90±1.93	73±1.38
4	178±1.41	144±1.10	122±1.64	102±1.22	90±1.58	83±1.69	125±1.79	104±1.03	80±1.83
5	179±1.37	157±1.84	134±1.54	111±1.41	99±1.72	85±1.43	131±1.52	114±1.74	95±1.14
6	183±1.32	165±1.21	140±1.42	115±1.82	104±1.44	91±1.28	143±1.45	124±1.06	101±1.60
72	185±1.20	168±1.50	144±1.61	125±1.62	108±1.51	97±1.54	147±1.28	132±1.53	104±1.14

Table E.1 (continue) Swelling power of different native and cross-linked MBS and BSM films with TA, MA and SA

Time (h)	Swelling power (%)								
	MBS25MA	MBS30MA	MBS10SA	MBS15SA	MBS20SA	MBS25SA	MBS30SA	BSM	BSM10TA
0	0	0	0	0	0	0	0	0	0
1	53±1.46	44±1.24	70±1.24	58±1.75	49±1.56	31±1.71	21±1.33	312±1.66	261±2.42
2	61±1.34	49±1.45	87±1.31	69±1.11	58±1.07	43±1.20	33±1.38	328±2.41	274±2.51
3	65±1.25	54±1.81	91±1.42	74±1.31	63±1.48	52±1.83	40±1.09	337±2.13	289±2.26
4	71±1.23	62±1.72	95±1.50	81±1.38	70±1.29	58±1.71	45±1.65	341±2.19	297±2.20
5	82±1.31	69±1.93	96±1.53	89±1.89	78±1.67	65±1.96	54±0.83	355±2.78	301±2.37
6	88±1.78	73±1.28	102±1.22	95±1.37	81±1.46	68±1.78	61±0.94	355±2.64	312±2.55
72	91±1.63	79±1.67	114±1.38	103±1.09	86±1.55	72±1.90	62±0.62	355±2.41	321±1.87

Table E.1 (continue) Swelling power of different native and cross-linked MBS and BSM films with TA, MA and SA

Time (h)	Swelling power (%)								
	BSM15TA	BSM20TA	BSM25TA	BSM30TA	BSM10MA	BSM15MA	BSM20MA	BSM25MA	BSM30MA
0	0	0	0	0	0	0	0	0	0
1	250±2.09	249±2.83	237±2.85	223±2.11	241±2.35	233±2.05	226±2.25	218±2.19	208±2.61
2	258±2.56	253±2.44	242±2.70	231±2.46	254±2.41	248±2.63	237±2.52	220±2.41	215±2.07
3	268±2.33	258±2.20	245±2.20	234±2.37	261±2.43	252±2.38	244±2.22	229±2.13	220±2.33
4	276±2.60	264±2.56	250±2.34	238±2.67	265±2.26	254±2.45	249±2.38	232±2.51	224±2.61
5	282±2.14	267±2.34	255±2.45	243±1.89	268±2.31	260±2.36	252±2.77	238±2.24	226±2.32
6	291±2.80	271±2.81	268±2.57	256±2.02	281±2.33	263±2.60	256±2.18	244±2.79	232±2.16
72	302±2.46	281±2.79	278±2.19	266±2.09	285±2.84	273±2.15	267±2.46	250±1.25	235±2.52

Table E.1 (continue) Swelling power of different native and cross-linked MBS and BSM films with TA, MA and SA

Time (h)	Swelling power (%)				
	BSM10SA	BSM15SA	BSM20SA	BSM25SA	BSM30SA
0	0	0	0	0	0
1	227±2.35	215±2.20	194±2.68	164±2.50	144±2.18
2	240±2.63	221±2.14	209±2.49	180±2.06	163±2.61
3	254±2.41	239±2.65	213±2.38	195±2.17	165±2.45
4	260±2.34	243±2.09	218±2.04	203±2.82	179±2.66
5	265±2.55	248±2.54	223±2.23	210±2.59	184±2.06
6	271±2.19	252±2.05	229±2.45	215±2.42	191±2.51
72	273±2.78	255±2.27	233±2.22	223±2.56	195±2.34

Appendix F

Appendix F

Water absorption

Table E.1 Water absorption of different native and cross-linked MBS and BSM films with TA, MA and SA

Days	Water absorption (%)								
	MBS	MBS10TA	MBS15TA	MBS20TA	MBS25TA	MBS30TA	MBS10MA	MBS15MA	MBS20MA
0	0	0	0	0	0	0	0	0	0
1	6.58±0.05	6.45±0.05	6.26±0.04	6.05±0.03	5.63±0.02	5.16±0.06	6.28±0.04	6.05±0.04	4.88±0.04
2	7.69±0.04	7.53±0.04	7.34±0.05	7.16±0.04	6.04±0.05	5.43±0.05	7.36±0.04	7.16±0.05	5.98±0.05
3	8.15±0.03	8.03±0.06	7.88±0.07	7.63±0.07	6.73±0.06	5.88±0.07	7.85±0.06	7.64±0.04	6.42±0.03
4	8.24±0.02	8.16±0.07	7.96±0.04	7.74±0.08	6.95±0.07	5.91±0.08	8.02±0.07	7.73±0.03	6.56±0.05
5	8.46±0.06	8.32±0.03	8.19±0.03	7.92±0.04	7.09±0.04	6.01±0.05	8.11±0.03	8.04±0.04	6.68±0.06
6	8.61±0.07	8.54±0.05	8.31±0.06	8.05±0.06	7.12±0.05	6.15±0.06	8.35±0.03	8.18±0.08	6.85±0.04
7	8.72±0.05	8.65±0.04	8.46±0.02	8.08±0.06	7.26±0.04	6.22±0.04	8.49±0.03	8.21±0.02	6.94±0.05
8	8.79±0.04	8.68±0.06	8.49±0.06	8.1±0.05	7.31±0.06	6.36±0.05	8.56±0.04	8.35±0.05	7.05±0.07
9	8.83±0.07	8.72±0.03	8.56±0.07	8.18±0.04	7.55±0.03	6.43±0.06	8.61±0.05	8.42±0.07	7.13±0.08
10	8.8±0.03	8.74±0.05	8.57±0.04	8.23±0.03	7.58±0.05	6.47±0.03	8.65±0.06	8.48±0.06	7.16±0.06
11	8.8±0.06	8.75±0.06	8.58±0.04	8.36±0.05	7.61±0.03	6.48±0.04	8.66±0.07	8.51±0.04	7.18±0.07
12	8.8±0.02	8.75±0.04	8.59±0.03	8.44±0.04	7.62±0.03	6.55±0.03	8.67±0.02	8.52±0.05	7.23±0.02

Table E.1 (continue) Water absorption of different native and cross-linked MBS and BSM films with TA, MA and SA

Days	Water absorption (%)								
	MBS25MA	MBS30MA	MBS10SA	MBS15SA	MBS20SA	MBS25SA	MBS30SA	BSM	BSM10TA
0	0	0	0	0	0	0	0	0	0
1	4.31±0.09	4.15±0.03	6.04±0.05	5.84±0.05	4.64±0.08	4.01±0.04	3.85±0.03	7.84±0.03	7.65±0.03
2	4.72±0.07	4.54±0.04	7.16±0.04	7.02±0.04	5.77±0.03	4.22±0.03	4.02±0.05	8.95±0.04	8.63±0.04
3	5.05±0.03	4.94±0.06	7.54±0.06	7.44±0.06	6.23±0.07	4.37±0.05	4.14±0.05	9.58±0.06	8.87±0.05
4	5.32±0.04	5.1±0.06	7.73±0.06	7.53±0.07	6.35±0.05	4.42±0.04	4.21±0.02	9.69±0.07	8.94±0.07
5	5.66±0.06	5.26±0.03	7.92±0.03	7.72±0.08	6.44±0.06	4.61±0.05	4.36±0.07	9.74±0.05	9.23±0.06
6	5.75±0.05	5.32±0.04	8.01±0.04	7.95±0.03	6.66±0.07	4.78±0.06	4.45±0.03	9.92±0.04	9.39±0.05
7	5.94±0.07	5.39±0.06	8.15±0.05	8.11±0.02	6.82±0.04	4.99±0.04	4.58±0.05	10.2±0.03	9.66±0.05
8	6.11±0.03	5.45±0.05	8.26±0.06	8.15±0.05	6.93±0.05	5.16±0.03	4.65±0.08	10.37±0.06	9.75±0.03
9	6.13±0.04	5.51±0.04	8.34±0.07	8.2±0.06	6.93±0.06	5.19±0.07	4.72±0.04	10.44±0.07	9.84±0.04
10	6.15±0.06	5.52±0.03	8.45±0.03	8.21±0.03	6.99±0.07	5.21±0.06	4.73±0.03	10.56±0.04	9.91±0.06
11	6.16±0.05	5.53±0.05	8.47±0.04	8.21±0.08	7.02±0.03	5.21±0.04	4.74±0.02	10.56±0.03	9.91±0.06
12	6.17±0.03	5.55±0.06	8.48±0.06	8.21±0.05	7.02±0.02	5.23±0.08	4.74±0.04	10.56±0.05	9.93±0.09

Table E.1 (continue) Water absorption of different native and cross-linked MBS and BSM films with TA, MA and SA

Days	Water absorption (%)								
	BSM15TA	BSM20TA	BSM25TA	BSM30TA	BSM10MA	BSM15MA	BSM20MA	BSM25MA	BSM30MA
0	0	0	0	0	0	0	0	0	0
1	7.15±0.03	6.98±0.03	6.31±0.03	5.62±0.04	7.52±0.02	6.72±0.03	5.3±0.02	5.82±0.04	5.39±0.06
2	8.13±0.04	7.05±0.04	6.63±0.04	6.18±0.05	8.55±0.04	8.47±0.05	6.9±0.05	6.56±0.05	6.16±0.04
3	8.76±0.03	7.54±0.05	7.02±0.03	6.31±0.06	8.74±0.03	8.64±0.06	7.41±0.05	7.02±0.04	6.34±0.05
4	8.85±0.05	7.69±0.05	7.15±0.02	6.65±0.02	8.82±0.06	8.7±0.03	7.57±0.06	7.19±0.05	6.45±0.06
5	8.93±0.03	7.92±0.06	7.42±0.05	6.89±0.03	8.89±0.04	8.89±0.04	7.65±0.03	7.54±0.06	6.88±0.03
6	9.09±0.04	8.03±0.06	7.64±0.06	7.25±0.04	9.16±0.08	8.92±0.06	7.78±0.070	7.62±0.02	7.14±0.02
7	9.13±0.06	8.12±0.07	7.81±0.04	7.35±0.05	9.23±0.02	9.13±0.07	7.83±0.04	7.75±0.03	7.32±0.03
8	9.2±0.07	8.24±0.02	7.9±0.07	7.44±0.07	9.44±0.03	9.24±0.04	7.95±0.02	7.79±0.04	7.39±0.04
9	9.31±0.02	8.31±0.03	7.94±0.04	7.52±0.02	9.65±0.04	9.35±0.05	8.16±0.07	7.84±0.06	7.48±0.05
10	9.48±0.05	8.48±0.02	7.99±0.03	7.59±0.06	9.74±0.06	9.35±0.03	8.24±0.06	7.85±0.07	7.48±0.06
11	9.48±0.03	8.5±0.04	8.12±0.03	7.63±0.04	9.87±0.08	9.36±0.05	8.28±0.08	7.86±0.03	7.50±0.04
12	9.48±0.07	8.53±0.06	8.23±0.07	7.63±0.04	9.87±0.04	9.36±0.03	8.31±0.05	7.87±0.02	7.50±0.03

Table E.1 (continue) Water absorption of different native and cross-linked MBS and BSM films with TA, MA and SA

Days	Water absorption (%)				
	BSM10SA	BSM15SA	BSM20SA	BSM25SA	BSM30SA
0	0	0	0	0	0
1	6.35±0.03	5.74±0.02	5.35±0.05	4.98±0.04	4.59±0.03
2	8.46±0.04	6.87±0.04	6.49±0.06	6.06±0.03	4.95±0.05
3	8.53±0.02	7.35±0.05	6.98±0.08	6.24±0.06	4.99±0.08
4	8.68±0.03	7.48±0.06	7.09±0.09	6.39±0.07	5.14±0.07
5	8.79±0.05	7.53±0.07	7.27±0.02	6.74±0.08	5.35±0.05
6	8.86±0.07	7.68±0.04	7.47±0.04	6.85±0.05	5.52±0.04
7	8.89±0.06	7.79±0.05	7.56±0.03	7.09±0.06	5.73±0.03
8	8.95±0.05	7.87±0.03	7.57±0.06	7.10±0.05	5.84±0.06
9	9.13±0.06	7.87±0.07	7.57±0.07	7.11±0.03	5.93±0.02
10	9.15±0.07	7.88±0.09	7.59±0.05	7.12±0.02	6.12±0.08
11	9.17±0.03	7.88±0.06	7.59±0.06	7.13±0.06	6.12±0.04
12	9.18±0.04	7.89±0.05	7.61±0.04	7.14±0.07	6.13±0.06

Appendix G

Appendix G

Mechanical properties

Table G.1 Mechanical properties of different native and cross-linked MBS and BSM films with TA, MA and SA

Samples	Mechanical properties		
	Tensile at maximum load (MPa)	Young's modulus (MPa)	Strain at maximum load (%)
MBS	24.0±0.23	459.33±5.4	4.5±0.12
MBS10TA	20.2±0.41	369.62±4.8	9.3±0.23
MBS15TA	18.3±0.32	321.89±3.6	13.7±0.20
MBS20TA	15.8±0.51	273.59±5.2	15.5±0.19
MBS25TA	14.4±0.21	242.83±6.3	18.6±0.17
MBS30TA	12.1±0.24	199.67±5.7	21.2±0.24
MBS10MA	21.9±0.25	404.43±5.5	8.3±0.42
MBS15MA	19.8±0.26	347.67±6.1	11.6±0.38
MBS20MA	18.8±0.32	333.62±3.7	12.7±0.44
MBS25MA	17.3±0.24	299.56±4.3	15.5±0.51
MBS30MA	16.2±0.18	275.04±5.9	17.8±0.39
MBS10SA	23.2±0.41	459.33±4.5	6.8±0.18

Table G.1 (continue) Mechanical properties of different native and cross-linked MBS and BSM films with TA, MA and SA

Samples	Mechanical properties		
	Tensile at maximum load (MPa)	Young's modulus (MPa)	Strain at maximum load (%)
MBS15SA	22±0.23	405.15+5.7	8.6+0.18
MBS20SA	21.1±0.31	384.68+5.5	9.7+0.22
MBS25SA	20.3±0.25	364.77+6.1	11.3+0.15
MBS30SA	18.7±0.17	329.22+4.2	13.6+0.19
BSM	17±0.23	242.85+4.9	40+0.82
BSM10TA	13.5±0.26	182.43+2.4	48+0.67
BSM15TA	12.1±0.16	157.75+5.7	53.4+0.72
BSM20TA	11.4±0.24	144.76+3.9	57.5+0.68
BSM25TA	10.4±0.28	127.92+4.3	62.6+0.84
BSM30TA	9.8±0.21	118.28+6.1	65.7+0.76
BSM10MA	15.3±0.25	212.5+4.2	44+0.45
BSM15MA	13.9±0.27	187.20+5.4	48.5+0.56
BSM20MA	13.3±0.31	174.77+3.8	52.2+0.37
BSM25MA	12.7±0.24	162.50+5.8	56.3+0.63
BSM30MA	12±0.16	149.53+6.7	60.5+0.44

Table G.1 (continue) Mechanical properties of different native and cross-linked MBS and BSM films with TA, MA and SA

Samples	Mechanical properties		
	Tensile at maximum load (MPa)	Young's modulus (MPa)	Strain at maximum load (%)
BSM10SA	16.5±0.22	232.39±4.4	42±0.56
BSM15SA	16±0.34	221.45±3.3	44.5±0.82
BSM20SA	15.4±0.25	209.80±3.9	46.8±0.79
BSM25SA	14.9±0.19	200.80±4.6	48.4±0.67
BSM30SA	14.4±0.41	191.23±5.1	50.6±0.93

Appendix H

Appendix H

Soil burial test

Table H.1 Soil burial test of different native and cross-linked MBS and BSM films with TA, MA and SA

Days	Samples	Mechanical properties		
		Stress at maximum load (MPa)	Young's modulus (MPa)	Strain at maximum load (%)
5	MBS	16.04±0.24	314±2.0	2.2±0.14
	MBS10TA	15.31±0.39	284.30±4.1	7.7±0.29
	MBS15TA	15.02±0.46	274.1±6.5	9.6±0.36
	MBS20TA	13.42±0.24	237.31±4.3	13.1±0.54
	MBS25TA	12.17±0.54	210.91±5.3	15.4±0.49
	MBS30TA	10.43±0.34	178.90±7.4	16.6±0.64
	MBS10MA	17.45±0.35	334.00±3.2	5.0±0.29
	MBS15MA	17.03±0.43	315.95±5.8	7.8±0.36
	MBS20MA	16.23±0.23	300.00±5.1	9.1±0.54
	MBS25MA	15.34±0.55	275.89±8.3	11.2±0.49
	MBS30MA	14.1±46	250.00±4.2	13.6±0.64
	MBS10SA	19.61+0.39	374±4.7	4.5±0.24

Table H.1 (continue) Soil burial test of different native and cross-linked MBS and BSM films with TA, MA and SA

Days	Samples	Mechanical properties		
		Stress at maximum load (MPa)	Young's modulus (MPa)	Strain at maximum load (%)
5	MBS15SA	18.21+0.46	341.33±5.1	6.7±0.15
	MBS20SA	17.82+0.34	327.0±3.7	8.1±0.54
	MBS25SA	16.57+0.33	299.99±6.8	10.5±0.37
	MBS30SA	15.93+0.45	280.0±3.2	12.4±0.44
	BSM	8.04+0.24	131.48±74	11.6±0.93
	BSM10TA	12.45+0.61	172.67±6.8	40.7±1.14
	BSM15TA	11.21+0.38	150.56±6.1	44.65±0.87
	BSM20TA	9.23+0.49	120.33±3.9	49.5±0.89
	BSM25TA	8.53+0.54	108.37±5.4	54.37±0.76
	BSM30TA	7.10+0.62	87.98±6.1	57.3±1.02
	BSM10MA	14.15+0.24	202.43±23	39.8±1.23
	BSM15MA	12.77+0.33	176.32±34	44.85±0.98
	BSM20MA	11.31+0.41	152.58±5.1	48.25±1.05
	BSM25MA	11.02+0.52	144.25±4.7	52.78±1.17
	BSM30MA	10.21+0.35	130.70±3.5	56.23±0.85

Table H.1 (continue) Soil burial test of different native and cross-linked MBS and BSM films with TA, MA and SA

Days	Samples	Mechanical properties		
		Stress at maximum load (MPa)	Young's modulus (MPa)	Strain at maximum load (%)
5	BSM10SA	15.38±0.33	222.86±6.3	38.02±1.21
	BSM15SA	14.19±0.24	202.43±6.5	40.19±0.97
	BSM20SA	13.32±0.46	187.07±5.7	42.4±1.32
	BSM25SA	13.07±0.31	180.7±6.2	44.61±1.15
	BSM30SA	12.82±0.29	175.00±5.1	46.51±0.92
10	MBS	13.26±0.53	262.0±6.1	1.3±0.43
	MBS10TA	13.12±0.41	249.4297±5.9	5.2±0.28
	MBS15TA	12.23±0.48	227.5349±4.6	7.5±0.83
	MBS20TA	11.84±0.37	211.99±7.4	11.7±0.44
	MBS25TA	10.1±0.39	177.8146±5.5	13.6±0.51
	MBS30TA	9.82±0.57	171.8285±4.8	14.3±0.62
	MBS10MA	15.04±0.31	291.0±3.1	3.9±0.23
	MBS15MA	14.7±0.42	278.14±5.5	5.7±0.46
	MBS20MA	14.42±0.56	269.0±4.7	8.2±0.57
	MBS25MA	14.04±0.37	254.574±3.9	10.3±0.43
	MBS30MA	13.31±0.48	239.0±5.1	12.4±0.72
	MBS10SA	17.42±0.34	335.0±7.7	3.4±0.35

Table H.1 (continue) Soil burial test of different native and cross-linked MBS and BSM films with TA, MA and SA

Days	Samples	Mechanical properties		
		Stress at maximum load (MPa)	Young's modulus (MPa)	Strain at maximum load (%)
10	MBS15SA	16.3±0.31	308.12±5.8	5.8±0.44
	MBS20SA	15.54±0.49	287.0±6.6	7.2±0.51
	MBS25SA	14.1±0.43	257.69±7.2	9.43±0.37
	MBS30SA	14.82±0.56	264.0±8.1	11.3±0.29
	BSM	4.30±0.33	77.06±6.3	11.6±0.98
	BSM10TA	11.04±0.34	156.92±5.6	40.7±0.87
	BSM15TA	9.21±0.45	127.34±1.9	44.65±0.76
	BSM20TA	7.42±0.52	99.26±4.2	49.5±0.91
	BSM25TA	6.54±0.56	84.73±3.9	54.37±1.02
	BSM30TA	5.31±0.37	67.51±4.3	57.3±1.09
	BSM10MA	13.44±0.55	198.23±1.8	35.6±0.73
	BSM15MA	11.25±0.34	160.86±3.7	39.87±0.68
	BSM20MA	9.42±0.58	130.11±4.5	44.79±0.94
	BSM25MA	9.07±0.29	122.21±2.5	48.43±1.12
	BSM30MA	8.65±0.37	113.50±3.6	52.41±0.89

Table H.1 (continue) Soil burial test of different native and cross-linked MBS and BSM films with TA, MA and SA

Days	Samples	Mechanical properties		
		Stress at maximum load (MPa)	Young's modulus (MPa)	Strain at maximum load (%)
10	BSM10SA	14.22±	213.27±3.3	33.35±1.23
	BSM15SA	12.39±	182.59±5.2	35.71±1.31
	BSM20SA	11.46±	165.73±4.7	38.29±0.95
	BSM25SA	11.05±	157.57±5.8	40.25±0.82
	BSM30SA	10.45±	146.67±3.6	42.49±0.74

Author Biography

Name	Miss. Naruenart Thessrimuang
Date of Birth	8 July 1988
Address	175 Moo.14 Tambol Wattart, Aumphor Muang, Nongkhai 43000
Education	(2010) Bachelor of science in industrial chemistry (King Mongkut's Institute of Technology Ladkrabang)
	(2013) Master of science in polymer technology (King Mongkut's Institute of Technology Ladkrabang)

Academic Publications

1. N.Thessrimuang and J.Prachayawarakorn. 2017. "Properties of cassava starch film cross-linked by tartaric acid." 1461-1464. in Pure and Applied Chemistry international conference 2017 (PACCON 2017), Bangkok.
2. N.Thessrimuang and J.Prachayawarakorn. 2017. "Preaparation and characterization of malic acid modified starch from cassava starch." 50-53 in International Polymer Conference of Thailand 2017 (PCT-7). Bangkok.
3. N.Thessrimuang and J.Prachayawarakorn. 2019, "Characterization and properties of high amylose mung bean starch biodegradable films cross-linked with malic or succinic acid." Journal of polymers and the environment. 2:234-244
4. N.Thessrimuang and J.Prachayawarakorn. 2019, "Development, modification and characterization of new biodegradable film from basil seed (Ocimum basilicum l.) mucilage." Journal of the science of food and agriculture.

BIOP-P2

Preparation and Characterization of Malic Acid Modified Starch from Cassava Starch

Naruenart Thessrimuang[1] and Jutarat Prachayawarakorn[1,2*]

[1]Department of Chemistry, Faculty of Science, King Mongkut's Institute of Technology Ladkrabang, Bangkok 10520

[2]Advanced Materials Research Unit, Faculty of Science, King Mongkut's Institute of Technology Ladkrabang, Bangkok 10520

Phone +66 2329 8400, Fax +66 2329 8428, *E-mail: jutarat.si@kmitl.ac.th

Abstract

The aim of this study was to examine the effectiveness of using malic acid, a dicarboxylic acid to enhance the properties of starch-based films. Starch/glycerol casted films were prepared with 0, 10, 15, 20, 25, and 30 wt% malic acid (starch wt% basis) and properties were, then, analyzed. It was found from FT-IR spectra that the additional peak position at 1730 cm^{-1}, assigned for the C=O stretching was observed. Moreover, the 30 wt% malic acid derived starch films caused the decreasing swelling property compared to the control film. There was also a significant increase of elongation at break of the starch film with the addition of 30 wt% malic acid. Finally, thermal stability of different acid-modified films was improved with the increased amounts of malic acid.

Keywords: cross-linking; malic acid; modified starch

1. Introduction

Starch is a renewable and abundant resource. However, starch exhibits several disadvantages such as a strong hydrophilic character (water sensitivity) and poor mechanical properties compared to conventional synthetic polymers [1], which make it undesirable for some applications such as packaging purposes.

Cross-linking is a common approach to improve the performance of starch for various applications. Starch and starch products have been cross-linked with various cross-linking agents [2]. Nevertheless, some of these cross-linking agents always display toxicity and thus their potential applications as biomaterials are limited. To overcome these disadvantages, certain nontoxic functional additives and simple modification techniques are required to improve mechanical properties and water resistibility of the starch films.

In this work, malic acid was chosen as the cross-linking agent because of its low cost and non-toxicity. As a result of its di-carboxylic structure, interaction could take place between the carboxyl groups of malic acid and the hydroxyl groups on the starch. Such an interaction would improve the water resistibility due to reducing available OH groups of starch [3]. Starch/glycerol casted films were prepared with different contents of malic acid and different properties were, then, different properties were examined.

2. Experimental methods

2.1 General

Cassava starch was obtained from Chaopraya Phuchrai 2999 Co., Ltd. (Kamphaengphet, Thailand). Glycerol (plasticizer) was provided by Lab System Co., Ltd. (Bangkok, Thailand) and malic acid (food grade) was purchased from Lab System Co. Ltd. (Bangkok, Thailand).

2.2 Sample preparation

Mixtures of soluble cassava starch (10 g), glycerol (2 g) and distilled water (100 ml) along with different amounts of malic acid, i.e. 0%, 10%, 15%, 20%, 25% and 30% (on the initial dry weight of starch) were prepared. All solutions were heated at the temperature of 65 °C for 30 min to ensure the completed starch gelatinization. The films were dried for 5 h. at the temperature of 70 °C in a hot air oven. Further curing at the temperature of 150 °C

for 10 min was performed. All films were, subsequently, conditioned at 60% RH (23 ± 1 °C) in a closed humidity chamber before assessing the film properties

2.3 IR spectroscopic study

A sample was characterized by IR using a Spectrum 200 GX spectrometer (PerkinElmer, USA) using KBr disk technique with a resolution of 6 cm^{-1} using 20 scans per sample.

2.4 Tensile properties

A film was cut into rectangular piece of 15 mm × 100 mm to test tensile properties. The film thickness was approximately 0.12 mm. The tensile testing was carried out using Universal Testing Machine (LLOYD Instrument, LR 5K, UK) with 100 N load cell and at a crosshead speed of 50 mm/min according to ASTM D-882. The sample was conditioned at the temperature of 23±1 °C and relative humidity of 60±5% before testing. At least 10 specimens were tested to obtain the averaged values.

2.5 Thermogravimetric analysis

A sample was scanned from the temperature of 50 °C to 600 °C using a thermogravimetric analyzer (Perkin Elmer, Pyris 1, Massachusetts, USA) at a rate of 10 °C/min in nitrogen atmosphere to characterize thermal decomposition temperature.

2.6 Swelling power

A sample was determined according to the method given by Yun and Yoon [4]. Accurately weighed dry film was immersed in distilled water at room temperature. At the end of soaking period, the film was taken out. The moisture on the surface was removed and the weight of the film was measured. The swelling power was calculated as follows:

$$\text{Swelling power} = (W_e - W_o)/W_o \qquad (1)$$

where W_o was the dry weight of the starch film and W_e was the weight of the film after being immersed in water.

3. Results & Discussion

3.1 IR spectroscopic study

FTIR spectra of the native starch film and the starch films cross-linked with 10, 15, 20, 25 and 30% malic acid are shown in Fig.1. It was found that all of the films showed similar peaks, except for the additional peak in the cross-linked film at 1730 cm^{-1}. The band at 1730 cm^{-1} (indicated in Figure 1) was ascribed to the ester carbonyl bands [5]. Since the films were thoroughly washed to remove the unbound malic acid, the presence of the carbonyl peak confirms the chemical linkages between malic acid and starch.

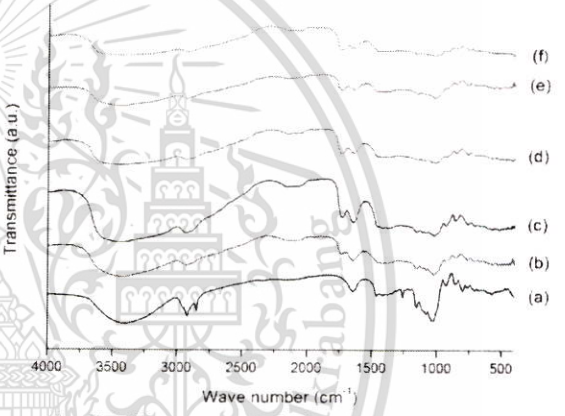

Figure 1. FT-IR spectra of the cassava starch films modified by different contents of malic acid (a) 0% (b) 10% (c) 15% (d) 20% (e) 25% and (f) 30%

3.2 Tensile property

Tensile properties of different cross-linked films are shown in Figure 2. It showed an increased softness of the film indicated by the decrease in the stress at maximum load and Young's modulus as well as the increase in strain at maximum load when malic acid contents were increased. As expected, the control cassava starch film was significantly stiffer than other malic acid-modified films. At the highest concentrations (30 wt% malic acid), lower stress and Young's modulus but higher strain were observed. This could be due to the cross-linking reaction by malic acid. However, there was excess cross-linking that limits the mobility of the starch molecules, leading to lower stress at maximum load. It should be noted that there was a significant increase of the strain at maximum load of

the malic acid modified cassava starch film, especially at high contents of malic acid. This should be due to the cross-linking reaction between malic acid and starch molecules.

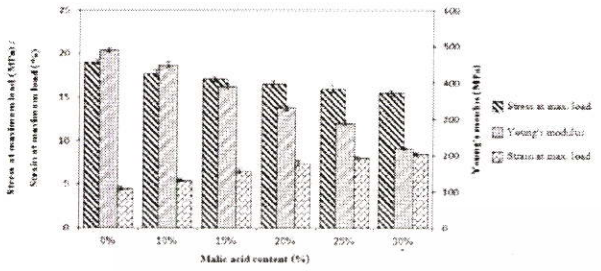

Figure 2. Mechanical properties of different malic acid-modified cassava starch films

3.3 Thermogravimetric analysis

Figure 3 presents thermogravimetric (TGA) and derivative thermogravimetric (DTG) graphs of native cassava starch film and different malic acid modified cassava starch films. The initial weight loss (DTG peak) below 100 °C was ascribed to the desorption of trace water. It seems that there is only one weight loss step on the DTG curve of native cassava starch film. However, there was four degradation steps for all derived films containing malic acid in a similar way to that of citric acid derived films by Shi et al. [6]. The second weight loss at around 180 °C was related to the glycerol, the third degradation weight loss above 150-250 °C may be due to acid hydrolysis of starch by malic acid [7]. The major weight loss at 320 °C was due to degradation of the chemical structure of starch and the fourth degradation weight loss above 350-370 °C may be because of the cross-link formation reaction of malic acid with starch polymer chains, respectively [8].

The third weight loss steps were strongly related to the interactions between starch and malic acid. It seems that the cross-linked starch films presented higher degradation temperature of the third weight loss and lower weight loss than the non-modified film. It was also observed that the residual weight percentage of the cross-linked starch films was more than that of the non-modified film. Moreover, the increase of malic acid content caused the residual weight percentage increased. This could be because, malic acid molecules were chemical bonded onto the starch chains [6].

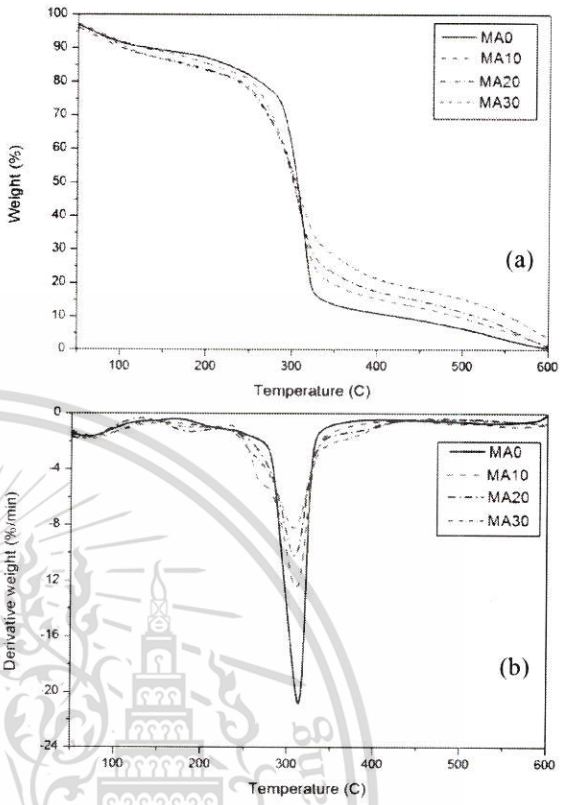

Figure 3. (a) TGA and (b) DTG thermograms of different cassava starch films modified by different contents of malic acid

3.4 Swelling power

The results of the swelling power measurements are shown in Fig 4. The cassava starch film showed the highest swelling power. Since native starch contains abundant hydroxyl groups that prefers to form hydrogen bonds with water. The swelling power of the starch films decreased with increasing malic acid concentration. Cross-linking and esterification reactions can reinforce the starch network both chemically and physically, thus resulting in lower swelling power [4].

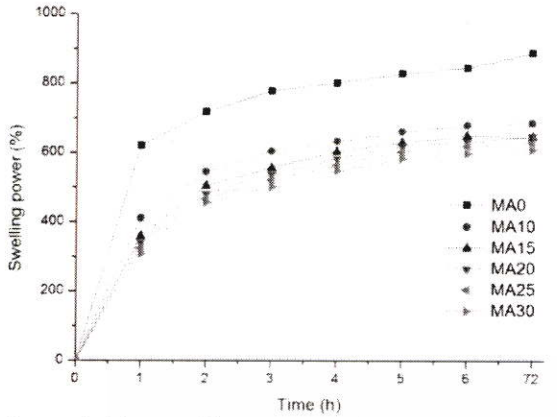

Figure 4. The swelling power of cross-linked cassava starch films modified by different contents of malic acid

Conclusion

Starch films cross-linked by different contents of malic acid were successfully prepared. It was found that the new FT-IR peak position at 1730 cm^{-1} was observed in different starch films modified by malic acid. Thermal decomposition temperatures were slightly increased with the increase of malic acid contents. Moreover, the improvement in tensile properties was detected by the significant increase of the strain at maximum load. Finally, the increasing of malic acid concentration caused the decrease of the swelling power. These films can be used in applications food and packaging.

Acknowledgement

The authors express their sincere appreciation to KMITL Research Fund for supporting the study financially.

References

[1] Averous, L. and Boquillon, N., "Biocomposites based on plasticized starch thermal and mechanical behaviours", *Carbohydrate Polymer.* :111–122 (2004).

[2] Hirsch, J.B. and Kokini, J.L., "Understanding the mechanism of cross-linking agents ($POCl_3$, STMP and EPI) through swelling behaviour and pasting properties of cross-linked waxy maize starches" *Cereal Chemistry.*: 102–107 (2002).

[3] Borredon, E., Bikiaris, D., Prinos, J. and Panayiotou, C., "Properties of fatty-acid esters of starch and their blends with LDPE", *Journal Apply Polymer Science* :705–721 (1997).

[4] Yun, Y.H., Wee, Y.J., Byun, H.S. and Yoon, S.D., "Biodegradability of chemically modified starch (RS4)/ PVA blend films Part 2", *Journal Polymer Environment.*: 12–18 (2008).

[5] Yang, C.Q. and Andrews, K., "Infrared spectroscopic studies of the non-formaldehyde durable press finishing of cotton fabrics by use of polycarboxylic acids", *Journal Apply Polymer Science.*:1609–1616 (1991).

[6] Shi, R., Zhang, Z., Liu, Q., Han, Y., Zhang, L. and Chen, D., "Characterization of citric acid/glycerol co-plasticized thermoplastic starch prepared by melt blending", *Carbohydrate Polymer.* :748–755 (2007).

[7] Ma, X., Chang, P.R. and Yu, J. and Stumborg, M. "Properties of biodegradable citric acid-modified granular starch/thermoplastic pea starch composites", *Carbohydrate Polymer.* :1–8 (2009).

[8] William N.G. and William D., "Starch composites with aconitic acid", *Carbohydrate Polymer.* :60–67 (2016).

Properties of cassava starch film cross-linked by tartaric acid

Naruenart Thessrimuang[1] and Jutarat Prachayawarakorn[1,2*]

[1]*Department of Chemistry, Faculty of Science, King Mongkut's Institute of Technology Ladkrabang, Thailand*
[2]*Advanced Materials Research Unit, Faculty of Science, King Mongkut's Institute of Technology Ladkrabang, Thailand*

*e-mail: jutarat.si@kmitl.ac.th

Abstract: The aim of this study was to examine the effectiveness of using tartaric acid, a dicarboxylic acid, to enhance properties of starch-based films. Starch/glycerol casted films were prepared with 0, 10, 15, 20 and 25 wt% tartaric acid (starch wt% basis) and the properties were, then, analysed. It was found from FT-IR spectra that an additional peak position at 1730 cm^{-1}, assigned for the C=O stretching was observed. It was shown that the increasing amount of tartaric acid led to a reduction in the percentage of swelling power. In addition, high content of tartaric acid increased the strain at maximum load. Moreover, thermal decomposition temperature of various films modified by different contents of tartaric acid was slightly higher than that of the non-modified film.

1. Introduction

Starch, an important and a large part of the available biomass, has received considerable attention because of its low cost, biodegradability, annually renewal and abundant supply throughout the world.[1] Starch is composed of two polymers of glucopyranose; amylose and amylopectin. Amylose is formed by glucose units joined by 1,4-glycosidic linkages and amylopectin is formed by glucose units joined by 1,4- as well as 1,6-glycosidic linkages. While linear amylose is a low molecular weight polymer consisting of 1000–10,000 glucose units, amylopectin is a larger branched macromolecule with degree of polymerization (DP), sometimes, exceeding one million.[2] However, starch has intrinsic disadvantages such as very weak resistance against shear and heat, very high susceptibility to thermal decomposition and high tendency to undergo retrogradation.[3]

Cross-linking is a way of improving properties of starch-based film, with improved mechanical properties and resistance to solubility. Tartaric acid (TA) is typically inexpensive and non-toxic organic acid used to cross-link starch. Tartaric acid is dicarboxylic acid that can react with the hydroxyl groups on the glucopyranose ring present in starch by forming ester bonds. Tartaric acid is soluble in water at room temperature. Glycerol plasticizer is not expected to esterify with organic acid since the esterification reaction is usually performed using homogeneous catalysts like sulfuric acid, p-toluenesulfonic acid, etc.[4] The aim of this study was to examine the effectiveness of using tartaric acid, a dicarboxylic acid, to enhance the properties of starch-based films. Starch/glycerol casted films were prepared with different contents of tartaric acid and the properties were, then, examined.

2. Materials and Methods

2.1 General

Cassava starch was obtained from Chaopraya Phuchrai 2999 Co., Ltd. (Kamphaengphet, Thailand). Glycerol (plasticizer) was provided by Lab System Co., Ltd. (Bangkok, Thailand) and tartaric acid (food grade) was purchased from Lab System Co., Ltd. (Bangkok, Thailand).

2.2 Sample preparation

Mixtures of soluble cassava starch (10 g), glycerol (3 g) and distilled water (100 ml) along with different amounts of tartaric acid added, i.e. 0%, 10%, 15%, 20% and 25% (on the initial dry weight of starch) were prepared. All solutions were heated at the temperature of 65 °C for 30 min to ensure the completed starch gelatinization. The films were dried for 5 h. at the temperature of 70 °C in a hot air oven. Further curing at the temperature of 150 °C for 10 min was performed. All films were, subsequently, conditioned at 60% RH (23 ± 1 °C) in a closed humidity chamber before assessing the film properties.

2.3 IR spectroscopic study

A sample was characterized by IR using a Spectrum 200 GX spectrometer (PerkinElmer, USA) using KBr disk technique with a resolution of 6 cm^{-1} using 20 scans per sample.

2.4 Tensile properties

A film was cut into rectangular piece of 15 mm × 100 mm dimensions to test tensile properties. The film thickness was approximately 0.12 mm. The tensile testing was carried out using Universal Testing Machine (LLOYD Instrument, LR 5K, UK) with 100 N load cell and at a crosshead speed of 50 mm/min according to ASTM D-882. The sample was conditioned at the temperature of 23±1 °C and relative humidity of 60±5% before testing. At least 10 specimens were tested to obtain the averaged values.

2.5 Thermogravimetric analysis

A sample was scanned from the temperature of 50 °C to 700 °C using a thermogravimetric analyzer (Perkin Elmer, Pyris 1, Massachusetts, USA) at a rate of 10 °C/min in nitrogen atmosphere to characterize thermal decomposition temperature.

2.6 Swelling test

The swelling power of a sample was determined according to the method given by Yun and Yoon[5]. Accurately weighed dry film was immersed in distilled water at room temperature (25 °C). At the end of soaking period, the film was taken out. The moisture on the surface was removed and the weight of the film was measured.

The swelling power was calculated as follows:

$$\text{Swelling power} = (w_e - w_o)/w_o$$

where w_o is the dry weight of the starch films and w_e is the weight of the film after being immersed in water.

3. Results & Discussion

3.1 IR spectroscopic study

FT-IR spectra of different films are presented in Figure 1. The hydrogen bonded hydroxyl group appeared as a main peak at 3430 cm^{-1} and the aliphatic C–H stretching was observed as a sharp peak at 2900 cm^{-1}. The sharp peak at 1730 cm^{-1} was assigned for the carbonyl stretching. The presence of ester bond can be confirmed by the presence of carbonyl peak at 1730 cm^{-1} in cross-linked cassava starch. Mathew and Abraham[6] reported the esterification of native potato starch with ferulic acid which showed the presence of carbonyl peak in the FT-IR spectrum at around 1726 cm^{-1}.

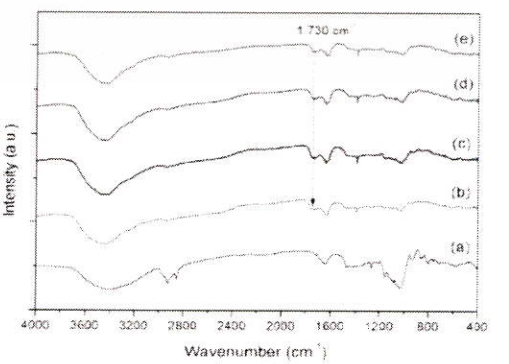

Figure 1. FT-IR spectra of the cassava starch films modified by different contents

of tartaric acid (a) 0% (b) 10% (c) 15% (d) 20% and (e) 25%.

3.2 Thermogravimetric analysis (TGA)

Figure 2 shows the thermogram of native cassava starch film and different tartaric acid-modified cassava starch films. The weight loss below 100 °C was ascribed to the desorption of trace water. The thermograms show that the native cassava starch film and different cross- linked cassava starch film started to degrade at the temperature of 260 °C. There was an increase of the degradation temperature of approximately 300 to 320 °C for the starch films modified by 0 to 25 wt% tartaric acid. The improved thermal degradation temperature was attributed to the cross-linking of tartaric acid with the starch polymer, in a similar way to that of citric acid-modified starch films.[7]

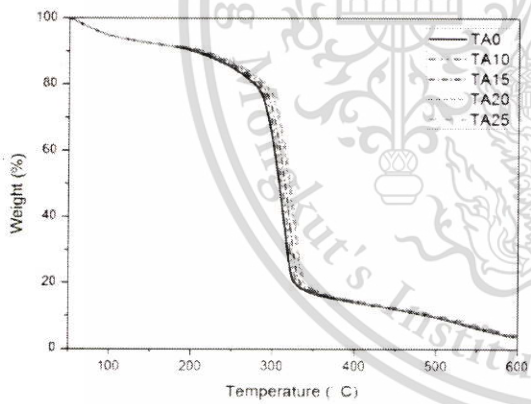

Figure 2. TGA thermograms of different cassava starch films modified by different contents of tartaric acid

3.3 Tensile properties

Stress-strain curves of the starch and modified starch films are shown in Figure 3. It can be seen that the film modified by 25 wt% tartaric acid showed lower stress and Young's modulus but higher strain than the non-modified film. This could be due to the cross-linking reaction by the tartaric acid.

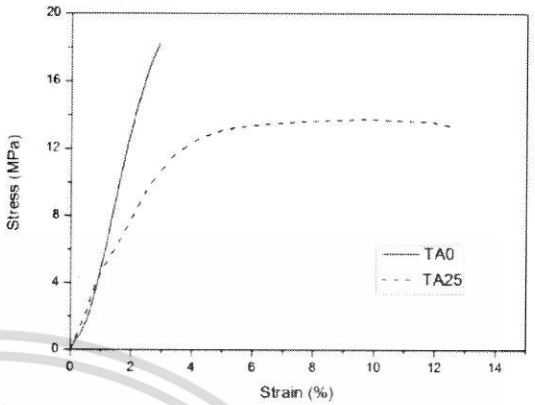

Figure 3. Stress–strain curves of cassava starch and modified cassava starch films

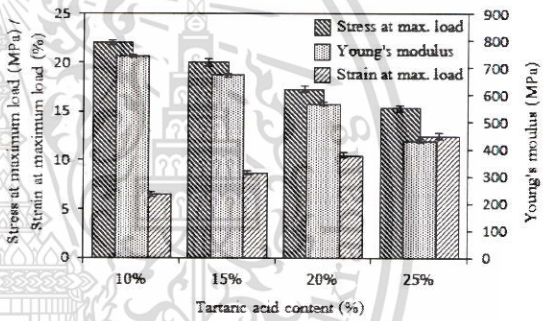

Figure 4. Mechanical properties of different tartaric acid-modified cassava starch films

Tensile properties of different cross-linked films are shown in Figure 4. The decrease in the stress at maximum load and Young's modulus as well as the increase in strain at maximum load was observed. As expected, the non-modified cassava starch film was significantly stiffer than other tartaric acid-modified films. At low concentrations of tartaric acid (10 wt% tartaric acid), there was not enough cross-linking between the starch molecules to improve the stress at maximum load of the films. At high concentrations (25 wt% tartaric acid); however, there was excess cross-linking that limits the mobility of the starch molecules, leading to lower tensile strength. It should be noted that there was a significant increase of the strain at

maximum load of the tartaric acid-modified cassava starch film, especially at high contents of the tartaric acid. This should be due to the cross-linking reaction between the tartaric acid and the starch molecules.

3.4 Swelling power

Figure 5 presents the swelling power of various cross-linked cassava starch films. It can be seen that the swelling power increased with increased immersion time for all starch films. The cassava starch film showed the highest swelling power. Since native starch contains abundant hydroxyl groups that prefer to form hydrogen bonds with water.[8] The swelling power for the cross-linked cassava starch film with 10 wt% tartaric acid was higher than those with 15, 20, 25 wt% tartaric acid, respectively. The swelling power tended to decrease as the concentration of tartaric acid increased due to the increase in the cross-linking density which hindered the penetration of water into the starch molecular network. The formation of a network structure prevented absorption of water. As explained earlier, cross-linking strengthens the polymer network reducing the absorption of water.

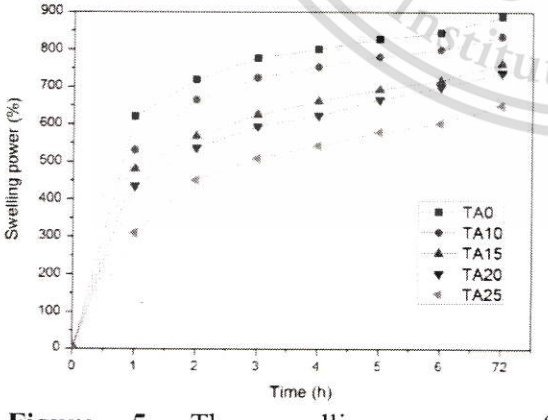

Figure 5. The swelling power of cross-linked cassava starch films modified by different contents of tartaric acid

4. Conclusions

Starch films cross-linked by different contents of tartaric acid were successfully prepared. It was found that the new FT-IR peak position at 1730 cm^{-1} was observed in different films modified by tartaric acid. Thermal decomposition temperatures were slightly increased with the increase of tartaric acid contents. Moreover, the improvement in tensile properties was detected by the significant increase of the strain at maximum load. Finally, the increasing of tartaric acid concentration caused the decrease of the swelling power. The cross-linked starch may be used as biodegradable mulching films.

Acknowledgement

The authors express their sincere appreciation to KMITL Research Fund for supporting the study financially.

References

1. Arvanitoyannis, I.; Kalichevsky, M.; Blanshard, J.M.V; Psomiadou, E. *Carbohydrate Polymers* **1994**, *24*, 1–15.
2. Du, X.; Jia, J.; Xu, S.; Zhou, Y. *Starch-Stärke* **2007**, *59*, 609–613.
3. Singh, J.; Kaur, L.; McCarthy, O.J. *Food Hydrocolloids* **2007**, *21*, 1–22.
4. Limin, Z.; Al-Zaini, E; Adesina, A.A. *Fuel* **2013**, *103*, 617–625.
5. Yun, Y.H.; Wee, Y.J.; Byun, H.S.; Yoon, S.D. *Journal of Polymers and the Environment* **2008**, *16*, 12–18.
6. Mathew, S.; Abraham, T.E. *Food Chemistry* **2007**, *105*, 579–589.
7. Ma, X.; Chang, P.R.; Yu, J.; Stumborg, M. *Carbohydrate Polymers* **2009**, *75*, 1–8.
8. Ayana, B.; Suin, S.; Khatua, B. *Carbohydrate Polymers* **2010**, *110*, 430–439.

Journal of Polymers and the Environment (2019) 27:234–244
https://doi.org/10.1007/s10924-018-1340-2

ORIGINAL PAPER

Characterization and Properties of High Amylose Mung Bean Starch Biodegradable Films Cross-linked with Malic Acid or Succinic Acid

Naruenart Thessrimuang[1] · Jutarat Prachayawarakorn[1,2]

Published online: 24 November 2018

Abstract
Because of weak mechanical and highly hydrophilic properties of starch, various applications for starch have been limited. In this study, mung bean starch (MBS), one type of high amylose starch, was chosen for its potential film forming biopolymers. MBS films were prepared and modified by different types and contents of natural di-carboxylic acids, i.e. malic acid (MA) and succinic acid (SA) with different acidity and chemical structures. It was found from FTIR spectra that the extra peak position of 1700 cm^{-1} were observed, the evidence of ester group formation for MA- or SA- modified MBS films. The incorporation of MA or SA into MBS film also caused the decrease in degree of crystallinity, as confirmed by XRD technique. Additionally, the maximum strain at maximum load was highly improved with the addition of 30% MA or SA. Moreover, swelling power and water vapor permeability (WVP) of MBS film modified by SA were lower than those by MA. Morphology, biodegradability and thermal property of different acid-modified MBS films were also investigated.

Keywords Cross-linked starch · Modified starch · Mung bean starch

Introduction

Among biopolymers, starch is suggested to be one of the most interesting materials for biodegradable films because of its low cost, renewability and natural abundance [1]. Starch is spontaneously unsuitable for most applications and; therefore, must be modified chemically or physically to improve their properties and applications, to afford products with improved functionality and minimize their defects [2]. The casted film from root and cereal starch has been widely investigated for their properties. However, studies on properties of starch films produced from legume starch i.e. mung bean starch (MBS) has been limited.

Mung bean (*Vigna radiate*), one type of legume starch, was generally grown in Southeast Asia countries, usually consumed as noodle. MBS consists of two types of molecules: amylose (linear 40–45%) and amylopectin (branched 55–60%) [3]. In general, intermediate amylose starch contains of approximately 25% amylose and 75% amylopectin; waxy starch consists of mostly amylopectin and 0–8% amylose; and high-amylose starch contains of 40–70% amylose [4]. Therefore, amylose-rich MBS was attractively chosen for film-forming bio-based polymers that offer high transparency and biodegradability [5, 6]. Nevertheless, poor mechanical properties and high hydrophilic characteristics of MBS are needed to be improved.

Generally, cross-linking process are normally used to cross-linked starch molecules to improve mechanical properties, thermal stability and swelling power [7]. Some cross-linking agents such as glutaraldehyde, urea formaldehyde are relatively toxic and expensive. Non-toxic cross-linker alternatives include natural carboxylic acids such as malic acid (MA), succinic acid (SA) or citric acid (CA); these acids are inexpensive and non-toxic chemicals. These are naturally organic acids presented in vegetables and fruits, which are synthesized during the fermentation process by microorganisms [8]. Di-carboxylic acids used as cross-linking agents can interconnect starch molecules between hydroxyl functional groups in D-glucopylanose units by covalent bonding. As a result, swelling property was reduced; while, molecular

✉ Jutarat Prachayawarakorn
jutarat.si@kmitl.ac.th

[1] Department of Chemistry, Faculty of Science, King Mongkut's Institute of Technology Ladkrabang (KMITL), Bangkok 10520, Thailand

[2] Advanced Materials Research Unit, Faculty of Science, King Mongkut's Institute of technology Ladkrabang (KMITL), Bangkok 10520, Thailand

weight and mechanical properties of cross-linked starch was improved [9, 10].

There have been many reports for di-carboxylic cross-linked starch films, normally for intermediate amylose starch. It was reported that water vapor barrier property of potato starch film were improved as aconitic acid percentage increased from 0 to 10 wt%; whereas, tensile strength decreased with 15 and 20 wt% [11]. Furthermore, degree of swelling and solubility of MA-, SA-modified corn starch films were lower than those of the native film [12]. Shen et al. used CA, SA, MA and 1,2,3,4-butanetetracarboxylic acid to modify corn starch films. It was found that the addition of the acids could improve tensile strain and permeability properties of corn starch films because of the crosslink sites that can interconnect the starch chains; simultaneously, starch chain hydrolysis was also observed [13]. Moreover, hydrophilicity of cross-linked potato starch was found to decrease as the contents of malonic acid increased. The increasing content of malonic acid also increased the extent of esterification, cross-linking of potato starch film [9]. It was also mentioned that cross-linking by MA and CA increased starch gelatinization temperature of wheat starch film. Besides, water absorption of wheat starch decreased when the contents of MA and CA increased [14]. Menzel et al. found that potato starch film cross-linked with 30 pph of CA were highly cross-linked, because film with 30% CA presented highest molecular weight and lowest water solubility [15].

To the best of our knowledge, there is no detailed study on the effect of content of di-carboxylic acids: i.e. MA or SA cross-linkers on properties of high amylose MBS film. Both di-carboxylic acids of MA and SA contain the same number of carbons atoms; however, MA contains 1 hydroxyl but there is no hydroxyl group on SA structure. MA also shows higher acidity than SA due to lower pKa_1 and pKa_2 [16, 17]. Native and cross-linked MBS films with different contents of MA and SA were characterized by Fourier transform infrared spectroscopy (FT-IR), thermogravimetric analysis (TGA), X-ray diffraction (XRD) and scanning electron microscopy (SEM). Moreover, water vapor permeability (WVP), swelling power, gel fraction, mechanical properties and biodegradable properties by soil buried test of different acid cross-linked MBS films were also examined.

Materials and Methods

MBS (60% amylopectin and 40% amylose) was obtained from Chaopraya Phuchrai 1999 Co., Ltd. (Kamphaengphet, Thailand). Glycerol (plasticizer) was obtained from Lab System Co., Ltd. (Bangkok, Thailand). MA and SA (food grade, Fig. 1) were provided by from Lab system, Co. Ltd. (Bangkok, Thailand).

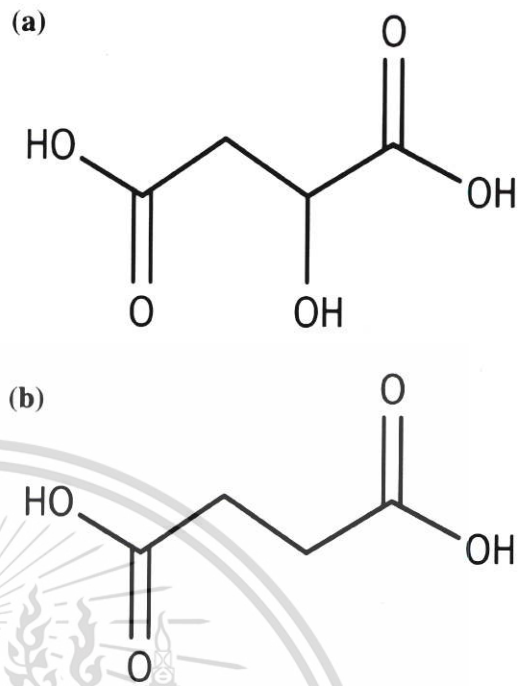

Fig. 1 Chemical structures of a MA and b SA

Experimental

Preparation of MBS Films

To prepare MBS film, MBS was gelatinized by adding 7 g of starch and 2.1 g (30 wt%) glycerol to 70 ml of distilled water. Either MA or SA with different contents of 10%, 20% and 30% (based on the initial dry weight of starch) were added. The solution was stirred consistently for 45 min at 65 °C on a hot plate with a magnetic stirrer (IKA, Germany). After cooling, MBS solution was casted on a polypropylene plate and dried in a hot-air oven (Memmert, Germany) for 10 h at 40 °C. The film was further heated in the oven at 150 °C for 10 min for completed cross-linking. The dried film was peeled off and kept in a closed in a desiccator containing magnesium nitrate at 60% relative humidity (RH) before characterization.

Characterization of Films

FTIR Spectroscopic Study

A sample was characterized by FTIR using a spectrum in transmission mode on a Spectrum 2000 GX spectrometer (Perkin Elmer, USA) using KBr disk technique. Absorption spectrum was collected in the range from 4000 to

400 cm^{-1}, using 20 scans at a resolution of 6 cm^{-1} while corrected against the background spectrum.

Swelling Power

The swelling power of a film was investigated by using a modified version of TG Dastidar et al. [9]. A film was immersed in water at room temperature (25 °C) for 3 days. The film was, then, taken out at the end of soaking period and removed moisture on the surface and the weight of the film was measured.

The swelling power was calculated using the following formula

$$\text{Swelling power} = \frac{W_2 - W_1}{W_1} \times 100 \quad (1)$$

where W_1 was the dry weight of MBS film and W_2 was the weight of the film after immersed in water for 3 days.

Gel Fraction

To determine gel fraction, precisely 0.2 g of a film was immersed in 5 mL DMSO under mild stirring for 24 h at 25 °C. After the treatment, DMSO was removed and the residual starch film was thoroughly washed in water. The dry weight of the sample after DMSO treatment was recorded to calculate weight loss. The experiment was performed in triplicate [9].

The gel fraction was calculated by using the following equation:

$$\text{Gel fraction} = \frac{M_g - M_b}{M_b} \times 100 \quad (2)$$

where M_b and M_g were the dry weight and wet weight of the film after immersed in DMSO for 24 h, respectively.

WVP

WVP of a film was carried out by ASTM method E96. The film (about 0.2 mm thickness) was cut into circles, sealed over the circular opening of cup and then stored in a desiccator at the temperature of 36 ± 2 °C. WVP was determined by the weight gain of the permeation specimen. After steady state condition was reached, accurate weight was recorded. WVP was examined by using the following Eq. 3:

$$\text{WVP} = \frac{W \times x}{t \times A \times \Delta P} \times 100 \quad (3)$$

where W/t was the slope of system weight gain versus time (g/day), x was the film thickness (mm), A was the area of the exposed surface of the film (32.15 cm^2) and ΔP = vapor pressure difference, mm Hg (1.333 × 102 Pa).

XRD

Wide-angle X-ray diffraction analysis was performed for a sample film. The sample was cut into approximately 30 mm × 30 mm rectangular shape and the measurement was performed by a D8 Advance X-ray diffractometer (Bruker, Madison, U.S.A) with CuKα wavelength of 1.542 Å. Radiation from the anode, operated at 40 kV and 35 mA. The diffractometer was equipped with 1° divergence slit, a 16 mm beam bask, a 0.2 mm receiving slit and a 1° scatter slit. Degree of film crystallinity (Xc) was determined using the method described by Chang et al. [18].

$$X_c = \frac{A_c}{A_c + A_a} \times 100 \quad (4)$$

where A_c was to the sum of the crystallised peak area above the amorphous area and A_a referred to the amorphous area on the X-ray diffractogram.

SEM

Morphology of a film was using a scanning electron microscope (FEI, Quanta 250, USA). Each tested sample was immersed into liquid nitrogen before fractured and, then, vacuum coated with thin layer of gold to prevent electrical charge.

Mechanical Properties

A film was cut into rectangular piece of 100 mm × 10 mm. The film thickness was approximately 0.4 mm. A film was conditioned at 60 ± 2% RH and at a temperature of 25 °C before testing. Tensile properties of a film was characterized using Universal Testing Machine (Lloyd Instrument, LR 5K, West Sussex, UK) with a 100 N load cell, a gauge length of 50 mm and the crosshead speed was maintained at 40 mm/min. Ten films were tested to obtain the averaged values.

Biodegradability

A film with the dimension of 100 mm × 10 mm was buried at approximately 10 cm under the soil surface with 10% moisture. The test was carried out over a period of 5 and 10 days in the laboratory. After that, the sample was collected from the pot, gently cleaned by brushing, tensile test of the soil-buried sample was, then, examined.

TGA

Thermogravimetric (TGA) and derivative thermal gravimetric (DTG) analyses of a film was scanned from 50 to 700 °C

using a thermogravimetric analyzer (Perkin Elmer, Pyris 1, Massachusetts, USA) at a rate of 10 °C/min in nitrogen atmosphere to characterize thermal stability and degradation temperature.

Results and Discussions

Chemical structures of MBS cross-linked by MA and SA is shown in Fig. 2. Either MA or SA can interconnect with hydroxyl groups on D-glucopyranose ring presented in MBS by forming ester bonds. Because of the presence of hydroxyl groups in MA structure, carboxyl group on MA was more difficult to react with hydroxyl groups on MBS molecules due to steric effect as compared to SA with no hydroxyl group. Furthermore, a simultaneous reaction to cross-linking is hydrolysis of MBS chain due to high acidity of the acids. Higher acidity of MA (pK_{a1} and pK_{a2} = 3.40 and 5.20, respectively) caused more efficient hydrolysis than lower acidity of SA (pK_{a1} and pK_{a2} = 4.20 and 5.60, respectively) [16, 17]. pH values of 6.5, 4.5 and 3.0 were found for MBS solution without acid, with 30% SA and with 30% MA, respectively.

Infrared Spectroscopy

Interaction between starch and acid cross-linker was analyzed by FTIR. FTIR spectra of different MBS films were presented in Fig. 3. It can be observed that the peak positions at 1080–1270 cm^{-1} and 1000–1200 cm^{-1} were attributed to the gluco-pyranose ring O–C stretching vibrations [19]. Water adsorbed by MBS molecules was ascribed by the peak position at 1640 cm^{-1} [13, 20]. The O–H stretching appeared as a very broad peak at 3500–3300 cm^{-1}, while the aliphatic C–H asymmetric stretching was observed as a sharp peak at 3000–2800 cm^{-1} [21]. It can be seen that both of the cross-linked MBS films with MA and SA showed similar IR peak pattern. It should be noted that the presence of esterification, allocated by the presence of carbonyl peak (1730 cm^{-1}) in both MA- and SA- cross-linked MBS film, was observed. Reddy et al. reported that cassava starch cross-linked with CA also showed the presence of carbonyl peak in the FTIR spectrum at around 1724 cm^{-1} [22]. In addition, gradual increase of intensity peak at 1730 cm^{-1} was observed as the contents of either MA or SA increased. This was suggested that there were an increase in the number of ester bonds formed with the increase contents of either MA or SA [9].

Swelling Power

The swelling power of native and different cross-linked MBS films is presented in Fig. 4. Native MBS film presented the highest in swelling power compared to those cross-linked films due to hydrophilic nature of the native film. However, the incorporation of different MA and SA contents caused the decrease in the degree of swelling power due to the increase in the ester bond formation, which decreased free hydroxyl groups of MBS molecules. Moreover, degree of swelling power of all cross-linked MBS films were greatly reduced by MA- and SA- cross-linking.

Furthermore, it can be observed that MBS films cross-linked by MA showed higher degree of swelling power than that of SA, considering at the same acid content. The result suggested that MBS film cross-linked with MA created lower ester linkage. This could be because of lower pK_a value of MA, resulting in more hydrolysis of the glycosidic linkages in MBS, leading to more hydrophilic character. In addition, higher degree of swelling power of MBS film with MA could also arise from steric hindrance by the present

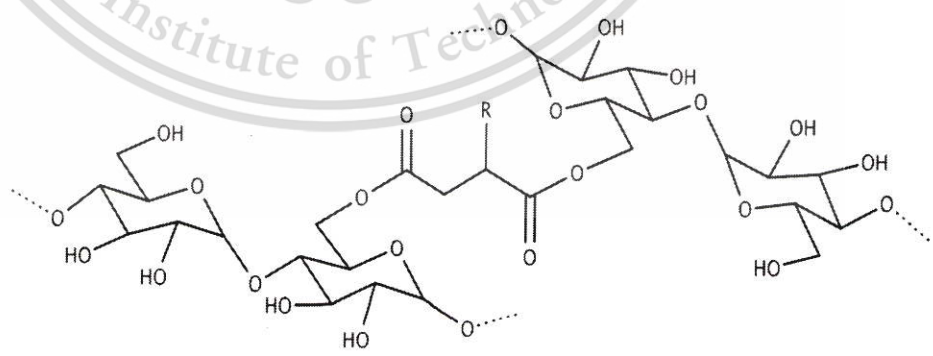

1) R = H (Succinic acid)

2) R = OH (Malic acid)

Fig. 2 Chemical structure of MBS cross-linked by MA and SA

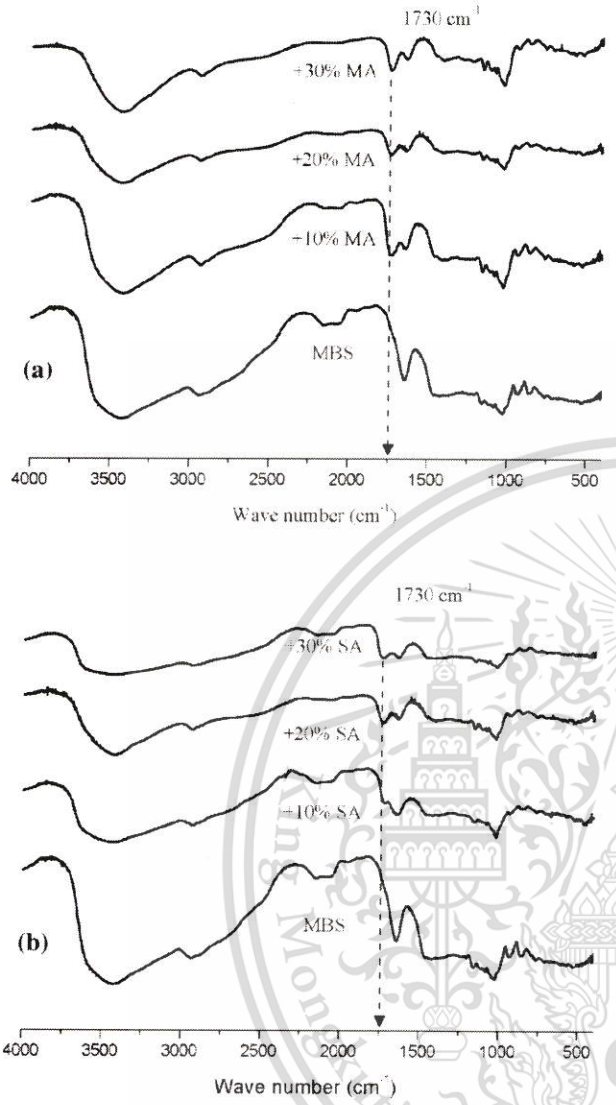

Fig. 3 FT-IR spectra of MBS films cross-linked by different contents of **a** MA and **b** SA

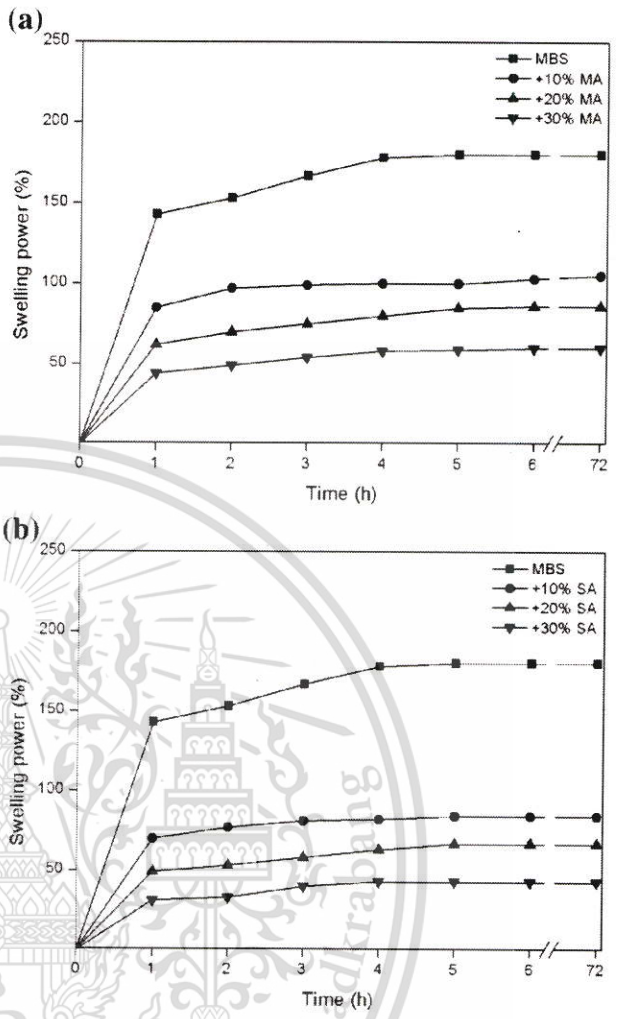

Fig. 4 Swelling power of different MBS films cross-linked by **a** MA and **b** SA

of hydroxyl group in MA, probably led to lower degree of cross-linking.

As expected, cross-linked MBS film with either 30% MA or SA exhibited the lowest swelling power due to the highest degree of esterification as confirmed by FT-IR spectra in Fig. 3. Cross-linking strengthened MBS molecules and decreased the penetration of water without disintegration, similar to those reported by Colivet et al. [23, 24]. Generally, crystalline structure of amylose in nature does not absorb water [25]. As a result, MBS film has contributed to the low degree of swelling due to its high amylose content. In addition, MBS film cross-linked by MA and SA showed lower swelling power than malonic acid cross-linked potato starch and cassava starch [9, 23].

Table 1 Gel fraction, WVTR and SA and degree of crystallinity of MBS films cross-linked by MA and SA

Acid types	Acid contents (%)	Gel fraction in DMSO (%)	WVP (g/mm/kPa/day/m^2)	Degree of crystallinity (%)
	0	0	4.43 ± 0.04	61.50 ± 0.04
MA	10	38 ± 0.05	3.62 ± 0.07	50.75 ± 0.02
	20	79 ± 0.03	2.58 ± 0.03	48.08 ± 0.03
	30	87 ± 0.07	1.44 ± 0.06	46.42 ± 0.02
SA	10	44 ± 0.04	2.54 ± 0.03	54.85 ± 0.04
	20	88 ± 0.06	1.03 ± 0.07	53.58 ± 0.03
	30	93 ± 0.03	0.56 ± 0.05	52.73 ± 0.02

Gel Fraction

Gel fraction of different MBS films is shown in Table 1. Native MBS film was absolutely soluble in DMSO. However, gel fraction of different MBS films increased with increasing contents of MA and SA. This could be associated with the increased content of cross-linking. Additionally, cross-linked MBS film with 30% MA and SA presented the highest gel fraction. This could be related to structural modification by cross-linking that increased hydrophobicity. Obviously, cross-linked MBS films by MA displayed lower gel fraction than that by SA at equal percentage because of more hydrolyzed MBS molecules. Moreover, steric effect of both acids affected gel fraction. Because of more steric effect of MA than that of SA, carboxyl groups on MA were more difficult to react with hydroxyl groups on MBS molecules. Therefore, SA showed higher degree of crosslinking and gel fraction than those of MA. The highest gel fraction was obtained from MBS film with 30% SA. In addition, MBS film cross-linked by MA and SA showed higher gel fraction than reported malonic acid cross-linked potato starch [9].

WVP

Table 1 also presents WVP of different cross-linked MBS films. Water vapor easily permeated native MBS film with the highest WVP. This was because the hydrophilicity of native MBS structure. When MA and SA contents were varied from 10 to 30%, WVP values slightly decreased. This was because the formation of hydrophobic of ester bonds via cross-linking that reduced the capacity of water vapor transmission.

In addition, both MBS films cross-linked by 30% MA and SA showed the lowest WVP, as compared with other acid contents. This caused by more covalent network, generated more hydrophobicity of the cross-linked MBS films. Seligra et al. reported the similar results for the cross-linked cassava starch film with CA due to cross-linking reaction [26].

Furthermore, MBS films cross-linked by SA showed lower WVP values than those by MA at the same content. This result should be related to more hydrophobicity and cross-linking. The WVP result also related to degree of swelling power (Fig. 4) and gel fraction (Table 1). WVP of cross-linked MBS films was lower than that of pea starch and rice starch film cross-linked with CA, when compared at the same humidity gradient [2].

XRD

Crystallinity of native and MBS cross-linked films by MA and SA films are presented in Table 1. Native MBS film showed the highest degree of crystallinity compared to those modified films. The addition of MA and SA resulted in the decrease of degree of crystallinity, which was ascribed to the replacement of hydroxyl group with di-carboxylic group during cross-linking process [9]. Therefore, the cross-linked MBS molecules cannot rearrange in crystal structures; this prohibited the recrystallization of the MBS molecules. Compared to native MBS film (61.50%), the relative crystallinity of cross-linked MBS films (46.42–54.85%) tended to decrease. According to Bruni et al. wheat starch cross-linked by sodium trimetaphosphate reduced the formation of crystalline regions in the wheat starch film [27].

In addition, the degree of crystallinity was lower in MBS films cross-linked by MA than those by SA at similar content. This was because of lower pK_a values of MA that enhanced hydrolysis, resulting in lower degree of crystallinity, compared to MBS films cross-linked by SA. Moreover, steric effect of MA caused lower degree of crystallinity. Additionally, the difference in MA and SA contents affected degree of crystallinity and also gel fraction. The increase of MA and SA contents resulted in an increase of degree of cross-linking. Hence, gel fractions of cross-linked films were increased. However, concurrent reaction to cross-linking is hydrolysis of MBS backbone chain. This was because acidity of MA and SA in the system. The increase of acid contents caused more starch hydrolysis, resulting in the decrease in degree of crystallinity.

SEM

Morphology of different MBS starch films were evaluated by SEM and the resulting images were shown in Fig. 5. The cross-section micrograph (Fig. 5a) illustrated that rough surface with starch some starch granules was observed in native MBS film; however, cross-linked MBS films with MA and SA showed homogeneous, smooth and continuous morphology without pores and cracks. It should be noted that the addition of MA and SA into MBS led to smoother structure compared to the native MBS film. Similar result was also observed for CA cross-linked corn starch film [22]. Moreover, the different types and contents of acids also exhibited the same phase morphology.

Mechanical Property

Mechanical properties of native and cross-linked MBS films are presented in Fig. 6. Due to high amylose content of MBS, high strength and stiffness of MBS film is expected. It was observed that native MBS film showed high stress at maximum load and Young's modulus but low strain at maximum load. This is due to excessive hydrogen bonds among MBS molecules. Amylose-rich MBS film was stronger than other polysaccharide films, e.g. wheat starch, potato starch, corn starch film [28].

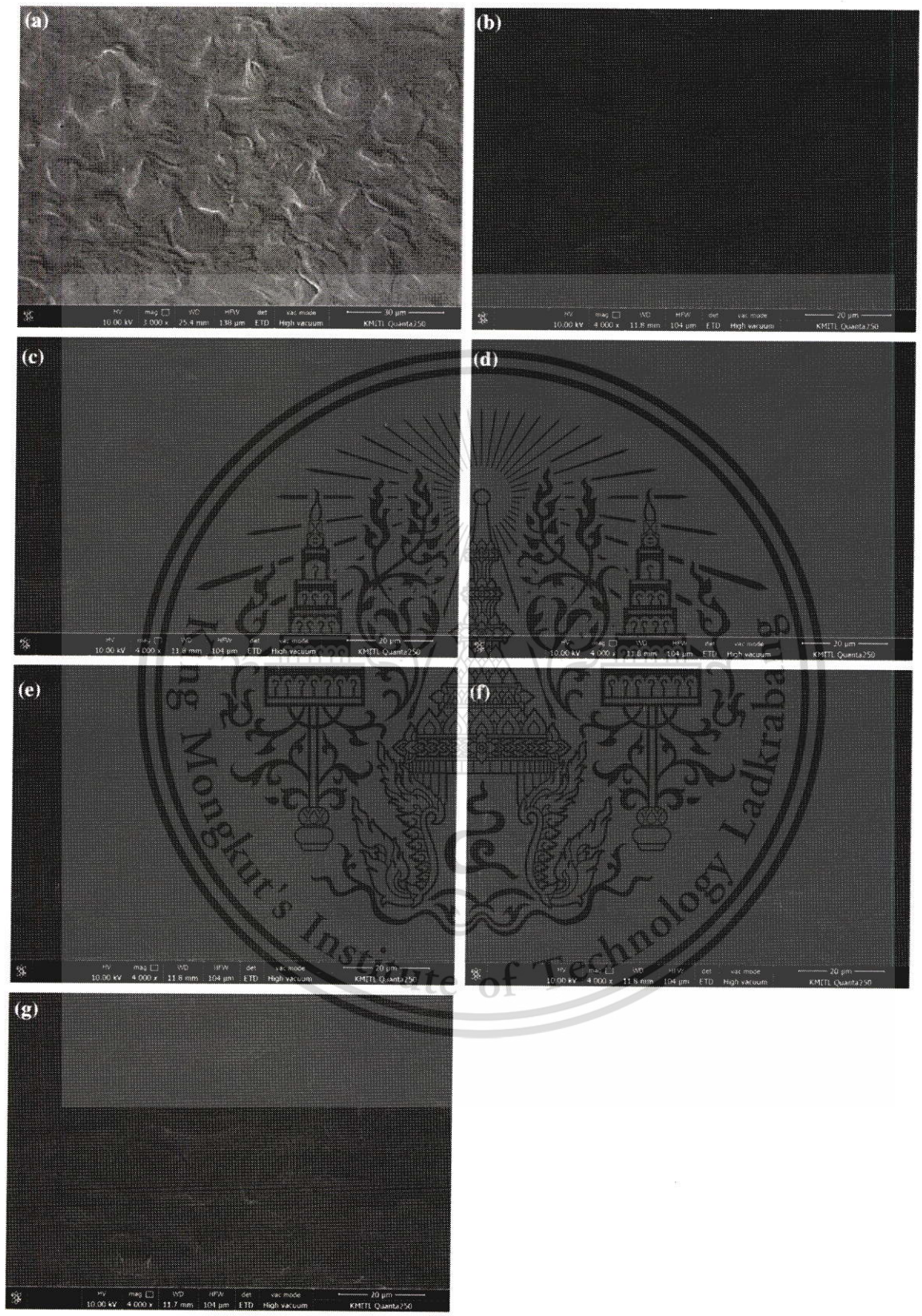

Fig. 5 Fractured surfaces of different contents of cross-linked MBS films **a** native MBS, **b** 10% MA, **c** 20% MA, **d** 30% MA, **e** 10% SA, **f** 20% SA and **g** 30% SA

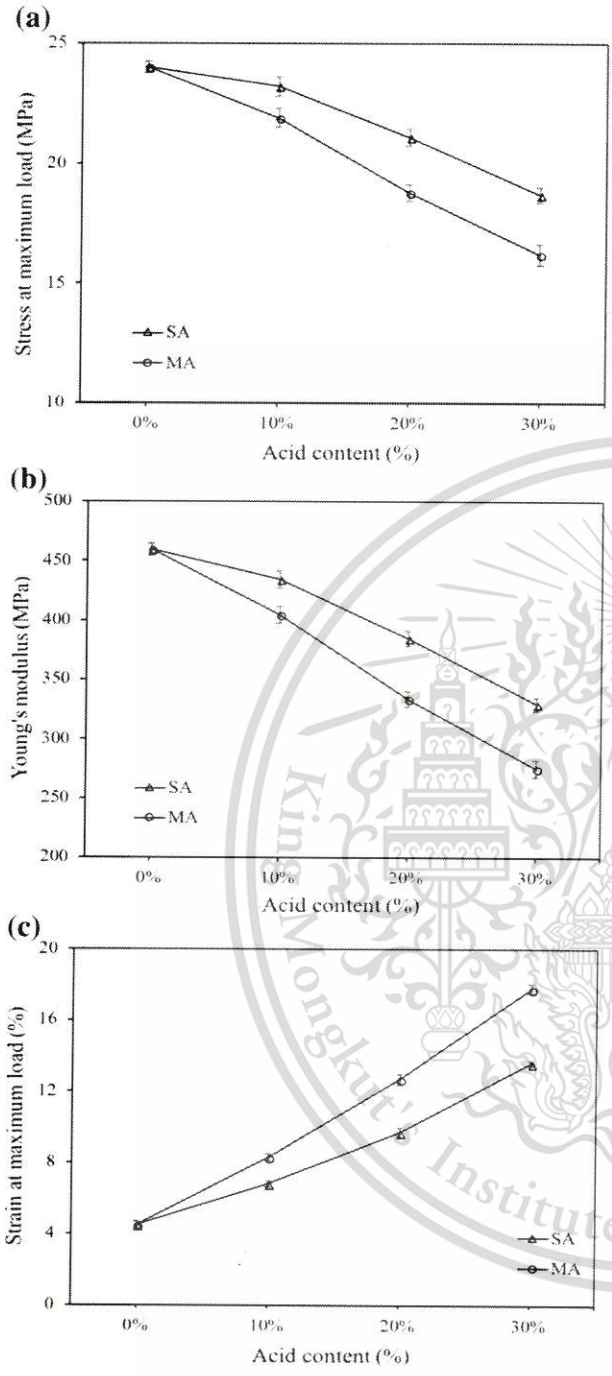

Fig. 6 Mechanical properties of different MBS films cross-linked with MA and SA **a** stress at maximum load, **b** Young's modulus and **c** strain at maximum load

On the contrary, cross-linked MBS films by either MA or SA exhibited lower stress at maximum load (Fig. 6a) and Young's modulus (Fig. 6b) than native MBS film. Consequently, strain at maximum load (Fig. 6c) was significantly increased, similar to that for aconitic acid cross-linked potato starch film [11]. This could be because the acid cross-linker reacted with hydroxyl groups in MBS molecules (Fig. 3) and formed ester linkages. The mechanical property results also confirmed the decrease of degree of crystallinity as shown in Table 1.

Moreover, it can observed that MBS film cross-linked by 30% MA or SA showed lower stress at maximum load and Young's modulus than those by 10% and 20% cross-linked by MA or SA. As a result, the increase in strain at maximum load was obtained. This is because there is more an excess of cross-linking bridges, resulting in lower chain stiffness and higher extendibility. This result was also in agreement with Reddy et al. who reported that high CA content caused by excess cross-linking led to the decrease of tensile strength [22].

Comparison between MA and SA, the results suggested that MBS film cross-linked by SA illustrated higher stress at maximum load and Young's modulus; and subsequently, lower strain at maximum load than that by MA. This is because of higher degree of crystallinity in SA cross-linked MBS film than MA cross-linked film as confirmed by XRD, gel fraction and swelling power (Table 1; Fig. 4, respectively). Moreover, higher acidity in MA resulting in more hydrolyzed MBS molecules, led to lower tensile strength than that in SA. Similar trends have been reported in corn starch/PVA blend films cross-linked by MA and SA [12]. In addition, stress at maximum load and Young's modulus of cross-linked MBS film with MA and SA is comparative to commercial LDPE film [29] and low-density polyethylene based nanocomposite films [30].

Soil Burial Test

Mechanical properties of different cross-linked MBS films by MA and SA after soil burial test were taken as stress at maximum load, Young's modulus and strain at maximum load of the films (Fig. 7). Mechanical properties of native and cross-linked MBS film were found to decrease after soil burial test. This could be due to the adsorption of moisture from soil, so the degradation occurred by hydrolysis and also microorganisms [31]. Interestingly, MBS films cross-linked by MA and SA could also biodegrade, confirmed by the decreased of tensile properties.

TGA

Figure 8 and Table 2 show TGA thermograms of different MBS films cross-linked by 0–30% MA and SA. The first step at about 70 °C being assigned to water evaporation from MBS films, the second step at approximately 180 °C related to glycerol plasticizer degradation [10]. The third peak around 290 °C due to the decomposition of hydrolyzed MBS [11]. The main degradation step at about 300 °C was

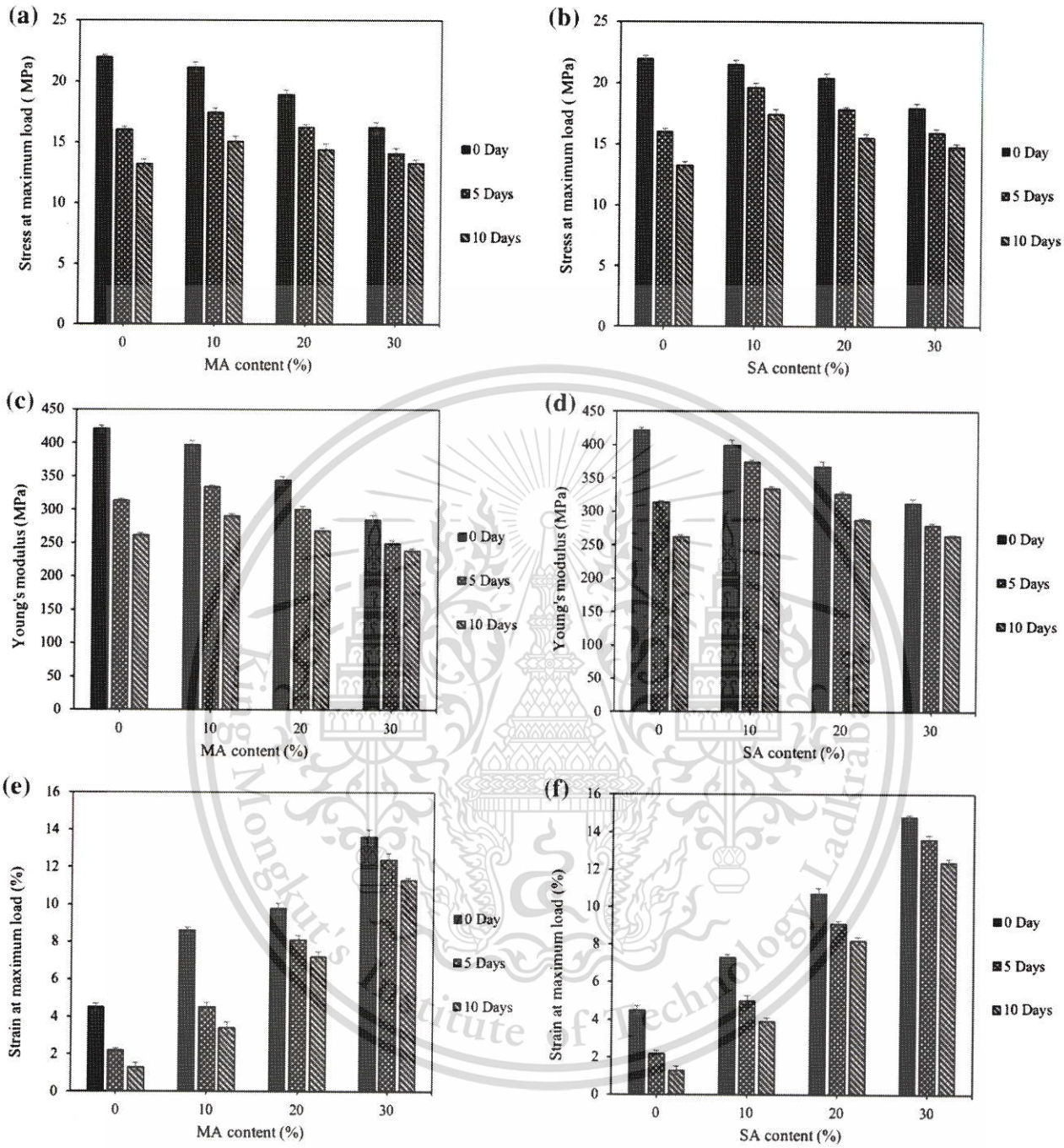

Fig. 7 Mechanical properties after biodegradation in soil of different films cross-linked by MA and SA **a, b** stress at maximum load, **a, d** Young's modulus and **e, f** strain at maximum load

due to thermal degradation of starch backbone [10] and the fifth step at around 370 °C was observed for degradation of cross-linked MBS [11].

It was found that, the main degradation step (step 4) of different cross-linked MBS films increased clearly, compared to native MBS film. It implies that the addition of different MA and SA could improve thermal degradation temperature because cross-linking could strengthen MBS backbone chains and created strong linkages; therefore, enhance thermal degradation temperature of cross-linked MBS films.

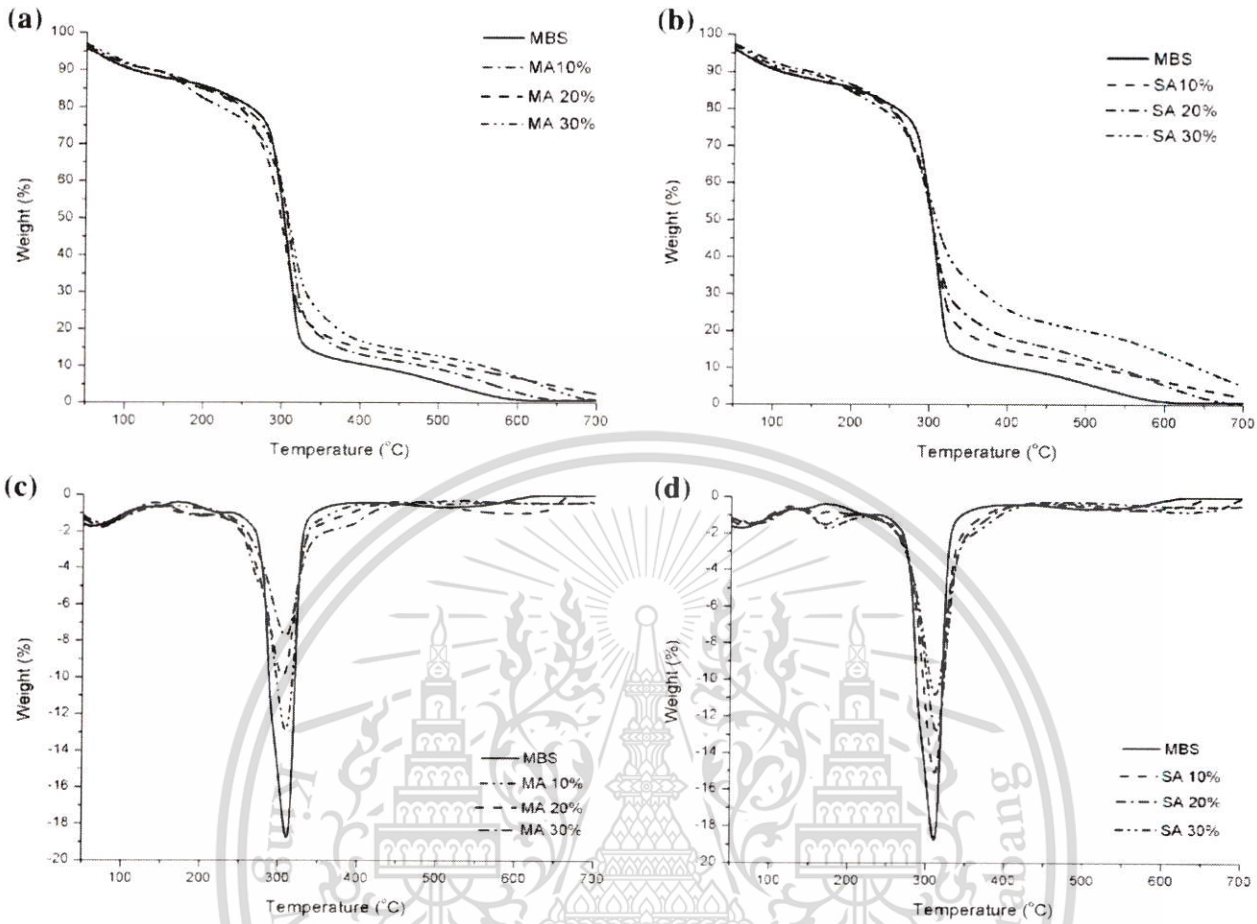

Fig. 8 **a, b** TGA and **c, d** DTG thermograms of different modified MBS films by MA and SA

Table 2 Decomposition temperatures and percentage weight losses of different cross-linked mung bean starch films obtained from TG and DTG thermograms

Samples	Acid contents (%)	Thermal decomposition temperature (°C)					Residues (%)
		Step 1 (°C)	Step 2 (°C)	Step 3 (°C)	Step 4 (°C)	Step 5 (°C)	600 °C
	0	72.6	172.4	–	301.4	–	0
	10	74.1	185.3	272.2	308.4	365.3	5.2
MA	20	68.2	186.2	274.5	309.8	370.4	8.4
	30	70.7	183.6	277.1	311.9	373.8	10.1
	10	65.5	184.4	–	311.6	370.2	6.5
SA	20	68.1	184.1	–	313.2	376.1	9.5
	30	74.3	187.9	–	315.8	377.8	15.2

Furthermore, the cross-linked MBS films by MA and SA exhibited higher residual weight percentage than native MBS film. It should be suggested that the residual weight percentage increased as the MA and SA contents increased which could be also ascribed to formation of strong cross-linkages between the acids and MBS chains.

Moreover, the degradation temperature and the residual weight percentage for MBS film cross-linked by SA was higher than that of MA at the same content. This was because SA acted as a strong cross-linker and formed the strongest film network as compared to MBS film cross-linked by MA at the same content. Thermal properties agreed with the results of swelling power (Fig. 4) and gel fraction (Table 1). Similar result was also reported for aconitic acid cross-linked potato starch film [11].

Conclusions

In this study, high amylose MBS film was successfully prepared and cross-linked by MA and SA. All cross-linked MBS films exhibited new ester bond formation observed by FTIR spectra. MA and SA also effectively decreased swelling power, WVP and degree of crystallinity but increased gel fraction of the cross-linked MBS films. In addition, MBS films with SA showed lower swelling power and WVP than those with MA at same acid content. Smooth fractured surface was noticed for different MBS films cross-linked by MA and SA. Moreover, both MA- and SA- modified MBS films showed the improvement of extendibility. All the MBS films also exhibited the capability to degrade after soil burial test. Furthermore, cross-linked MBS films showed higher thermal degradation temperature and higher residual weight percentage as compared to native MBS film. From this study, MBS film with 30% SA presented extendibility of film and highest gel fraction, lowest degree of swelling power and WVP value.

Acknowledgements The authors express their sincere appreciation to KMITL Research Fund (Grant No. KREF 046108) for supporting the study financially.

References

1. Ketkaew S, Kasemsiri P, Hiziroglu S, Mongkolthanaruk W, Wannasutta R, Pongsa U, Chindaprasirt P (2018) J Polym Environ 26:311–318
2. Ma X, Chang PR, Yu J, Stumborg M (2009) Carbohydr Polym 75:1–8
3. Hoover R, Li YX, Hynes G, Senanayake N (1997) Food Hydrocol 4:401–408
4. Shen X, Shang W, Strappe P, Chen L, Li X, Zhou Z (2018) Food Hydrocol 77:40–48
5. Bae HJ, Cha DS, Whiteside WS, Park HJ (2008) Food Chem 106:96–105
6. Rompothi O, Pradipasena P, Tananuwong K, Somwangthanaroj A, Janjarasskul T (2017) Carbohydr Polym 157:748–756
7. Ghaffar AMA, Ali HE, Nasef SM, El-Bialy HA (2018) J Polym Environ 26:3226–3236
8. Olivato JB, Grossmann MVE, Bilck AP, Yamashita F (2012) Carbohydr Polym 90:159–164
9. Dastidar TG, Netravali AN (2012) Carbohydr Polym 90:1620–1628
10. Sun S, Liu P, Ji N, Hou H, Dong H (2018) Food Hydrocol 77:964–975
11. Gilfillan WN, Doherty WOS (2016) Carbohydr Polym 141:60–67
12. Yoon SD, Chough SH, Park HR (2005) Appl Polym Sci 100:3733–3740
13. Shen L, Xu H, Kong L, Yang Y (2015) Polym Environ 23:588–594
14. Majzoobi M, Beparva P, Farahnaky A, Badii F (2014) Starch/Stärke 66:491–495
15. Menzel C, Olsson E, Plivelic TS, Andersson R, Johansson C, Kuktaite R, Järnström L, Koch K (2013) Carbohydr Polym 96:270–276
16. Wikipedia, Malic acid. https://en.wikipedia.org/wiki/Malic_acid
17. Wikipedia, Succinic acid. https://en.wikipedia.org/wiki/Succinic_acid
18. Chang FF, He X, Huang Q (2013) J Cereal Sci 58:89–95
19. Dai H, Chang PR, Yu J, Geng F, Ma X (2010) Carbohydr Polym 80:139–144
20. Menzel C, Seisenbaeva G, Agback P, Gällstedt M, Boldizar A, Koch K (2017) Carbohydr Polym 172:365–373
21. Liu J, Wang B, Lin L, Zhang J, Liu W, Xie J, Ding Y (2014) Food Hydrocol 36:45–52
22. Reddy N, Yang Y (2010) Food Chem 118:702–711
23. Colivet J, Carvalho RA (2017) Ind Crop Prod 95:599–607
24. Yoon SD (2014) J Agric Food Chem 62:1755–1764
25. Riouxa B, Ispas-Szabob P, AÈõt-Kadic A, Mateescub MA, JuhaÂsza J (2002) Carbohydr Polym 50:371–378
26. Seligra PG, Jaramillo CM, Famá L, Goyanes S (2016) Carbohydr Polym 138:66–74
27. Bruni GP, Oliveira JP, Halal SLME, Flores WH, Gunde A, Miranda MZ, Dias ARG, Zavareze ER (2018) Starch/Stärke. https://doi.org/10.1002/star.201700192
28. Basiak E, Lenarta A, Debeaufort F (2017) Int J Biol Macromol 98:348–356
29. MatWeb material property data, Dow LDPE6821 low density polyethylene, film grade. http://www.matweb.com/reference/tensilestrength.aspx
30. Majeed K, AlMaadeed MAA, Zagho MM (2018) Chin J Chem Eng 26:428–435
31. Wang H, Wei D, Zheng A, Xiao H (2015) Polym Degrad Stab 116:14–22

Research Article

Received: 25 September 2018 Revised: 26 March 2019 Accepted article published: 17 May 2019 Published online in Wiley Online Library:

(wileyonlinelibrary.com) DOI 10.1002/jsfa.9812

Development, modification and characterization of new biodegradable film from basil seed (*Ocimum basilicum* L.) mucilage

Naruenart Thessrimuang[a] and Jutarat Prachayawarakorn[a,b*]

Abstract

BACKGROUND: Biodegradable films from basil seed mucilage (BSM) were formed and modified with several di-carboxylic acid crosslinkers; i.e. tartaric acid (TA), malic acid (MA) and succinic acid (SA) with varying acidity and chemical structures, to enhance mechanical properties and water barrier ability. Basil seeds have a reasonable mucilage content and valuable properties; thus, it has the potential to develop valuable new biodegradable films.

RESULT: We characterized BSM films with the three crosslinkers using Fourier-transform infrared (FTIR) spectra and observed a 1730 cm^{-1} C=O stretching peak, which confirmed ester linkage between the mucilage and crosslinkers. The crosslinked films showed higher gel fraction than native films. The crosslinked films showed better swelling and water vapor permeability with SA than with TA and MA. Crosslinking led to significant improvement in strain at maximum load. Further, the stress maximum load was comparable to that of commercial low-density polyethylene (LDPE) film. Crosslinked films showed additional homogeneous morphology and an increase in thermal degradation temperatures.

CONCLUSION: Crosslinking with dicarboxylic acids improved all the key properties of BSM films, including excellent stress and strain at maximum load, improved barrier capability and thermal properties. Thus, these films showed good potential as biodegradable films, especially for food packaging.

Keywords: basil seed mucilage; biodegradable film; crosslinking; polysaccharide

INTRODUCTION

In recent years, biodegradable films have been studied extensively driven by a demand for inexpensive, non-toxic and biodegradable films. Biodegradable films commonly are derived from polysaccharides and proteins and there is considerable interest in finding new renewable resources for forming bio-based films.[1]

Basil seed (*Ocimum basilicum* L.) is a novel mucilaginous polysaccharide, which is grown in various regions of Asia, Africa, America and Europe.[2] Basil is an aromatic herb that is used extensively to add a distinctive aroma and flavor to food. The leaves can be used fresh or dried for use as a spice. Essential oils extracted from fresh leaves and flowers can be used as additives in food, pharmaceuticals and cosmetics.[3] Basil seed mucilage (BSM) is an acidic polysaccharide, which has an uronic acid content of approximately 7%. Uronic acid has two major components of glucomannan (43%) and (1,4)-linked xylan (24%) and a minor fraction of glucan (2.3%).[4] Compared with other polysaccharides, BSM is an interesting material and it has attractive advantages, such as low production cost, biocompatibility, biodegradability and good rheological properties, which are factors that enable it to have excellent potentiality as a film-forming agent.[5] Basil seed contains a large quantity of mucilage with good functional properties.[6] BSM has been used as a stabilizing and thickening ingredient in food systems.[7] BSM has shown potential for removing chromium[8] and as a pharmaceutical excipient.[9] Khazaei *et al.* also showed that BSM could produce films with good appearance and satisfactory mechanical properties.[5]

In general, bio-based films show low stability and poor mechanical properties and crosslinking has been used to improve their functional properties.[10,11] However, some crosslinkers, such as boric acid, epichlorohydrin and glutaraldehyde, are expensive and toxic to humans.[12] Therefore, natural crosslinkers, such as tartaric acid (TA), malic acid (MA) and succinic acid (SA), are preferred. These are natural organic acids, present, in vegetables and fruits, synthesized during fermentation by microorganisms. They can be produced in large quantities, by biotechnological techniques, and can be used to modify polysaccharides.[13] The two carboxylic acid groups can produce chemical bridges between hydroxyl groups of the polysaccharide molecules. Crosslinking can reduce hydrophilicity of polysaccharides, improve water vapor permeability (WVP), mechanical and also thermal properties.[14–16]

Olsson *et al.* observed that the potato starch film, with 30 pph citric acid (CA) added, led to a significant reduction in equilibrium

* *Correspondence to: J Prachayawarakorn, Faculty of Science, King Mongkut's Institute of Technology Ladkrabang (KMITL), Bangkok, Thailand. E-mail: jutarat.si@kmitl.ac.th*

a *Department of Chemistry, Faculty of Science, King Mongkut's Institute of Technology Ladkrabang (KMITL), Bangkok, Thailand*

b *Advanced Materials Research Unit, Faculty of Science, King Mongkut's Institute of Technology Ladkrabang (KMITL), Bangkok, Thailand*

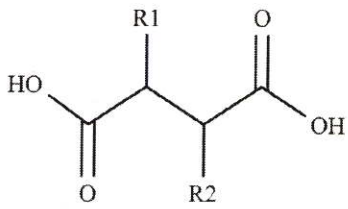

Succinic acid ; $R_1 = H$, $R_2 = H$

Malic acid ; $R_1 = OH$, $R_2 = H$

Tartaric acid ; $R_1 = OH$, $R_2 = OH$

Figure 1. Chemical structures of tartaric acid (TA), malic acid (MA) and succinic acid (SA).

moisture content, diffusion coefficient and WVP at high relative humidity (RH) which suggested that crosslinking occurred.[17] Furthermore, scanning electron microscopy (SEM) images showed that ascorbic acid (AsA) reduced the interfacial tension between the potato starch and polyvinyl alcohol (PVA) blended films, resulting in more homogeneous morphology: swelling of the blended film decreased when AsA content was increased.[18] CA-modified thermoplastic pea starch improved water vapor barrier properties.[19] Shen *et al.* reported that corn starch film crosslinked with CA, MA, SA and 1,2,3,4-butanetetracarboxylic acid showed enhanced tensile strain.[20] The degree of swelling and solubility of aconitic acid crosslinked potato starch films was lower than that of the native film.[21] Another report showed that adipic acid, as a crosslinking agent, enhanced gel fraction of chitosan/corn cob composite films.[22]

We developed a new biodegradable film from BSM and studied the effect of steric hindrance of hydroxyl (OH) groups in chemical structures of di-carboxylic acids; i.e. TA, MA and SA on properties of BSM films. Native and crosslinked BSM films with TA, MA and SA were characterized by Fourier-transform infrared spectroscopy (FTIR), SEM, X-ray diffraction (XRD) and thermogravimetric analysis (TGA). Furthermore, WVP, swelling ability and gel fraction of different BSM films were also examined.

MATERIALS AND METHODS

Materials

Basil seeds were obtained from Thai Baan Rai Co. Ltd (Bangkok, Thailand). Glycerol was obtained from Lab System Co. Ltd (Bangkok, Thailand). TA, MA and SA (food grade, Fig. 1) were obtained from Lab System Co. Ltd.

Mucilage extraction procedure

The mucilage was extracted using a modification of Beigomi *et al.*'s method.[23] About 50 g of basil seeds were first washed to remove all dust and dirt. The seeds were immersed in distilled water at a ratio of 1:50 (seeds/distilled water) for 2 h at room temperature. After that, the swollen seeds were stirred with a rod paddle blender (IKA, Konigswinter, Germany) at 71×*g* for 10 min to scrub the mucilage layer off the seed surface. The mucilage was separated from the seeds by filtering the swollen seeds through cheesecloth to remove the remaining small seed particles, and then centrifuged (Universal320, Hettich, Salford, UK) at 4200×*g* for 5 min to remove seed residue. Mucilage was separately prepared for each experiment to ensure freshness.

Preparation of BSM films

To prepare BSM film, 70 g of mucilage obtained from previous extraction was mixed with 30 g kg^{-1} (based on BSM weight) glycerol as a plasticizer. TA, MA and SA (30 g kg^{-1}, based on the initial weight of BSM) were then added. The solution was stirred continuously for 45 min at 60 °C. BSM was cast by pouring the mixture onto a polypropylene plate and dried in a hot-air oven (Memmert, Schwabach, Germany) for 10 h at 40 °C. The BSM film was further heated in the oven at 150 °C for 10 min to complete crosslinking. The dried BSM film was peeled off and stored in desiccators, containing a saturated solution of magnesium nitrate (60 ± 2% RH) for 48 h, before characterization.

FTIR spectroscopic study

FTIR spectra were scanned in transmission mode on a Spectrum 2000 GX spectrometer (Perkin Elmer, Waltham, MA, USA) using KBr disks. Normally, 20 scans averaged for each spectrum at a resolution of 6 cm^{-1}. The absorption spectrum was baseline-corrected from 4000 to 400 cm^{-1}.

Swelling ability

A film (30 × 30 mm^2) was dried at 105 °C for 2 h and immersed in distilled water at room temperature for 3 days. Film swelling was determined following Dastidar *et al.*[24] The wet film was weighed after removing water from the surface of the film with blotting paper.

Swelling was calculated as:

$$\text{Swelling ability} = \frac{W_2 - W_1}{W_1} \times 100 \quad (1)$$

where W_1 was the original weight of the sample and W_2 was the weight of the film after immersed in water for 3 days.

Gel fraction

To determine gel fraction, 0.2 g of BSM film was soaked in 25 mL dimethyl sulfoxide (DMSO) and stirred for 24 h at 25 °C.[24] Then, residual BSM film was washed thoroughly with water and dried at 70 °C. The gel fraction was

$$\text{Gel fraction} = \frac{M_g - M_b}{M_b} \times 100 \quad (2)$$

where M_b is the dry and M_g the wet weight of the film immersed in DMSO for 24 h.

Water vapor permeability (WVP)

Film WVP was determined following Qin *et al.*[25] Circular test cups containing desiccant (0% RH) were sealed with film (effective film area ~0.0036 m^2). The film was stored in a desiccator maintained at 75% RH with saturated sodium chloride. Water-vapor transport was determined from the weight gain:

$$\text{WVP} = \frac{W \times x}{t \times A \times \Delta P} \quad (3)$$

where W/t was the slope of system weight gain *versus* time (in g d^{-1}), x was the film thickness (in millimeters), A was the area of the exposed film surface (3220 mm^2) and ΔP the vapor pressure difference (1.333 × 10^2 Pa).

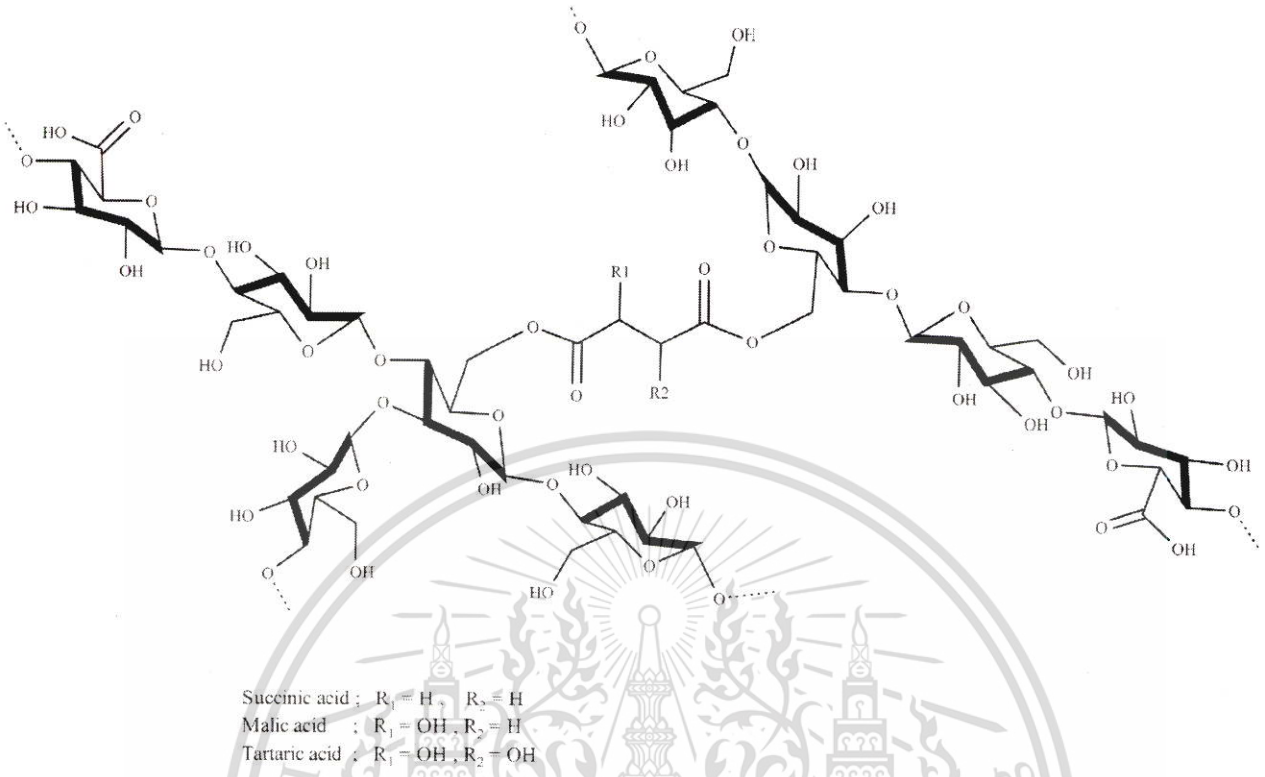

Figure 2. Chemical structure of basil seed mucilage (BSM) crosslinked by tartaric acid (TA), malic acid (MA) or succinic acid (SA).

Table 1. The pKa, swelling ability, gel fraction, water vapor permeability (WVP) and degree of crystallinity of basil seed mucilage (BSM) films crosslinked by 30% tartaric acid (TA), malic acid (MA) or succinic acid (SA)

Samples	pKa		Swelling ability (%)			Gel fraction in dimethyl sulfoxide (%)	WVP (g mm m^{-2} d^{-1} kPa^{-1})	Degree of crystallinity (%)
	pKa_1	pKa_2	1 h	5 h	72 h			
BSM	–	–	312	355	364	0	3.38 ± 0.07	46.5 ± 0.09
+TA	2.89	4.40	223	246	251	77 ± 0.05	2.69 ± 0.06	28.0 ± 0.06
+MA	3.40	5.20	208	226	239	92 ± 0.04	1.62 ± 0.03	34.3 ± 0.03
+SA	4.20	5.60	174	187	193	97 ± 0.02	1.04 ± 0.05	40.9 ± 0.05

X-Ray diffraction (XRD)

Wide-angle XRD spectra were recorded with a D8 Advance X-ray diffractometer (Bruker, Madison, WI, USA) with 1.542 Å CuKα radiation. A sample was cut into ~30 × 30 mm^2 rectangles with a smooth surface.

The degree of crystallinity (X_c) was determined from:

$$X_c = \frac{A_c}{A_c + A_a} \times 100 \quad (4)$$

where A_c is the integrated area of the crystal peak above the amorphous area and A_a is the amorphous area on the X-ray diffractogram.

Scanning electron microscopy (SEM)

The cross-sectional morphology of the film was studied by SEM (Quanta 250, FEI company, Oregon, USA). The film was fractured in liquid nitrogen and sputtered with a thin layer of gold to prevent electrical charge accumulation.

Mechanical properties

Mechanical properties of a film were determined by tensile testing, using a Universal Testing Machine (Lloyd Instrument, LR 5K, Bognor Regis, UK). The film was cut in rectangular 100 mm × 15 mm strips and preconditioned for 24 h at 25 °C and 60 ± 2% RH. The deformation was recorded at a crosshead speed at 40 mm min^{-1} and a 50 mm gauge length. Averages were calculated from 10 replicates of each sample.

Biodegradability

A film was cut into 100 mm × 10 mm strips and buried at ~100 mm depth in soil with 10% moisture for a period 5–10 days in the laboratory, then tested for tensile properties.

Thermogravimetric analysis (TGA)

TGA and derivative thermogravimetry (DTG) analyses used a thermogravimetric analyzer (Perkin Elmer, Pyris 1). Films were scanned from 50 °C to 700 °C at a 10 °C min^{-1} in a nitrogen atmosphere to characterize thermal stability and degradation temperature.

RESULTS AND DISCUSSION

The chemical structure of BSM crosslinked by TA, MA and SA films is presented in Fig. 2. The dicarboxylic acids (TA, MA or SA) can react with the hydroxyl groups of BSM via esterification. Because of the steric hindrance of two hydroxyl groups of TA and one hydroxyl group of MA, the TA or MA carboxyl groups could not link to the BSM hydroxyl groups as easily as SA which lacks a hydroxyl group, so as the number of hydroxyl groups increased, steric hindrance of the crosslinkers also increased. Further, both esterification and acid hydrolysis of BSM backbone chain occur. The acidity of the crosslinkers increased in the sequence of TA > MA > SA. Solution pH values were SA 4.0, MA 3.0, TA 2.5 and native BSM 4.5. The pKa values of TA, MA and SA are presented in Table 1.

FTIR

FTIR spectra of various BSM films crosslinked with different crosslinkers are shown in Fig. 3. The peak positions, 3300–3500 cm^{-1}, were attributed to hydroxyl group O—H stretching and 2800–3000 cm^{-1} to CH_2 group C—H stretching.[26] The 1600 cm^{-1} peak was assigned to carboxylic group asymmetric stretching. The 1080–1270 cm^{-1} and 1000–2000 cm^{-1} peaks were assigned to C—O bonds of the saccharide unit.[27] Note that carboxylic group symmetric stretching, appeared at 1400 cm^{-1}, reflecting the presence of uronic acid in BSM polysaccharides.[28] Several BSM films presented similar IR peak patterns. However, a new sharp peak in the crosslinked BSM films appeared at 1730 cm^{-1}. This was the carbonyl peak from the ester links between acids and BSM molecules. Similarly, Reddy and Yang reported a carbonyl peak at ~1730 cm^{-1} in cassava starch crosslinked with CA.[27]

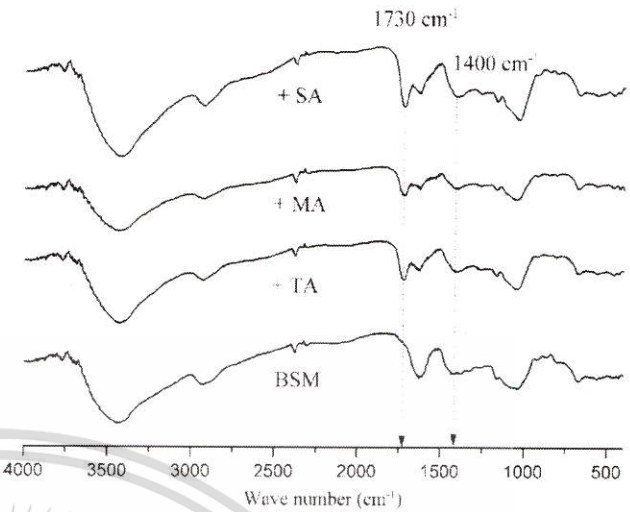

Figure 3. FTIR spectra of basil seed mucilage (BSM) films crosslinked by tartaric acid (TA), malic acid (MA) and succinic acid (SA).

Swelling ability and gel fraction

Table 1 shows swelling *versus* time for native and crosslinked BSM films. Native BSM film showed the highest swelling due to its hydrophilic nature. The polysaccharides of BSM directly affected its absorption, since it contains both uronic acid and polyelectrolyte structures. However, adding crosslinkers reduced the swelling, because the crosslinks used the OH groups and reduced the hydrophilic nature of the backbone, thus crosslinking significantly decreased absorption of water and consequent swelling.

Swelling with crosslinked TA was the highest, followed by MA and SA: the higher acidity of TA led to more extensive hydrolysis and a more hydrophilic property, compared to MA and SA. Further, the two hydroxyl groups of TA easily bonded with H_2O, enhancing hydrophilic properties. From Table 1, we see that BSM film, crosslinked by SA, had a lower swelling than MA, signifying a higher degree of crosslinking. As the number of crosslinks

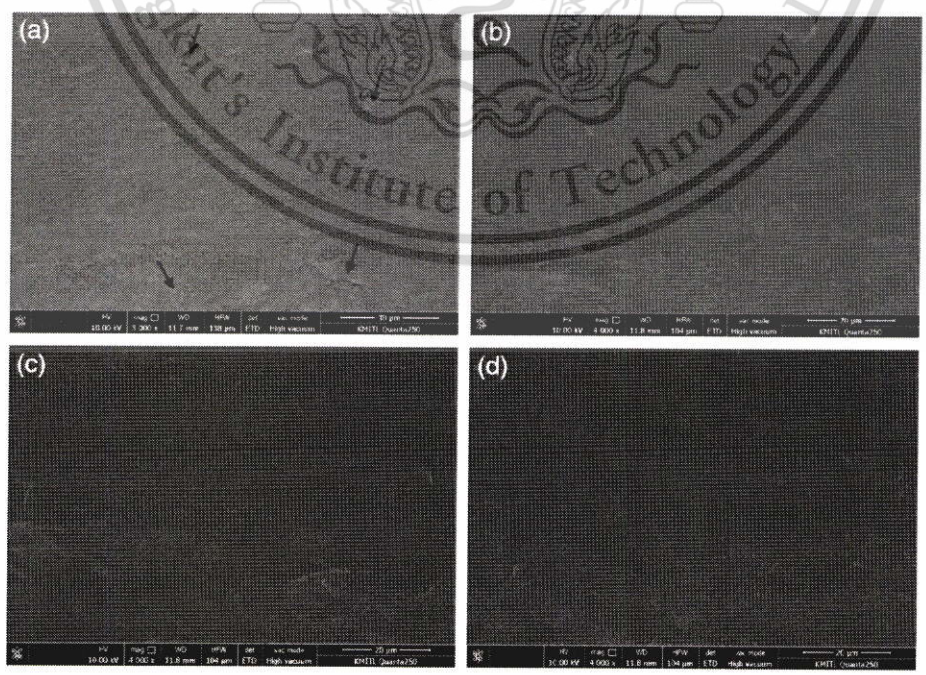

Figure 4. Chemical structure of basil seed mucilage (BSM) crosslinked by tartaric acid (TA), malic acid (MA) or succinic acid (SA).

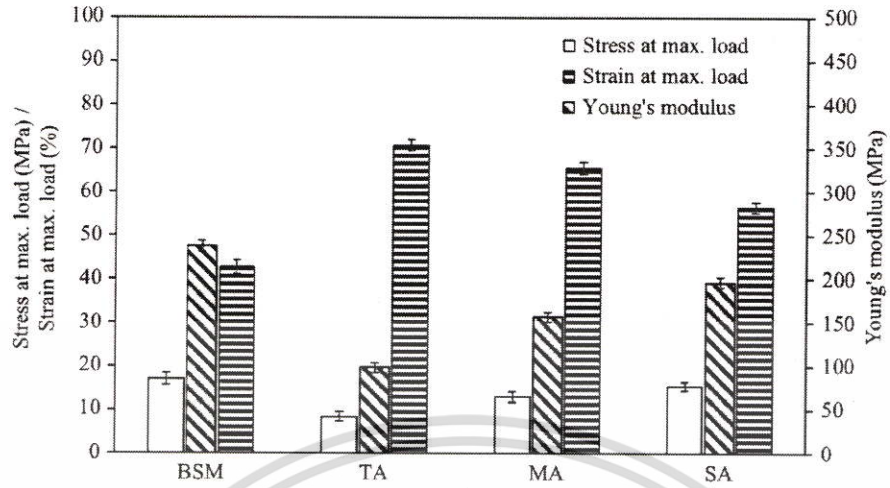

Figure 5. Mechanical properties of basil seed mucilage (BSM) films crosslinked with tartaric acid (TA), malic acid (MA) and succinic acid (SA).

Table 2. Film properties

Samples	WVP	Stress at maximum load (MPa)	Strain at maximum load (%)	Gel fraction (%)	References
Crosslinked basil seed mucilage (BSM) film with succinic acid	1.04 ± 0.05	15.4 ± 1.02	56.6 ± 1.2	97 ± 0.02	This work
Starch/poly vinyl alcohol (PVA) with ZnO	–	6.7	0.26	N/A	14
Starch/PVA with epichlorohydrin	–	6	0.46	N/A	14
Starch/PVA with borax	–	22	0.08	N/A	14
Starch/PVA with formaldehyde	–	6.5	0.2	N/A	14
PVA/xylan composite film with citric acid (CA)	2.48	7.6	35.5	N/A	17
CA modified granular pea starch/thermoplastic pea starch	2.6	N/A	N/A	–	19
CA modified granular rice starch/thermoplastic rice starch	2	N/A	N/A	–	19
Corn starch film with CA + sodium hypophosphate as catalyst	–	26.83 ± 4.39	4.35 ± 1.49	–	20
Potato starch film with aconitic acid	–	1.25	101.7	N/A	21
Chitosan/corn corb composite film with epichlorohydrin	–	46.9 ± 0.9	8.2 ± 0.4	79.64 ± 2.7	22
Chitosan/corn corb composite film with adipic acid	–	37.1 ± 2.01	12.18 ± 0.3	71.69 ± 2.8	22
Chitosan/corn corb composite film with glutaraldehyde	–	42.0 ± 1.6	7.7 ± 0.2	–	22
Potato starch film with malonic acid + sodium hypophosphite as catalyst	–	23.17	1.58	81	24
Corn starch film with CA	N/A	7	N/A	N/A	27
Sesame protein film with CA	N/A	6.56 ± 0.30	2.56 ± 0.05	–	32
Sesame protein film with succinic acid	N/A	7.03 ± 0.15	1.39 ± 0.34	–	32
Sesame protein film with malic acid	N/A	5.79 ± 0.45	4.76 ± 0.25	–	32
Low-density polyethylene (LDPE)	N/A	12.8 ± 0.53	156 ± 4.6	–	30
LDPE/organo modified montmorillonite (OMMT)	N/A	13.3 ± 0.83	154.5 ± 4.6	–	30
LDPE/OMMT/LLDPE-grafted maleic anhydride (MA)	N/A	10.2 ± 0.71	135.1 ± 5.07	–	30
LDPE/OMMT/natural rubber (ENR)	N/A	7.8	155	–	30
LDPE/OMMT/LLDPE-g-MA/ENR	N/A	9	160	–	30
Carbon nanotubes (NTs)/LDPE nanocomposite film	–	9.5	–	–	31
Halloysite NT/LDPE nanocomposite film	–	8.5	–	–	31
Titania NT/LDPE nanocomposite film	–	8	–	–	31

N/A, not available; WVP, water vapor permeability.

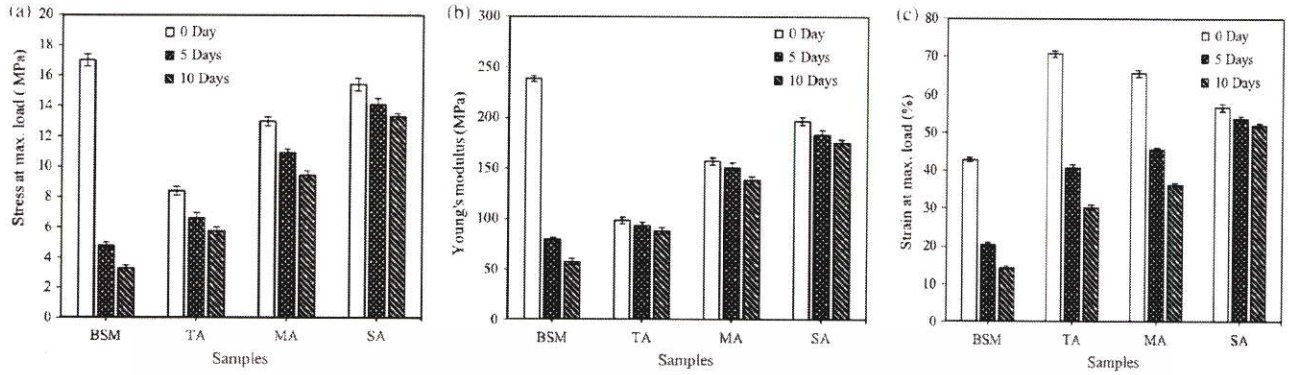

Figure 6. Mechanical properties after biodegradation in soil of basil seed mucilage (BSM) films crosslinked by tartaric acid (TA), malic acid (MA) and succinic acid (SA): (a) stress at maximum load, (b) Young's modulus and (c) strain at maximum load.

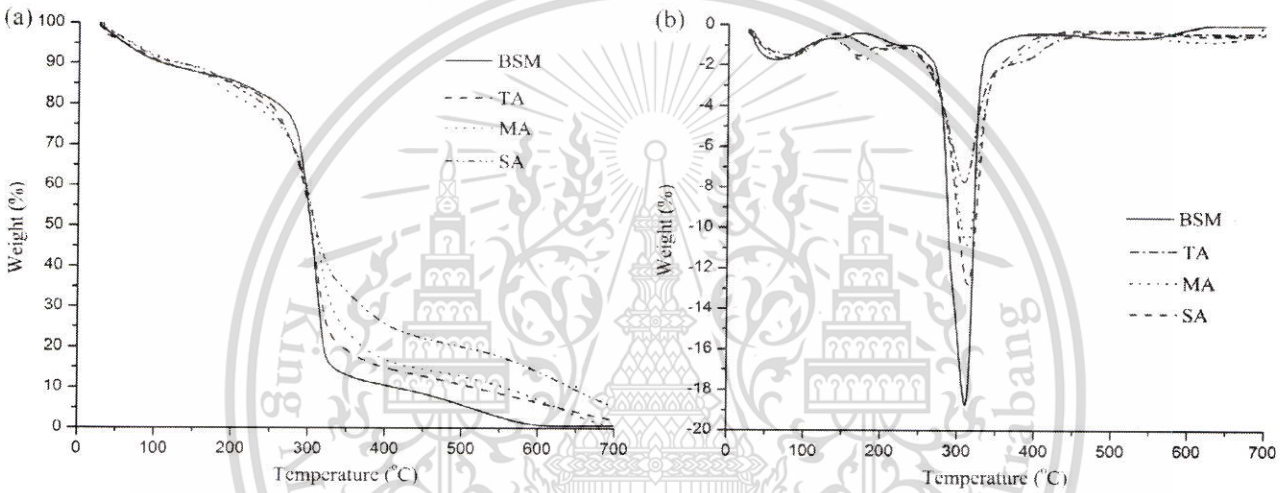

Figure 7. (a) Thermogravimetric analysis (TGA) and (b) derivative thermogravimetry (DTG) thermograms of basil seed mucilage (BSM) films crosslinked by tartaric acid (TA), malic acid (MA) and succinic acid (SA).

increased, the film became more resistant to water. Crosslinking strengthened BSM polymers prevented absorption of water and reduced disintegration. This trend is consistent with the report of Dastidar and Netravali, who crosslinked potato and cassava starch with CA.[24] The gel fraction measurements in Table 1 follow the same pattern for the same reason. Gel fraction for the crosslinked BSM film (97%) was clearly higher than those reported for the other bio-based films, which ranged from 71 to 81%.[22,24]

WVP

WVP for native and crosslinked BSM films is also shown in Table 1. The highest WVP was observed for the native BSM film, due to the abundance of hydroxyl groups in the polysaccharide molecules. All the crosslinked films showed lower WVP than native BSM film. The formation of a dense networked structure after crosslinking inhibits absorption of water and also restricts the movement of molecules, causing the difficulty for diffusion of water and lower vapor permeability.

Moreover, WVP of BSM film with SA tended to be the lowest, followed by MA and TA crosslinked BSM films because the tight ester bond formation after crosslinking extremely reduced water penetration. This agreed with Olsson *et al.* who reported that CA crosslinked potato starch film improved water vapor barrier of film.[17] WVP value of the crosslinked BSM film in this study was evidently lower than other bio-based films, which were ranged from 2 to 2.6 g mm m^{-2} d^{-1} kPa^{-1}.[17,19]

XRD

Crystallinity of native and various BSM films crosslinked by TA, MA and SA are also illustrated in Table 1. Crosslinked BSM film showed the reduction of degree of crystallinity compared to the native BSM film. After the crosslinking process, hydroxyl groups of BSM structure were replaced by C=O groups; therefore, the crosslinked BSM molecules could retard the re-association of the polysaccharide chains and prevent the recrystallization of the crosslinked BSM molecules. According to Dastidar and Netravali, the formation of crystal structures of potato and cassava starch films decreased after crosslinking with malonic acid.[24]

Moreover, degree of crystallinity values of different crosslinked BSM films were ranked as TA < MA < SA. The result also indicated that the highest acidity of TA enhanced hydrolysis BSM backbone chain, resulting in the lowest degree of crystallinity, as compared to BSM film crosslinked by MA and SA. In addition, the steric effect of TA caused the lowest degree of crystallinity. However, BSM film crosslinked by SA showed the highest degree of crystallinity because of the lowest acidity and steric hindrance of SA. In spite

Table 3. Decomposition temperatures and residual weight percentage of different crosslinked basil seed mucilage (BSM) films obtained from thermogravimetric and derivative thermogravimetry thermograms

Samples	Acid contents (%)	Thermal decomposition temperature (°C)					Residues (%) 600 °C
		Zone 1	Zone 2	Zone 3	Zone 4	Zone 5	
	0	72.6	172.4	–	305.4	–	0
Tartaric acid (TA)	30	98.8	187.7	260.4	312.6	373.5	10.4
Malic acid (MA)	30	70.7	189.6	262.8	317.2	381.4	11.9
Succinic acid (SA)	30	74.3	188.7	264.7	325.2	387.9	16.4

of the decrease in degree of crystallinity of crosslinked BSM films, the degree of crystallinity was still higher than that of bio-based films.[27,29]

SEM

SEM images of native and crosslinked BSM films are shown in Fig. 4. The cross-section micrograph of the native film (Fig. 4(a)) displayed a rough surface. However, the crosslinked films (Fig. 4(b–d)) illustrated homogenous and continuous morphology without pores or cracks. We ascribe this to crosslinking interactions between the BSM hydroxyl groups and functional groups in the crosslinkers. Furthermore, the homogenous and continuous morphology of the crosslinked film was assisted by the partial chain scission from the acid hydrolysis reaction. No marked difference can be seen in the films with TA, MA and SA.

Mechanical properties

Mechanical properties of native and crosslinked BSM films are displayed in Fig. 5. The uronic acid functional group has a strong affinity for water, allowing BSM films to easily form hydrogen bonds and retain water. Therefore, BSM films showed excellent strain at maximum load compared with other starch films.[14,22,24]

It can be observed that native BSM film presented the highest stress at maximum load and Young's modulus but lowest strain at maximum load. Excessive hydrogen bonds in the BSM molecules caused strong cohesive energy density.

However, crosslinked BSM films presented lower stress at maximum load and Young's modulus than the native film. Consequently, the strain at maximum load was increased. Higher extendibility was attributed to numerous crosslinks between side chains. This correlated with the decrease of degree of crystallinity presented in Table 1. Reddy and Yang reported similar results with CA crosslinked corn starch films.[27] Films exhibiting good extensibility are sought for food packaging applications, where the greater flexibility is desired.

Moreover, BSM film with TA demonstrated lower stress at maximum load and Young's modulus than the others. Strain at maximum load was correspondingly increased. The higher acidity of TA caused excessive hydrolysis of the polysaccharide chains: shorter chains are usually associated with low stress at maximum load and Young's modulus but higher strain at maximum load of the BSM film. Furthermore, this is consistent with the degree of crystallinity (Table 1). The lowest degree of crystallinity of film with TA resulted in the lowest stress at maximum load and Young's modulus, but showed the highest strain at maximum load. BSM film showed noticeable stress at maximum load, comparable with low-density polyethylene (LDPE) film, as seen in Table 2.[30,31] Moreover, BSM films exhibited excellent strain at maximum load relative to other bio-based films and protein films.[14,16,20–22,24,27,30–32]

Soil burial test

In the soil burial test (Fig. 6), we compared mechanical properties before and after degradation for native and crosslinked BSM films. After burial, there was a significant drop in tensile properties for all samples. The absorption of moisture from the soil during burial and also microorganisms led to this reduction.[32] Moreover, it was observed that all crosslinked BSM films would biodegrade, resulting in decreased tensile properties. TA crosslinked films showed the lowest strength and elasticity, i.e. they were more strongly degraded in the soil, due to acid hydrolysis.

TGA

TGA and DTG thermograms of native and crosslinked BSM films are shown in Fig. 7 and Table 3. The first step corresponded to water evaporation which occurred at ~100 °C; the second step at ~180 °C was associated with the degradation of the glycerol-rich phase. In addition, all crosslinked BSM films showed a third step from 260 °C, due to decomposition of hydrolyzed BSM molecules, thus reducing the molecular weight and thermal resistance of the film (Fig. 7 and Table 3).[21]

The main degradation step at 300 °C was assigned to thermal degradation of the saccharide backbone.[22] A further thermal degradation step for crosslinked film was observed at 370 °C.[21] This was attributed to the increased thermal degradation corresponding to breaking of the stronger ester bonds between the acids and BSM chains.

The temperature of the main degradation step (step 4) of crosslinked films increased significantly, compared to the native film. The TA, MA and SA enhanced intermolecular interactions between the BSM backbone chains by crosslinking, with strong covalent bonds, resulting in a higher thermal degradation temperature of the crosslinked films.

Crosslinked films also showed higher thermal degradation and higher char residue than the native films, explained by the effect of crosslinking between the acids and BSM chains. It should be noted that SA crosslinked films showed the highest residual weight percentage and a higher thermal degradation temperature than the others. With the lowest steric hindrance, SA created the highest degree of crosslinking.

CONCLUSION

Biodegradable BSM film was successfully prepared and crosslinked by TA, MA and SA. All crosslinked BSM films showed new ester bond formation, observed in FTIR spectra. After crosslinking, swelling, WVP and degree of crystallinity of BSM film were significantly decreased and gel fraction clearly increased. BSM films with SA showed the lowest swelling and WVP and the highest gel fraction compared to TA and MA. SEM images showed

that the crosslinked films were smoother than the native film. In addition, all the crosslinked films showed enhanced extendibility and thermal properties were improved by crosslinking. As a crosslinker, SA showed the lowest water permeability and swelling ability, the highest gel fraction and extendibility.

ACKNOWLEDGEMENTS

The authors thank the King Mongkut's Institute of Technology Ladkrabang (KMITL) Research Fund (KREF 046108) for financial support and the Department of Chemistry, KMITL, for facility support and also John Morris, KRIS, KMITL who checked and compressed this manuscript to a more readable form.

REFERENCES

1 Kokoszka S, Debeaufort F, Hambleton A, Lenart A and Voilley A, Protein and glycerol contents affect physico-chemical properties of soy protein isolate-based edible films. *Innovative Food Sci Emerging Technol* **11**:503–510 (2010).
2 Kurd F, Fathi M and Shekarchizadeh H, Basil seed mucilage as a new source for electrospinning: production and physicochemical characterization. *Int J Biol Macromol* **95**:689–695 (2017).
3 Javanmardi J, Khalighi A, Kashi A, Bais H and Vivanco J, Chemical characterization of basil (*Ocimum basilicum* L.) found in local accessions and used in traditional medicines in Iran. *J Agric Food Chem* **50**:5878–5883 (2002).
4 Salehi F, Kashaninejad M, Tadayyon A and Arabameri F, Modeling of extraction process of crude polysaccharides from Basil seeds (*Ocimum basilicum* L.) as affected by process variables. *J Food Sci Technol* **52**:5220–5227 (2015).
5 Khazaei N, Esmaiili M, Djomeh ZE, Ghasemlou M and Jouki M, Characterization of new biodegradable edible film made from basil seed (*Ocimum basilicum* L.) gum. *Carbohydr Polym* **102**:199–206 (2014).
6 Allafchiana A, Jalalib SAH, Hosseinia F and Massoudd M, *Ocimum basilicum* mucilage as a new green polymer support for silver in magnetic nanocomposites: production and characterization. *J Environ Chem Eng* **5**:5912–5920 (2017).
7 Rafe A, Razavi S and Khan S, Rheological and structural properties of β-lactoglobulin and basil seed gum mixture: effect of heating rate. *Food Res Int* **49**:32–38 (2012).
8 Melo J and D'souza S, Removal of chromium by mucilaginous seeds of *'Ocimum basilicum*. *Bioresour Technol* **92**:151–155 (2004).
9 Kadam PV, Yadav KN, Jagdale SK, Shivatare RS, Bhilwade SK and Patil MJ, Evaluation of *Ocimum sanctum* and *Ocimum basillicum* mucilage as a pharmaceutical excipient. *J Chem Pharm Res* **4**:1950–1955 (2012).
10 Zhuang C, Tao F and Cui Y, Anti-degradation gelatin films crosslinked by active ester based on cellulose. *R Soc Chem* **5**:52183–52193 (2015).
11 Sun S, Liu P, Ji N, Hou H and Dong H, Effects of various cross-linking agents on the physicochemical properties of starch/PHA composite films produced by extrusion blowing. *Food Hydrocolloids* **77**:964–975 (2018).
12 Reddy N, Reddy R and Jiang Q, Crosslinking biopolymers for biomedical applications. *Trends Biotechnol* **33**:362–369 (2015).
13 Xu H, Shen L, Xu L and Yanga Y, Low-temperature crosslinking of proteins using non-toxic citric acid in neutral aqueous medium: mechanism and kinetic study. *Ind Crops Prod* **74**:234–240 (2015).
14 Das K, Ray D, Bandyopadhyay NR, Gupta A, Sengupta S, Sahoo S *et al.*, Preparation and characterization of cross-linked starch/poly(vinyl alcohol) green films with low moisture absorption. *Ind Eng Chem Res* **49**:176–2185 (2010).
15 Abdillahi H, Chabrat E, Rouilly A and Rigal L, Influence of citric acid on thermoplastic wheat flour/poly(lactic acid) blends. II. Barrier properties and water vapor sorption isotherms. Indust. *Crop Prod* **50**:104–111 (2013).
16 Wang S, Ren J, Li W, Sun R and Liu S, Properties of polyvinyl alcohol/xylan composite films with citric acid. *Carbohydr Polym* **103**:94–99 (2014).
17 Olsson E, Hedenqvist MS, Johansson C and Järnström L, Influence of citric acid and curing on moisture sorption, diffusion and permeability of starch films. *Carbohydr Polym* **94**:765–772 (2013).
18 Yoon SD, Cross-linked potato starch-based blend films using ascorbic acid as a plasticizer. *J Agric Food Chem* **62**:1755–1764 (2014).
19 Ma X, Chang PR, Yu J and Stumborg M, Properties of biodegradable citric acid-modified granular starch/thermoplastic pea starch composites. *Carbohydr Polym* **75**:1–8 (2009).
20 Shen L, Xu H, Kong L and Yang Y, Non-toxic crosslinking of starch using polycarboxylic acids: kinetic study and quantitative correlation of mechanical properties and crosslinking degrees. *J Polym Environ* **23**:588–594 (2015).
21 Gilfillan WN and Doherty WOS, Starch composites with aconitic acid. *Carbohydr Polym* **141**:60–67 (2016).
22 Yeng CM, Husseinsyah S and Ting SS, A comparative study of different crosslinking agent-modified chitosan/corn cob biocomposite films. *Polym Bull* **72**:791–808 (2015).
23 Beigomi M, Mohsenzadeh M and Salari A, Characterization of a novel biodegradable edible film obtained from *Dracocephalum moldavica* seed mucilage. *Int J Biol Macromol* **108**:874–883 (2018).
24 Dastidar TG and Netravali AN, 'Green' crosslinking of native starches with malonic acid and their properties. *Carbohydr Polym* **90**:1620–1628 (2012).
25 Qin Y, Zhang S, Yu J, Yang J, Xiong L and Sun Q, Effects of chitin nano-whiskers on the antibacterial and physicochemical properties of maize starch films. *Carbohydr Polym* **147**:372–378 (2016).
26 Naji-Tabasia S, Razavi SMA and Mehditabar H, Fabrication of basil seed gum nanoparticles as a novel oral delivery system of glutathione. *Carbohydr Polym* **157**:1703–1713 (2017).
27 Reddy N and Yang Y, Citric acid cross-linking of starch films. *Food Chem* **118**:702–711 (2009).
28 Naji-Tabasi S, Razavi SMA, Mohebbi M and Malaekeh-Nikouei B, New studies on basil (*Ocimum bacilicum* L.) seed gum. Part I – fractionation, physicochemical and surface activity characterization. *Food Hydrocolloids* **52**:350–358 (2016).
29 Vanier NL, Oliveira JP, Bruni GP, Halal SLME, Villanova FA, Elessandra RZ *et al.*, Characteristics of starch from different bean genotypes and its effect on biodegradable films. *J Sci Food Agric* **99**:1207–1214 (2018).
30 Attaran SA, Hassan A and Wahit MU, Effects of ENR and OMMT on barrier and tensile properties of LDPE nanocomposite film. *Iran Polym J* **24**:367–378 (2015).
31 Majeed K, AlMaadeed MAA and Zagho MM, Comparison of the effect of carbon, halloysite and titania nanotubes on the mechanical and thermal properties of LDPE based nanocomposite films. *Chin J Chem Eng* **26**:428–435 (2018).
32 Wang H, Wei D, Zheng A and Xiao H, Soil burial biodegradation of antimicrobial biodegradable PBAT films. *Polym Degrad Stab* **116**:14–22 (2015).

